New Nuclear Medicine Techniques for the Assessment of Myocardial Viability

Riemer H.J.A. Slart

RIJKSUNIVERSITEIT GRONINGEN

New Nuclear Medicine Techniques for the Assessment of Myocardial Viability

Proefschrift

ter verkrijging van het doctoraat in de
Medische Wetenschappen
aan de Rijksuniversiteit Groningen
op gezag van de
Rector Magnificus, dr. F. Zwarts,
in het openbaar te verdedigen op
maandag 27 juni 2005
om 13.15 uur

door

Riemer Harmand Johan Anne Slart

geboren op 10 april 1969

te Emmercompascuum

Promotores:	Prof. Dr. D.J. van Veldhuisen Prof. Dr. E.E. van der Wall
Co-promotores:	Dr. P.L. Jager Dr. J.J. Bax

Beoordelingscommissie	Prof. Dr. R.A.J.O. Dierckx Prof. Dr. F. Zijlstra Prof. Dr. B.L.F. van Eck-Smit
Paranimfen:	drs. F.J.N. van der Sluis S.J.L. Mantel

ISBN 90-367-2275-6

Cover: photo by L.H. Veeman & Stichting Het Groninger Landschap.
Design by Reclamebureau Pieterman, Groningen.

Financial support by the Netherlands Heart Foundation and Stichting Onderzoek en Opleiding Nucleaire Geneeskunde Groningen for the publication of this thesis is gratefully acknowledged.

Publication of this thesis was also financially supported by:

Van Buchem Stichting
Tromp Medical Engineering B.V.
I.D.B. Holland B.V.
Tyco Healthcare / Mallinckrodt Medical B.V.
GE Healthcare Medical Diagnostics
Groningen Institute of Drug Exploration (GUIDE)
Medrad Europe B.V.
Bristol-Myers Squibb B.V.
Veenstra instrumenten B.V.
Pfizer B.V.
Guidant Nederland B.V.

Voor mijn ouders

Contents

SECTION I

Introduction and outline of the thesis

Chapter 1

Imaging techniques in nuclear cardiology for the assessment of myocardial viability Adapted from the *submitted* version

INTRODUCTION

1. Clinical importance of identifying viable myocardium

Assessment of myocardial viability in patients with coronary artery disease (CAD) and left ventricle (LV) dysfunction is of major importance for prognosis (1-3). Patients with this condition are at high risk for cardiac death and usually have significant limitations in their lifestyles. It is well known that LV dysfunction is not necessarily an irreversible process. Dysfunctional but viable myocardium has the potential to recover after restoration of myocardial blood flow by either coronary arterial bypass grafting (CABG) or percutaneous transluminal coronary angioplasty (PTCA), whereas scarred tissue will not recover (4-7). Patients with CAD and severe dysfunction but viable LV have a poor prognosis when treated with medical therapy alone (8). In selected patients with sufficient viable myocardium, coronary revascularization appears to afford a long-term survival benefit (9,10). Nuclear imaging techniques like positron emission tomography (PET) or single positron emission computed tomography (SPECT) play a major role in the assessment of myocardial viability (11-14). Further improvement for the detection of myocardial viability will be expected, because of new technique development in the nuclear cardiology field, like attenuation corrected SPECT, dual isotope simultaneous acquisition (DISA) SPECT and gated FDG PET. Also the combination of multislice computed tomography scanners with PET opens possibilities of adding coronary calcium scoring and noninvasive coronary angiography to myocardial perfusion imaging and quantification.
In the next paragraphs we describe several conventional and new nuclear techniques, a radiopharmaceutical overview and pathophysiogical backgrounds of myocardial viability.

2. Pathophysiology of myocardial contractile dysfunction

LV dysfunction may be caused by (1) (repetitive) stunning, (2) widespread hibernation or by (3) infarcted necrotic myocardium. Myocardial stunning is a condition of prolonged, postischemic dysfunction of viable tissue that can be salvaged by reperfusion (15). Stunning may occur after acute coronary occlusion followed by thrombolysis, but also after a period of unstable angina or exercise-induced ischemia. Repetitive stunning is a phenomenon defined as repeated episodes of ischemia inducing reduction in contractility. It appears that one of the mechanisms responsible for myocardial stunning ischemia is an alteration of contractile proteins resulting in decreased responsiveness of the contractile machinery to Ca^{2+}, so that the myocardium generates less force (16). In this sense, myocardial stunning could be viewed as a disturbance of myofilament function.
Hibernation means chronically reduced myocardial perfusion at rest associated with impairment in contractile function, which can be reversed after revascularization. The reduction of contractile function associated with hibernation may be a protective

response of the myocardium in order to meet the reduced supply of oxygen and substrates, leading to a new situation of perfusion-contraction matching, which prevents apoptosis and cell death (17,18). In hibernating myocardium, myocytes are in a stable non-contractile state. Cell membrane and cellular metabolism remain intact and little or no evidence of apoptosis is present (19,20). Elsasser et al. biopsied areas of hibernating myocardium during coronary artery bypass graft (CABG) (21). They found an enlarged extracellular space with cellular debris, macrophages, fibroblasts and collagen, associated with basement membrane thickening and increased collagen fibrils and fibroblasts. There also appears to be an alternation of structural proteins, metabolism to a more fetal form, disorganization of the cytoskeleton, loss of myofilaments, occurence of large fields with glycogen, and sarcomeric instability (22). Unclear is if these findings are typical related to hibernated myocardial tissue or also to other tissue conditions.
The time course of functional recovery of hibernating myocardium may vary considerably, and depends on several factors including the duration and severity of myocardial ischemia, the time and completeness of myocardial revascularisation, and the extent of ultrastructural alterations within the dysfunctional myocardium (23). There is increasing evidence that cell death after myocardial ischemia and reperfusion may begin as apoptosis rather than necrosis (24). The induction of apoptosis and necrosis is regulated by many of the same biochemical intermediates, including alterations in high-energy phosphates, intracellular calcium accumulation, and reactive oxygen species. Apoptosis, first descibed by Kerr and coworkers, is characterized by morphologic changes, including cell shrinkage and formation of membrane-bound apoptotic bodies (25). In contrast, necrosis is characterized by cell swelling, depletion of high energy stores, disruption of the cellular membrane involving fluid and electrolyte alterations and fragmentation of DNA, due to mechanisms such as ischemia and thrombosis (26). These findings suggest that necrosis into scar formation occurs continuously due to myocytes loss and that early revascularization would enhance recovery of function.
Several imaging techniques are based on the detection of viable myocardium in order to select those patients who will benefit from revascularization. These techniques will be outlined in the next paragraphs

3. Methods for the detection of myocardial viability

What is the gold standard for viability studies? The choice of gold standard or reference technique for viability is still a long debate. There have been many end-points proposed for viability studies, including preserved cellular metabolism (27), histological examination of biopsied tissue (28), preserved regional wall contraction by low-dose dobutamine echography, gated SPECT or magnetic resonance imaging (MRI) (29-32), regional or global functional recovery (33-36), symptom improvement (37,38) and improved survival (39,40) (Table 1). From a pathophysiological point of view, biological signals as generated from PET and SPECT or histological examination provide important insights into viability

at the cellular or molecular level. ^{18}F-fluorodeoxyglucose (FDG) uptake in myocardial tissue indicates preserved viability (41). High ^{99m}Tc-annexin V affinity to the cellular wall, due to phosphatidyl-serine overexpression indicates apoptosis, associated with programmed cell death (42). Short duration of apoptosis can be reversible, whereas longer existing apoptosis is mostly an irreversible process and results in depletion of sarcomeres and extensive interstitial fibrosis, indicating absent viable myocardium (43).
Regional dysfunctional contractility of the left ventricle, can be transiently reversed by positive inotropic stimulation. During stimulation with dobutamine infusion (used in MRI, gated SPECT or echography), systolic wall thickness will increase in viable, but not in scarred myocardium, because only viable cells are able to response to the inotropic stimulus. Assessment of regional or global functional recovery of the LV after restoration of blood flow is also relevant because it is directly associated with the definition of stunned or hibernating myocardium. From a clinical point of view, the improved survival and symptoms following revascularization are optimal endpoint of viability studies, because these are considered as the main goals of revascularization procedures, but this requires a long follow-up period. Probably, the global improvement of LV function and reduction in end-systolic and end-diastolic volume (reverse remodeling) after revascularization is an acceptable alternative, because this is easy to measure and is likely to be associated with improved prognosis (44). PET is an attractive technique for the assessment of myocardial viability. This will be outlined in the next paragraph.

3.1 PET

PET imaging differs from conventional radionuclide imaging because it uses radionuclides that decay with positron emission. A positron has the same mass as an electron but has a positive charge. The positron travels a short distance, up to a few millimeters, interacts with an electron, and the two undergo a mutual annihilation, resulting in the pro-

Table 1: Outline of different referent methods for the assessment of myocardial viability.

Assessment viability	Technique
Cellular function	Biopsy
	^{99m}Tc-annexin V
	FDG
	^{11}C-acetate
	^{11}C-palmitate
	^{99m}Tc-sestamibi/^{99m}Tc-tetrofosmin
	^{201}Tl
Regional LV contractility	Dobutamine stress MRI
	Dobutamine stress echocardiography
	Dobutamine stress gated SPECT
Clinical	Cardiac events
	Symptoms
	LV recovery post-revascularization

duction of two 511-kev gamma photons, 180° apart from each other. PET imaging consists of detection of these photons in coincidence in a ring detector system. Imaging by PET leads to high acquisition efficiency, resulting in high-quality images.
The clinical utility of PET imaging to identify viable myocardial tissue was first described by Tillisch et al. in the middle eighties (45). The accuracy of FDG (with or without an additional perfusion tracer) imaging for predicting improvement in LV function after revascularization, as reported in several previous studies, is high, with a negative predicting value ranging from 76% to 90% and a positive predicting value ranging from 82% to 100% (46-51). Therefore, PET is recognized as an accurate technique for the quantification of metabolism and perfusion of the myocardium, resulting in high diagnostic accuracy for the detection of myocardial viability (52,53).

3.1.1 Metabolic imaging: FDG

Free fatty acids, glucose, and lactate are the major energy sources of the heart (54-56). Fatty acids play a major role in the metabolism of the non-ischemic heart, whereas glucose becomes the major substrate for the myocardium during ischemic conditions (57-59). FDG closely resembles glucose and is therefore a suitable tracer to visualize glucose metabolism.
A prerequisite for FDG imaging of the heart is high myocardial uptake. For most studies using FDG, glucose loading either by oral glucose administration or by insulin clamp is essential. Acipimox, a nicotinic acid derivate, may be an alternative to clamping. Acipimox inhibits peripheral lipolysis and therefore reduces plasma free-fatty acid levels, and, indirectly stimulates cardiac FDG uptake in this way (60). Previous data have shown that good image quality can be obtained using acipimox (comparable with clamping and superior to oral glucose load) (61).
The clinical applicability of FDG is based on the effective intracellular trapping after phosphorylation of FDG into FDG-6-phosphate. In contrast to glucose-6-phosphate, FDG-6-phosphate is not a substrate for further metabolism. Therefore, FDG enables detection of metabolic changes at the cellular level during ischemia. The preserved or increased glucose utilization, and subsequent FDG uptake in hypoperfused and dysfunctional myocardium (flow-metabolism mismatch) is regarded as a metabolic marker of cell survival and viability, whereas concordant reduction in both blood flow and FDG uptake (matched defect) is indicative of scar (Figure 1). Thus, FDG PET provides a biological signal on cellular viability, and is considered to be one of the most accurate non-invasive techniques to identify viable tissue, as supported by a number of studies using PET (62-68).
Image are usually interpreted semi-quantitatively, based on the relative regional uptake of FDG (69). Absolute quantification of regional myocardial glucose utilization by dynamic imaging and compartment modeling does not appear to enhance the diagnostic accuracy of FDG PET to detect viable myocardium, probably because of high variability in glucose utilization rates in individual patients, even in comparison with a normal database (70). In general, the relative FDG uptake is considered clinically sufficient for this purpose. PET studies can be displayed in polarmaps or short and long axes of the left ventricle.

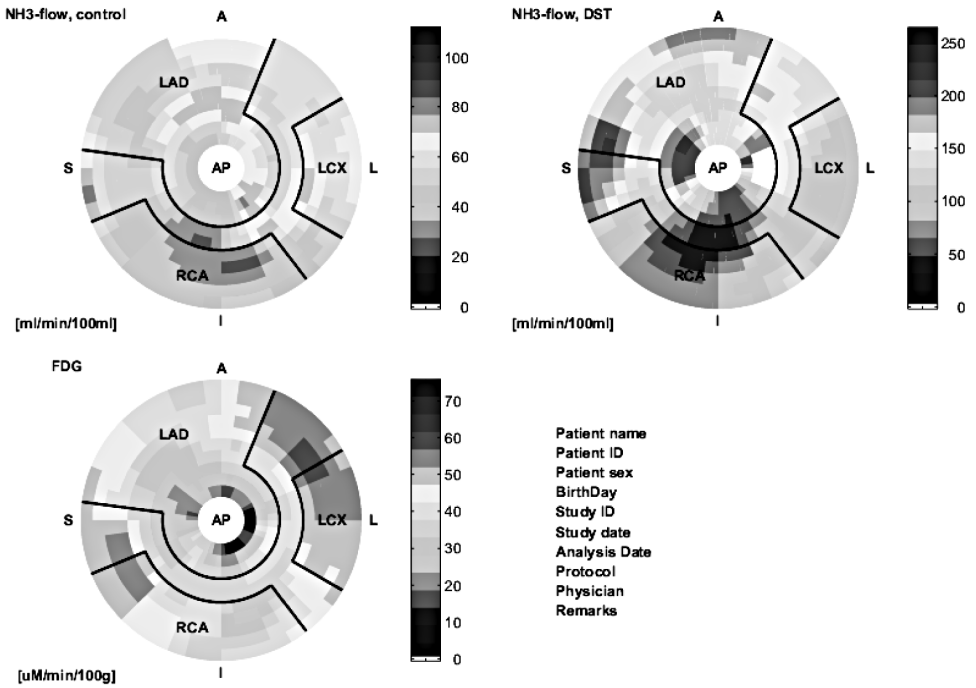

Figure 1: PET polarmaps display. The first polarmap illustrates rest ^{13}N-ammonia perfusion of the left ventricle. In the mid-inferior wall a relative small defect is visible and becomes lager on the second, dypiridamole (DST) stress ^{13}N-ammonia perfusion polarmap, indicating insufficient flow reserve. ^{18}F-fluorodeoxyglucose (FDG) in the inferior wall is largely preserved on the lowermost polarmap, indicating ischemia and viability. A minor FDG defect is persisting in the mid-inferior region, indicating a small infarcted area.

3.1.2 Metabolic imaging: fatty acids

Under aerobic conditions, the heart uses predominantly fatty acids, but after carbohydrate loading, the inhibitory effect of insulin on release of fatty acids from adipocytes diminishes circulating fatty acids and up-regulates glucose use by the heart. During myocardial ischemia, fatty acid metabolism is diminished and glucose uptake is enhanced (71). Normal (relative to flow) or enhanced glucose metabolism serves as the metabolic signature of ischemic myocardium. Stunned or hibernating myocardium also demonstrate preserved oxygen use relative to perfusion and function (72).

Because the diminished use of fatty acids is a key metabolic feature of myocardial ischemia, early interest with PET focused on the use of fatty acids such as ^{11}C-palmitate (Table 2) (73). However, because of its relatively complicated synthesis, the need for an on-site cyclotron, and the complex tracer kinetics, this tracer is not currently used for identification of viable myocardium.

^{11}C-acetate is an another PET tracer for studying myocardial oxidative metabolism and a

Table 2: Single-photon emitting and positron emitting (*) tracers for cardiac imaging.

Tracer	Assessment	Uptake mechanism
^{201}Tl	Perfusion/viability	Na^+/K^+-ATPase celmembrane pump
^{99m}Tc-sestamibi	Perfusion (viability)	Mitochondrial K^+-ATP channel
^{99m}Tc-tetrofosmin	Perfusion (viability)	Mitochondrial K^+-ATP channel
^{15}O-water*	Perfusion	Diffuses freely across cell membrane
^{13}N-ammonia*	Perfusion	Diffuses freely across cell membrane. The ammonium form is intracellularly trapped in glutamine via the enzyme glutamine synthase
^{82}Rb*	Perfusion/viability	Na^+/K^+-ATPase celmembrane pump
FDG*	Glucose consumption	Intracellular trapping after phosphorylation of FDG to FDG-6-phosphate
^{11}C-acetate*	Oxidative metabolism/ perfusion	Converted intracellular to acetyl-CoA and further metabolized in the Krebs cycle of the mitochondrium to $^{11}CO_2$
^{11}C-palmitate*	Free fatty acid metabolism	FFA intracellularly converted to FFA-CoA, cleavage of carbon fragments of FFA-CoA during β-oxidation and further metabolized in the Krebs cycle of the mitochondrium to $^{11}CO_2$

marker of regional myocardial blood flow, because of its relatively high first-pass extraction in myocardial tissue. However, this tracer also requires a cyclotron in addition to the assessment of wash-out kinetics, thereby making this tracer somewhat less useful for most centers.

3.1.3 Flow Tracers

The ideal tracer for the assessment of myocardial perfusion would possess the following properties: distribution in the myocardium in linear proportion to blood flow (without plateau effect at high flow rates) over the full range of values experienced in health and disease, efficient myocardial extraction from the blood on the first passage through the myocardium, stable retention within the myocardium during data acquisition, rapid elimination allowing rapid repeat studies, good availability, competitive pricing and good imaging characteristics (short half-live, high photon flux, adequate energy, low radiation burden to the patient). No current tracer possesses all of these properties and comprimises have to be made.

Absolute quantification of myocardial blood flow is feasible using PET and tracer kinetic models (74,75). In clinical practice, FDG PET is often combined with a flow tracer to assess myocardial perfusion. Although FDG PET imaging without a flow tracer has sufficient sensitivity and specificity for detecting viable tissue (76), a combination of flow and metabolism provides more comprehensive information on viability and herein the differentiation between hibernation and stunning (77-79). Stunned myocardium exhibits slightly reduced or normal perfusion, whereas in hibernating myocardium perfusion is

severely reduced. Stunned myocardium is likely to demonstrate early recovery of function, whereas hibernating myocardium may take a longer time to (fully) recover in function after revascularization (80).

3.1.3.1 ^{13}N-ammonia

In the bloodstream, ^{13}N-ammonia consists of neutral ammonia (NH_3) in equilibrium with its charged ammonium (NH_4) ion. The neutral NH_3 molecule readily diffuses across plasma and cell membranes. Inside the cell, it re-equilibrates with its ammonium form, which is trapped in glutamine via the enzyme glutamine synthase (81,82). Despite back diffusion, the first-pass trapping of ^{13}N ammonia at rest is high, although decreasing with higher blood flow. ^{13}N-ammonia allows quantification of perfusion both at rest and after application of vasodilatating agents to assess myocardial perfusion reserve, such as dipyridamole or adenosine (83,84). With the use of a 2- or 3-compartmental model, satisfactory reproducibility and accuracy can be obtained (85,86).
The suitability of ^{13}N-ammonia as a myocardial flow tracer is established in numerous studies (87-92). Kitsiou et al. demonstrated that ^{13}N-ammonia retention rather than absolute myocardial blood flow was a good marker of cellular viability (93). The use of ^{13}N-ammonia is restricted to sites with a cyclotron.

3.1.3.2 ^{15}O-Water

Unlike ^{13}N-ammonia, ^{15}O-water diffuses freely across plasma membranes and makes this tracer a favorite for quantification of myocardial blood flow. In theory, ^{15}O-water is considered to be an ideal tracer for measurement of myocardial blood flow without plateau effect at high flow rates (94,95). However, poor contrast between the myocardium and cardiac blood pool, due to the properties of ^{15}O-water (necessity for subtraction of blood pool activity), and a very short physical half-life time may cause heterogeneity of flow measurements, as demonstrated by Nitzsche et al (96).
A unique feature of ^{15}O-water PET imaging is that the proportion of the total tissue that is capable of rapidly exchanging water (water perfusable tissue index, PTI) can be used as a marker of tissue viability (97,98). Although more work needs to be done before its clinical utility is determined, this technique appears to provide information on tissue viability. The use of ^{15}O-water is restricted to sites with a cyclotron.

3.1.3.3 Rubidium-82 (^{82}Rb)

^{82}Rb is produced in a commercially available generator by decay from strontium-82 attached to an elution column. ^{82}Rb decays by positron emission with a short half-life of 75 s. Therefore it facilitates the rapid completion of a series of resting and stress myocardial perfusion studies. ^{82}Rb, like ^{201}Thallium (^{201}Tl), is a cation and an analog of potassium. It is extracted from plasma by myocardial cells via the Na^+/K^+-ATPase pump. Myocardial extraction of ^{82}Rb is similar to (^{201}Tl) and slightly less than ^{13}N-ammonia, decreasing during hyperemia (99). ^{82}Rb extraction can be altered by severe acidosis, hypoxia, and ischemia (100). Thus, uptake of ^{82}Rb is a function of both blood flow and of myocardial

cell integrity. Unlike ^{201}Tl, there are minimal problems with liver or bowel uptake. The disadvantages of ^{82}Rb include the high energy of its positron (3.3 MeV) and a rather low extraction fraction (65%). However, PET imaging with ^{82}Rb has proven to be highly accurate in the detection and functional assessment of coronary artery stenoses and infarct size imaging (101,102).

3.2 Gated FDG PET

Compared to echography, MRI, CT, gated SPECT, gated blood pool SPECT, PET systems also offer the capability to perform an electrocardiograph (ECG)-gated acquisition and to generate systolic and diastolic images of the heart (103,104). In combination with myocardial perfusion, gated FDG PET permits a complete LV evaluation, using a single modality for evaluation of major myocardial parameters, including glucose metabolism, flow reserve and LV function. Obtaining functional information of the LV requires no extra scan or tracer injection. Assessment of cardiac function by gated FDG PET without the need for other clinical modalities will significantly reduce the time and costs of pre-revascularization work-up. While MRI is considered the reference method for the assessment of LV function, most studies compared gated FDG PET with other techniques like gated SPECT, left ventriculography, and 2D echocardiography (105-110).
Other PET techniques including gated blood pool PET after red blood-cell labelling with C^{15}O (111,112) or gated ^{13}N-ammonia (113) also provide information about LV volumes and function, but give no information about metabolism. Furthermore, gated FDG PET studies for the prediction of functional recovery after revascularization are currently not available, using FDG uptake and wall thickening as viability parameters.

3.3 SPECT

Myocardial perfusion scintigraphy (MPS) SPECT is an established imaging technique that is already an integral part of the managing of coronay artery disease and is included in a number of professional guidelines. Many studies has assessed the diagnostic accuracy of MPS for the detection of coronary artery disease (114-116). In the largest study of 2,560 patients randomized to each of the three tracers (^{99m}Tc-sestamibi, ^{99m}Tc-tetrofosmin and ^{201}Tl) and using mainly adenosine stress (the ROBUST study, UK based), overall sensitivity in the subset of patients undergoing angiography was 91% and specificity 87%, with no significant difference between the three tracers (117). For many patients with coronary artery disease, the assessment of prognosis, or likelihood of future cardiac events, is an essential step in choosing between medical management and revascularization. The power of MPS for predicting future coronary events has been demonstrated in large number of studies and in many of thousand of patients. It is perhaps the area of nuclear cardiology where the evidence is most strong (118-120). The

most important variables that predict the likelihood of future events are the extent and severity of induced ischemia (121) but other predictors are increased lung uptake of ^{201}Tl (122), stress-induced ventricular dilatation (123). MPS has incremental prognostic value even after clinical assessment, exercise electrocardiography, and coronary angiography (124). In contrast, a normal MPS indicates good clinical outcome with < 0.6% event rate of major cardiac events yearly as reported in a multicenter registry of 4,728 patients (125). Further, ^{99m}Tc-labeled myocardial perfusion tracers reflect not only flow, but also myocardial viability (126).

PET imaging is an established technique to distinguish viable from scarred myocardium, howvever its relative limited availability, dependency of cyclotrons and high costs has limited the widespread use in clinical practice. PET has several technical advantages over gamma-technique SPECT such as higher counting sensitivity, higher spatial resolution, routine use of attenuation correction and absolute quantification of myocardial perfusion flow and metabolism. However, most of these technical advantages of PET over SPECT for accurate assessment of myocardial viability are not strongly required, although attenuation correction systems might be beneficial (127). To meet the advantages of attenuation correction, some SPECT systems are equipped with attenuation correction systems at present. Substantial efforts have been made for further improvement of the less expensive and much more widely available SPECT technique for the assessment of viability. Presently, several traditional and novel tracers for the detection of ischemia and viability are used with SPECT.

3.3.1 ^{201}Thallium

The active uptake of ^{201}Tl by myocardial cells is dependent on myocardial blood flow and active transport (128). ^{201}Tl is a potassium analog that is actively transported into myocytes by a Na^+/K^+-ATPase-dependent mechanism. Its uptake thus requires an intact, functional cell membrane. Therefore, myocardial ^{201}Tl uptake represents both myocardial perfusion and cellular viability. It has been shown that delayed imaging 3–4 hours after stress injection of ^{201}Tl frequently underestimates the presence of viable myocardium as compared to metabolic imaging with FDG PET (129). Modified ^{201}Tl protocols such as reinjection technique (130,131) enhanced the detection of viable myocardium, although viability in myocardium may still be underestimated by ^{201}Tl as compared with FDG PET (132). Kitsiou et al. showed that stress induced reversible defects are highly predictive of functional recovery after revascularization (133). Therefore, the use of stress and redistribution imaging protocol is preferred. Images are usually interpreted visually, but relative quantitation of regional tracer uptake within the dysfunctional myocardium may provide more objective and accurate results than visual assessment of myocardial viability (134).

3.3.2 ^{99m}Tc-sestamibi and ^{99m}Tc-tetrofosmin

Technetium-99m labeled flow tracers such as ^{99m}Tc-sestamibi and ^{99m}Tc-tetrofosmin are lipophilic and positive charged, and now widely available as alternatives to ^{201}Tl. Compared with ^{201}Tl, these ^{99m}Tc-labeled agents emit higher energy photons yielding better

image quality, and the shorter half-life time of ^{99m}Tc allows the administration of higher dosage. At high flow rates the detection of CAD is underestimated by ^{99m}Tc-labeled flow tracers (135,136). A more important characteristic of these tracers is that, unlike ^{201}Tl, they do not show significant redistribution over time, and there have been controversies regarding the use of ^{99m}Tc-labeled agents as a viability tracer (137). However, experimental studies demonstrated that myocardial retention of both ^{99m}Tc-sestamibi and ^{99m}Tc-tetrofosmin requires cellular viability (138). Uptake and retention of ^{99m}Tc-sestamibi and ^{99m}Tc-tetrofosmin is dependent on cell membrane integrity and mitochondrial function (139). Myocardial ischemia is interfering with mitochondrial K^+-ATP channel activation (140) thereby changing its mitochondrial membrane potential (141), and finally reducing cellular ^{99m}Tc-sestamibi uptake (142). Further, regional ^{99m}Tc-sestamibi (143) or ^{99m}Tc-tetrofosmin (144) activity is closely correlated with ^{201}Tl, indicating viability.
Udelson et al. (145) described the utility of ^{99m}Tc-sestamibi for the prediction of functional recovery after revascularization, which was comparable to that of ^{201}Tl in severe CAD patients. Similar results have been reported for ^{99m}Tc-tetrofosmin, a relative newer ^{99m}Tc-labeled flow tracer, whereas ^{99m}Tc-tetrofosmin uptake also predicted functional recovery as did rest injected ^{201}Tl (146).

3.4.1 Methods to enhance the detection of viability: nitrates

Nitrates improve collateral blood flow to hypoperfused myocardial regions as demonstrated in previous studies using ^{201}Tl imaging (147). Bisi et al (148). proposed that nitrates might have an role in improving the ability of ^{99m}Tc-sestamibi imaging to predict myocardial viability. Several, more recent studies demontrated that the use of nitrates further improves the diagnostic accuracy of viability tests with flow tracers (149,150). Sciagra et al. (151) found that nitrate induced changes in ^{99m}Tc-sestamibi activity are an accurate marker of potentially reversible myocardium for regional (152) and global (153) functional recovery. Furthermore, the prognostic value of nitrate enhanced ^{99m}Tc-sestamibi imaging has been validated by the same authors (154).

3.4.2 Attenuation correction

It is well known that attenuation artifacts may unfavorably affect the diagnostic accuracy of myocardial perfusion SPECT imaging. The non-uniform attenuation of the emitted radiation may produce severe artefacts which may result in fixed defects on SPECT images that could easily be mistaken for myocardial infarction. Common causes of attenuation artefacts are associated with breast attenuation in women, and diaphragmatic attenuation in men.
Attenuation correction using transmission scans may help in distinguishing attenuation artefacts from myocardial infarction patterns, especially in the posterior, posterolateral and posteroseptal wall, where misinterpretation is most common. Hendel et al. performed the first prospective multicenter trial, using a dual-detector camera equipped with a Gadolinium-153 line source (155). In their study the normalcy rate (n=88), was significantly improved (86% vs 96%, respectively), and false positive perfusion images were

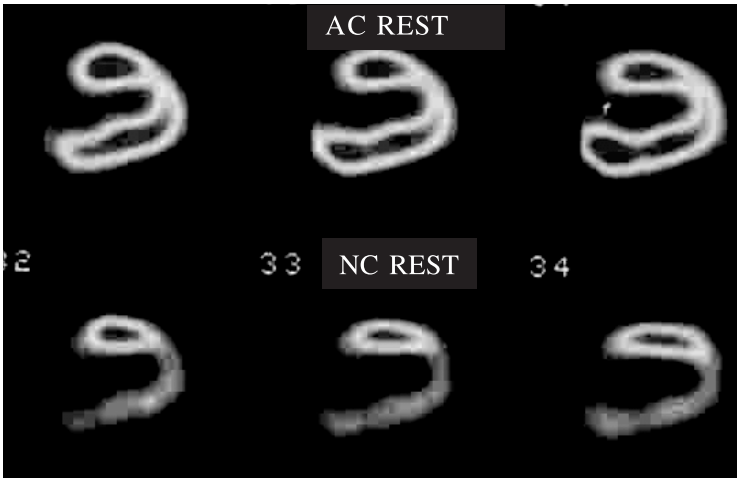

Figure 2: Improvement generated by attenuation correction (AC). Lower row shows myocard perfusion rest vertical long axis slices without correction, showing a marked inferior defect originally judged to be an infarction. Upper row shows corresponding images after AC, now correctly normal.

reduced by more than 4-fold (from 14% to 4%). Several methods for transmission scan based attenuation correction have become available now (156). Commercialized SPECT attenuation correction systems measure the nonhomogeneous attenuation distribution utilizing external collimated radionuclide sources (157) or X-ray CT with hibrid sytems (158). Attenuation correction may considerably change the appearance of images that readers have long been used to (Figure 2). In addition to the variability in methods of attenuation correction, these systems usually also employ different acquisition and reconstruction protocols, and may or may not also incorporate scatter correction algorithms or depth-dependent resolution correction methods.

3.5 Gated SPECT

The widespread application of ^{99m}Tc-labeled myocardial perfusion tracers and data processing capacityhave made ECG-gated SPECT imaging part of the clinical routine in nuclear imaging laboratories (159). The ^{99m}Tc-labeled perfusion tracers, permit assessment of regional myocardial wall motion and wall thickening throughout the cardiac cycle, due to their high count rates and stable myocardial distribution with time. The automatic quantification of LV volumes, ejection fraction (EF), regional myocardial wall motion and thickening from gated SPECT is rapid and accurate, with minimal operator interaction, and is therefore widely used (Figure 3). Gated SPECT is also valuable in its ability to enhance artifact identification by differentiating scarred tissue from attenuation artifacts, because these artifacts reveal normal wall motion and thickening. DePuey and Rozanski demonstrated that false-positive perfusion studies could be reduced from 14% to 3% by incorporating regional wall motion data in the interpretation of perfusion imaging (160). The combination of gating and attuenation correction provide the highest diagnostic accuracy and should be considered complementary (161). Gated SPECT imaging has

also shown to have an important role in the risk assessment of patients with known or suspected CAD (162). Travin et al. demonstrated in a group of 3207 patients that abnormal gated SPECT wall motion score was associated with an annual event rate of 6.1% compared with 1.6% for a normal score, and an abnormal left ventricular ejection fraction was associated with an event rate of 7.4% compared with 1.8% for normal patients (163). Dobutamine stress gated SPECT using ^{99m}Tc-labeled perfusion tracer provides information on both perfusion and contractile reserve in a single study as recently documented by Yoshinaga et al., who compared the accuracy of low-dose dobutamine stress gated myocardial SPECT with the accuracy of dobutamine stress echocardiography in identifying viable myocardium in patients with previous myocardial infarction (164). Because SPECT is more objective and reproducible than echo-cardiography, gated SPECT with pharmacological intervention may become an indispensable diagnostic tool for viability testing.

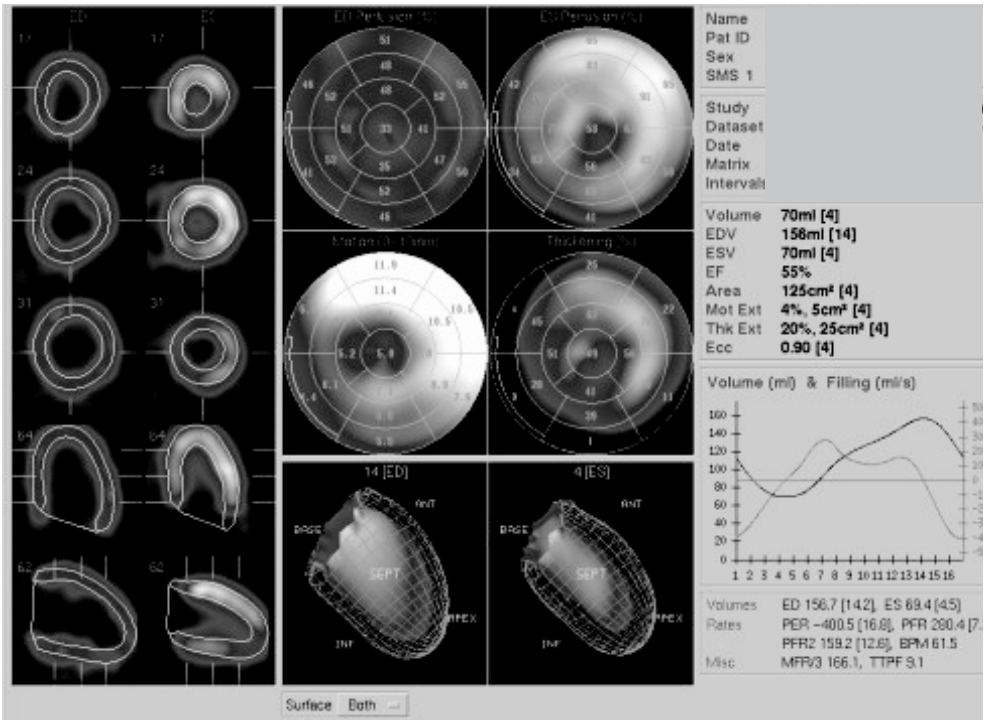

Figure 3: Polarmap display of gated SPECT. Perfusion of the end-diastolic and end-systolic phase is automatical quantified (upper row polarmaps). Wall motion (mm) and wall thickening (%) is also automatical quantified (middle row). The end-diastolic and end-systolic phase of the left ventricle (LV) is displayed in the lower row, showing endocard and epicard contours. End-diastolic, end-systolic and LV ejection fraction is calculated automatically and displayed on the right side. The short and long axes with the detection contours are displayed in the vertical row on the left side on the overview.

3.6 FDG SPECT and DISA SPECT

Substantial effort has been invested in the development of SPECT using extra-high energy collimators, which may permit larger scale clinical use of FDG imaging (165-167). Several clinical studies have shown that FDG SPECT offers diagnostic information similar to PET, and it compares favorably with other imaging modalities, including rest redistribution (168), stress-reinjection ^{201}Tl imaging (169), or low dose dobutamine echocardiography (170). Despite the difference in resolution of both systems FDG SPECT shows a good agreement (94%) with FDG PET (171). As with PET studies, metabolic activity measured by FDG SPECT is generally interpreted in combination with a flow tracer. For this purpose, a dual-isotope simultaneous acquisition (DISA) SPECT protocol with FDG and ^{99m}Tc-perfusion tracer is attractive because it enables assessment of myocardial glucose utilization and perfusion in a single study (Figure 4) (172-174). DISA SPECT shortens the duration of procedure, with the advantage of an identical geometric registration of the different isotope images. Direct comparison of the perfusion tracers ^{99m}Tc-sestamibi/FDG DISA SPECT and ^{13}N-ammonia PET are scarce. Only Matsunari et al. published a small study about the concordance and discordance of ^{99m}Tc-sestamibi/FDG DISA SPECT and ^{13}N-ammonia/FDG PET in 10 patients with CAD, by using the difference between the perfusion tracer and FDG of both techniques (175). They found a good overall concordance between the activity distribution of FDG and flow tracers of both techniques. Different FDG-perfusion patterns can be observed in the left ventricle with contractile dysfunction (Table 3).
ECG-gated FDG SPECT or DISA SPECT is additional technique to assess LV function (176). Thereby DISA SPECT has the potential to assess myocardial glucose utilization, perfusion, and LV function in a single study. Despite these potential advantages, DISA SPECT imaging has not been compared directly with PET imaging for the prediction of LV recovery in patients with LV dysfunction.

3.7 SPECT-CT and PET-CT

The introduction of combination of CT scans into SPECT and PET systems is a recent development. In oncology combined SPECT and CT or PET and CT in a single combined unit become the preferred approach for SPECT and PET approach for imaging. For cardiological purposes CT could be used for attenuation correction, calcium score, functional LV assessment and visualization of coronary arteries and accompanying stenoses. On the other hand, CT attenuation correction is more susceptible to artifacts produced by metallic implants or pacemakers, than pin source-produced attenuation maps. Other potential beneficials of SPECT-CT and PET-CT systems in cardiac imaging are: the scout CT scan can, in a few seconds to check the proper positioning of the patient. A very short scanning time for the CT attenuation map may under-sample the position of the heart and diaphragm, due to cardiac contraction, and respiratory movement. The transmission scan

Table 3: N = normal; ↓ = decreased; ↓ ↓ = severely decreased; ↑ = increased

	contraction	perfusion	FDG uptake	Recovery after revasularization
Normal myocardium	N	N	N	
Repetive stunning	↓	N	N tot ↑	+
Hibernation	↓	↓	N tot ↑	+
Transmural scar	↓	↓ ↓	↓ ↓	–
Non-transmural scar	↓	↓	↓	–/+

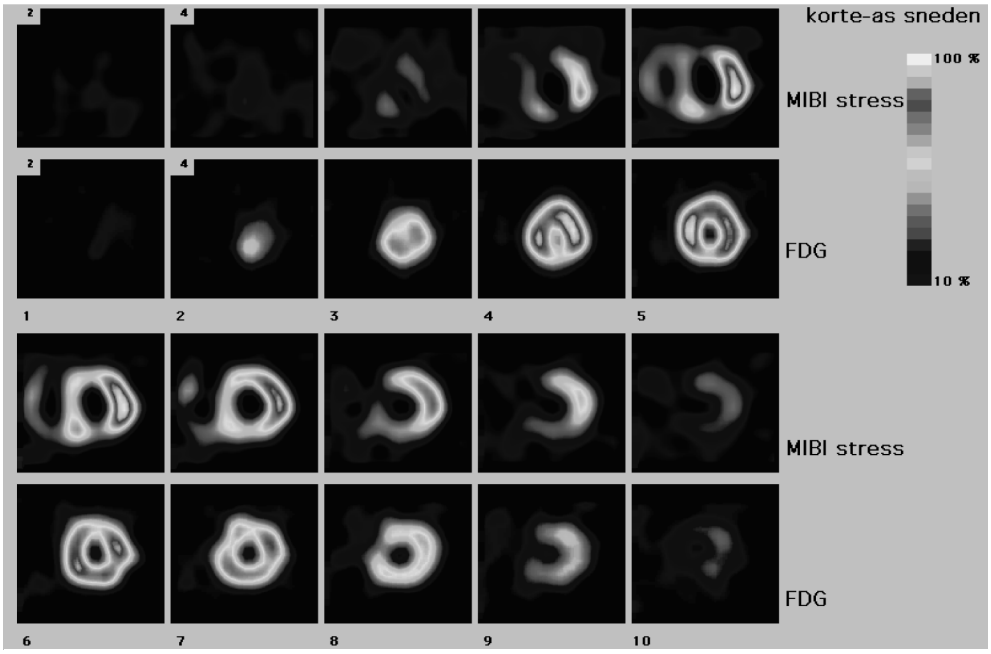

Figure 4: Short-axis view of a dual isotope simultaneous acquisition (DISA) SPECT image. The first row demostrates row is shows a large perfusion defect in the apex, mid-anterior, septal and inferior wall after (dypiridamole) stress ^{99m}Tc-sestamibi. The simultaneous performed FDG study on the second row shows adequate uptake in these regions, indicating ischemia or preserved viability.

needs to be obtained over a sufficient number of respiratory and cardiac cycles, to match the average position of the heart during the emission scan at rest and again during stress.

Another potential application of the single combined unit is the possibility of obtaining coronary calcium scores at the same imaging session as the SPECT or PET scan, which is feasible with an 8- or 16-slice multidetector CT scanner. The clinical value of coronary calcium scoring is at this time still an open question in clinical practice and their interaction and significance needs to be explored (177,178).

An intriguing possibility is the potential value of CT coronary angiography performed

together with PET rest and stress for viability imaging. Multislice (16 slices or greater) CT (MSCT) scans have been found to have sufficient temporal resolution to image, with intravenous contrast, coronary arteries with a diameter or 1.5 mm or greater, with a initial reported sensitivity for 50% or greater coronary lesions of 86% to 92%, a specificity of 93% to 99%, and accuracy of 93% compared with invasive coronary angiography (179). Electron beam CT (EBCT) and MSCT show similarly high levels of accuracy for determining and ruling out significant coronary artery stenoses (180). MSCT is capable of providing good image quality in more coronary segments than EBCT because of its better contrast to noise ratio and higher spatial resolution. Motion artefacts seen at heart rates of > 75 beats/min and a higher radiation exposure are the main limitations of MSCT (181).
There are limitations in visualizing lesions in the smallest distal vessels, and in the presence of heavy calcifications. The latter limitation can be overcome with the aid of the PET or SPECT perfusion results.
It is conceivable that patients with known or suspected disease could be studied with sequential stress-rest perfusion imaging and CT angiography and ventriculography, allowing acquisitions of superimposed images of both coronary anatomy, perfusion, wall motion, and viability. This complete set of spatially mapped information could add precision and ease to decision-making for interventions in multivessel disease intervention planning, or in patients with physiologically abnormal perfusion but anatomically normal coronary arteries. This proposition still needs to be evaluated in clinical studies, because the experience of PET-CT or SPECT-CT is scarce at present.

Outline of the thesis

In the present thesis we evaluated the value of (a) attenuation corrected myocardial perfusion scintigraphy, (b) DISA SPECT and (c) gated FDG PET for the assessment of myocardial viability and LV function in patients with coronary artery disease.

SECTION II evaluates the value of attenuation correction in myocardial perfusion and viability detection. The first aim of this work was to determine, as described in **chapter 2**: (a) the yield of attenuation correction with regard to sensitivity and specificity, and (b) to determine the influence of 1 year 's clinical experience of routinely applied attenuation correction on the interpretation of myocardial perfusion scintigraphy are analyzed. In **chapter 3** the impact of attenuation correction on the assessment of viability with resting ^{99m}Tc-tetrofosmin SPECT is reported. Both non-corrected images and corrected images were compared with the viable segments on FDG SPECT imaging that served as the reference method.
SECTION III evaluates the value of DISA SPECT for the detection of myocardial viability. In **chapter 4**, the first main goal of that study was to analyse the quality of the ^{99m}Tc-sestamibi images of DISA SPECT. Therefore, ^{99m}Tc-sestamibi images of single and dual iso-

tope acquisition were quantitatively and qualitatively compared. The second goal was to investigate whether signs of myocardial viability could be detected with FDG SPECT in irreversible perfusion defects present on previous rest-stress ^{99m}Tc-sestamibi. In **chapter 5,** a head-to-head comparison between ^{99m}Tc-sestamibi/FDG DISA SPECT and ^{13}N-ammonia/FDG PET of normal and dysfunctional LV segments was performed using both visual and quantitative analysis. In **chapter 6**, the diagnostic performance between ^{99m}Tc-sestamibi/FDG DISA SPECT and ^{13}N-ammonia/FDG PET was compared for the prediction of regional function, global LV function and LV remodelling in 47 patients with chronic ischemic LV dysfunction undergoing revascularization. MRI was used to assess LV function before and after revascularization.

Section IV evaluates the value of gated FDG PET for the assessment of LV function and viability. In **chapter 7**, the value of gated FDG PET for the prediction of LV recovery was analyzed, by using MRI as an independent reference method for the assessment of LV function before and after revascularization. In **chapter 8,** the accuracy of gated FDG PET for the assessment of LV function, LV volumes and regional wall motion was evaluated in 38 patients with chronic coronary artery disease and depressed LVEF in comparison with the reference method MRI. **Chapter 9** contains the summary, including future perspectives and conclusions. **Chapter 10** contains the summary, including future perspectives and conclusions in Dutch.

Reference List

1. Di Carli MF, Davidson M, Little R, Khanna S, Mody FV, Brunken RC et al. Value of metabolic imaging with positron emission tomography for evaluating prognosis in patients with coronary artery disease and left ventricular dysfunction. *Am J Cardiol.* 1994; 73(8):527-533.
2. Rahimtoola SH. The hibernating myocardium. *Am Heart J.* 1989; 117(1):211-221.
3. Tillisch J, Brunken R, Marshall R, Schwaiger M, Mandelkern M, Phelps M et al. Reversibility of cardiac wall-motion abnormalities predicted by positron tomography. *N Engl J Med.* 1986; 314(14):884-888.
4. Dilsizian V, Rocco TP, Freedman NM, Leon MB, Bonow RO. Enhanced detection of ischemic but viable myocardium by the reinjection of thallium after stress-redistribution imaging. *N Engl J Med.* 1990; 323(3):141-146.
5. Tamaki N, Kawamoto M, Tadamura E, Magata Y, Yonekura Y, Nohara R et al. Prediction of reversible ischemia after revascularization. Perfusion and metabolic studies with positron emission tomography. *Circulation.* 1995; 91(6):1697-1705.
6. Tillisch J, Brunken R, Marshall R, Schwaiger M, Mandelkern M, Phelps M et al. Reversibility of cardiac wall-motion abnormalities predicted by positron tomography. *N Engl J Med.* 1986; 314(14):884-888.
7. Bonow RO. Identification of viable myocardium. *Circulation.* 1996; 94(11):2674-2680.
8. Emond M, Mock MB, Davis KB, Fisher LD, Holmes D-RJ, Chaitman BR et al. Long-term survival of medically treated patients in the Coronary Artery Surgery Study (CASS) Registry. *Circulation.* 1994; 90(6):2645-2657.
9. Baker DW, Jones R, Hodges J, Massie BM, Konstam MA, Rose EA. Management of heart failure. III. The role of revascularization in the treatment of patients with moderate or severe left ventricular systolic dysfunction. *JAMA.* 1994; 272(19):1528-1534.
10. Bounous EP, Mark DB, Pollock BG, Hlatky MA, Harrell F-EJ, Lee KL et al. Surgical survival benefits for coronary disease patients with left ventricular dysfunction. *Circulation.* 1988; 78(3 Pt 2):I151-I157.
11. Dilsizian V, Rocco TP, Freedman NM, Leon MB, Bonow RO. Enhanced detection of ischemic but viable myocardium by the reinjection of thallium after stress-redistribution imaging. *N Engl J Med.* 1990; 323(3):141-146.
12. Ragosta M, Beller GA, Watson DD, Kaul S, Gimple LW. Quantitative planar rest-redistribution 201Tl imaging in detection of myocardial viability and prediction of improvement in left ventricular function after coronary bypass surgery in patients with severely depressed left ventricular function. *Circulation.* 1993; 87(5):1630-1641.
13. Tamaki N, Yonekura Y, Yamashita K, Saji H, Magata Y, Senda M et al. Positron emission tomography using fluorine-18 deoxyglucose in evaluation of coronary artery bypass grafting. *Am J Cardiol.* 1989; 64(14):860-865.
14. Tillisch J, Brunken R, Marshall R, Schwaiger M, Mandelkern M, Phelps M et al. Reversibility of cardiac wall-motion abnormalities predicted by positron tomography. *N Engl J Med.* 1986; 314(14):884-888.
15. Braunwald E, Kloner RA. The stunned myocardium: prolonged, postischemic ventricular dysfunction. *Circulation.* 1982; 66(6):1146-1149.
16. Kloner RA, Bolli R, Marban E, Reinlib L, Braunwald E. Medical and cellular implications of stunning, hibernation, and preconditioning: an NHLBI workshop. *Circulation.* 1998; 97(18):1848-1867.
17. Braunwald E, Rutherford JD. Reversible ischemic left ventricular dysfunction: evidence for the “hibernating myocardium”. *J Am Coll Cardiol.* 1986; 8(6):1467-1470.
18. Rahimtoola SH. The hibernating myocardium. *Am Heart J.* 1989; 117(1):211-221.

19. Dispersyn GD, Ausma J, Thone F, Flameng W, Vanoverschelde JL, Allessie MA et al. Cardiomyocyte remodelling during myocardial hibernation and atrial fibrillation: prelude to apoptosis. *Cardiovasc Res.* 1999; 43(4):947-957.
20. Wilson JM. Reversible congestive heart failure caused by myocardial hibernation. *Tex Heart Inst J.* 1999; 26(1):19-27.
21. Elsasser A, Schlepper M, Zimmermann R, Muller KD, Strasser R, Klovekorn WP et al. The extracellular matrix in hibernating myocardium--a significant factor causing structural defects and cardiac dysfunction. *Mol Cell Biochem.* 1998; 186(1-2):147-158.
22. Frangogiannis NG. The pathological basis of myocardial hibernation. *Histol Histopathol.* 2003; 18(2):647-655.
23. Vanoverschelde JL, Depre C, Gerber BL, Borgers M, Wijns W, Robert A et al. Time course of functional recovery after coronary artery bypass graft surgery in patients with chronic left ventricular ischemic dysfunction. *Am J Cardiol.* 2000; 85(12):1432-1439.
24. Gottlieb RA, Burleson KO, Kloner RA, Babior BM, Engler RL. Reperfusion injury induces apoptosis in rabbit cardiomyocytes. *J Clin Invest.* 1994; 94(4):1621-1628.
25. Kerr JF, Wyllie AH, Currie AR. Apoptosis: a basic biological phenomenon with wide-ranging implications in tissue kinetics. *Br J Cancer.* 1972; 26(4):239-257.
26. Haunstetter A, Izumo S. Apoptosis: basic mechanisms and implications for cardiovascular disease. *Circ Res.* 1998; 82(11):1111-1129.
27. Di Carli MF, Davidson M, Little R, Khanna S, Mody FV, Brunken RC et al. Value of metabolic imaging with positron emission tomography for evaluating prognosis in patients with coronary artery disease and left ventricular dysfunction. *Am J Cardiol.* 1994; 73(8):527-533.
28. Zimmermann R, Mall G, Rauch B, Zimmer G, Gabel M, Zehelein J et al. Residual 201Tl activity in irreversible defects as a marker of myocardial viability. Clinicopathological study. *Circulation.* 1995; 91(4):1016-1021.
29. Baer FM, Voth E, Schneider CA, Theissen P, Schicha H, Sechtem U. Comparison of low-dose dobutamine-gradient-echo magnetic resonance imaging and positron emission tomography with [18F]fluorodeoxyglucose in patients with chronic coronary artery disease. A functional and morphological approach to the detection of residual myocardial viability. *Circulation.* 1995; 91(4):1006-1015.
30. Baer FM, Voth E, Deutsch HJ, Schneider CA, Horst M, de Vivie ER et al. Predictive value of low dose dobutamine transesophageal echocardiography and fluorine-18 fluorodeoxyglucose positron emission tomography for recovery of regional left ventricular function after successful revascularization. *J Am Coll Cardiol.* 1996; 28(1):60-69.
31. Qureshi U, Nagueh SF, Afridi I, Vaduganathan P, Blaustein A, Verani MS et al. Dobutamine echocardiography and quantitative rest-redistribution 201Tl tomography in myocardial hibernation. Relation of contractile reserve to 201Tl uptake and comparative prediction of recovery of function. *Circulation.* 1997; 95(3):626-635.
32. Leoncini M, Sciagra R, Maioli M, Bellandi F, Marcucci G, Sestini S et al. Usefulness of dobutamine Tc-99m sestamibi-gated single-photon emission computed tomography for prediction of left ventricular ejection fraction outcome after coronary revascularization for ischemic cardiomyopathy. *Am J Cardiol.* 2002; 89(7):817-821.
33. Tamaki N, Kawamoto M, Tadamura E, Magata Y, Yonekura Y, Nohara R et al. Prediction of reversible ischemia after revascularization. Perfusion and metabolic studies with positron emission tomography. *Circulation.* 1995; 91(6):1697-1705.
34. Tillisch J, Brunken R, Marshall R, Schwaiger M, Mandelkern M, Phelps M et al. Reversibility of cardiac wall-motion abnormalities predicted by positron tomography. *N Engl J Med.* 1986; 314(14):884-888.
35. Udelson JE, Coleman PS, Metherall J, Pandian NG, Gomez AR, Griffith JL et al. Predicting

recovery of severe regional ventricular dysfunction. Comparison of resting scintigraphy with 201Tl and 99mTc-sestamibi. *Circulation.* 1994; 89(6):2552-2561.
36. vom-Dahl J, Eitzman DT, al Aouar ZR, Kanter HL, Hicks RJ, Deeb GM et al. Relation of regional function, perfusion, and metabolism in patients with advanced coronary artery disease undergoing surgical revascularization. *Circulation.* 1994; 90(5):2356-2366.
37. Bax JJ, Poldermans D, Elhendy A, Cornel JH, Boersma E, Rambaldi R et al. Improvement of left ventricular ejection fraction, heart failure symptoms and prognosis after revascularization in patients with chronic coronary artery disease and viable myocardium detected by dobutamine stress echocardiography. *J Am Coll Cardiol.* 1999; 34(1):163-169.
38. Di Carli MF, Asgarzadie F, Schelbert HR, Brunken RC, Laks H, Phelps ME et al. Quantitative relation between myocardial viability and improvement in heart failure symptoms after revascularization in patients with ischemic cardiomyopathy. *Circulation.* 1995; 92(12):3436-3444.
39. Bax JJ, Poldermans D, Elhendy A, Cornel JH, Boersma E, Rambaldi R et al. Improvement of left ventricular ejection fraction, heart failure symptoms and prognosis after revascularization in patients with chronic coronary artery disease and viable myocardium detected by dobutamine stress echocardiography. *J Am Coll Cardiol.* 1999; 34(1):163-169.
40. Di Carli MF, Davidson M, Little R, Khanna S, Mody FV, Brunken RC et al. Value of metabolic imaging with positron emission tomography for evaluating prognosis in patients with coronary artery disease and left ventricular dysfunction. *Am J Cardiol.* 1994; 73(8):527-533.
41. Di Carli MF, Davidson M, Little R, Khanna S, Mody FV, Brunken RC et al. Value of metabolic imaging with positron emission tomography for evaluating prognosis in patients with coronary artery disease and left ventricular dysfunction. *Am J Cardiol.* 1994; 73(8):527-533.
42. Thimister PW, Hofstra L, Liem IH, Boersma HH, Kemerink G, Reutelingsperger CP et al. In vivo detection of cell death in the area at risk in acute myocardial infarction. *J Nucl Med.* 2003; 44(3):391-396.
43. Maes A, Flameng W, Nuyts J, Borgers M, Shivalkar B, Ausma J et al. Histological alterations in chronically hypoperfused myocardium. Correlation with PET findings. *Circulation.* 1994; 90(2):735-745.
44. Bax JJ, Poldermans D, Elhendy A, Cornel JH, Boersma E, Rambaldi R et al. Improvement of left ventricular ejection fraction, heart failure symptoms and prognosis after revascularization in patients with chronic coronary artery disease and viable myocardium detected by dobutamine stress echocardiography. *J Am Coll Cardiol.* 1999; 34(1):163-169.
45. Tillisch J, Brunken R, Marshall R, Schwaiger M, Mandelkern M, Phelps M et al. Reversibility of cardiac wall-motion abnormalities predicted by positron tomography. *N Engl J Med.* 1986; 314(14):884-888.
46. Baer FM, Voth E, Schneider CA, Theissen P, Schicha H, Sechtem U. Comparison of low-dose dobutamine-gradient-echo magnetic resonance imaging and positron emission tomography with [18F]fluorodeoxyglucose in patients with chronic coronary artery disease. A functional and morphological approach to the detection of residual myocardial viability. *Circulation.* 1995; 91(4):1006-1015.
47. Knuuti MJ, Saraste M, Nuutila P, Harkonen R, Wegelius U, Haapanen A et al. Myocardial viability: fluorine-18-deoxyglucose positron emission tomography in prediction of wall motion recovery after revascularization. *Am Heart J.* 1994; 127(4 Pt 1):785-796.
48. Lucignani G, Paolini G, Landoni C, Zuccari M, Paganelli G, Galli L et al. Presurgical identification of hibernating myocardium by combined use of technetium-99m hexakis 2-methoxy-isobutylisonitrile single photon emission tomography and fluorine-18 fluoro-2-deoxy-D-glucose positron emission tomography in patients with coronary artery disease. *Eur J Nucl Med.* 1992; 19(10):874-881.
49. Maes AF, Borgers M, Flameng W, Nuyts JL, van de Werf F, Ausma JJ et al. Assessment of

myocardial viability in chronic coronary artery disease using technetium-99m sestamibi SPECT. Correlation with histologic and positron emission tomographic studies and functional follow-up. *J Am Coll Cardiol.* 1997; 29(1):62-68.
50. Schoder H, Campisi R, Ohtake T, Hoh CK, Moon DH, Czernin J et al. Blood flow-metabolism imaging with positron emission tomography in patients with diabetes mellitus for the assessment of reversible left ventricular contractile dysfunction. *J Am Coll Cardiol.* 1999; 33(5):1328-1337.
51. Tamaki N, Kawamoto M, Tadamura E, Magata Y, Yonekura Y, Nohara R et al. Prediction of reversible ischemia after revascularization. Perfusion and metabolic studies with positron emission tomography. *Circulation.* 1995; 91(6):1697-1705.
52. Tamaki N, Kawamoto M, Tadamura E, Magata Y, Yonekura Y, Nohara R et al. Prediction of reversible ischemia after revascularization. Perfusion and metabolic studies with positron emission tomography. *Circulation.* 1995; 91(6):1697-1705.
53. vom-Dahl J, Eitzman DT, al Aouar ZR, Kanter HL, Hicks RJ, Deeb GM et al. Relation of regional function, perfusion, and metabolism in patients with advanced coronary artery disease undergoing surgical revascularization. *Circulation.* 1994; 90(5):2356-2366.
54. Opie LH. Metabolism of the heart in health and disease. I. *Am Heart J.* 1968; 76(5):685-698.
55. Opie LH. Metabolism of the heart in health and disease. II. *Am Heart J.* 1969; 77(1):100-122.
56. Opie LH. Metabolism of the heart in health and disease. 3. *Am Heart J.* 1969; 77(3):383-410.
57. Camici P, Ferrannini E, Opie LH. Myocardial metabolism in ischemic heart disease: basic principles and application to imaging by positron emission tomography. *Prog Cardiovasc Dis.* 1989; 32(3):217-238.
58. King LM, Opie LH. Glucose delivery is a major determinant of glucose utilisation in the ischemic myocardium with a residual coronary flow. *Cardiovasc Res.* 1998; 39(2):381-392.
59. Opie LH. Effects of regional ischemia on metabolism of glucose and fatty acids. Relative rates of aerobic and anaerobic energy production during myocardial infarction and comparison with effects of anoxia. *Circ Res.* 1976; 38(5 Suppl 1):I52-I74.
60. Knuuti MJ, Yki-Jarvinen H, Voipio-Pulkki LM, Maki M, Ruotsalainen U, Harkonen R et al. Enhancement of myocardial [fluorine-18]fluorodeoxyglucose uptake by a nicotinic acid derivative. *J Nucl Med.* 1994; 35(6):989-998.
61. Bax JJ, Veening MA, Visser FC, Van Lingen A, Heine RJ, Cornel JH et al. Optimal metabolic conditions during fluorine-18 fluorodeoxyglucose imaging; a comparative study using different protocols. *Eur J Nucl Med.* 1997; 24(1):35-41.
62. Di Carli MF, Davidson M, Little R, Khanna S, Mody FV, Brunken RC et al. Value of metabolic imaging with positron emission tomography for evaluating prognosis in patients with coronary artery disease and left ventricular dysfunction. *Am J Cardiol.* 1994; 73(8):527-533.
63. Haas F, Haehnel CJ, Picker W, Nekolla S, Martinoff S, Meisner H et al. Preoperative positron emission tomographic viability assessment and perioperative and postoperative risk in patients with advanced ischemic heart disease. *J Am Coll Cardiol.* 1997; 30(7):1693-1700.
64. Tamaki N, Yonekura Y, Yamashita K, Saji H, Magata Y, Senda M et al. Positron emission tomography using fluorine-18 deoxyglucose in evaluation of coronary artery bypass grafting. *Am J Cardiol.* 1989; 64(14):860-865.
65. Tamaki N, Kawamoto M, Takahashi N, Yonekura Y, Magata Y, Nohara R et al. Prognostic value of an increase in fluorine-18 deoxyglucose uptake in patients with myocardial infarction: comparison with stress thallium imaging. *J Am Coll Cardiol.* 1993; 22(6):1621-1627.
66. Tillisch J, Brunken R, Marshall R, Schwaiger M, Mandelkern M, Phelps M et al. Reversibility of cardiac wall-motion abnormalities predicted by positron tomography. *N Engl J Med.* 1986; 314(14):884-888.
67. Udelson JE, Coleman PS, Metherall J, Pandian NG, Gomez AR, Griffith JL et al. Predicting

recovery of severe regional ventricular dysfunction. Comparison of resting scintigraphy with 201Tl and 99mTc-sestamibi. *Circulation.* 1994; 89(6):2552-2561.
68. vom-Dahl J, Eitzman DT, al Aouar ZR, Kanter HL, Hicks RJ, Deeb GM et al. Relation of regional function, perfusion, and metabolism in patients with advanced coronary artery disease undergoing surgical revascularization. *Circulation.* 1994; 90(5):2356-2366.
69. vom-Dahl J, Eitzman DT, al Aouar ZR, Kanter HL, Hicks RJ, Deeb GM et al. Relation of regional function, perfusion, and metabolism in patients with advanced coronary artery disease undergoing surgical revascularization. *Circulation.* 1994; 90(5):2356-2366.
70. Knuuti MJ, Nuutila P, Ruotsalainen U, Teras M, Saraste M, Harkonen R et al. The value of quantitative analysis of glucose utilization in detection of myocardial viability by PET. *J Nucl Med.* 1993; 34(12):2068-2075.
71. Bergmann SR. Cardiac positron emission tomography. *Semin Nucl Med.* 1998; 28(4):320-340.
72. Camici P, Ferrannini E, Opie LH. Myocardial metabolism in ischemic heart disease: basic principles and application to imaging by positron emission tomography. *Prog Cardiovasc Dis.* 1989; 32(3):217-238.
73. Rosamond TL, Abendschein DR, Sobel BE, Bergmann SR, Fox KA. Metabolic fate of radiolabeled palmitate in ischemic canine myocardium: implications for positron emission tomography. *J Nucl Med.* 1987; 28(8):1322-1329.
74. Hutchins GD, Schwaiger M, Rosenspire KC, Krivokapich J, Schelbert H, Kuhl DE. Noninvasive quantification of regional blood flow in the human heart using N-13 ammonia and dynamic positron emission tomographic imaging. *J Am Coll Cardiol.* 1990; 15(5):1032-1042.
75. Iida H, Kanno I, Takahashi A, Miura S, Murakami M, Takahashi K et al. Measurement of absolute myocardial blood flow with H215O and dynamic positron-emission tomography. Strategy for quantification in relation to the partial-volume effect. *Circulation.* 1988; 78(1):104-115.
76. Baer FM, Voth E, Deutsch HJ, Schneider CA, Horst M, de Vivie ER et al. Predictive value of low dose dobutamine transesophageal echocardiography and fluorine-18 fluorodeoxyglucose positron emission tomography for recovery of regional left ventricular function after successful revascularization. *J Am Coll Cardiol.* 1996; 28(1):60-69.
77. Bax JJ, Visser FC, Poldermans D, Elhendy A, Cornel JH, Boersma E et al. Time course of functional recovery of stunned and hibernating segments after surgical revascularization. *Circulation.* 2001; 104(12 Suppl 1):I314-I318.
78. Haas F, Augustin N, Holper K, Wottke M, Haehnel C, Nekolla S et al. Time course and extent of improvement of dysfunctioning myocardium in patients with coronary artery disease and severely depressed left ventricular function after revascularization: correlation with positron emission tomographic findings. *J Am Coll Cardiol.* 2000; 36(6):1927-1934.
79. Haas F, Jennen L, Heinzmann U, Augustin N, Wottke M, Schwaiger M et al. Ischemically compromised myocardium displays different time-courses of functional recovery: correlation with morphological alterations? *Eur J Cardiothorac Surg.* 2001; 20(2):290-298.
80. Bax JJ, Visser FC, Poldermans D, Elhendy A, Cornel JH, Boersma E et al. Time course of functional recovery of stunned and hibernating segments after surgical revascularization. *Circulation.* 2001; 104(12 Suppl 1):I314-I318.
81. Bax JJ, Visser FC, Poldermans D, Elhendy A, Cornel JH, Boersma E et al. Time course of functional recovery of stunned and hibernating segments after surgical revascularization. *Circulation.* 2001; 104(12 Suppl 1):I314-I318.
82. Schelbert HR, Phelps ME, Huang SC, MacDonald NS, Hansen H, Selin C et al. N-13 ammonia as an indicator of myocardial blood flow. *Circulation.* 1981; 63(6):1259-1272.
83. Hutchins GD, Schwaiger M, Rosenspire KC, Krivokapich J, Schelbert H, Kuhl DE. Noninvasive quantification of regional blood flow in the human heart using N-13 ammonia and dynamic positron emission tomographic imaging. *J Am Coll Cardiol.* 1990; 15(5):1032-1042.

84. Schelbert HR, Phelps ME, Huang SC, MacDonald NS, Hansen H, Selin C et al. N-13 ammonia as an indicator of myocardial blood flow. *Circulation.* 1981; 63(6):1259-1272.
85. Hutchins GD, Schwaiger M, Rosenspire KC, Krivokapich J, Schelbert H, Kuhl DE. Noninvasive quantification of regional blood flow in the human heart using N-13 ammonia and dynamic positron emission tomographic imaging. *J Am Coll Cardiol.* 1990; 15(5):1032-1042.
86. Sawada S, Muzik O, Beanlands RS, Wolfe E, Hutchins GD, Schwaiger M. Interobserver and interstudy variability of myocardial blood flow and flow-reserve measurements with nitrogen 13 ammonia-labeled positron emission tomography. *J Nucl Cardiol.* 1995; 2(5):413-422.
87. Endo M, Yoshida K, Iinuma TA, Yamasaki T, Tateno Y, Masuda Y et al. Noninvasive quantification of regional myocardial blood flow and ammonia extraction fraction using nitrogen-13 ammonia and positron emission tomography. *Ann Nucl Med.* 1987; 1(1):1-6.
88. Hutchins GD, Schwaiger M, Rosenspire KC, Krivokapich J, Schelbert H, Kuhl DE. Noninvasive quantification of regional blood flow in the human heart using N-13 ammonia and dynamic positron emission tomographic imaging. *J Am Coll Cardiol.* 1990; 15(5):1032-1042.
89. Krivokapich J, Smith GT, Huang SC, Hoffman EJ, Ratib O, Phelps ME et al. 13N ammonia myocardial imaging at rest and with exercise in normal volunteers. Quantification of absolute myocardial perfusion with dynamic positron emission tomography. *Circulation.* 1989; 80(5):1328-1337.
90. Krivokapich J, Stevenson LW, Kobashigawa J, Huang SC, Schelbert HR. Quantification of absolute myocardial perfusion at rest and during exercise with positron emission tomography after human cardiac transplantation. *J Am Coll Cardiol.* 1991; 18(2):512-517.
91. Muzik O, Beanlands RS, Hutchins GD, Mangner TJ, Nguyen N, Schwaiger M. Validation of nitrogen-13-ammonia tracer kinetic model for quantification of myocardial blood flow using PET. *J Nucl Med.* 1993; 34(1):83-91.
92. Nagamachi S, Czernin J, Kim AS, Sun KT, Bottcher M, Phelps ME et al. Reproducibility of measurements of regional resting and hyperemic myocardial blood flow assessed with PET. *J Nucl Med.* 1996; 37(10):1626-1631.
93. Kitsiou AN, Bacharach SL, Bartlett ML, Srinivasan G, Summers RM, Quyyumi AA et al. 13N-ammonia myocardial blood flow and uptake: relation to functional outcome of asynergic regions after revascularization. *J Am Coll Cardiol.* 1999; 33(3):678-686.
94. Huang SC, Schwaiger M, Carson RE, Carson J, Hansen H, Selin C et al. Quantitative measurement of myocardial blood flow with oxygen-15 water and positron computed tomography: an assessment of potential and problems. *J Nucl Med.* 1985; 26(6):616-625.
95. Iida H, Kanno I, Takahashi A, Miura S, Murakami M, Takahashi K et al. Measurement of absolute myocardial blood flow with H215O and dynamic positron-emission tomography. Strategy for quantification in relation to the partial-volume effect. *Circulation.* 1988; 78(1):104-115.
96. Nitzsche EU, Choi Y, Czernin J, Hoh CK, Huang SC, Schelbert HR. Noninvasive quantification of myocardial blood flow in humans. A direct comparison of the [13N]ammonia and the [15O]water techniques. *Circulation.* 1996; 93(11):2000-2006.
97. De Silva R, Yamamoto Y, Rhodes CG, Iida H, Nihoyannopoulos P, Davies GJ et al. Preoperative prediction of the outcome of coronary revascularization using positron emission tomography. *Circulation.* 1992; 86(6):1738-1742.
98. Yamamoto Y, De Silva R, Rhodes CG, Araujo LI, Iida H, Rechavia E et al. A new strategy for the assessment of viable myocardium and regional myocardial blood flow using 15O-water and dynamic positron emission tomography. *Circulation.* 1992; 86(1):167-178.
99. Becker L, Ferreira R, Thomas M. Comparison of 86Rb and microsphere estimates of left ventricular bloodflow distribution. *J Nucl Med.* 1974; 15(11):969-973.
100. Goldstein RA, Mullani NA, Marani SK, Fisher DJ, Gould KL, O'Brien H-AJ. Myocardial perfu-

sion with rubidium-82. II. Effects of metabolic and pharmacologic interventions. *J Nucl Med.* 1983; 24(10):907-915.
101. Gould KL. Identifying and measuring severity of coronary artery stenosis. Quantitative coronary arteriography and positron emission tomography. *Circulation.* 1988; 78(2):237-245.
102. Grover-McKay M, Ratib O, Schwaiger M, Wohlgelernter D, Araujo L, Nienaber C et al. Detection of coronary artery disease with positron emission tomography and rubidium 82. *Am Heart J.* 1992; 123(3):646-652.
103. Boyd HL, Gunn RN, Marinho NV, Karwatowski SP, Bailey DL, Costa DC et al. Non-invasive measurement of left ventricular volumes and function by gated positron emission tomography. *Eur J Nucl Med.* 1996; 23(12):1594-1602.
104. Hoffman EJ, Phelps ME, Wisenberg G, Schelbert HR, Kuhl DE. Electrocardiographic gating in positron emission computed tomography. *J Comput Assist Tomogr.* 1979; 3(6):733-739.
105. Hattori N, Bengel FM, Mehilli J, Odaka K, Ishii K, Schwaiger M et al. Global and regional functional measurements with gated FDG PET in comparison with left ventriculography. *Eur J Nucl Med.* 2001; 28(2):221-229.
106. Hoffmeister HM, Helber U, Franow A, Feine U, Bares R, Seipel L et al. ECG-gated 18F-FDG positron emission tomography. *Int J Cardiovasc Imaging.* 2002; 18(5):363-372.
107. Hor G, Kranert WT, Maul FD, Schroder O, Karimian-Tatriz A, Geb O et al. Gated metabolic positron emission tomography (GAPET) of the myocardium: 18F-FDG-PET to optimize recognition of myocardial hibernation. *Nucl Med Commun.* 1998; 19(6):535-545.
108. Khorsand A, Graf S, Frank H, Kletter K, Sochor H, Maurer G et al. Model-based analysis of electrocardiography-gated cardiac (18)F-FDG PET images to assess left ventricular geometry and contractile function. *J Nucl Med.* 2003; 44(11):1741-1746.
109. Schaefer WM, Lipke CS, Nowak B, Kaiser HJ, Buecker A, Krombach GA et al. Validation of an evaluation routine for left ventricular volumes, ejection fraction and wall motion from gated cardiac FDG PET: a comparison with cardiac magnetic resonance imaging. *Eur J Nucl Med Mol Imaging.* 2003; 30(4):545-553.
110. Schaefer WM, Lipke CS, Nowak B, Kaiser HJ, Reinartz P, Buecker A et al. Validation of QGS and 4D-MSPECT for quantification of left ventricular volumes and ejection fraction from gated 18F-FDG PET: comparison with cardiac MRI. *J Nucl Med.* 2004; 45(1):74-79.
111. Boyd HL, Gunn RN, Marinho NV, Karwatowski SP, Bailey DL, Costa DC et al. Non-invasive measurement of left ventricular volumes and function by gated positron emission tomography. *Eur J Nucl Med.* 1996; 23(12):1594-1602.
112. Rajappan K, Livieratos L, Camici PG, Pennell DJ. Measurement of ventricular volumes and function: a comparison of gated PET and cardiovascular magnetic resonance. *J Nucl Med.* 2002; 43(6):806-810.
113. Yamashita K, Tamaki N, Yonekura Y, Ohtani H, Saji H, Mukai T et al. Quantitative analysis of regional wall motion by gated myocardial positron emission tomography: validation and comparison with left ventriculography. *J Nucl Med.* 1989; 30(11):1775-1786.
114. Kapur A, Latus KA, Davies G, Dhawan RT, Eastick S, Jarritt PH et al. A comparison of three radionuclide myocardial perfusion tracers in clinical practice: the ROBUST study. *Eur J Nucl Med Mol Imaging.* 2002; 29(12):1608-1616.
115. Mahmarian JJ, Boyce TM, Goldberg RK, Cocanougher MK, Roberts R, Verani MS. Quantitative exercise thallium-201 single photon emission computed tomography for the enhanced diagnosis of ischemic heart disease. *J Am Coll Cardiol.* 1990; 15(2):318-329.
116. Van Train KF, Garcia EV, Maddahi J, Areeda J, Cooke CD, Kiat H et al. Multicenter trial validation for quantitative analysis of same-day rest-stress technetium-99m-sestamibi myocardial tomograms. *J Nucl Med.* 1994; 35(4):609-618.
117. Kapur A, Latus KA, Davies G, Dhawan RT, Eastick S, Jarritt PH et al. A comparison of three

radionuclide myocardial perfusion tracers in clinical practice: the ROBUST study. *Eur J Nucl Med Mol Imaging.* 2002; 29(12):1608-1616.
118. Brown KA. Prognostic value of thallium-201 myocardial perfusion imaging. A diagnostic tool comes of age. *Circulation.* 1991; 83(2):363-381.
119. Brown KA. Prognostic value of cardiac imaging in patients with known or suspected coronary artery disease: comparison of myocardial perfusion imaging, stress echocardiography, and position emission tomography. *Am J Cardiol.* 1995; 75(11):35D-41D.
120. Brown KA. Prognostic value of myocardial perfusion imaging: state of the art and new developments. *J Nucl Cardiol.* 1996; 3(6 Pt 1):516-537.
121. Ladenheim ML, Pollock BH, Rozanski A, Berman DS, Staniloff HM, Forrester JS et al. Extent and severity of myocardial hypoperfusion as predictors of prognosis in patients with suspected coronary artery disease. *J Am Coll Cardiol.* 1986; 7(3):464-471.
122. Gill JB, Ruddy TD, Newell JB, Finkelstein DM, Strauss HW, Boucher CA. Prognostic importance of thallium uptake by the lungs during exercise in coronary artery disease. *N Engl J Med.* 1987; 317(24):1486-1489.
123. Weiss AT, Berman DS, Lew AS, Nielsen J, Potkin B, Swan HJ et al. Transient ischemic dilation of the left ventricle on stress thallium-201 scintigraphy: a marker of severe and extensive coronary artery disease. *J Am Coll Cardiol.* 1987; 9(4):752-759.
124. Iskandrian AS, Chae SC, Heo J, Stanberry CD, Wasserleben V, Cave V. Independent and incremental prognostic value of exercise single-photon emission computed tomographic (SPECT) thallium imaging in coronary artery disease. *J Am Coll Cardiol.* 1993; 22(3):665-670.
125. Shaw LJ, Hendel R, Borges-Neto S, Lauer MS, Alazraki N, Burnette J et al. Prognostic value of normal exercise and adenosine (99m)Tc-tetrofosmin SPECT imaging: results from the multicenter registry of 4,728 patients. *J Nucl Med.* 2003; 44(2):134-139.
126. Maes AF, Borgers M, Flameng W, Nuyts JL, van de Werf F, Ausma JJ et al. Assessment of myocardial viability in chronic coronary artery disease using technetium-99m sestamibi SPECT. Correlation with histologic and positron emission tomographic studies and functional follow-up. *J Am Coll Cardiol.* 1997; 29(1):62-68.
127. Matsunari I, Boning G, Ziegler SI, Nekolla SG, Stollfuss JC, Kosa I et al. Attenuation-corrected 99mTc-tetrofosmin single-photon emission computed tomography in the detection of viable myocardium: comparison with positron emission tomography using 18F-fluorodeoxyglucose. *J Am Coll Cardiol.* 1998; 32(4):927-935.
128. Leppo JA. Myocardial uptake of thallium and rubidium during alterations in perfusion and oxygenation in isolated rabbit hearts. *J Nucl Med.* 1987; 28(5):878-885.
129. Brunken RC, Mody FV, Hawkins RA, Nienaber C, Phelps ME, Schelbert HR. Positron emission tomography detects metabolic viability in myocardium with persistent 24-hour single-photon emission computed tomography 201Tl defects. *Circulation.* 1992; 86(5):1357-1369.
130. Bonow RO, Dilsizian V, Cuocolo A, Bacharach SL. Identification of viable myocardium in patients with chronic coronary artery disease and left ventricular dysfunction. Comparison of thallium scintigraphy with reinjection and PET imaging with 18F-fluorodeoxyglucose. *Circulation.* 1991; 83(1):26-37.
131. Dilsizian V, Rocco TP, Freedman NM, Leon MB, Bonow RO. Enhanced detection of ischemic but viable myocardium by the reinjection of thallium after stress-redistribution imaging. *N Engl J Med.* 1990; 323(3):141-146.
132. Bonow RO, Dilsizian V, Cuocolo A, Bacharach SL. Identification of viable myocardium in patients with chronic coronary artery disease and left ventricular dysfunction. Comparison of thallium scintigraphy with reinjection and PET imaging with 18F-fluorodeoxyglucose. *Circulation.* 1991; 83(1):26-37.

133. Kitsiou AN, Srinivasan G, Quyyumi AA, Summers RM, Bacharach SL, Dilsizian V. Stress-induced reversible and mild-to-moderate irreversible thallium defects: are they equally accurate for predicting recovery of regional left ventricular function after revascularization? *Circulation.* 1998; 98(6):501-508.
134. Qureshi U, Nagueh SF, Afridi I, Vaduganathan P, Blaustein A, Verani MS et al. Dobutamine echocardiography and quantitative rest-redistribution 201Tl tomography in myocardial hibernation. Relation of contractile reserve to 201Tl uptake and comparative prediction of recovery of function. *Circulation.* 1997; 95(3):626-635.
135. Glover DK, Ruiz M, Edwards NC, Cunningham M, Simanis JP, Smith WH et al. Comparison between 201Tl and 99mTc sestamibi uptake during adenosine-induced vasodilation as a function of coronary stenosis severity. *Circulation.* 1995; 91(3):813-820.
136. Glover DK, Ruiz M, Koplan BA, Watson DD, Beller GA. 99mTc-tetrofosmin assessment of myocardial perfusion and viability in canine models of coronary occlusion and reperfusion. *J Nucl Med.* 1999; 40(1):142-149.
137. Marzullo P, Parodi O, Reisenhofer B, Sambuceti G, Picano E, Distante A et al. Value of rest thallium-201/technetium-99m sestamibi scans and dobutamine echocardiography for detecting myocardial viability. *Am J Cardiol.* 1993; 71(2):166-172.
138. Takahashi N, Reinhardt CP, Marcel R, Leppo JA. Myocardial uptake of 99mTc-tetrofosmin, sestamibi, and 201Tl in a model of acute coronary reperfusion. *Circulation.* 1996; 94(10):2605-2613.
139. Travin MI, Bergmann SR. Assessment of myocardial viability. *Semin Nucl Med.* 2005; 35(1):2-16.
140. Cohen MV, Baines CP, Downey JM. Ischemic preconditioning: from adenosine receptor of KATP channel. *Annu Rev Physiol.* 2000; 62:79-109.
141. Holmuhamedov EL, Jovanovic S, Dzeja PP, Jovanovic A, Terzic A. Mitochondrial ATP-sensitive K+ channels modulate cardiac mitochondrial function. *Am J Physiol.* 1998; 275(5 Pt 2):H1567-H1576.
142. Crane P, Laliberte R, Heminway S, Thoolen M, Orlandi C. Effect of mitochondrial viability and metabolism on technetium-99m-sestamibi myocardial retention. *Eur J Nucl Med.* 1993; 20(1):20-25.
143. Udelson JE, Coleman PS, Metherall J, Pandian NG, Gomez AR, Griffith JL et al. Predicting recovery of severe regional ventricular dysfunction. Comparison of resting scintigraphy with 201Tl and 99mTc-sestamibi. *Circulation.* 1994; 89(6):2552-2561.
144. Matsunari I, Fujino S, Taki J, Senma J, Aoyama T, Wakasugi T et al. Quantitative rest technetium-99m tetrofosmin imaging in predicting functional recovery after revascularization: comparison with rest-redistribution thallium-201. *J Am Coll Cardiol.* 1997; 29(6):1226-1233.
145. Udelson JE, Coleman PS, Metherall J, Pandian NG, Gomez AR, Griffith JL et al. Predicting recovery of severe regional ventricular dysfunction. Comparison of resting scintigraphy with 201Tl and 99mTc-sestamibi. *Circulation.* 1994; 89(6):2552-2561.
146. Matsunari I, Fujino S, Taki J, Senma J, Aoyama T, Wakasugi T et al. Quantitative rest technetium-99m tetrofosmin imaging in predicting functional recovery after revascularization: comparison with rest-redistribution thallium-201. *J Am Coll Cardiol.* 1997; 29(6):1226-1233.
147. He ZX, Medrano R, Hays JT, Mahmarian JJ, Verani MS. Nitroglycerin-augmented 201T1 reinjection enhances detection of reversible myocardial hypoperfusion. A randomized, double-blind, parallel, placebo-controlled trial. *Circulation.* 1997; 95(7):1799-1805.
148. Bisi G, Sciagra R, Santoro GM, Fazzini PF. Rest technetium-99m sestamibi tomography in combination with short-term administration of nitrates: feasibility and reliability for prediction of postrevascularization outcome of asynergic territories. *J Am Coll Cardiol.* 1994; 24(5):1282-1289.
149. He ZX, Medrano R, Hays JT, Mahmarian JJ, Verani MS. Nitroglycerin-augmented 201T1 rein-

jection enhances detection of reversible myocardial hypoperfusion. A randomized, double-blind, parallel, placebo-controlled trial. *Circulation.* 1997; 95(7):1799-1805.
150. Sciagra R, Bisi G, Santoro GM, Agnolucci M, Zoccarato O, Fazzini PF. Influence of the assessment of defect severity and intravenous nitrate administration during tracer injection on the detection of viable hibernating myocardium with data-based quantitative technetium 99m-labeled sestamibi single-photon emission computed tomography. *J Nucl Cardiol.* 1996; 3(3):221-230.
151. Sciagra R, Bisi G, Santoro GM, Zerauschek F, Sestini S, Pedenovi P et al. Comparison of baseline-nitrate technetium-99m sestamibi with rest-redistribution thallium-201 tomography in detecting viable hibernating myocardium and predicting postrevascularization recovery. *J Am Coll Cardiol.* 1997; 30(2):384-391.
152. Sciagra R, Bisi G, Santoro GM, Zerauschek F, Sestini S, Pedenovi P et al. Comparison of baseline-nitrate technetium-99m sestamibi with rest-redistribution thallium-201 tomography in detecting viable hibernating myocardium and predicting postrevascularization recovery. *J Am Coll Cardiol.* 1997; 30(2):384-391.
153. Sciagra R, Leoncini M, Marcucci G, Dabizzi RP, Pupi A. Technetium-99m sestamibi imaging to predict left ventricular ejection fraction outcome after revascularisation in patients with chronic coronary artery disease and left ventricular dysfunction: comparison between baseline and nitrate-enhanced imaging. *Eur J Nucl Med.* 2001; 28(6):680-687.
154. Sciagra R, Pellegri M, Pupi A, Bolognese L, Bisi G, Carnovale V et al. Prognostic implications of Tc-99m sestamibi viability imaging and subsequent therapeutic strategy in patients with chronic coronary artery disease and left ventricular dysfunction. *J Am Coll Cardiol.* 2000; 36(3):739-745.
155. Hendel RC, Berman DS, Cullom SJ, Follansbee W, Heller GV, Kiat H et al. Multicenter clinical trial to evaluate the efficacy of correction for photon attenuation and scatter in SPECT myocardial perfusion imaging. *Circulation.* 1999; 99(21):2742-2749.
156. Corbett JR, Ficaro EP. Clinical review of attenuation-corrected cardiac SPECT. *J Nucl Cardiol.* 1999; 6(1 Pt 1):54-68.
157. Bailey DL. Transmission scanning in emission tomography. *Eur J Nucl Med.* 1998; 25(7):774-787.
158. Bocher M, Balan A, Krausz Y, Shrem Y, Lonn A, Wilk M et al. Gamma camera-mounted anatomical X-ray tomography: technology, system characteristics and first images. *Eur J Nucl Med.* 2000; 27(6):619-627.
159. Germano G, Kiat H, Kavanagh PB, Moriel M, Mazzanti M, Su HT et al. Automatic quantification of ejection fraction from gated myocardial perfusion SPECT. *J Nucl Med.* 1995; 36(11):2138-2147.
160. DePuey EG, Rozanski A. Using gated technetium-99m-sestamibi SPECT to characterize fixed myocardial defects as infarct or artifact. *J Nucl Med.* 1995; 36(6):952-955.
161. Links JM, DePuey EG, Taillefer R, Becker LC. Attenuation correction and gating synergistically improve the diagnostic accuracy of myocardial perfusion SPECT. *J Nucl Cardiol.* 2002; 9(2):183-187.
162. Sharir T, Germano G, Kavanagh PB, Lai S, Cohen I, Lewin HC et al. Incremental prognostic value of post-stress left ventricular ejection fraction and volume by gated myocardial perfusion single photon emission computed tomography. *Circulation.* 1999; 100(10):1035-1042.
163. Travin MI, Heller GV, Johnson LL, Katten D, Ahlberg AW, Isasi CR et al. The prognostic value of ECG-gated SPECT imaging in patients undergoing stress Tc-99m sestamibi myocardial perfusion imaging. *J Nucl Cardiol.* 2004; 11(3):253-262.
164. Yoshinaga K, Morita K, Yamada S, Komuro K, Katoh C, Ito Y et al. Low-dose dobutamine electrocardiograph-gated myocardial SPECT for identifying viable myocardium: comparison with

dobutamine stress echocardiography and PET. *J Nucl Med.* 2001; 42(6):838-844.
165. Delbeke D, Videlefsky S, Patton JA, Campbell MG, Martin WH, Ohana I et al. Rest myocardial perfusion/metabolism imaging using simultaneous dual-isotope acquisition SPECT with technetium-99m-MIBI/fluorine-18-FDG. *J Nucl Med.* 1995; 36(11):2110-2119.
166. Fukuchi K, Katafuchi T, Fukushima K, Shimotsu Y, Toba M, Hayashida K et al. Estimation of myocardial perfusion and viability using simultaneous 99mTc-tetrofosmin--FDG collimated SPECT. *J Nucl Med.* 2000; 41(8):1318-1323.
167. Sandler MP, Videlefsky S, Delbeke D, Patton JA, Meyerowitz C, Martin WH et al. Evaluation of myocardial ischemia using a rest metabolism/stress perfusion protocol with fluorine-18 deoxyglucose/technetium-99m MIBI and dual-isotope simultaneous-acquisition single-photon emission computed tomography. *J Am Coll Cardiol.* 1995; 26(4):870-878.
168. Bax JJ, Cornel JH, Visser FC, Fioretti PM, Van Lingen A, Huitink JM et al. Comparison of fluorine-18-FDG with rest-redistribution thallium-201 SPECT to delineate viable myocardium and predict functional recovery after revascularization. *J Nucl Med.* 1998; 39(9):1481-1486.
169. Bax JJ, Cornel JH, Visser FC, Fioretti PM, Van Lingen A, Reijs AE et al. Prediction of recovery of myocardial dysfunction after revascularization. Comparison of fluorine-18 fluorodeoxyglucose/thallium-201 SPECT, thallium-201 stress-reinjection SPECT and dobutamine echocardiography. *J Am Coll Cardiol.* 1996; 28(3):558-564.
170. Bax JJ, Cornel JH, Visser FC, Fioretti PM, Van Lingen A, Reijs AE et al. Prediction of recovery of myocardial dysfunction after revascularization. Comparison of fluorine-18 fluorodeoxyglucose/thallium-201 SPECT, thallium-201 stress-reinjection SPECT and dobutamine echocardiography. *J Am Coll Cardiol.* 1996; 28(3):558-564.
171. Srinivasan G, Kitsiou AN, Bacharach SL, Bartlett ML, Miller-Davis C, Dilsizian V. [18F]fluorodeoxyglucose single photon emission computed tomography: can it replace PET and thallium SPECT for the assessment of myocardial viability? *Circulation.* 1998; 97(9):843-850.
172. Fukuchi K, Katafuchi T, Fukushima K, Shimotsu Y, Toba M, Hayashida K et al. Estimation of myocardial perfusion and viability using simultaneous 99mTc-tetrofosmin--FDG collimated SPECT. *J Nucl Med.* 2000; 41(8):1318-1323.
173. Matsunari I, Kanayama S, Yoneyama T, Matsudaira M, Nakajima K, Taki J et al. Myocardial distribution of (18)F-FDG and (99m)Tc-sestamibi on dual-isotope simultaneous acquisition SPET compared with PET. *Eur J Nucl Med Mol Imaging.* 2002; 29(10):1357-1364.
174. Sandler MP, Videlefsky S, Delbeke D, Patton JA, Meyerowitz C, Martin WH et al. Evaluation of myocardial ischemia using a rest metabolism/stress perfusion protocol with fluorine-18 deoxyglucose/technetium-99m MIBI and dual-isotope simultaneous-acquisition single-photon emission computed tomography. *J Am Coll Cardiol.* 1995; 26(4):870-878.
175. Matsunari I, Kanayama S, Yoneyama T, Matsudaira M, Nakajima K, Taki J et al. Myocardial distribution of (18)F-FDG and (99m)Tc-sestamibi on dual-isotope simultaneous acquisition SPET compared with PET. *Eur J Nucl Med Mol Imaging.* 2002; 29(10):1357-1364.
176. Matsunari I. Electrocardiographic-gated dual-isotope simultaneous acquisition SPECT using (18)F-FDG and (99m)Tc-sestamibi to assess myocardial viability and function in a single study. 2005.
177. Kuettner A, Kopp AF, Schroeder S, Rieger T, Brunn J, Meisner C et al. Diagnostic accuracy of multidetector computed tomography coronary angiography in patients with angiographically proven coronary artery disease. *J Am Coll Cardiol.* 2004; 43(5):831-839.
178. Kuettner A, Trabold T, Schroeder S, Feyer A, Beck T, Brueckner A et al. Noninvasive detection of coronary lesions using 16-detector multislice spiral computed tomography technology: initial clinical results. *J Am Coll Cardiol.* 2004; 44(6):1230-1237.
179. Ropers D, Baum U, Pohle K, Anders K, Ulzheimer S, Ohnesorge B et al. Detection of coronary artery stenoses with thin-slice multi-detector row spiral computed tomography and multiplanar

reconstruction. *Circulation.* 2003; 107(5):664-666.
180. Leber AW, Knez A, Becker C, Becker A, White C, Thilo C et al. Non-invasive intravenous coronary angiography using electron beam tomography and multislice computed tomography. *Heart.* 2003; 89(6):633-639.
181. Leber AW, Knez A, Becker C, Becker A, White C, Thilo C et al. Non-invasive intravenous coronary angiography using electron beam tomography and multislice computed tomography. *Heart.* 2003; 89(6):633-639.

SECTION II

The value of attenuation correction in myocardial perfusion scintigraphy and viability detection

Chapter 2

Effect of attenuation correction on the interpretation of ^{99m}Tc-sestamibi myocardial perfusion scintigraphy: the impact of 1 year 's experience

Riemer H.J.A. Slart[1], Tjin H. Que[1], Dirk J. van Veldhuisen[2], Lieke Poot[1], Paul K. Blanksma[2], D. Albertus Piers[1], Pieter L. Jager[1]

Department of Nuclear Medicine and Molecular Imaging[1] and Cardiology[2]
University Medical Center Groningen, The Netherlands

Eur J Nucl Med Mol Imaging 2003 Nov;30(11):1505-9.

Abstract

Aim: To determine the yield of attenuation correction in myocardial perfusion imaging (MPI), before and after a 1-year experience period.
Methods: In 48 consecutive patients referred for MPI, both non-corrected (NC) and attenuation corrected (AC) images were analyzed by 3 independent readers shortly after implementation of AC. The same images were re-analyzed one year later, after having obtained experience in AC on a routine basis in >500 patients with clinical feedback. Results were compared with gold standards for ischemia and infarction based on coronary angiography, follow-up, ultrasound and gated blood pool imaging.
Results: Sensitivity and specificity for detection of coronary artery disease were 95% and 45% respectively for NC images, and 77% and 70% for AC images at first readings. After one year of AC experience, NC sensitivity/specificity was 100%/61%, and AC results were 89%/92%.
Conclusion: Attenuation correction improves the performance of MPI interpretation. With attenuation correction, specificity is increased and sensitivity is similar as compared with non-corrected images. However, attenuation correction requires experience and is associated with a learning curve.

Keywords: myocardial perfusion imaging, ^{99m}Tc-sestamibi, attenuation correction, learning curve.

Introduction

Although single-photon emission computed tomography (SPECT) using tracers such as ^{99m}Tc-sestamibi, ^{99m}Tc-tetrofosmin or thallium-201 is an accurate, noninvasive diagnostic method for the detection of coronary artery disease (CAD), attenuation artefacts reduce the specificity of this technique (1,2). The non-uniform attenuation of the emitted radiation may produce severe artefacts which may result in fixed defects on SPECT images that could easily be mistaken for myocardial infarction. Common causes of attenuation artefacts are associated with breast attenuation in women, and diaphragmatic attenuation in men (2-4). Attenuation correction using transmission scans may help in distinguishing attenuation artefacts from myocardial infarction patterns, especially in the posterior, posterolateral and posteroseptal wall, where misinterpretation is most common (5,6). Recently, several methods for transmission scan based attenuation correction (AC) have become available (4). Some authors have reported considerable improvements in the accuracy, but others found no improvement or even decreasing accuracy (4, 6-12). Attenuation correction may considerably change the appearance of images that readers have long been used to. For this reason centers that obtained attenuation correction, discontinue using it after a short period. In addition to the variability in methods of attenuation correction, these systems usually also employ different acquisition and reconstruction protocols, and may or may not also incorporate scatter correction algorithms or depth-dependent resolution correction methods. These factors contribute to confusion as to the real clinical impact (13).

Apart from the variations in systems and methods, it is likely that a significant learning effect exists in interpretation of AC images. The impact of this learning effect may even be greater than the differences between various systems and methods. In this study we report our experience with attenuation correction using a multiple-line array of gadolinium-153 (^{153}Gd) rods. The aims of this study were (a) to determine the yield of attenuation correction with regard to sensitivity and specificity, and (b) to determine the influence of 1 year's clinical experience of routinely applied attenuation correction on the interpretation of myocardial perfusion scintigraphy. For this purpose three independent readers evaluated 48 studies shortly after implementation of the attenuation correction system and blindly re-analyzed the same studies again after obtaining this experience.

Materials and methods

Forty-eight consecutive patients suspected of coronary artery disease or referred for risk stratification analysis (35 male, 13 female, mean age 58 ± 13 (SD), range 27 - 87 years) were included. These patients were referred between May and July 2000 for routine myocardial perfusion SPECT imaging. Twenty-one patients of this group had a history of myocardial infarction (Table 1).

Six-hundred MBq of ^{99m}Tc-sestamibi was injected at rest and the next day after dipyri-

damole or bicycle stress. SPECT images were acquired one hour after tracer administration using a double headed gammacamera (Siemens E.Cam) equipped with low-energy high-resolution collimators. The camera heads were in perpendicular position. Other acquisition parameters were: 32 steps rotation, 20 sec per step, 128 x 128 matrix size, rotation from the 45° right anterior oblique to the 135° left posterior oblique position with the patient laying supine. The attenuation correction system consists of an array of ^{153}Gd external line sources incorporated in retractable 'wings' on the camera, and is called 'profile attenuation correction'. These wings form a 180° degree arc opposite to the perpendicular camera heads. A shutter opens and closes the external sources. In this study simultaneous emission and transmission images were obtained, using a 20% window over the ^{99m}Tc-photopeak and a 20% window over the ^{153}Gd photopeak. No scatter correction was performed. Non-corrected (NC) emission scans were reconstructed after filtered-back-projection using a Butterworth 0.30/6 filter. Attenuation corrected images were reconstructed from the emission and transmission images using iterative reconstruction (Wallace) methods on Siemens ICON computers (version 8.5). The manufacturer considers these methods standard and dedicated to this application. All data were reorientated in order to produce short-axis (SA), horizontal long-axis (HLA) and vertical long-axis (VLA) sections. Both an uncorrected printout and an attenuation corrected printout was obtained.

NC and AC myocardial perfusion images of individual patients were analyzed together by three independent nuclear medicine physicians, blinded for the clinical pretest likelihood of coronary artery disease, final diagnosis or each other's results. Differences in the interpretation of a study as normal or abnormal or differences confined to individual segments were resolved by a fourth experienced reader in a blind manner. The NC and AC perfusion images were scored into 3 categories (0 = normal, 1 = ischemia, 2 = infarction) using a 9-segment polar map (basal and distal anterior, lateral, inferior and septal walls, and one for the apex). Images were read according to the standard procedure in our department, meaning that non-severe irreversible defects on NC images could be attributed to attenuation correction and scored as normal, based on the experience of the reader. To correlate results with vessel territories, anterior, septal and apical segments were assigned to the left anterior descending artery (LAD), lateral segments to the left circumflex artery (RCX), and inferior segments to the right coronary artery (RCA).

The first reading took place shortly after the implementation of the AC system, and the exact same reading and scoring system was applied by the same three readers one year later. In the intervening period the readers had obtained experience in > 500 MPI patients undergoing routinely evaluation for clinical purposes with and without AC, incorporating feedback from clinicians. These MPI routine studies were always evaluated in cooperation with experienced cardiologists. Available CAG and clinical information were compared to the NC and AC MPI results. In cases of discordance between CAG and the MPI results, other techniques were available to detect or exclude CAD, like positron emission tomography (PET).

The results of the 3 readers were pooled, and average values are presented. A reduction

Table 1. Demographic data

	No.
Patients	48
Male	35
Female	13
Mean age (yrs)	58 ± 13
CAD*	26
Infarction only	13
Infarction and ischemia	8
Ischemia only	5
CAG	26
1-vessel disease	9
2-vessel disease	4
3-vessel disease	0

* Assessed by coronary angiography (CAG), MUGA, ultrasound or X-ray ventriculography

in vessel diameter of > 70% on coronary angiography was considered as the gold standard for the presence of ischemia. However, coronary angiography was available in only 26 of the patients; in the remaining 22, the likelihood of coronary artery disease was assessed on the basis of follow-up data recorded over 1 year. For assessment of myocardial infarction, we relied on the patient's history, e.g. ECG changes clearly suggestive of myocardial infarction accompanied by an increase in myocardium-specific enzymes or the presence of wall motion disorders such as akinesia or dyskinesia on ultrasound or blood pool imaging (information of one type ot the other was available in all patients). At the time of attenuation correction acquisition, gated SPECT was not available. Both NC and AC images were compared with the gold standard for each segment, before and after the 1-year experience period. From these data sensitivities and specificities per patient for the overall detection of coronary artery disease, for detection of ischemia only and for detection of infarction only were calculated.

Statistical analysis

Data were expressed as mean ± SD. McNemar's test with Yate's correction was used to determine the differences in sensitivity and specificity for paired data samples. A P value of <0.05 was considered significant.

Results

Gold standard

Thirteen patients were diagnosed with ischemia in one or more segments, all based on coronary angiography. Nine had single-vessel disease and four had two-vessel disease.

In the other 35 patients no signs of ischemia were found, based on coronary angiography in 13, and on unremarkable follow-up combined with low clinical likelihood of coronary disease (14). In 21 patients, a previous infarction was confirmed by MUGA, ultrasound, X-ray ventriculography or combinations thereof. In the others, combinations of these available tests ruled out unknown infarctions. In total 26 patients had coronary artery disease, with a mean of 1.7 abnormal segments (Table 1).

Initial assessments

A total of 432 segments in 48 patients were evaluated and compared with the gold standard. On average 1.9 segments per patient were scored as abnormal with the NC study. Sensitivity for the detection of CAD was 95% for the NC images, at a specificity of 45%. For the AC images sensitivity was 77% (not significantly different from NC, $P = 0.13$) at a specificity of 70% ($P = 0.13$). Mean accuracy with an average difference between the 3 readers of the NC and AC studies was 68% (average difference 1.3%) and 73% (average difference 3.6%). Considering only the detection of ischemia, NC sensitivity was 72% and specificity 80%. Using the attenuation corrected images these figures were 30% and 87% (sensitivity and specificity NC vs AC; P =0.24 and 0.37, respectively). Considering only the detection of infarctions, NC subgroup sensitivity and specificity were 86% and 62% respectively, while for AC studies the sensitivity and specificity were 79% and 80% respectively (sensitivity and specificity NC vs AC; P =NS and 0.045 respectively).

Assessments after one year

Analyzing the same patient data after 1 year of experience with attenuation correction, the sensitivity of NC for the detection of CAD on the patient level was now 100% (P = NS vs initial reading), and the specificity had improved to 61% for the NC readings ($P < 0.001$). The sensitivity of the AC images for CAD was 89%; it had improved with the initial readings, but not significantly ($P = 0.71$). Specificity of AC MPI was 92%, showing a significant improvement compared with the initial assessments ($P = 0.023$, Table 2). Mean accuracy of the NC and AC studies was 83% (average difference between the 3 readers

Table 2. Sensitivity and specificity in detection of CAD in 38 patients without and after 1 year of attenuation correction experience.

Approach	Sensitivity (%)	Specificity (%)
Initial assessment		
NC	95	45
AC	77	70
	$P = 0.13$	$P = 0.13$
After 1 year's experience		
NC	100	61
AC	89	92
	$P = 0.71$*	$P = 0.023$*

* Initial AC reading vs AC reading after 1 year's experience

was 4.6%) and 88% (average difference 1.6 %) respectively.
Considering only the detection of ischemia, the sensitivity of NC studies was 68% and the specificity, 83%. For the AC studies, these values were 48% and 94% respectively.
Considering only the detection of infarctions, the sensitivity and specificity of NC studies were 93% and 71% respectively, while sensitivity and specificity of AC studies were 97% and 97% respectively (sensitivity and specificity of NC vs AC; both P = NS). Re-analyzing NC studies after 1 year changed the final diagnosis in 16% of the patients. Re-analyzing AC studies after 1 year's experience AC changed the final diagnosis in 15% of the patients.

Discussion

At time of the first reading, shortly after the implementation of attenuation correction system, we found that attenuation correction led to an increase in specificity for the detection of CAD as compared with NC studies; the difference was not, however, statistically significant. The sensitivity of the AC images tended to be lower than that of the NC images, leading to a mixed positive/negative yield. However, after 1 year of experience, the sensitivity of the AC studies had increased to approach the level previously achieved with NC image interpretation, though the improvement was not significant. Specificity in CAD detection with AC images had also increased and was significant better compared with the specificity of AC images 1 year earlier. The specificity of NC images for detection of CAD had similarly increased significantly compared with the initial NC reading.
The overall results of attenuation correction therefore appear to be beneficial, and performance in interpretation of MPI is improved (Figure 1). However, this study demonstrates that this improvement requires experience and is associated with a learning curve. In addition, we found that also the NC reading performance, and especially differentiation of attenuation artefacts from infarction, improved after using attenuation correction for 1 year, suggesting that performance in general increases with this new feature.
While our data, in agreement with many other reports, mainly showed improvements in specificity as result of attenuation correction, others have also reported increased sensitivities (4,7,8,10,12). Usually in these studies, sensitivity for overall detection of CAD is given, thereby aggregating the detection of infarcted areas with the more important detection of ischemia. In our setting, we apparently read our images with high sensitivity, at lower specificity. Therefore, it may not be surprising that especially specificity increased after we implemented the attenuation correction system. All centers have their own 'set-point' in the trade-off between sensitive or specific reading of MPI, and it thus seems logical that in some centers sensitivity may increase by attenuation correction. It should be noted that in other studies, scatter correction and motion correction also assisted in the detection of artificial fixed defects (6,7).
We found not only that attenuation correction resulted in no overall improvement in sensitivity, but also that it yielded considerably worse sensitivity in (small) subgroup of pa-

tients with validated ischemia (Figure 2a and 2b). In the subgroup of patients with myocardial infarctions, on the other hand, sensitivity was similar for NC and AC imaging, at considerable better specificity. Therefore, some caution is advised in basing a diagnosis of ischemia solely on AC images, while a diagnosis of infarction appears to be more reliable using AC. Although combined reading of AC and NC studies is complex, in our opinion the NC and AC images should be used in conjunction at present. As the feature of AC is truly additional, the conjunct reading poses no problems.

Our study is too small to draw conclusions on the performance of AC for each of the three vessel territories. Other limitations of this study include the retrospective nature and associated problems such as verification bias (for instance there was lack of accurate confirmation of infarcted myocardial tissue with ^{18}F-fluorodeoxyglucose (FDG)). Also gated SPECT for evaluation of wall motion and wall thickening was not available in our center at the time of MPI acquisition. However, we believe that the relatively high frequency of coronary angiography in this study and the availability of clinical follow-up data probably minimized the likelihood of errors in this study.

Despite the improvement in MPI interpretation that is offered by attenuation correction, further advances in the AC method would be welcome. Especially the increase in subdiaphragmatic activity induced by attenuation correction may interfere with assessment of the inferior wall. This problem may be reduced by better reconstruction methods. It is also conceivable in the near future, better tracers with less gastrointestinal activity will become available, leading to reduced subdiaphragmatic activity (^{99m}Tc-tetrofosmin has already represented an advance in this direction). It is also to be noted that in general, the quality of the attenuation correction appears to be related to the quality of the transmission map (μ map). In a recent report by O'Connor et al. (15), the best attenuation correction was found using computed tomography (CT) for transmission imaging. The high photon flux produced by CT generates better correction than the lower flux methods incorporating radioactive sources, such as the array of ^{153}Gd rods used in this study. This approach might also decrease costs in the long run, as replacement of ^{153}Gd rods is not longer be necessary. In addition, improved methods for scatter compensation, motion correction and collimator resolution modelling will also contribute to better diagnostic performance (7,16).

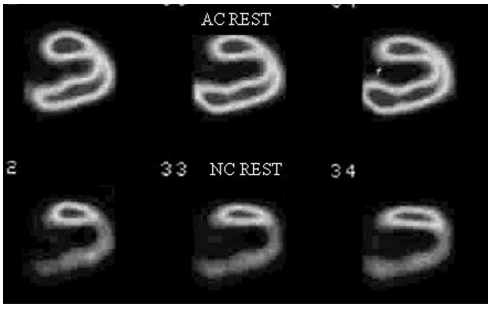

Figure 1. Improvement generated by AC. Lower row shows MPI rest vertical long axis slices without correction, showing a marked inferior defect originally judged to be an infarction. Upper row shows corresponding images after AC, now correctly normal.

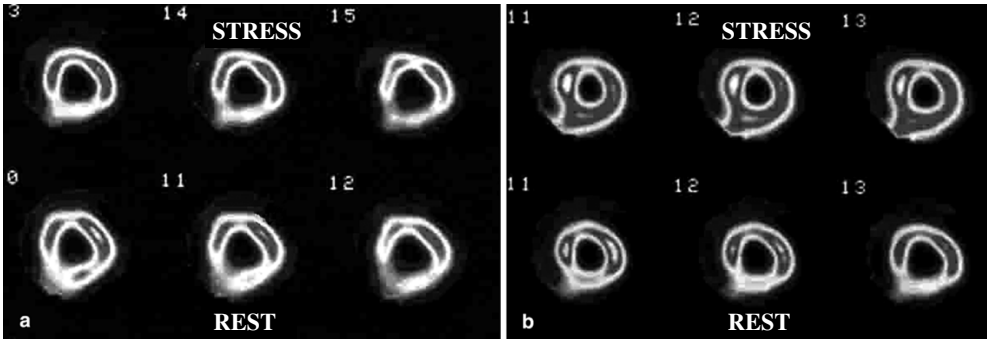

Figure 2. Deteriorating effect of AC. MPI transversal slices in a patient with ischemia inferior showing modest reversibility in the inferior wall on non-corrected images (A). The corresponding AC images (B) were read as normal by all observers.

Conclusion

In this study attenuation correction resulted in an increase in the specificity of myocardial perfusion scintigraphy at similar sensitivity as compared with non-corrected images. However, the method requires experience and is associated with a learning curve. From this and other studies it slowly becomes clear that attenuation correction should be part of the standard myocardial perfusion imaging method, as recently stated by the American Society of Nuclear Cardiology (17). With future technical improvements, and given appropriate experience with this method, attenuation correction might further improve myocardial perfusion imaging, which will ultimately translate into a beneficial clinical effect.

Reference List

1. DePuey EG. How to detect and avoid myocardial perfusion SPECT artifact. *J Nucl Med* 1994;35:699-702.
2. DePuey EG, Garcia EV. Optimal specificity of thallium-201 SPECT through recognition of imaging artifacts. *J Nucl Med* 1989;30:441-449.
3. Miles J, Cullom SJ, Case JA. An introduction to attenuation correction. *J Nucl Cardiol* 1999;6:449-457.
4. Corbett JR, Ficaro EP. Clinical review of attenuation-corrected cardiac SPECT. *J Nucl Cardiol* 1999;6:54-68
5. Gallowitsch HJ, Sykora J, Mikosch P, Kresnik E, Unterweger O, Molnar M et al. Attenuation-corrected thallium-201 single photon emission tomography using a gadolinium-153 moving line source: clinical value and the impact of attenuation correction on the extent and severity of perfusion abnormalities. *Eur J Nucl Med* 1998;25:220-228.
6. Kjaer A, Cortsen A, Rahbek B, Hasseldam H, Hesse B. Attenuation and scatter correction in myocardial SPET: improved diagnostic accuracy in patients with suspected coronary artery disease. Eur *J Nucl Med Mol Imaging* 2002;29:1438-1442.
7. Links JM, DePuey EG, Taillefer R, Becker LC. Attenuation correction and gating synergistically improve the diagnostic accuracy of myocardial perfusion SPECT. *J Nucl Cardiol* 2002;9:183-187.
8. Shotwell M, Singh BM, Fortman C, Bauman BD, Lukes J, Gerson MC. Improved coronary disease detection with quantitative attenuation-corrected Tl-201 images. *J Nucl Cardiol* 2002;9:52-62.
9. Gallowitsch HJ, Unterweger O, Mikosch P, Kresnik E, Sykora J, Grimm G et al. Attenuation correction improves the detection of viable myocardium by thallium-201 cardiac tomography in patients with previous myocardial infarction and left ventricular dysfunction. *Eur J Nucl Med* 1999;26:459-466.
10. Hendel RC, Berman DS, Cullom SJ, Follansbee W, Heller GV, Kiat H et al. Multicenter clinical trial to evaluate the efficacy of correction for photon attenuation and scatter in SPECT myocardial perfusion imaging. *Circulation* 1999;99:2742-2749.
11. Lee DS, So Y, Cheon GJ, Kim KM, Lee MM, Chung JK, Lee MC. Limited incremental diagnostic values of attenuation-noncorrected gating and ungated attenuation correction to rest/stress myocardial perfusion SPECT in patients with an intermediate likelihood of coronary artery disease. *J Nucl Med* 2000;41:852-859; discussion 860-862.
12. Vidal R, Buvat I, Darcourt J, Migneco O, Desvignes P, Baudouy M, Bussiere F. Impact of attenuation correction by simultaneous emission/transmission tomography on visual assessment of 201Tl myocardial perfusion images. *J Nucl Med* 1999;40:1301-1309.
13. Wackers FJ. Should SPET attenuation correction be more widely employed in routine clinical practice? Against. *Eur J Nucl Med Mol Imaging* 2002;29:412-415.
14. Diamond GA, Forrester JS. Analysis of probability as an aid in the clinical diagnosis of coronary-artery disease. *N Eng J Med* 1979;300:1350-1358.
15. O'Connor MK, Kemp B, Anstett F, Christian P, Ficaro EP, Frey E et al. A multicenter evaluation of commercial attenuation compensation techniques in cardiac SPECT using phantom models. *J Nucl Cardiol* 2002;9(4):361-376.
16. Wacker FJTh. Attenuation correction, or the emperor's new clothes? [editorial] *J Nucl Med* 1999;40:1310-1312.
17. Hendel RC, Corbett JR, Cullom SJ, DePuey EG, Garcia EV, Bateman TM. The value and practice of attenuation correction for myocardial perfusion SPECT imaging: a joint position statement from the American Society of Nuclear Cardiology and the Society of Nuclear Medicine. *J Nucl Cardiol* 2002;9:135-143.

Chapter 3

Added value of attenuation corrected ^{99m}Tc-tetrofosmin SPECT for the detection of viability: Comparison with FDG SPECT

Riemer H.J.A. Slart[1], Jeroen J. Bax[2], Wim J. Sluiter[3], Dirk J. van Veldhuisen[4], Pieter L. Jager[1]

Department of Nuclear Medicine and Molecular Imaging[1], University Medical Center Groningen, Department of Cardiology[2], Leiden University Medical Center, Department of Endocrinology[3], University Medical Center Groningen, Department of Cardiology [4], University Medical Center Groningen, The Netherlands.

J Nucl Cardiol 2004 Nov-Dec;11(6):689-96.

Abstract

The aim of this study was to evaluate the value of attenuation correction (AC) of ^{99m}Tc-tetrofosmin single photon emission computed tomography (SPECT) imaging for the detection of myocardial viability.

Methods: A head-to-head comparison between resting ^{99m}Tc-tetrofosmin SPECT and ^{18}F-fluorodeoxyglucose (FDG) SPECT was performed. Both the non-corrected (NC) and AC ^{99m}Tc-tetrofosmin SPECT images were compared with the FDG images that served as the reference for viability. Consecutive patients (n=33) with chronic coronary artery disease and left ventricular dysfunction were included. Segmental ^{99m}Tc-tetrofosmin and FDG data were displayed in polar maps (17-segment model) and the segments were normalized to peak activity using the 4D-MSPECT software program. Segments with normalized FDG activity greater than 50% were considered viable. A similar cutoff to assess viability was used for the NC and AC ^{99m}Tc-tetrofosmin images. Regional contractile function was determined from the gated ^{99m}Tc-tetrofosmin images and scored as normokinesia, hypokinesia or akinesia/dyskinesia.

Results: Of all segments, 482 (85%) were viable on FDG SPECT. Of these, 427 (89%) were classified as viable with NC ^{99m}Tc-tetrofosmin. Thus 55 (11%) were underestimated with NC ^{99m}Tc-tetrofosmin SPECT; these segments were mainly located in the inferior and inferoseptal regions. AC changed 39 segments (70%) of the underestimated segments into viable. By the use of attenuation correction, the agreement between ^{99m}Tc-tetrofosmin and FDG imaging improved from 84% to 90%. Similar observations were made when the analysis was restricted to the dysfunctional segments.

Conclusion: The addition of attenuation correction to ^{99m}Tc-tetrofosmin SPECT significantly improved detection of myocardial viability in patients with chronic artery disease, although minimal underestimation of viability remained as compared with FDG SPECT imaging.

Keywords: attenuation correction, ^{99m}Tc-tetrofosmin, ^{18}F-fluorodeoxyglucose, single photon emission computed tomography, myocardial viability.

Introduction

Myocardial viability assessment is an important clinical issue in patients with coronary artery disease (CAD) and left ventricular (LV) dysfunction. Patients with viable myocardium have been demonstrated to benefit from revascularization, with an improvement in LV function and a favourable prognosis after revascularization (1-3).
Various techniques have been proposed for the detection of viable myocardium, including nuclear imaging with ^{18}F-fluorodeoxyglucose (FDG), thallium-201 and technetium-99m (^{99m}Tc) labeled agents (4-10). In addition, other imaging modalities have been used for the assessment of viability, including magnetic resonance imaging and dobutamine stress or contrast echocardiography (11-13).
For clinical use, ^{99m}Tc-labeled agents may be preferred (4,14,15). The feasibility of ^{99m}Tc-sestamibi and ^{99m}Tc-tetrofosmin imaging to assess viability has been demonstrated (4,14). Still, as compared with FDG imaging, the ^{99m}Tc-labeled agents appear to underestimate the presence of residual viable myocardium, in particular in severely dysfunctional regions (5,7,16-18). This underestimation of viability may partially be ascribed to attenuation artefacts, scatter and partial volume effects (19-22). In particular, the non-uniform attenuation of the emitted radiation of ^{99m}Tc-labeled tracers may produce severe artefacts, resulting in defects on single photon emission computed tomography (SPECT) imaging, leading to underestimation of viability (22-24). Attenuation correction (AC) by the use of transmission scans may help in distinguishing attenuation artefacts from myocardial infarction patterns, especially in the posterior wall, where misinterpretation is most common (21,25). Recently, several methods for transmission scan-based attenuation correction have become available, and clinical results have shown its utility to improve the detection of CAD (23,26). Data on the added value of attenuation correction in viability assessment are scarce (27). In this study we report the impact of attenuation correction on assessment of viability with resting ^{99m}Tc-tetrofosmin SPECT. Both non-corrected (NC) images and corrected images were compared with the viable segments on FDG imaging that served as the reference method.

Material and methods

Patients

This study included 33 consecutive patients with chronic CAD and LV dysfunction (23 men, mean age 63 ± 11 years [range 37-80]). Of these, 22 (66%) had a history of myocardial infarction and 19 (57%) had undergone previous revascularization (both > 3 months before the study).
The mean number of stenosed coronary arteries on angiography was 1.6 ± 1.0
The mean LV ejection fraction (LVEF) in the study population was 41 ± 13 %. Ten patients had diabetes mellitus type 2. All patients underwent a resting gated SPECT ^{99m}Tc-tetrofosmin and a resting FDG SPECT in random order. None of the patients had cardiac events or therapeutic interventions during the study.

Resting ^{99m}Tc-tetrofosmin SPECT: Data acquisition, Analysis and Viability Criteria

At rest, 600 MBq ^{99m}Tc-tetrofosmin was injected. SPECT images, including gated images in 16 frames with an R-R interval of ± 10%, were acquired 1 hr after tracer administration using a dual-headed gamma camera (Siemens E.Cam, Siemens Medical Systems, Hoffman Estates, Ill, USA) equipped with low-energy high-resolution collimators. This system has a spatial resolution of 7.4 mm full-width at half maximum (FWHM). The camera heads were in perpendicular position (90° opposed). Other acquisition parameters were: 32 steps, 20 s per step, 128 matrix size, zoom 1.0 and rotation from 45° right anterior oblique to 135° left posterior oblique position with the patient in the supine position. The AC system consisted of an array of ^{153}Gd external line sources incorporated in retractable "wings" on the camera. This system is called Profile Attenuation Correction (Siemens Medical Systems). These wings form a 180° arc opposite the perpendicular camera heads. A shutter opens and closes the external sources. In this study simultaneous emission and transmission images were obtained, using a 20% window over the ^{99m}Tc-photopeak and a 20% window over the ^{153}Gd-photopeak. No scatter correction was performed. After filtered backprojection reconstruction, NC emission slices were two-dimensionally filtered using a Butterworth filter with cutoff frequency of 0.30 cycles/pixel of Nyquist frequency and order 6. AC images were reconstructed from the emission and transmission images using iterative reconstruction (Wallis and Miller (28)) methods on Siemens ICON computers (version 8.5). All data from the ^{99m}Tc-tetrofosmin SPECT studies were reorientated in short-axis, horizontal and vertical long-axis sections. Data were analyzed and displayed in a 17-segment polar map (as recently proposed (29)), using the 4D-MSPECT program, a commercially available gated cardiac software package (developed by the University of Michigan Medical Center, Ann Arbor, MI, USA) (30).

Average counts per segment were obtained from the 17 segments and the measured counts were normalized to the segment with the highest average counts. NC and AC segments were regarded as viable when the normalized activity was greater than 50% (^{99m}Tc-tetrofosmin > 50%), and non-viable when activity was 50% or lower (^{99m}Tc-tetrofosmin ≤ 50%) (31).

The quantitative 4D-MSPECT analysis program was also used for assessing LV volumes, LVEF and regional wall motion. The 4D-MSPECT model uses a cylindric-spheric coordinate system, with cylindric coordinates to sample from the basal to the distal wall and spheric coordinates to sample the apex. Weighted spline and thresholding techniques were used to refine surface estimates. Fitted to a Gaussian function, wall position and wall thickness were estimated. LV wall motion was classified visually in 3 categories (0 = normal 1, = hypokinesia, 2 = akinesia/dyskinesia) by use of the 17-segment model.

FDG SPECT: Data acquisition, Analysis and Viability Criteria

FDG SPECT acquisition was performed on a separate day. Patients received a glucose-enriched breakfast. Acipimox (a nicotinic acid derivative, 500 mg) was administered orally to lower the circulating free fatty acids. To prevent side effects of acipimox (eg. skin rash), 250 mg of aspirin was administered orally 5 minutes before acipimox intake. Guided by

the plasma glucose levels, patients received additional insulin as previously described (32).

Ninety minutes after acipimox administration, 200 MBq FDG was injected at rest. Sixty minutes thereafter, data acquistion was started. A Siemens MultiSPECT dual-headed gamma camera with extra-high energy (EHE) collimators (Siemens) was used, with only one head activated during acquisition set at an energy window of 511 keV (± 15%). This system has a spatial resolution of 12.3 mm full width at half maximum. Sixty-four projections were acquired over a circular orbit of 180° (45° right anterior oblique to 45° left posterior oblique; 30 s per angle). The total acquisition time was 35 min. The planar FDG images were corrected for the decay of ^{18}F during data acquisition. Short-axis, vertical - and horizontal long-axis images of FDG were reconstructed using filtered back projection with a Butterworth filter (Nf 0.5, order 6). Further analysis of data was performed using the 4D-MSPECT program, similarly to the ^{99m}Tc-tetrofosmin data and displayed in polar maps (17-segment model). Average counts per segment were obtained from the 17 segments and the measured counts were normalized to the segment with the highest average counts. Segments were considered as non-viable, when the normalized FDG activity was ≤ 50% and as viable when the activity was > 50%.

Comparison between ^{99m}Tc-tetrofosmin and FDG SPECT

A head-to-head comparison for each corresponding segment was performed between ^{99m}Tc-tetrofosmin and FDG in all segments. In addition, the comparison was repeated in the dysfunctional segments, since viability is mainly important in dysfunctional myocardium. The normalized activities were compared and agreement between the 2 techniques (for assessment of viability and scar tissue) was determined.

Statistical analysis

Data were expressed as mean ± SD.

The agreement for viability detection using ^{99m}Tc-tetrofosmin and FDG was assessed by the use of weighted K-statistics. K-values of < 0.4, of 0.4 - 0.75, and of > 0.75 were considered to present poor, fair to good, and excellent agreement respectively, on the basis of the Fleiss classification (33). McNemar and Chi square tests were used to evaluate concordance/discordance and agreement/differences between NC ^{99m}Tc-tetrofosmin and AC ^{99m}Tc-tetrofosmin respectively. A *P* value <0.05 was considered significant.

Results

All segments

Of all 561 segments, 482 (85%) segments were viable on FDG SPECT (FDG >50%); the mean activity was 74 ± 12% (range 51% to 98%).

Of these, 427 (89%) were classified as viable when NC ^{99m}Tc-tetrofosmin images were used (Figure 1). The mean activity was 73 ± 13 (range 51 to 98%). The agreement on a

segmental basis between NC ^{99m}Tc-tetrofosmin and FDG SPECT was 84%, with a K-statistic of 0.41 (95% confidence interval (CI) 0.27-0.54, *P* <0.0001).
Of the 482 FDG viable segments, 55 (11%) were underestimated with NC ^{99m}Tc-tetrofosmin (Figure 1). Underestimation with NC ^{99m}Tc-tetrofosmin was mainly localized in the inferior and inferoseptal regions (see Table 1).
Of the 482 FDG viable segments, 466 (97%) were classified as viable when AC ^{99m}Tc-tetrofosmin images were used, reducing the number of underestimated segments by 70% (from 55 to 16, Figure 1). The mean AC ^{99m}Tc-tetrofosmin activity was 75 ± 11% (range 51% to 98%). The total agreement on a segmental basis between AC ^{99m}Tc-tetrofosmin and FDG SPECT was 90%, with a K-statistic of 0.48 (95% CI 0.31-0.64, *P* <0.0001).
Of the total of 55 underestimated NC ^{99m}Tc-tetrofosmin segments, 70% were correctly reclassified as viable segments after AC, in particular in the inferior and inferoseptal regions (Figure 2).

Segments with contractile dysfunction

Of all 222 dysfunctional segments, 164 (73%) segments were viable on FDG SPECT and the mean activity was 71 ± 11% (range 51 to 97%).
Of these 164 segments, 134 (81%) were classified as viable when NC ^{99m}Tc-tetrofosmin images were used (Figure 3). The mean activity was 70 ± 12% (range 51 to 98%). The total agreement on a segmental basis between NC ^{99m}Tc-tetrofosmin and FDG SPECT was 77%, with a K-statistic of 0.43 (95% CI 0.27-0.59, *P* <0.0001). Of the 164 FDG viable segments, 30 (18%) were underestimated with NC ^{99m}Tc-tetrofosmin. Underestimation with NC ^{99m}Tc-tetrofosmin was mainly localized in the inferior, inferolateral and inferoseptal regions (see Table 2). Of the 164 FDG viable segments, 159 (97%) were classified as

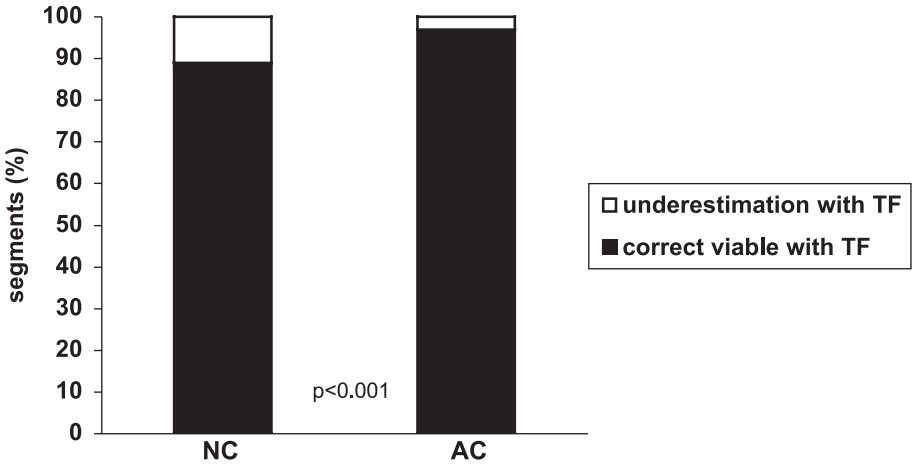

Figure 1. Bar graph showing the assessment for viability of NC ^{99m}Tc-tetrofosmin (89%) and AC ^{99m}Tc-tetrofosmin (97%) out of 482 FDG SPECT viable segments.
NC = non-corrected; AC = attenuation-corrected; TF = rest ^{99m}Tc-tetrofosmin.

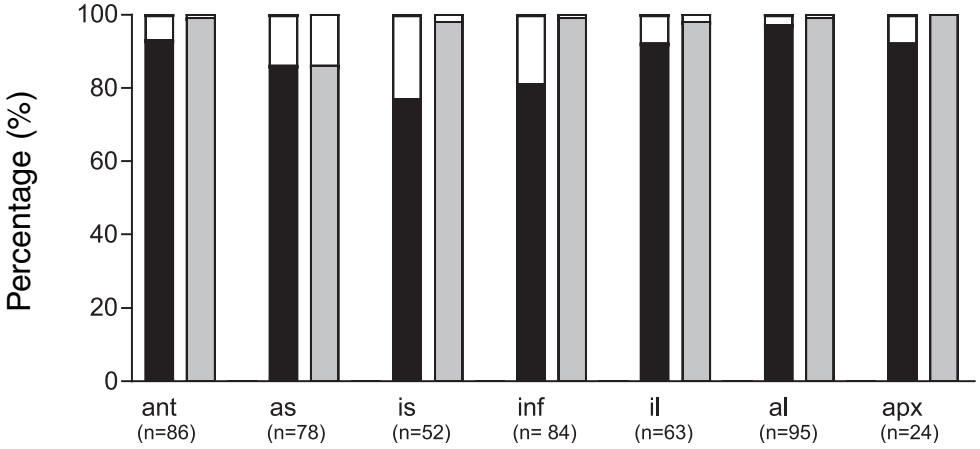

Figure 2. Bar graph showing the added value of attenuation correction for assessment of viability according to the different regions. The largest underestimation is observed in the inferoseptal (is) and inferior (inf) regions, and attenuation correction corrects the most in these regions.
Ant: anterior wall; as: anteroseptal; il: inferolateral; al: anterolateral; apx: apex.
NC = non-corrected; AC = attenuation-corrected.

viable when AC ^{99m}Tc-tetrofosmin images were used (Figure 3). The mean ^{99m}Tc-tetrofosmin activity was 73 ± 11% (range 51 to 98%). The total agreement on segmental basis between AC ^{99m}Tc-tetrofosmin and FDG SPECT was 83%, with a K-statistic of 0.51 (95% CI 0.32-0.69, P <0.0001).
Of the 30 underestimated NC ^{99m}Tc-tetrofosmin segments, 25 (83%) were correctly

Table 1. Detection of viability with NC and AC ^{99m}Tc-tetrofosmin in the 7 main regions of all viable segments

FDG-viable segments (No.)	No. of segments (%) underestimated	
	NC	AC
ANT (86)	6 (7%)	1 (1%)
AS (78)	11 (14%)	11 (14%)
IS (52)	12 (23%)	1 (2%)
INF (84)	16 (19%)	1 (1%)
IL (63)	5 (8%)	1 (2%)
AL (95)	3 (3%)	1 (1%)
Apex (24)	2 (8%)	0 (0%)
Total (482)	55 (11%)	16 (3%)

Viability detection in the inferior and inferoseptal regions was especially less underestimated after attenuation correction. *ANT*, anterior wall; *AS*, anteroseptal; *IS*, inferoseptal; *INF*, inferior; *IL*, inferolateral; *AL*, anterolateral; *NC* = non-corrected; *AC* = attenuation-corrected.

reclassified as viable segments when the AC ^{99m}Tc-tetrofosmin images were used, in particular in the inferior, inferoseptal and inferolateral regions (Figures 4 and 5).

Discussion

^{99m}Tc-labeled tracers to assess myocardial viability

^{99m}Tc-labeled tracers including ^{99m}Tc-tetrofosmin and ^{99m}Tc-sestamibi are lipophilic myocardial perfusion tracers that have been used extensively over the past decade. It has been shown that the uptake and retention of these ^{99m}Tc-labeled agents is associated with mitochondria function and may reflect cellular viability (34).

Various comparative studies between ^{99m}Tc-sestamibi SPECT and other viability techniques have been performed (9,17,35,36). Kaltoft et al. evaluated 50 patients with ^{99m}Tc-sestamibi SPECT to assess viability, and the results were compared with FDG PET (17). Considering FDG PET as the gold standard, ^{99m}Tc-sestamibi SPECT had a sensitivity of 87% with a specificity of 82% for the detection of viable myocardium (17). Additional studies have used ^{99m}Tc-sestamibi to predict improvement of function after revascularization. When the 10 available ^{99m}Tc-sestamibi studies (with 207 patients) were pooled, a sensitivity and specificity of 87% and 71%, respectively, were obtained for the prediction of improvement of regional LV function after revascularization (37). Less experience has been obtained with ^{99m}Tc-tetrofosmin SPECT. Both ^{99m}Tc-labeled tracers have been demonstrated to yield comparable image quality, and provided comparable accuracy for the detection of coronary artery disease (8,14,38,39). Few studies have used ^{99m}Tc-tetrofosmin SPECT for the assessment of viability. Matsunari et al. performed a head-to-head

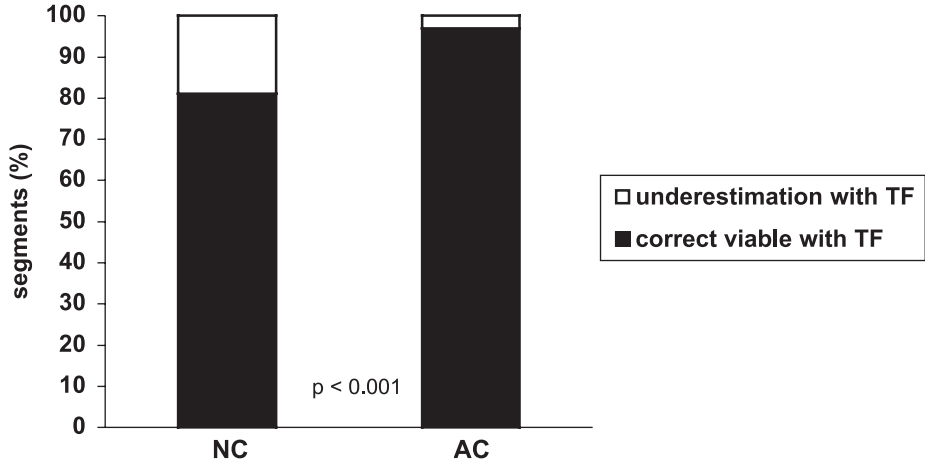

Figure 3. Bar graph showing the assessment for viability of NC ^{99m}Tc-tetrofosmin (81%) and AC ^{99m}Tc-tetrofosmin (97%) out of 164 dysfunctional but FDG SPECT viable segments.
NC = non-corrected; AC = attenuation-corrected; TF = rest ^{99m}Tc-tetrofosmin.

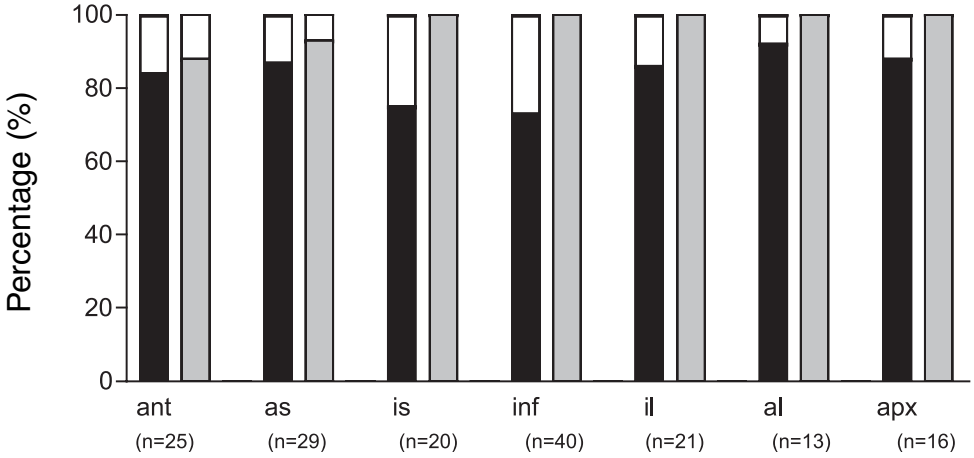

Figure 4. Bar graph showing the added value of attenuation correction for assessment of viability according to the different regions of dysfunctional segments. The largest underestimation is observed in the inferoseptal (is), inferior (inf) and inferolateral (il) regions, and attenuation correction corrects the most in these regions.

Ant: anterior wall; as: anteroseptal; al: anterolateral; apx: apex.

NC = non-corrected; AC = attenuation-corrected.

comparison between ^{99m}Tc-tetrofosmin SPECT and FDG PET in 24 patients (27). Considering FDG PET as the gold standard, they demonstrated a diagnostic accuracy of 80% for the detection of viable myocardium.

^{99m}Tc-tetrofosmin, attenuation correction and FDG SPECT

Despite the good results with the ^{99m}Tc-labeled tracers, several studies demonstrated

Table 2. Detection of viability with NC and AC TF in the 7 main regions of all viable, but dysfunctional segments.

FDG viable segments: n	NC underestimated per region: n (%)	AC underestimated per region: n (%)
ANT (n=25)	4 (16%)	3 (12%)
AS (n=29)	4 (13%)	2 (7%)
IS (n=20)	5 (25%)	0 (0%)
INF (n=40)	11 (27%)	0 (0%)
IL (n=21)	3 (14%)	0 (0%)
AL (n=13)	1 (8%)	0 (0%)
Apex (n=16)	2 (12%)	0 (0%)
Total (n=164)	30 (18%)	5 (3%)

Viability detection in the inferior (INF), inferolateral (IL) and inferoseptal (IS) regions was less underestimated after AC. ANT: anterior wall; AS: anteroseptal; AL: anterolateral. NC = non-corrected; AC = attenuation-corrected.

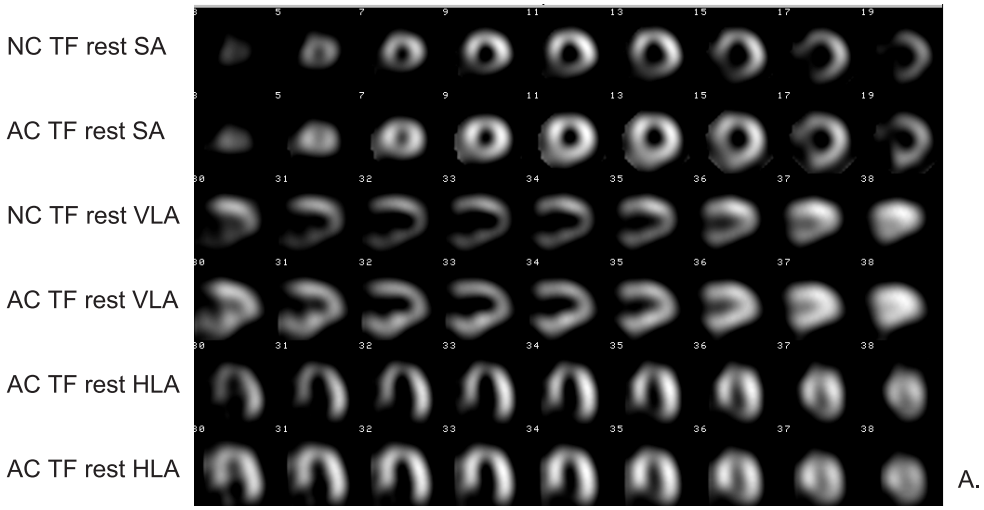

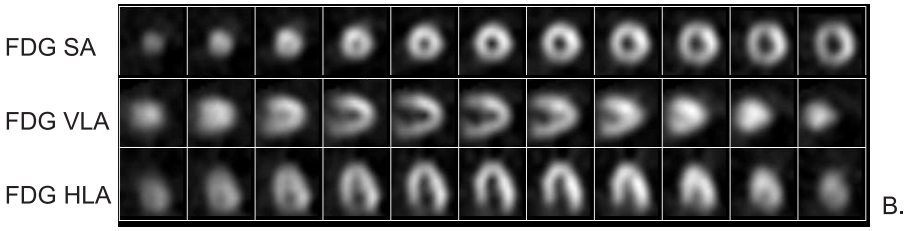

Figure 5.

A. Non-corrected (NC) and attenuation corrected (AC) rest ^{99m}Tc-tetrofosmin (TF) images divided in short-axis (SA), horizontal (HLA) and vertical long axis (VLA) slices from the apex to the base of the left ventricle. The NC rest ^{99m}Tc-tetrofosmin study improved from an activity ⩽ 50% to an activity > 50% after AC in the apex, septal and inferior wall, suggesting viable myocardial tissue.

B. FDG SPECT divided in SA-axis, HLA-axis and VLA-axis of the left ventricle in the same patient. FDG activity > 50% confirmed the presence of viable myocardial tissue in the corresponding apex, septal and inferior wall.

that ^{99m}Tc-sestamibi SPECT underestimated viability in patients with CAD (5,17,18,40,41). Altehoefer et al. compared ^{99m}Tc-sestamibi and FDG PET in 111 patients and demonstrated FDG uptake in 23% of the defects on ^{99m}Tc-sestamibi SPECT (40). Matsunari et al. reported a comparable underestimation of viability by ^{99m}Tc-tetrosfosmin SPECT as compared with FDG PET: 20% of the FDG PET viable segments was considered nonviable on ^{99m}Tc-tetrofosmin SPECT (27). In our study, with a head-to-head comparison between ^{99m}Tc-tetrofosmin SPECT and FDG imaging, 11% of the FDG viable segments were considered nonviable by ^{99m}Tc-tetrofosmin SPECT. Underestimation of

viability by the ^{99m}Tc-labeled agents may to some extent be explained by the different tracer properties of ^{99m}Tc-labeled tracers and FDG, but is also related to attenuation artefacts as observed with ^{99m}Tc-tetrofosmin SPECT (27,42,43). Soufer et al. already pointed out that underestimation of viability by ^{99m}Tc-sestamibi was predominantly observed in the inferior and septal regions, where attenuation artefacts are likely to occur (41). Also, in the present study, the majority (51%) of the underestimated segments was located in the inferior and septal regions (Table 1).

More recently, the use of AC has been introduced, and various studies have demonstrated the value of AC and ^{99m}Tc-sestamibi imaging to detect CAD (20,23,26,44). Indeed, attenuation correction using transmission scans can help in distinguishing attenuation artefacts from myocardial infarction patterns, in particular in the inferior, posterior and septal regions (21,25). Thus far, 1 study has systematically compared NC and AC ^{99m}Tc-tetrofosmin for the assessment of viability. In a direct comparison with FDG PET, the authors demonstrated an improvement for assessing viability when AC was used (27). In particular, the defect extent on ^{99m}Tc-tetrofosmin SPECT decreased significantly from 19.8 ± 15.2% on the NC images to 9.7% ± 12.6% on the AC images (P=0.01). Moreover, the percentage of dysfunctional segments classified nonviable by ^{99m}Tc-tetrofosmin SPECT that were viable on FDG PET decreased from 24.5% on the NC images to 13.7% on the AC images, thus a reduction of 44% in underestimation of viability when AC was applied to the ^{99m}Tc-tetrofosmin SPECT images. In our study, a similar reduction in underestimated segments was shown when AC was applied to the ^{99m}Tc-tetrofosmin SPECT images. The number of ^{99m}Tc-tetrofosmin nonviable but FDG viable segments decreased from 11% to 3% when AC was used. A similar reduction (from 18% to 3%) was observed when the analysis was restricted to the dysfunctional segments only. In addition, the largest reduction in underestimated segments was observed in the inferior and septal regions (Table 2).

Still, despite AC, some underestimation of myocardial viability remained as observed by Matsunari et al. (27) and confirmed in our study.

Limitations

The major limitation of the study is the lack of assessment of outcome after revascularization. Whether AC will result in an improved prediction of recovery of function post-revascularization remains to be demonstrated. In addition, larger patient populations need to be studied to confirm the added value of AC for assessment of viability with ^{99m}Tc-tetrofosmin SPECT.

Although the spatial resolution of FDG SPECT is lower as compared with FDG PET, the detection of viability with NC and AC ^{99m}Tc-tetrofosmin SPECT was still significant different. Using a PET technique may have resulted in higher differences between NC and AC ^{99m}Tc-tetrofosmin SPECT for the detection of myocardial viability. Attenuation-correction was not performed for the FDG SPECT studies, but the quality of FDG SPECT images will be less hampered by attenuation due to the high photon energy of ^{18}F. Matsunari et al. used attenuation-corrected static FDG PET images performed on a dedicated PET

system (27). PET may reduce potential attenuation artefacts in FDG studies, although small differences were noticed in myocardial activity distribution between FDG SPECT and FDG PET (45).
Left ventricular function in the subjects was relatively modestly depressed (LVEF: 41 ± 13%) probably based on relatively high prevalence of viable segments. The difference in detection of viability between NC and AC ^{99m}Tc-tetrofosmin SPECT may also be higher in patients with more severely depressed LV function, in whom more extensive and severe perfusion defects might be identified.

Conclusion

The addition of attenuation correction to ^{99m}Tc-tetrofosmin SPECT significantly improved detection of myocardial viability in patients with chronic CAD, although minimal underestimation of viability remained as compared with FDG SPECT imaging.

Acknowledgement

We gratefully acknowledge J. ter Veen for technical assistance.

Reference List

1. Di Carli MF, Davidson M, Little R, Khanna S, Mody FV, Brunken RC et al. Value of metabolic imaging with positron emission tomography for evaluating prognosis in patients with coronary artery disease and left ventricular dysfunction. *Am J Cardiol.* 1994; 73(8):527-533.
2. Rahimtoola SH. The hibernating myocardium. *Am Heart J.* 1989; 117(1):211-221.
3. Tillisch J, Brunken R, Marshall R, Schwaiger M, Mandelkern M, Phelps M et al. Reversibility of cardiac wall-motion abnormalities predicted by positron tomography. *N Engl J Med.* 1986; 314(14):884-888.
4. Acampa W, Cuocolo A, Petretta M, Bruno A, Castellani M, Finzi A et al. Tetrofosmin imaging in the detection of myocardial viability in patients with previous myocardial infarction: comparison with sestamibi and Tl-201 scintigraphy. *J Nucl Cardiol.* 2002; 9(1):33-40.
5. Altehoefer C, vom-Dahl J, Biedermann M, Uebis R, Beilin I, Sheehan F et al. Significance of defect severity in technetium-99m-MIBI SPECT at rest to assess myocardial viability: comparison with fluorine-18-FDG PET. *J Nucl Med.* 1994; 35(4):569-574.
6. Bax JJ, Cornel JH, Visser FC, Fioretti PM, Van Lingen A, Reijs AE et al. Prediction of recovery of myocardial dysfunction after revascularization. Comparison of fluorine-18 fluorodeoxyglucose/thallium-201 SPECT, thallium-201 stress-reinjection SPECT and dobutamine echocardiography. *J Am Coll Cardiol.* 1996; 28(3):558-564.
7. Dilsizian V, Arrighi JA, Diodati JG, Quyyumi AA, Alavi K, Bacharach SL et al. Myocardial viability in patients with chronic coronary artery disease. Comparison of 99mTc-sestamibi with thallium reinjection and [18F]fluorodeoxyglucose. *Circulation.* 1994; 89(2):578-587.
8. Kapur A, Latus KA, Davies G, Dhawan RT, Eastick S, Jarritt PH et al. A comparison of three radionuclide myocardial perfusion tracers in clinical practice: the ROBUST study. *Eur J Nucl Med Mol Imaging.* 2002; 29(12):1608-1616.
9. Kauffman GJ, Boyne TS, Watson DD, Smith WH, Beller GA. Comparison of rest thallium-201 imaging and rest technetium-99m sestamibi imaging for assessment of myocardial viability in patients with coronary artery disease and severe left ventricular dysfunction. *J Am Coll Cardiol.* 1996; 27(7):1592-1597.
10. Matsunari I, Fujino S, Taki J, Senma J, Aoyama T, Wakasugi T et al. Myocardial viability assessment with technetium-99m-tetrofosmin and thallium-201 reinjection in coronary artery disease. *J Nucl Med.* 1995; 36(11):1961-1967.
11. Baer FM, Voth E, Deutsch HJ, Schneider CA, Horst M, de Vivie ER et al. Predictive value of low dose dobutamine transesophageal echocardiography and fluorine-18 fluorodeoxyglucose positron emission tomography for recovery of regional left ventricular function after successful revascularization. *J Am Coll Cardiol.* 1996; 28(1):60-69.
12. Kuijpers D, Ho KY, van Dijkman PR, Vliegenthart R, Oudkerk M. Dobutamine cardiovascular magnetic resonance for the detection of myocardial ischemia with the use of myocardial tagging. *Circulation.* 2003; 107(12):1592-1597.
13. Iliceto S, Galiuto L, Marchese A, Cavallari D, Colonna P, Biasco G et al. Analysis of microvascular integrity, contractile reserve, and myocardial viability after acute myocardial infarction by dobutamine echocardiography and myocardial contrast echocardiography. *Am J Cardiol.* 1996; 77(7):441-445.
14. Acampa W, Cuocolo A, Sullo P, Varrone A, Nicolai E, Pace L et al. Direct comparison of technetium 99m-sestamibi and technetium 99m-tetrofosmin cardiac single photon emission computed tomography in patients with coronary artery disease. *J Nucl Cardiol.* 1998; 5(3):265-274.
15. Freeman I, Grunwald AM, Hoory S, Bodenheimer MM. Effect of coronary occlusion and myocardial viability on myocardial activity of technetium-99m-sestamibi. *J Nucl Med.* 1991; 32(2):292-298.

16. Burt RW, Perkins OW, Oppenheim BE, Schauwecker DS, Stein L, Wellman HN et al. Direct comparison of fluorine-18-FDG SPECT, fluorine-18-FDG PET and rest thallium-201 SPECT for detection of myocardial viability. *J Nucl Med.* 1995; 36(2):176-179.
17. Kaltoft A, Bottcher M, Sand NP, Flo C, Nielsen TT, Rehling M. 99mTc-Sestamibi SPECT is a useful technique for viability detection: results of a comparison with NH3/FDG PET. *Scand Cardiovasc J.* 2001; 35(4):245-251.
18. Sawada SG, Allman KC, Muzik O, Beanlands RS, Wolfe E-RJ, Gross M et al. Positron emission tomography detects evidence of viability in rest technetium-99m sestamibi defects. *J Am Coll Cardiol.* 1994; 23(1):92-98.
19. DePuey EG. How to detect and avoid myocardial perfusion SPECT artifacts. *J Nucl Med.* 1994; 35(4):699-702.
20. Hendel RC, Berman DS, Cullom SJ, Follansbee W, Heller GV, Kiat H et al. Multicenter clinical trial to evaluate the efficacy of correction for photon attenuation and scatter in SPECT myocardial perfusion imaging. *Circulation.* 1999; 99(21):2742-2749.
21. Kjaer A, Cortsen A, Rahbek B, Hasseldam H, Hesse B. Attenuation and scatter correction in myocardial SPET: improved diagnostic accuracy in patients with suspected coronary artery disease. *Eur J Nucl Med Mol Imaging.* 2002; 29(11):1438-1442.
22. Miles J, Cullom SJ, Case JA. An introduction to attenuation correction. *J Nucl Cardiol.* 1999; 6(4):449-457.
23. Corbett JR, Ficaro EP. Clinical review of attenuation-corrected cardiac SPECT. *J Nucl Cardiol.* 1999; 6(1 Pt 1):54-68.
24. DePuey EG, Garcia EV. Optimal specificity of thallium-201 SPECT through recognition of imaging artifacts. *J Nucl Med.* 1989; 30(4):441-449.
25. Gallowitsch HJ, Sykora J, Mikosch P, Kresnik E, Unterweger O, Molnar M et al. Attenuation-corrected thallium-201 single-photon emission tomography using a gadolinium-153 moving line source: clinical value and the impact of attenuation correction on the extent and severity of perfusion abnormalities. *Eur J Nucl Med.* 1998; 25(3):220-228.
26. O'connor MK, Kemp B, Anstett F, Christian P, Ficaro EP, Frey E et al. A multicenter evaluation of commercial attenuation compensation techniques in cardiac SPECT using phantom models. *J Nucl Cardiol.* 2002; 9(4):361-376.
27. Matsunari I, Boning G, Ziegler SI, Nekolla SG, Stollfuss JC, Kosa I et al. Attenuation-corrected 99mTc-tetrofosmin single-photon emission computed tomography in the detection of viable myocardium: comparison with positron emission tomography using 18F-fluorodeoxyglucose. *J Am Coll Cardiol.* 1998; 32(4):927-935.
28. Wallis JW, Miller TR. Rapidly converging iterative reconstruction algorithms in single-photon emission computed tomography. *J Nucl Med.* 1993; 34(10):1793-1800.
29. Cerqueira MD, Weissman NJ, Dilsizian V, Jacobs AK, Kaul S, Laskey WK et al. Standardized myocardial segmentation and nomenclature for tomographic imaging of the heart: a statement for healthcare professionals from the Cardiac Imaging Committee of the Council on Clinical Cardiology of the American Heart Association. *J Nucl Cardiol.* 2002; 9(2):240-245.
30. Ficaro EP, Kritzman JN, Corbett JR. Development and clinical validation of normal Tc-99m sestamibi database: comparison of 3D-MSPECT to Cequal [abstract]. [abstract]. *J Nucl Med.* 1999; 40(suppl)(125P).
31. Maes AF, Borgers M, Flameng W, Nuyts JL, van de Werf F, Ausma JJ et al. Assessment of myocardial viability in chronic coronary artery disease using technetium-99m sestamibi SPECT. Correlation with histologic and positron emission tomographic studies and functional follow-up. *J Am Coll Cardiol.* 1997; 29(1):62-68.

32. Schinkel AF, Bax JJ, Valkema R, Elhendy A, van Domburg RT, Vourvouri EC et al. Effect of diabetes mellitus on myocardial 18F-FDG SPECT using acipimox for the assessment of myocardial viability. *J Nucl Med.* 2003; 44(6):877-883.
33. Fleiss JL. *Statistical Methods for Rates and Proportions.* 2nd ed. ed. New York, NY: Wiley; 1981:212-236.
34. Platts EA, North TL, Pickett RD, Kelly JD. Mechanism of uptake of technetium-tetrofosmin. I: Uptake into isolated adult rat ventricular myocytes and subcellular localization. *J Nucl Cardiol.* 1995; 2(4):317-326.
35. Lee VS, Resnick D, Tiu SS, Sanger JJ, Nazzaro CA, Israel GM et al. MR imaging evaluation of myocardial viability in the setting of equivocal SPECT results with (99m)Tc sestamibi. *Radiology.* 2004; 230(1):191-197.
36. Marzullo P, Parodi O, Sambuceti G, Reisenhofer B, Gimelli A, Giorgetti A et al. Myocardial viability: nuclear medicine versus stress echocardiography. *Echocardiography.* 1995; 12(3):291-302.
37. Bax JJ, Wijns W, Cornel JH, Visser FC, Boersma E, Fioretti PM. Accuracy of currently available techniques for prediction of functional recovery after revascularization in patients with left ventricular dysfunction due to chronic coronary artery disease: comparison of pooled data. *J Am Coll Cardiol.* 1997; 30(6):1451-1460.
38. Flamen P, Bossuyt A, Franken PR. Technetium-99m-tetrofosmin in dipyridamole-stress myocardial SPECT imaging: intraindividual comparison with technetium-99m-sestamibi. *J Nucl Med.* 1995; 36(11):2009-2015.
39. Shaw LJ, Hendel R, Borges-Neto S, Lauer MS, Alazraki N, Burnette J et al. Prognostic value of normal exercise and adenosine (99m)Tc-tetrofosmin SPECT imaging: results from the multicenter registry of 4,728 patients. *J Nucl Med.* 2003; 44(2):134-139.
40. Altehoefer C, Kaiser HJ, Dorr R, Feinendegen C, Beilin I, Uebis R et al. Fluorine-18 deoxyglucose PET for assessment of viable myocardium in perfusion defects in 99mTc-MIBI SPET: a comparative study in patients with coronary artery disease. *Eur J Nucl Med.* 1992; 19(5):334-342.
41. Soufer R, Dey HM, Ng CK, Zaret BL. Comparison of sestamibi single-photon emission computed tomography with positron emission tomography for estimating left ventricular myocardial viability. *Am J Cardiol.* 1995; 75(17):1214-1219.
42. Banzo I, Pena FJ, Allende RH, Quirce R, Carril JM. Prospective clinical comparison of non-corrected and attenuation- and scatter-corrected myocardial perfusion SPECT in patients with suspicion of coronary artery disease. *Nucl Med Commun.* 2003; 24(9):995-1002.
43. Kluge R, Sattler B, Seese A, Knapp WH. Attenuation correction by simultaneous emission-transmission myocardial single-photon emission tomography using a technetium-99m-labelled radiotracer: impact on diagnostic accuracy. *Eur J Nucl Med.* 1997; 24(9):1107-1114.
44. Slart RH, Que TH, Van Veldhuisen DJ, Poot L, Blanksma PK, Piers DA et al. Effect of attenuation correction on the interpretation of (99m)Tc-sestamibi myocardial perfusion scintigraphy: the impact of 1 year's experience. Eur J *Nucl Med Mol Imaging.* 2003; 30(11):1505-1509.
45. Matsunari I, Kanayama S, Yoneyama T, Matsudaira M, Nakajima K, Taki J et al. Myocardial distribution of (18)F-FDG and (99m)Tc-sestamibi on dual-isotope simultaneous acquisition SPET compared with PET. *Eur J Nucl Med Mol Imaging.* 2002; 29(10):1357-1364.

SECTION III

DISA SPECT for the detection of myocardial viability

Chapter 4

Comparison of ^{99m}Tc-sestamibi-^{18}F-fluorodeoxyglucose dual isotope simultaneous acquisition and rest-stress ^{99m}Tc-sestamibi SPECT for the assessment of myocardial viability

Jaep de Boer[1], Riemer H.J.A. Slart[1], Paul K. Blanksma[2], Antoon T.M. Willemsen[1], Pieter L. Jager[1], Anne M.J. Paans[1], Willem Vaalburg[1], D. Albertus Piers[1].

Departments of Nuclear Medicine and Molecular Imaging[1], Cardiology[2], University Medical Center Groningen, The Netherlands.

Nucl Med Commun 2003 Mar;24(3):251-7.

Abstract

Background: Dual isotope simultaneous acquisition (DISA) SPECT offers the advantage of obtaining information on myocardial perfusion using ^{99m}Tc-sestamibi and metabolism using ^{18}F-fluorodeoxyglucose (FDG) in a single study. The prerequisite is that the ^{99m}Tc-sestamibi images are not degraded by scattered 511 keV photons or poor count statistics due to a lower efficiency of the extra high energy collimator (EHE). Therefore, we compared the registered ^{99m}Tc-sestamibi uptake and image quality of a DISA SPECT and single isotope SPECT acquisition. Furthermore we investigated whether DISA SPECT yields additional information for the assessment of myocardial viability in comparison with rest-stress ^{99m}Tc-sestamibi.

Methods: 19 patients with known coronary artery disease and irreversible perfusion defects on previous rest-stress MIBI test studies were studied. After oral glucose loading and simultaneous injection of 600 MBq ^{99m}Tc-sestamibi and 185 MBq FDG at rest, DISA SPECT was performed using energy windows of 140 ± 15%, 170 ± 20% and 511 ± 15% keV. Planar 140 keV images were corrected for scatter by subtraction using the 170 keV window. The single and dual isotope ^{99m}Tc-sestamibi images were both displayed in a polar map with 128 segments normalized to maximum counts. FDG and ^{99m}Tc-sestamibi images were visually scored for a perfusion-metabolism mismatch pattern using 9 regions per heart.

Results: There was an excellent correlation (r =0.93, P <0.0001) of the ^{99m}Tc-sestamibi uptake as detected in the single and dual isotope acquisition. The average difference of the dual and single isotope ^{99m}Tc-sestamibi uptake was -1.2% (NS from zero) and the coefficient of variation of the difference was 8.7**%**

Of the 79 regions with irreversible perfusion defects on prior rest-stress ^{99m}Tc-sestamibi, 6 regions in 5 patients (7.6%, P <0.0034) showed a perfusion-metabolism mismatch pattern.

Conclusion: We conclude that in DISA SPECT acquisition does not affect the quality of the ^{99m}Tc-sestamibi images. Furthermore ^{99m}Tc-sestamibi-FDG DISA SPECT may show viability in a small but significant number of regions with irreversible perfusion defects on rest-stress ^{99m}Tc-sestamibi.

Keywords: Dual Isotope Simultaneous Acquisition, SPECT, ^{99m}Tc-sestamibi, ^{18}F-fluorodeoxyglucose, myocardial viability

Introduction

In patients with coronary artery disease and poor left ventricular function identification of viable myocardium is needed prior to revascularization. When viable tissue is revascularized, left ventricular function and ejection fraction improve significantly (1,2), the frequency of cardiac events is reduced and life expectancy is increased (3,4). For routine practice dobutamine-echocardiography and nuclear imaging techniques can be used for the assessment of myocardial viability. ^{201}Tl-rest-redistribution scintigraphy shows intact myocardial membrane function (5,6). Intact myocardial glucose metabolism can be shown by ^{18}F-fluorodeoxyglucose (FDG) imaging (2,3,7) and intact myocardial mitochondrial uptake is demonstrated by ^{99m}Tc-sestamibi scintigraphy (8,9). While scintigraphy with single photon emission computed tomography (SPECT) tracers ^{201}Tl- and ^{99m}Tc-sestamibi are used routinely mostly, FDG positron emission tomography (PET) has emerged as the most sensitive and specific technique (10). FDG is transportable due to its relatively long half-life (110 min) and, as a result of the limited availability of PET cameras, acquisition with SPECT using extra high energy (EHE) collimators (511 keV) is considered as a clinically useful alternative (11-14). In addition, SPECT dual isotope simultaneous acquisition (DISA) using a 140 keV and a 511 keV window has the advantage that information on myocardial perfusion with ^{99m}Tc-sestamibi and metabolism with FDG can be obtained at the same time (14,15). This results in a fast, patient-friendly protocol and identically oriented metabolism and perfusion images. However, the prerequisite is that the ^{99m}Tc-sestamibi images are not degraded by scatter of 511 keV photons and poor count statistics due to the lower efficiency of the EHE collimator.

The first main goal of our study was to evaluate the quality of the ^{99m}Tc-sestamibi images of the DISA SPECT acquisition. Therefore we compared quantitatively and qualitatively the ^{99m}Tc-sestamibi images of a single and dual isotope acquisition.

From other comparative studies, it is known that ^{99m}Tc-sestamibi tends to underestimate myocardial viability in comparison with FDG PET (8,9,16-18). Therefore, our second goal was to investigate whether signs of myocardial viability could be detected with FDG SPECT in irreversible perfusion defects present on previous rest-stress ^{99m}Tc-sestamibi.

Materials and methods

Patients

We studied 19 patients with known coronary artery disease and no signs of stress induced ischemia (i.e. only irreversible perfusion defects) on prior rest-stress ^{99m}Tc-sestamibi. Patients with diabetes mellitus were excluded. Patients were studied because of chest pain, congestive heart failure, ventricular fibrillation or recent infarction. The median delay between the rest-stress ^{99m}Tc-sestamibi and DISA SPECT studies was 27 days (range 1-63 days). No cardiac events occurred between the studies. Patient characteristics are summarized in Table 1. All patients gave informed consent. The study was approved by the Local Medical Ethics Committee.

Table 1. Demographic and clinical characteristics of 19 patients.

Characteristic	Value
Sex (male/female)	17/2
Age: years	62 (range 38-75)
Previous myocardial infarction	14
Prior revascularization:	
CABG	8
PTCA	3
Symptoms:	
Angina	15
Congestive heart failure	5
Ventricular fibrillation	2
Angiographic findings:	
Single vessel disease	7
Double vessel disease	5
Triple vessel disease	3
Unavailable	4
Ejection fraction:	
>50%	8
30-50%	7
<30%	3
Not available	1

CABG: coronary artery bypass graft; PTCA: percutaneous transluminal coronary angioplasty.

Rest-stress ^{99m}Tc-sestamibi imaging

Patients were studied after an overnight fast and refrained from caffeine and theophylline. Using a two day protocol and a single-headed gamma camera (Siemens Orbiter) with a low-energy high-resolution collimator (Siemens) ^{99m}Tc-sestamibi images were acquired one hour after intravenous injection of 600 MBq ^{99m}Tc-sestamibi at rest and at peak exercise (8 patients) or 4 minutes after intravenous dipyridamole (0.56 mg/kg body weight in 4 min) infusion (11 patients). Chocolate and coffee were given after the injection to promote liver clearance of ^{99m}Tc-sestamibi. With the patient in supine position, 64 projections were acquired in a circular orbit of 180° (45° right anterior oblique (RAO) to 45° left posterior oblique (LPO)); 20 s each angle, energy peak at 140 keV ± 15%. Images were reconstructed using filtered backprojection with a Butterworth filter (N_f 0.5, order 6) and reoriented along the short axis, vertical long axis and horizontal long axis of the heart.

DISA SPECT imaging

Patients were instructed to have a glucose rich breakfast and were given a 75 g oral glucose load 45 min prior to the simultaneous injection of 600 MBq ^{99m}Tc-sestamibi and 185 MBq FDG at rest. After the injection a chocolate bar and coffee were given to enhance the

hepatic clearance of ^{99m}Tc-sestamibi. Sixty minutes post injection, DISA SPECT was started. A Siemens Multispect double-headed gamma camera with EHE collimators (Siemens) was used, with one head activated during acquisition. In this way, image qualities of the double-headed camera were not favoured relative to the images of the single-headed gamma camera. Three energy windows were set at 140 ± 15%, 170 ± 20% and 511 ± 15% keV. Sixty-four projections were acquired over a circular orbit of 180° (45° RAO to 45° LPO; 30 s per angle). The total acquisition time was 35 min. Planar 140 keV images were corrected for scatter by subtraction of the 170 keV images using a convolution based correction method (19). The planar FDG images were corrected for decay of ^{18}F during acquisition. Short axis, vertical long axis and horizontal long axis images of ^{99m}Tc-sestamibi and FDG were reconstructed using identical axes and filtered backprojection with a Butterworth filter (N_f 0.5, order 6 for both the FDG and ^{99m}Tc-sestamibi study). In this way, identically oriented FDG and ^{99m}Tc-sestamibi images were obtained from DISA SPECT.

Comparison of detected uptake of ^{99m}Tc-sestamibi in single versus dual isotope acquisition

Both studies were analysed quantitatively en qualitatively. Visual analysis and quantitative analysis was done separately. It was assumed that the orientation of the separately acquired single and dual isotope ^{99m}Tc-sestamibi scans was comparable after reorientation. Eight short axis slices were analyzed, starting at the apex. First, for each slice, the epi- and endocardial contours were determined automatically as described previously (20). Each slice was divided into 16 equiangular segments between the two contours. For each segment the mean activity was calculated resulting in a total of 128 activity values per study. These values were normalized and expressed as percentage of the maximum of each image. Least-squares linear regression analysis and the method of Bland and Altman (21) were used to evaluate the segmental ^{99m}Tc-sestamibi uptake of the single isotope acquisition versus the dual isotope acquisition.

Viability assessment

Short and long axis images of the rest-stress ^{99m}Tc-sestamibi images and DISA SPECT images, viewed on a computer screen, were read by four experienced readers in consensus. A nine-region heart model was used. One region was assigned to the apex. The anterior, septal, inferior and lateral walls were divided into a distal and basal region. The regions of the rest-stress ^{99m}Tc-sestamibi studies were classified into two categories: 1) *normal perfusion:* normal stress ^{99m}Tc-sestamibi uptake or a mildly irreversibly reduced ^{99m}Tc-sestamibi uptake such as seen in cases of attenuation; 2) *irreversible perfusion defect*: moderate to severe irreversibly reduced uptake of ^{99m}Tc-sestamibi, indicative of scar tissue. Reversible perfusion defects were not found due to the inclusion criteria.

The regions of the DISA SPECT studies regions were classified into three categories: 1) *normal perfusion and metabolism*: intact ^{99m}Tc-sestamibi and FDG uptake; 2) *perfusion-metabolism mismatch defect:* a moderately to severely reduced ^{99m}Tc-sestamibi uptake in combination with an intact or relatively increased FDG uptake representing viable

myocardium; 3) *perfusion-metabolism match defects:* moderately to severely decreased uptake of both ^{99m}Tc-sestamibi and FDG indicative of scar tissue. The results of viability assessment were tested for significance using the Wilcoxon test for paired data. $P < 0.05$ was considered significant.

Results

Comparison of detected uptake of ^{99m}Tc-sestamibi of single versus dual isotope acquisition

In a total of 2432 segments, the ^{99m}Tc-sestamibi activity of the dual and single isotope acquisition correlated well ($r = 0.93$, $P < 0.0001$) (Figure 1A). Visual inspection showed no noticeable difference in quality of the rest ^{99m}Tc-sestamibi and DISA SPECT ^{99m}Tc-sestamibi studies (Figure 2). The average difference of the dual and single isotope ^{99m}Tc-sestamibi uptake was -1.2% (NS from zero) and the coefficient of variation of the difference was 8.7**%** (Figure 1B). Minor deviations were seen in the apical and basal slices of the heart due to partial volume effect and patient misalignment inherent to the separate acquisitions of the resting single isotope ^{99m}Tc-sestamibi and the DISA SPECT studies.

Viability assessment

Rest-stress ^{99m}Tc-sestamibi showed irreversible perfusion defects in 79 of 171 regions obtained from the 19 patients. Of these 79 regions 73 regions showed a match defect with DISA SPECT which is statistically significantly less ($P = 0.034$) than the 79 defects from the rest-stress ^{99m}Tc-sestamibi. With DISA SPECT 6 of the 79 (7.6%) irreversible ^{99m}Tc-sestamibi regions showed a perfusion-metabolism mismatch pattern indicating myocardial viability. These 6 regions were obtained in 5 patients. In 3 patients viability was found in the inferior wall, in 2 patients in the lateral wall and in one patient in the basal anterior wall (Figure 2).

Discussion

This study shows that after correction dual isotope ^{99m}Tc-sestamibi images are not degraded by scatter of the 511 keV photons in comparison with the separately acquired single isotope ^{99m}Tc-sestamibi images. In addition 7.6% (6/79) of the regions with irreversible perfusion defects on rest-stress ^{99m}Tc-sestamibi were viable with DISA SPECT as demonstrated by a perfusion metabolism mismatch pattern.

Dual isotope SPECT imaging

Myocardial FDG imaging with SPECT is a useful alternative in the absence of PET technology (11-14). In addition dual isotope simultaneous acquisition allows simultaneous imaging of either rest (22) or stress (14) perfusion with ^{99m}Tc-sestamibi and metabolism

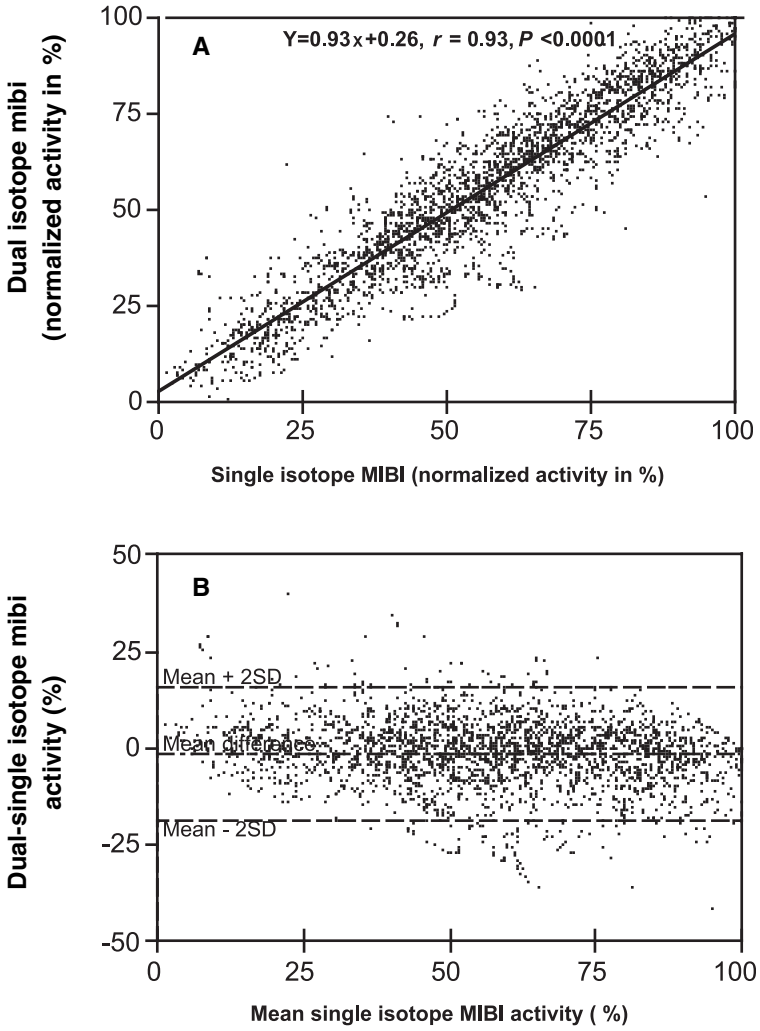

Figure 1

A. Correlation of normalized single isotope ^{99m}Tc-sestamibi uptake (x-axis) and normalized dual isotope ^{99m}Tc-sestamibi (y-axis). *MIBI = ^{99m}Tc-sestamibi*

B. Bland and Altman plot. Normalized mean single isotope ^{99m}Tc-sestamibi uptake (x-axis) against the difference between the dual versus normalized single isotope ^{99m}Tc-sestamibi uptake (y-axis). *MIBI = ^{99m}Tc-sestamibi*

with FDG. This results in a fast, patient friendly protocol that can be performed in any nuclear medicine department. These practical points advocate the use of cardiac FDG imaging with DISA SPECT (23). Despite the increasing clinical application of DISA SPECT, only a small number of clinical studies have been performed to evaluate the quality of the ^{99m}Tc-sestamibi images of the DISA SPECT acquisition (15,22). A comparable

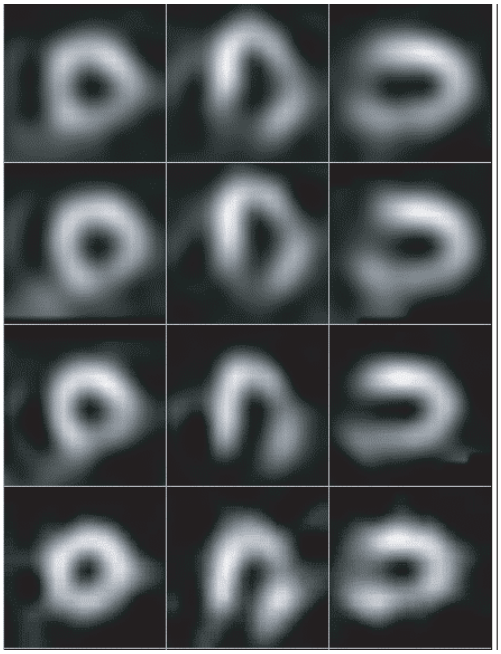

Figure 2. Example of a patient with an irreversible perfusion defect in the infero-lateral with rest-stress ^{99m}Tc-sestamibi and a perfusion-metabolism mismatch in this area with MIBI/FDG DISA SPECT.
Left row: short axis. Middle row: horizontal long axis. Right row: vertical long axis. MIBI = ^{99m}Tc-sestamibi

study with ^{99m}Tc-tetrofosmin-FDG was performed by Fukuchi et al. (24), which showed a good correlation between single-rest ^{99m}Tc-tetrofosmin and ^{99m}Tc-tetrofosmin images obtained from a scatter corrected DISA SPECT ^{99m}Tc-tetrofosmin-FDG study.
Although theoretically ^{99m}Tc-sestamibi images could be degraded by scattered 511 keV photons and poor count statistics due to the EHE collimator, our results showed no difference between the normalized dual and single isotope ^{99m}Tc-sestamibi uptake. The efficiency ratio in count detecting of our EHE collimator compared to the LEHR collimator in the 140 keV window is about 30%. Visual inspection showed no noticeable difference in quality of the rest ^{99m}Tc-sestamibi and DISA SPECT ^{99m}Tc-sestamibi studies. The results in our patients are in accordance with other comparable studies (15,22,24), and a cardiac-phantom study (22). Scatter distribution in the technetium window can become significant in physiologically unlikely situations of a fourfold increase of metabolism in combination with a twofold reduced perfusion (22).
In all patients, the FDG scans were interpretable. However, in some patients image quality was suboptimal due to a heterogeneous FDG uptake. This has also been reported by others (25,26). Image quality can be increased with an euglycemic hyperinsulinemic clamp or the use of acipimox in order to lower the circulating free fatty acids and increase the blood insulin concentration. This results in a more homogeneous myocardial glucose and FDG uptake (25,27).

FDG as a viability tracer

FDG is considered an excellent tracer for the detection of myocardial viability. The feasibly of SPECT acquisition of FDG with extra high energy collimators has been described (11,28) and improvement of ventricular wall motion after revascularization could be detected with a sensitivity and specificity of 84% and 86%, respectively (25). The FDG uptake of SPECT and PET were highly concordant in three studies (12,13,29). Although in these studies patients were not revascularized, it is to be expected that acquisition with SPECT may replace PET for routine purposes.
We also found a small (7.6%) but significant increase in the number of viable regions with FDG SPECT in comparison with rest-stress ^{99m}Tc-sestamibi. This is in accordance with the general finding that ^{99m}Tc-sestamibi has a sensitivity somewhat lower than FDG for detection of myocardial viability.

^{99m}Tc-sestamibi as a viability tracer

The application of ^{99m}Tc-labeled perfusion agents for the assessment of myocardial viability has been debated. While some publications (30-32) indicate that ^{99m}Tc-sestamibi SPECT can be used, other comparative studies report that ^{99m}Tc-sestamibi SPECT underestimates myocardial viability in comparison with ^{201}Tl (16,33) and FDG PET imaging (8,16-18,34). Myocardial perfusion defects are usually larger with ^{99m}Tc-sestamibi than with ^{13}N-ammonia PET (17). However, Siebelink (35) et al. demonstrated no difference in patient outcome and cardiac event free survival between management based on ^{13}N-ammonia/FDG PET and stress/rest ^{99m}Tc-sestamibi SPECT imaging.
In only in a small percentage (7.6%) of the irreversible perfusion defects a perfusion metabolism mismatch consistent with myocardial viability was found. This may have 2 causes. In the first place this might be due to a selection bias since we excluded patients with reversible perfusion defects. This suggests that we might have excluded patients with viable myocardium, which also indicates that ^{99m}Tc-sestamibi might be a rather good viability tracer in the majority of patients. However, our results also indicate that FDG may give additional information in a selected group of patients that have already undergone a rest-stress ^{99m}Tc-sestamibi study. Secondly, because we were not able to analyse wall motion in all the patients it is possible that regions with wall motion abnormalities but normal perfusion, which, by definition, were scored as normal in our study were in fact dysfunctional (due to stunning) but viable myocardium.

Limitations

In this study we compared two scintigraphic techniques. Most patients were not revascularized and also no systematic data on wall motion abnormalities were obtained from all patients. Therefore, the detection of myocardial viability, i.e. improvement of local wall motion after revascularization, could not be determined.

Conclusion

This study shows that, without loss of image quality rest ^{99m}Tc-sestamibi images can be acquired simultaneously with FDG using DISA SPECT. Therefore, dual isotope acquisition with FDG and ^{99m}Tc-sestamibi may become a clinically applicable routine method for the assessment myocardial viability. Furthermore, signs of viability were found with ^{99m}Tc-sestamibi-FDG DISA SPECT in a small, but significant number (7.6%) of regions with irreversible perfusion defects on rest-stress ^{99m}Tc-sestamibi.

Reference List

1. DiCarli MF, Asgarzadie F, Schelbert HR *et al*. Quantitative relation between myocardial viability and improvement in heart failure symptoms after revascularization in patients with ischemic cardiomyopathy. *Circulation* 1995;92:3436-3444.
2. Tillisch J, Brunken R, Marshall R *et al*. Reversibility of cardiac wall-motion abnormalities predicted by positron tomography. *N Engl J Med* 1986;314:884-888.
3. DiCarli MF, Davidson M, Little R *et al*. Value of metabolic imaging with positron emission tomography for evaluating prognosis in patients with coronary artery disease and left ventricular dysfunction. *Am J Cardiol* 1994;73:527-533.
4. Eitzman D, al Aouar Z; Kanter HL *et al*. Clinical outcome of patients with advanced coronary artery disease after viability studies with positron emission tomography. *J Am Coll Cardiol* 1992;20:559-565.
5. Dilsizian V, Rocco TP, Freedman NM, Leon MB, Bonow RO. Enhanced detection of ischemic but viable myocardium by the reinjection of thallium after stress-redistribution imaging. *N Engl J Med* 1990;323: 141-146.
6. Kiat H, Berman DS, Maddahi J *et al*. Late reversibility of tomographic myocardial thallium-201 defects: an accurate marker of myocardial viability. *J Am Coll Cardiol* 1988;12:1456-1463.
7. Bax JJ, Cornel JH, Visser FC *et al*. Prediction of improvement of contractile function in patients with ischemic ventricular dysfunction after revascularization by fluorine-18 fluorodeoxyglucose single-photon emission computed tomography. *J Am Coll Cardiol* 1997;30:377-383.
8. Altehoefer C, vom-Dahl J, Biedermann M *et al*. Significance of defect severity in technetium-99m-MIBI SPECT at rest to assess myocardial viability: comparison with fluorine-18-FDG PET. *J Nucl Med* 1994;35:569-574.
9. Lucignani G, Landoni C, Mengozzi G *et al*. Relation between dobutamine trans-thoracic echocardiography, 99mTc-MIBI and 18FDG uptake in chronic coronary artery disease. *Nucl Med Commun* 1995;16:548-557.
10. Bax JJ, Wijns W, Cornel JH, Visser FC, Boersma E, Fioretti PM. Accuracy of currently available techniques for prediction of functional recovery after revascularization in patients with left ventricular dysfunction due to chronic coronary artery disease: comparison of pooled data. *J Am Coll Cardiol* 1997;30:1451-1460.
11. Bax JJ, Visser FC, van Lingen A *et al*. Feasibility of assessing regional myocardial uptake of 18F-fluorodeoxyglucose using single photon emission computed tomography. *Eur Heart J* 1993;14:1675-1682.
12. Burt RW, Perkins OW, Oppenheim BE *et al*. Direct comparison of fluorine-18-FDG SPECT, fluorine-18-FDG PET and rest thallium-201 SPECT for detection of myocardial viability. *J Nucl Med* 1995;36:176-179.

13. Chen EQ, MacIntyre WJ, Go RT *et al*. Myocardial viability studies using fluorine-18-FDG SPECT: a comparison with fluorine-18-FDG PET. *J Nucl Med* 1997;38:582-586.
14. Sandler MP, Videlefsky S, Delbeke D *et al*. Evaluation of myocardial ischemia using a rest metabolism/stress perfusion protocol with fluorine-18 deoxyglucose/technetium-99m MIBI and dual-isotope simultaneous-acquisition single-photon emission computed tomography. *J Am Coll Cardiol* 1995;26:870-878.
15. Stoll HP, Hellwig N, Alexander C, Ozbek C, Schieffer H, Oberhausen E. Myocardial metabolic imaging by means of fluorine-18 deoxyglucose/technetium-99m sestamibi dual-isotope single-photon emission tomography. *Eur J Nucl Med* 1994;21:1085-1093.
16. Dilsizian V, Arrighi JA, Diodati JG *et al*. Myocardial viability in patients with chronic coronary artery disease. Comparison of 99mTc-sestamibi with thallium reinjection and [18F]fluorodeoxyglucose. *Circulation* 1994;89: 578-587.
17. Sawada S, Elsner G, Segar DS *et al*. Evaluation of patterns of perfusion and metabolism in dobutamine-responsive myocardium. *J Am Coll Cardiol* 1997;29:55-61.
18. Soufer R, Dey HM, Ng CK, Zaret BL. Comparison of sestamibi single-photon emission computed tomography with positron emission tomography for estimating left ventricular myocardial viability. *Am J Cardiol* 1995;75:1214-1219.
19. Kool W, Willemsen ATM, Paans AMJ, Piers DA. Convolution based triple enery window crosstalk correction for disa spect. *J Nucl Med* 1997; 38:89p (Abstract).
20. Blanksma PK, Willemsen AT, Meeder JG *et al*. Quantitative myocardial mapping of perfusion and metabolism using parametric polar map displays in cardiac PET. *J Nucl Med* 1995;36:153-158.
21. Bland JM, Altman DG. Statistical methods for assessing agreement between two methods of clinical measurement. *Lancet* 1986;1:307-310.
22. Delbeke D, Videlefsky S, Patton JA *et al*. Rest myocardial perfusion/metabolism imaging using simultaneous dual-isotope acquisition SPECT with technetium-99m-MIBI/fluorine-18-FDG. *J Nucl Med* 1995;36:2110-2119.
23. Sandler MP, Bax JJ, Patton JA, Visser FC, Martin WH, Wijns W. Fluorine-18-fluorodeoxyglucose cardiac imaging using a modified scintillation camera. *J Nucl Med* 1998;39:2035-2043.
24. Fukuchi K, Katafuchi T, Fukushima K *et al*. Estimation of myocardial perfusion and viability using simultaneous 99m-Tc-tetrofosmin-FDG collimated SPECT. *J Nucl Med* 2000;41:1318-1323.
25. Bax JJ, Veening MA, Visser FC et al. Optimal metabolic conditions during fluorine-18 fluorodeoxyglucose imaging; a comparative study using different protocols. *Eur J Nucl Med* 1997;24:35-41.
26. Martin WH, Jones RC, Delbeke D, Sandler MP. A simplified intravenous glucose loading protocol for fluorine-18 fluorodeoxyglucose cardiac single-photon emission tomography. *Eur J Nucl Med* 1997;24:1291-1297.
27. Knuuti MJ, Yki Jarvinen H, Voipio Pulkki LM *et al*. Enhancement of myocardial [fluorine-18]fluorodeoxyglucose uptake by a nicotinic acid derivative. *J Nucl Med* 1994;35:989-998.
28. Hoflin F, Ledermann H, Noelpp U, Weinreich R, Rosler H. Routine 18F-2-deoxy-2-fluoro-D-glucose (18F-FDG) myocardial tomography using a normal large field of view gamma-camera. *Angiology* 1989;40:1058-1064.
29. Bax JJ, Visser FC, Blanksma PK *et al*. Comparison of myocardial uptake of fluorine-18-fluorodeoxyglucose imaged with PET and SPECT in dyssynergic myocardium. *J Nucl Med* 1996;37:1631-1636.
30. Dakik HA, Howell JF, Lawrie GM *et al*. Assessment of myocardial viability with 99mTc-sestamibi tomography before coronary bypass graft surgery: correlation with histopathology and postoperative improvement in cardiac function. *Circulation* 1997;96:2892-2898.

31. Senior R, Raval U, Lahiri A. Technetium 99m-labeled sestamibi imaging reliably identifies retained contractile reserve in dyssynergic myocardial segments. *J Nucl Cardiol* 1995;2:296-302.
32. Udelson JE, Coleman PS, Metherall J *et al*. Predicting recovery of severe regional ventricular dysfunction. Comparison of resting scintigraphy with 201-Tl and 99mTc-sestamibi. *Circulation* 1994;89:2552-2561.
33. Cuocolo A, Pace L, Ricciardelli B, Chiariello M, Trimarco B, Salvatore M. Identification of viable myocardium in patients with chronic coronary artery disease: comparison of thallium-201 scintigraphy with reinjection and technetium-99m-methoxyisobutyl isonitrile. *J Nucl Med* 1992;33:505-511.
34. Sand NP, Bottcher M, Madsen MM, Nielsen TT, Rehling M. Evaluation of regional myocardial perfusion in patients with severe left ventricular dysfunction: comparison of 13N-ammonia PET and 99mTc sestamibi SPECT. *J Nucl Cardiol* 1998;5:4-13.
35. Siebelink HM, Blanksma PK, Crijns HJGM, *et al*. No different cardiac event free survival in positron emission tomography and single photon emission computed tomography guided patient management. A prospective randomized comparison in patients with suspicion of jeopardized myocardium. *J Am Coll Cardiol* 2001;37:81-88.

Chapter 5

Comparison of ^{99m}Tc-sestamibi/FDG DISA SPECT with PET for the detection of viability in patients with coronary artery disease and left ventricular dysfunction

Riemer H.J.A. Slart[1], Jeroen J. Bax[2], Jaep de Boer[3], Antoon T.M. Willemsen[1]
Piet H. Mook[4], Matthijs Oudkerk[4], Ernst E. van der Wall[2], Dirk J. van Veldhuisen[5];
Pieter L. Jager[1]

Department of Nuclear Medicine and Molecular Imaging[1], University Medical Center Groningen; Department of Cardiology[2], Leiden University Medical Center; Department of Nuclear Medicine[3], Diaconessenhuis Meppel; Department of Radiology[4], University Medical Center Groningen; Department of Cardiology[5], University Medical Center Groningen, The Netherlands.

Eur J Nucl Med Mol Imaging 2005. In press.

Abstract

Aim: Dual isotope simultaneous acquisition (DISA) SPECT is an attractive technique as it permits assessment of both myocardial glucose metabolism and perfusion within in a single session, but few data on its accuracy for assessment of viability are available as yet. In the present study, DISA SPECT was compared with PET for the detection of myocardial viability in normal and dysfunctional left ventricle (LV) myocardium.
Methods: Fifty-eight patients with chronic coronary artery disease and LV dysfunction (LV ejection fraction 33 ± 12%) were studied. Patients underwent a 1-day dipyridamole stress ^{99m}Tc-sestamibi/FDG DISA SPECT and ^{13}N-ammonia/FDG PET protocol. Within 1 week, resting MRI was performed to assess contractile function. Comparison of PET and SPECT data was performed using both visual and quantitative analysis.
Results: The correlation of normalized activities of the flow tracers ^{99m}Tc-sestamibi and ^{13}N-ammonia was good, ($r = 0.82$; $P < 0.001$). The correlation between both FDG studies was also good ($r = 0.83$; $P < 0.001$). The agreement for the assessment of viability for all segments between DISA SPECT and PET was 82%, with a κ-statistic of 0.59 (95% CI 0.53 - 0.64), without a significant difference; in dysfunctional segments only, the agreement was 82%, with a κ-statistic of 0.63 (95% CI 0.56 - 0.70), without a significant difference. When the DISA SPECT data were analyzed visually, the agreement between DISA SPECT and PET was 83%, with a κ-statistic of 0.58 (95% CI 0.52 - 0.63), without a significant difference. Moreover, there was no significant difference between visual and quantitative DISA SPECT analysis for the detection of viability.
Conclusion: This study shows an overall good agreement between ^{99m}Tc-sestamibi/FDG DISA SPECT and PET for the assessment of myocardial viability in patients with severe LV dysfunction. Quantitative or visual analysis of the SPECT data did not influence the agreement with PET, suggesting that visual assessment may be sufficient for clinical purposes.

Keywords: myocardial viability, acipimox, FDG, DISA SPECT, PET.

Introduction

The assessment of myocardial viability has become an important aspect of the diagnostic and prognostic work up of patients with coronary artery disease (CAD) and left ventricular (LV) dysfunction. Patients with viable myocardium have been demonstrated to benefit from revascularization, with an improvement in LV function and a favourable prognosis after revascularization (1-4).

Positron emission tomography (PET) imaging using fluorine –18 fluorodeoxyglucose (FDG) combined with a flow tracer such as nitrogen-13 ammonia (^{13}N-ammonia) is an accurate non-invasive diagnostic technique to distinguish viable myocardium from scar tissue in patients with chronic coronary artery disease (4,5). However, the clinical use of the technique is still limited owing to the restricted availability of PET equipment. To meet the increasing demand, substantial effort has been invested in the development of single photon emission computed tomography (SPECT) using extra-high energy collimators, which may permit larger scale clinical use of FDG imaging (6-8). Another advantage of SPECT with FDG is the possibility of dual-isotope simultaneous acquisition (DISA) in which ^{99m}Tc-labeled myocardial perfusion agent and FDG can be imaged in a single acquisition session. Besides the time saving effect of DISA, the simultaneous acquisition also guarantees identical geometric registration of the patient for both sets of images. To date, only two small patient studies have described the agreement in tracer distribution between DISA SPECT and PET (7,9). In order to meet the clinical demand of viability studies, the DISA SPECT protocol needs further adaptation to simplify the procedure, to ensure high patient throughput. In particular, visual analysis of data may be preferred over quantitative analysis, but currently no study has addressed this topic. Moreover, the metabolic circumstances during FDG imaging are important and imaging following acipimox (Nedios®, Byk, The Netherlands), a nicotinic acid derivative, has been proposed as the most simple approach, even in patients with diabetes mellitus (10-12). However, FDG SPECT imaging following acipimox has also not been compared directly with PET imaging. We performed a head-to-head comparison between DISA SPECT and PET using both visual and quantitative analysis with patient preparation using acipimox, to study the degree of agreement between these methods.

Materials and methods

Patients

Fifty-eight patients with chronic CAD and LV dysfunction were included (46 men, mean age 65 ± 9 years, range 41-83). Thirty-eight patients (65%) had a history of myocardial infarction (>3 months ago) and 17 patients (29%) had undergone previous revascularization (>3 months before the study). The mean LV ejection fraction (LVEF) in the patient group was 33 ± 12% and LVEF data was obtained with previous clinical multigated equilibrium radionuclide angiography (ERNA) or gated SPECT (< 3 months before the study).

Twelve patients had diabetes mellitus type 2, which was well regulated by oral hypoglycemics and/or insulin.
Patients with unstable angina and/or heart failure requiring hospitalization were excluded. None of the patients had cardiac events or therapeutic interventions during the study. All subjects signed an informed consent form based on the guidelines of the institutional ethics committee prior to participation in the study.
The PET and DISA acquisitions were performed on the same day, starting with PET (schematic outline, see Figure 1). One minute after ^{13}N-ammonia injection, 600 MBq of ^{99m}Tc-sestamibi was injected intravenously with the purpose for DISA acquisition later. The DISA acquisition was performed later during the day, using the same FDG as injected shortly before the PET images. Perfusion was studied during dipyridamole stress to analyse viability in segments with chronic and/or reduced flow reserve; using this protocol, discrimination between stress-induced ischemia and viability (with resting hypoperfusion) is not possible, but for clinical purposes both represent jeopardized myocardium which need to be revascularized.

Positron emission tomography
All anti-anginal medication and caffeine containing beverages were withdrawn at least 24 hr prior to the PET studies. Patients were prepared with a glucose-enriched breakfast. Ninety minutes prior to FDG injection acipimox (500) mg was administered orally to lower the circulating free fatty acids (11). To prevent side effects of acipimox (eg. skin rash), 250 mg of aspirin was administered orally 5 minutes before acipimox intake. Guided by the plasma glucose levels, patients received additional insulin as previously described (12).
PET acquisition was performed on an ECAT-951/31 PET system (Siemens/CTI, Knoxville, TN, USA) imaging 31 planes over a total axial length of 10.8 cm. Following the transmission scan (^{68}Ge/^{68}Ga rod sources), dipyridamole infusion (0.56 mg/kg/body weight in 6 minutes) was started. The dynamic acquisition procedure was started immediately after injection of 400 MBq of ^{13}N-ammonia, 6 minutes after start of dipyridamole infusion, and continued for 15 minutes. After completion of the ^{13}N-ammonia data acquisition, 400 MBq of FDG was injected intravenously, followed by the PET dynamic acquisition procedure. The total FDG PET acquisition time was 40 minutes, with the last 20 minutes acquired in

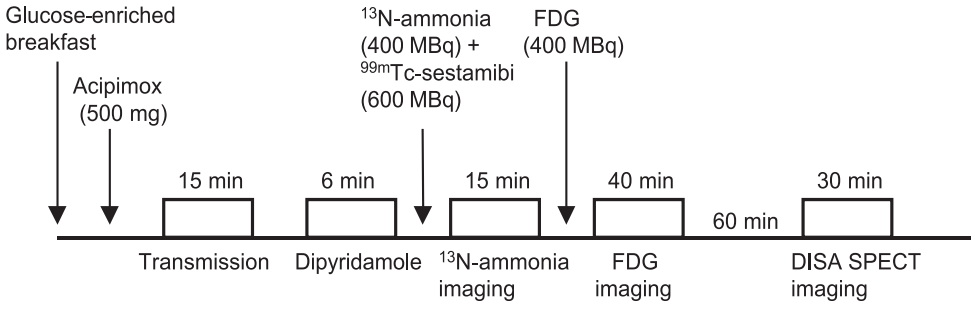

Figure 1. Schematic outline of DISA SPECT and PET protocol.

gated mode with 16 frames per cardiac cycle. The myocardial count rate was higher than 10 kcps (true coincidents). All gated FDG PET scans were obtained in phased mode, that is, the length of each gate was optimized for the current RR-interval. The RR-interval was allowed to vary by ± 10%. Data were corrected for attenuation with the transmission scan and were reconstructed using filtered back-projection (Hann filter: 0.5 pixels/cycle).
After manual reorientation, 12 short-axis images of FDG and ^{13}N-ammonia were obtained with a plane thickness from 7 to 9 mm at an in-plane resolution of approximately 7 mm. Myocardial tissue was corrected for spillover of activity from the blood pool in the LV myocardium. For equal comparison of PET versus DISA, the dynamic PET studies were transformed into static studies, as proposed by the clinical guidelines for interpretation and reporting (13). Frames of gated FDG PET were summed and used for further data analysis. Similarly, the frames of the last 8 minutes of the ^{13}N-ammonia acquisition were summed and used for further analysis.

DISA SPECT

DISA SPECT acquisition was performed on the same day, 1 hr after completion of the PET scan. In the 1-hour waiting time, patients received chocolate and coffee to enhance hepatic clearance of ^{99m}Tc-sestamibi. A Siemens MultiSPECT dual-headed gamma camera with extra-high energy (EHE) collimators (Siemens) was used, with only one head activated during acquisition (360 degrees had no better results) (14,15). The resolution of the EHE collimator is 10.4 mm full-width at half-maximum (FWHM) for ^{18}F and 9.2 mm for ^{99m}Tc at 10 cm distance from the collimator face. Three energy windows were set at 140 (± 15%), 170 (± 20%) and 511 keV (± 15%). Sixty-four projections were acquired over a circular orbit of 180° (45° RAO to 45° LPO; 30 s per angle). The total acquisition time was 30 min. Planar 140 keV images were corrected for scatter by subtraction of the 170 keV images using a convolution-based correction method (14,15). The planar FDG images were corrected for the decay of ^{18}F during acquisition. Short-, vertical -, and horizontal long-axis images of FDG were reconstructed using filtered back projection with a Butterworth filter (Nyquist frequency 0.5, order 6 for both the FDG and ^{99m}Tc-sestamibi study). In this way identically oriented FDG and ^{99m}Tc-sestamibi images were obtained from the DISA SPECT acquisition.

Data analysis and viability criteria for PET and DISA SPECT

All data from the PET and DISA SPECT studies were re-orientated to short-axis, horizontal and vertical long-axis sections. Data of FDG, ^{13}N-ammonia and ^{99m}Tc-sestamibi were analysed quantitatively and displayed in a 17-segment polar map as recently proposed (16), using the 4D-MSPECT program, a commercially available cardiac software package (developed by the University of Michigan Medical Center, Ann Arbor, MI, USA) (17). Average counts per segment were obtained from the 17 segments and the measured counts were normalized to the segment with the highest average counts.
For both PET and DISA segments were considered to be viable when the perfusion activity was $\geqslant$75% or perfusion activity was $<$75% but FDG activity $\geqslant$10% than the perfusion

activity (perfusion - FDG mismatch). Mismatch patterns can be caused by hibernation (i.e. reduced resting flow with increased FDG uptake), but also (since dipyridamole perfusion was used) by (post-ischemic) stunning or stress-induced ischemia.
Segments were considered non-viable, when the normalized activity was $<$75% and the difference in activities between the perfusion tracer and FDG was 10%. Segments were subdivided in non-transmural scar tissue when the normalized perfusion activity was >25% and $<$75% with a FDG - perfusion tracer difference $<$10%. Segments were considered as transmural scar tissue when the normalized perfusion activity was $\leq$25% with a FDG - perfusion tracer difference $<$10%.
For DISA SPECT, segmental ^{99m}Tc-sestamibi and FDG uptake were also scored visually by two experienced observers in agreement using a 4-grade scoring system: 1 = normal tracer uptake (activity 75-100%), 2 = moderately reduced tracer uptake (activity 50-75%), 3 = severely reduced tracer uptake (activity 25-50%) 4 = absent tracer uptake (activity $<$25%). Segments were considered viable when the perfusion tracer score was 1 or when the FDG uptake grade score was higher than the ^{99m}Tc-sestamibi uptake score (perfusion - FDG mismatch). Segments were considered as non-transmural scar tissue when a perfusion defect (score 2 or 3) exhibited concordantly reduced FDG uptake (mild to moderate match pattern). Segments were considered transmural scar tissue when a perfusion defect (score 4) exhibited concordantly reduced FDG uptake (severe match pattern). PET was used as the reference method for verification of all DISA SPECT data.

MRI to assess contractile function
Images were acquired on a 1.5 Tesla MRI system (Vision, Siemens Medical Systems, Erlangen, Germany) equipped with high performance gradients (maximum gradient strength = 40 mT/m; maximum slew rate = 200 mT/m/ms). Patients were examined in the supine position using a flexible body array coil for signal reception.
Scout images depicting the myocardium were acquired in the coronal and sagital imaging planes using a 2-D FLASH ECG-triggered sequence (one slice per heartbeat; TR = 40 – 100 ms, TE = 6 ms, flip angle = 58°, field of view (FOV) = 300 – 350 mm, slice thickness = 8 mm) after which the short-axis plane was determined. The short-axis plane was defined perpendicular to the LV long-axis from the center of the mitral annulus to the apex. Slices were acquired at 8 to10 LV base to apex short-axis locations during repeated breath-holds (± 15 seconds). Images were reconstructed using 2D-Fourier reconstruction with in-plane matrix of 128 x 256 (reconstructed voxel size = 17.6 mm^3). The TR were varied depending on the R-R interval of the patient and the number of cardiac phases to be imaged. A Sparc workstation (Sun Microsystems, Mountain View, CA, USA) was used for further analysis of data. LV volumes were calculated from the MR images using previously validated automated software (MR Analytical Software System [MASS], Leiden, The Netherlands) (18). The window width and window level settings were determined automatically by scaling to the maximum grey scale. For the assessment of regional wall motions, MRI images were visually interpreted by a single, experienced observer blinded to the PET results. A 17-segment model was used and each segment was assigned a

wall motion score using a 4-point scoring system. 1 = normal wall motion, 2 = hypokinesia, 3 = akinesia, 4 = aneurysm pattern**.**

Statistical analysis

All results were expressed as mean ± SD. The comparison of segmental tracer uptake for PET and DISA SPECT was evaluated by linear regression and correlation analysis (Pearson correlation coefficient). The degree of agreement between segmental tracer uptake in the same segments in PET and DISA studies was tested by Bland-Altman analysis (19). Limits of agreement were calculated using the mean of the differences ± SD. Agreement for viability in normal and dysfunctional segments was assessed from 2 x 2 and 3 x 3 tables using weighted kappa statistics. Kappa values of <0.4, between 0.4 and 0.75, and >0.75 were considered to represent poor, fair to good, and excellent agreement, respectively, based on the Fleiss classification (20). The kappa values are reported with their 95% confidence intervals (95% CI) and their SEs. McNemar test was used to analyse concordancy in segments between DISA SPECT and PET. Statistical significance was defined as $P<0.05$.

Results

Of 986 segments, 24 (2%) segments were excluded from further analysis because of interfering overprojection of infra-diaphagmatical activity or misalignment of the left ventricle in the field of view in the PET camera. Accordingly, 962 segments were used for further analysis.

DISA SPECT versus PET, normalized tracer activities.

Linear regression revealed a high correlation between the normalized activity of the perfusion tracers ^{99m}Tc-sestamibi and ^{13}N-ammonia ($r=0.82$; $y=0.89x+4.0$; $P<0.001$). The highest correlation was in the distal anterior segment ($r=0.92$; $P<0.001$), the lowest in the basal inferior septal segment, although still significant ($r=0.58$; $P<0.001$).

Bland-Altman analysis revealed a difference of higher mean activity ratio of ^{13}N-ammonia versus ^{99m}Tc-sestamibi of 3.1 ± 10.7, but without a significant trend and within limits of 24 to -18%, (95% CI: 3.1 - 3.8, see Figure 2A). There was no tendency toward greater differences at different mean uptake values.

The correlation between both FDG studies was also high ($r=0.83$; $y=0.95-0.24$; $P<0.001$). The highest correlation between both studies was in the distal anterior segment ($r=0.90$; $P<0.001$), the lowest in the basal inferior septal segment, although still significant ($r=0.56$; $P<0.001$). Bland-Altman analysis revealed a difference of higher mean activity ratio of FDG PET versus FDG DISA SPECT of 3.6 ± 9.6, but without a significant trend and within limits of 22 to -15% (CI: 3.6 - 4.2, see Figure 2B).

There was also no tendency toward greater differences at different mean uptake values.

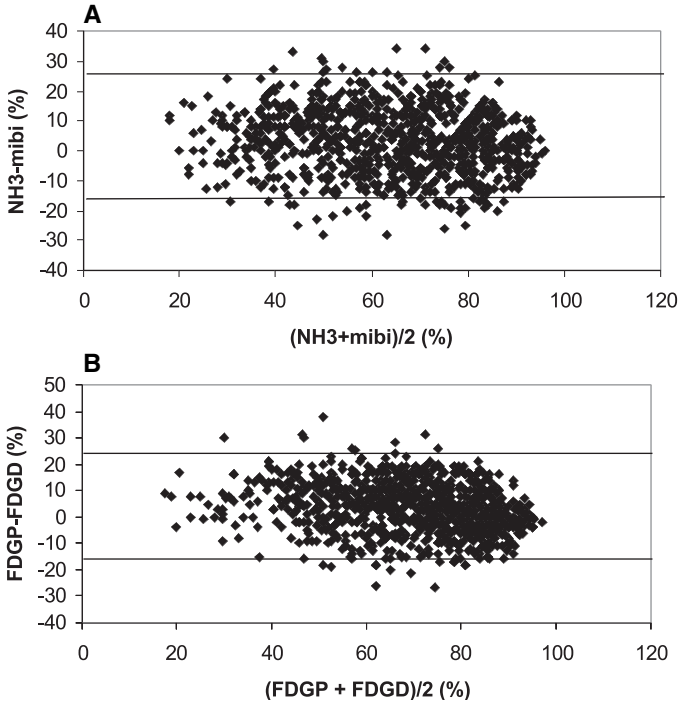

Figure 2. Bland-Altman plots illustrating the absolute difference between ^{99m}Tc-sestamibi versus ^{13}N-ammonia (A) and FDG DISA SPECT (FDGD) versus FDG PET (FDGP) (B).

DISA SPECT versus PET: quantitative assessment of viability in all segments

The agreement for tissue characterization in the 962 segments between DISA SPECT and PET was 82%, with a κ-statistic of 0.59 (95% CI 0.53 - 0.64; SE 0.027; see Figure 3). There was no significant difference between DISA SPECT and PET in the detection of viability in these segments (*P* = NS). Most discordant segments for the detection of viability with DISA SPECT in comparison to PET were located in the basal anterior wall (25 of 51 (49%) segments), whereas the least false positive or false negative segments were observed in the mid-inferior wall (3 of 58 (5%) segments).

DISA SPECT versus PET: quantitative assessment of viability in dysfunctional myocardium

On MRI, 457 (47%) segments showed normal wall motion, whereas 505 (53%) segments revealed abnormal wall motion. In particular, 368 segments were hypokinetic, 121 akinetic and 16 dyskinetic.

The agreement for the detection viability between DISA SPECT and PET in all 505 dysfunctional segments was 82%, with a κ-statistic of 0.63 (95% CI 0.56 - 0.70; SE 0.034). There was no significant difference between DISA and PET in the detection of viability in segments (*P* = NS).

When the non-viable segments were divided into non-transmural and transmural scars, the agreement was 79%, with a κ-statistic of 0.62 (95% CI 0.53 - 0.70; SE 0.045; see Table 1). According to PET, 239 (65%) of 368 hypokinetic segments were classified as

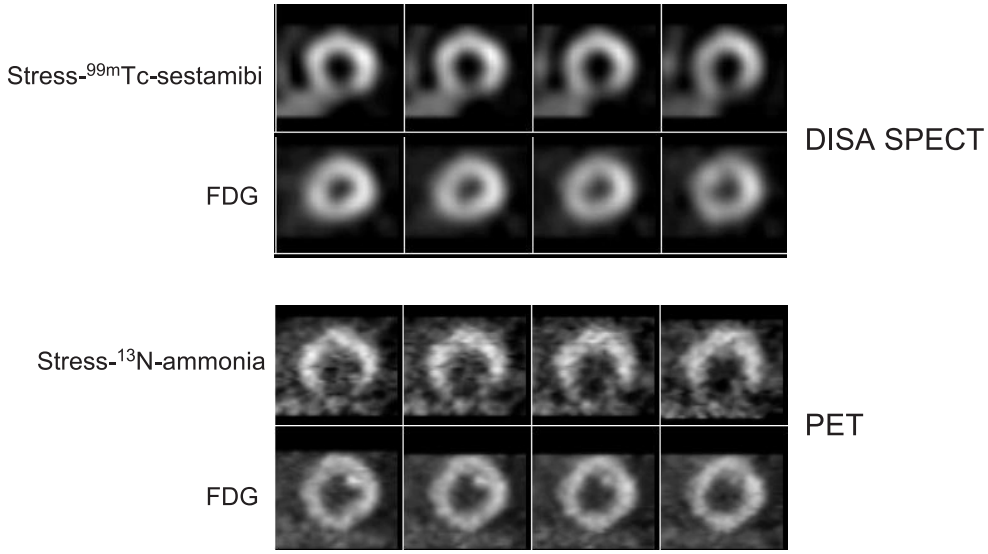

Figure 3. Short-axis series of a corresponding DISA SPECT and PET study. Of note, both series (PET and DISA SPECT) show reduced myocardial perfusion with preserved FDG uptake in the inferior wall, indicating viable tissue.

viable, as compared to 215 (58%) on DISA SPECT (agreement 79%). In the 137 a- and dyskinetic segments, the agreement between PET and DISA SPECT was 83% (with 66 segments classified as viable on PET and 61 on DISA SPECT).

Visual analysis of DISA SPECT versus PET: assessment of viability in all segments

The agreement for tissue characterization in the 962 segments between visual analysis of DISA SPECT and quantitative PET was 83%, with a κ-statistic of 0.58 (95% CI 0.52 - 0.63; SE 0.029; see Table 2). There was no significant difference between DISA SPECT and PET in the detection of viability in these segments (P = NS).

Visual analysis of DISA SPECT: assessment of viability in dysfunctional myocardium.

The agreement for the detection of viability between visual analysis of DISA SPECT and

Table 1. Agreement for the detection of viable, non-transmural (NTM) and transmural (TM) dysfunctional segments of DISA SPECT vs PET (n = 505 segments).

	PET viable	PET NTM	PET TM
DISA viable	245	31	0
DISA NTM	59	154	3
DISA TM	1	8	4

Table 2. Agreement PET and visual analysis DISA SPECT (V-DISA) for the detection of in all viable and non-viable segments (n = 962 segments).

	PET viable	PET non-viable
V-DISA viable	667	44
V-DISA non-viable	36	215

PET in all 505 dysfunctional segments was 89%, with a κ-statistic of 0.79 (95% CI 0.72 - 0.83; SE 0.028).
When the visual and quantitative SPECT data were compared directly, there was no significant difference between the visual and quantitative DISA SPECT analysis in the detection of viability in all segments (P = NS). The agreement for the detection viability in all 505 dysfunctional segments between visual and quantitative analysis DISA SPECT was 86%, with a κ-statistic of 0.72 (95% CI 0.65 - 0.77; SE 0.031).

Discussion

The most important finding of this study was a good agreement between DISA SPECT and PET for the assessment of viability for all or dysfunctional segments, without a significant discordance. In addition, visually or quantitatively analyzed DISA SPECT data compared equally with the PET data. These observations suggest that DISA SPECT provides adequate information on myocardial viability and visual analysis of data may be sufficient for clinical purposes.

Comparison to previous studies
The normalized regional acitivity of ^{99m}Tc-sestamibi correlated well with ^{13}N-ammonia, as was the case for the normalized FDG SPECT and PET activities. These findings are in line with previous studies: Srinivasan et al. analyzed the correlation between FDG DISA SPECT and FDG PET in 28 patients with CAD and found an overall good agreement (94%) and correlation (r = 0.81, slope = 0.79), with a mean difference of 9.6% between both techniques (21). Also the study of Fukuchi et al. resulted in comparable FDG findings in 18 patients with CAD, using ^{99m}Tc-tetrofosmin/ FDG DISA SPECT in comparison to PET (r = 0.86, κ-statistic of 0.67) (7). Direct comparison of the perfusion tracers ^{99m}Tc-sestamibi/ FDG DISA SPECT and ^{13}N-ammonia PET are scarce. The only such study to have been publicated was a small investigation by Matsunari et al., who analyzed the concordance and discordance of ^{99m}Tc-sestamibi/FDG DISA SPECT and ^{13}N-ammonia/ FDG PET in ten patients with CAD on the basis on the difference between the perfusion tracer and FDG with the two techniques (9).
Similar to the agreement in perfusion values, we also found a very good overall agreement using PET or DISA for the assessment of myocardial viability, both in segments with normal wall motion and in dysfunctional segments. In dysfunctional myocardium in par-

Table 3: Head-to-head comparison between FDG SPECT or DISA SPECT and FDG PET for the evaluation of myocardial viability (131 patients, 6 studies)

Author (ref)	Patients (n)	Imaging approach	Metabolic circumstances	Perfusion tracer	Data analysis	LVEF(%)	Agreement(%) or Kappa (κ)
Burt (34)	20	sequential	oral glucose load	^{201}Tl at rest	Visual	NA	93
Martin (35)	9	sequential	oral glucose load	MIBI or ^{201}Tl at rest	Visual	NA	100
Bax (36)	20	sequential	clamp	^{201}Tl at rest	Quant	39±16	76
Chen (37)	36	sequential	oral glucose load	^{82}Rb stress & rest	Quant	NA	90
Srinivasan (21)	28	sequential	oral glucose load	^{201}Tl stress & rest	Quant	33±15	94
Fukuchi (7)	18	DISA	oral glucose load	^{99m}Tc-tetrof. at rest	Quant	35±9	κ = 0.67
Present study	58	DISA	Acipimox	MIBI stress	Quant	33±12	82

Ref = reference; LVEF = left ventricular ejection fraction; DISA; dual isotope simultaneous acquisition; MIBI = ^{99m}Tc-sestamibi; ^{99m}Tc-tetrof = ^{99m}Tc-tetrofosmin; Quant = quantitative; NA = not available.

ticular, the assessment of viability is important, since these regions need to be considered for revascularization (3,22,23). The agreement in dysfunctional segments was 82% when quantitative DISA SPECT was compared with PET and also 82% when visually analyzed DISA SPECT was compared with PET. These observations are in line with previous studies comparing FDG PET and SPECT in the same patients. The available studies are summarized in detail in Table 3. This summary indicates also that the direct comparisons between PET and SPECT are still limited (n= 6, with 131 patients). This pool will be enlarged by the addition of our data, which also focus on other important issues not addressed previously.

A first difference between published studies and the current one is that the majority of these studies (5 out of 6) did not perform DISA SPECT, but rather performed sequential perfusion and FDG SPECT imaging. Currently, state-of-the-art FDG imaging with SPECT may utilize dual-isotope imaging and simultaneous acquisition, as used in the current study. DISA SPECT offers important advantages, including shorter imaging time and perfect alignment between perfusion and FDG images.

A second difference is that 3 out of 6 studies were not performed in patients with severe LV dysfunction, although these are the patients who need viability assessment in order to justify the enhanced risk of revascularization (24-27). For this reason, only patients with a LVEF $<$ 35% were included in the current study, and the findings indicate that FDG SPECT also compares well to PET in this subset of patients.

A third difference is that the majority of the available studies performed visual or quantitative analysis of the data, whereas both quantitative and visual analysis were performed in the present study. Furthermore, the metabolic conditions during which FDG imaging is performed are important. This is the first study that reports on FDG imaging with both SPECT and PET after administration of acipimox, which is the most simple and patient-friendly approach and ensures good image quality in virtually all patients, even in those with diabetes if whom insulin is co-administered (12).

Finally, the imaging protocol used in the present study was not used previously (Table 3),

namely perfusion was assessed during pharmacological stress. Although omission of the resting perfusion images no longer allows discrimination between repetitively stunned myocardium (with normal resting perfusion) and hibernating myocardium (with reduced resting perfusion), this information is mainly of interest for research purposes. Other studies have demonstrated that resting perfusion was near normal in chronic dysfunctional myocardium (28,29). Vanoverschelde et al. observed similar levels of perfusion with PET in regions with normal contraction and regions with chronic dysfunction (29). These authors showed that instead of resting flow, flow reserve was reduced in dysfunctional but viable myocardium (29). Based on their observations, Vanoverschelde and co-workers suggested that repeated ischemic attacks may result in chronic dysfunction, with flow remaining normal or mildly reduced, a condition referred to as repetitive stunning (30). The current DISA SPECT study, however aimed at providing a simple protocol for detection of viability of hibernating myocardium and dysfunctional myocardium based on reduced flow reserve.

In the present study, most segments that yielded discordant results for assessment of viability were located in the basal anterior wall; the precise reason for that finding is unclear. Considering the difference in photon energies between ^{18}F and ^{99m}Tc, one would anticipate the most discrepancies in the inferior and septal regions, which are the regions most susceptible to attenuation. The present data, however, suggest that attenuation does not markedly influence the identification of viable myocardium using DISA SPECT. Most importantly, no specific over- or underestimation of viability by SPECT was observed.

Furthermore, 65% of the hypokinetic segments were classified as viable on PET, as compared to 58% on DISA SPECT (agreement 79%). In hypokinetic segments more viability would be presumed. However, many dysfunctional segments showed severe hypokinesia, probably due to the presence of non-viable myocardial tissue. This may explain the high percentage of severe hypokinetic, but non-viable segments. The observation is in line with previous studies (31).

Clinical implications

The protocol described for DISA SPECT is a simple approach, and may allow high patient throughput, in order to meet the increasing demand for viability studies with the exponentially increasing number of patients presenting with ischemic cardiomyopathy (32). In particular, the use of acipimox may further simplify the procedure and still ensure good image quality.

One open issue was the analysis of data. Quantitative analysis is considered the most accurate form of analyzing the data, although for routine clinical purposes visual analysis may be preferred. To date, a systematic comparison of visual and quantitative analysis of FDG SPECT data is not available. The findings in the current study indicate that both analyses compared equally to FDG PET suggesting that visual analysis may be sufficient in the clinical setting.

All analyses of data were performed with 4D-MSPECT. Besides extensive analysis of the perfusion and FDG data, this program does also allow assessment of function when data

are acquired in the gating mode. This may particularly be attractive in patients with severe LV dysfunction who need viability testing, since LVEF, LV volumes and regional wall motion may then be determined in one imaging session.

Study limitations

The major limitation of the study is the lack of assessment of outcome after revascularization. A direct comparison between DISA SPECT and PET against the gold standard i.e. improvement of wall motion after revascularization is needed before definitive conclusions can be drawn.

Another, technical limitation hampering the current direct comparison of DISA SPECT and PET is that the SPECT data were not corrected for attenuation. Attenuation correction may improve the accuracy for detection of myocardial viability (33). Additional studies specifically addressing the issue of (correction for) attenuation are needed. Also the delay of FDG injection and DISA SPECT acquisition may possibly influence the quality of the DISA SPECT images. To overcome the problems of radiation decay patients were injected with 400 MBq FDG instead of the usual dose of 200 MBq in our hospital.

Conclusion

This study shows good overall agreement between ^{99m}Tc-sestamibi/FDG DISA SPECT and PET for the assessment of myocardial viability in patients with severe LV dysfunction. Agreement with PET was similar with quantitative or visual analysis of the SPECT data, suggesting that visual assessment may be sufficient for clinical purposes. The use of acipimox simplifies the DISA SPECT procedure and still ensures reliable assessment of myocardial viability with FDG.

Acknowledgment

We thank Wim J. Sluiter and Hans J. Hillege for their assistance in statistical data analysis.

Reference List

1. Allman KC, Shaw LJ, Hachamovitch R, Udelson JE. Myocardial viability testing and impact of revascularization on prognosis in patients with coronary artery disease and left ventricular dysfunction: a meta-analysis. *J Am Coll Cardiol.* 2002; 39(7):1151-1158.
2. Baer FM, Voth E, Deutsch HJ, Schneider CA, Horst M, de Vivie ER et al. Predictive value of low dose dobutamine transesophageal echocardiography and fluorine-18 fluorodeoxyglucose positron emission tomography for recovery of regional left ventricular function after successful revascularization. *J Am Coll Cardiol.* 1996; 28(1):60-69.
3. Bax JJ, Cornel JH, Visser FC, Fioretti PM, Van Lingen A, Reijs AE et al. Prediction of recovery of myocardial dysfunction after revascularization. Comparison of fluorine-18 fluorodeoxyglucose/thallium-201 SPECT, thallium-201 stress-reinjection SPECT and dobutamine echocardiography. *J Am Coll Cardiol.* 1996; 28(3):558-564.
4. Tillisch J, Brunken R, Marshall R, Schwaiger M, Mandelkern M, Phelps M et al. Reversibility of cardiac wall-motion abnormalities predicted by positron tomography. *N Engl J Med.* 1986; 314(14):884-888.
5. Tamaki N, Kawamoto M, Tadamura E, Magata Y, Yonekura Y, Nohara R et al. Prediction of reversible ischemia after revascularization. Perfusion and metabolic studies with positron emission tomography. *Circulation.* 1995; 91(6):1697-1705.
6. Delbeke D, Videlefsky S, Patton JA, Campbell MG, Martin WH, Ohana I et al. Rest myocardial perfusion/metabolism imaging using simultaneous dual-isotope acquisition SPECT with technetium-99m-MIBI/fluorine-18-FDG. *J Nucl Med.* 1995; 36(11):2110-2119.
7. Fukuchi K, Katafuchi T, Fukushima K, Shimotsu Y, Toba M, Hayashida K et al. Estimation of myocardial perfusion and viability using simultaneous 99mTc-tetrofosmin--FDG collimated SPECT. *J Nucl Med.* 2000; 41(8):1318-1323.
8. Sandler MP, Videlefsky S, Delbeke D, Patton JA, Meyerowitz C, Martin WH et al. Evaluation of myocardial ischemia using a rest metabolism/stress perfusion protocol with fluorine-18 deoxyglucose/technetium-99m MIBI and dual-isotope simultaneous-acquisition single-photon emission computed tomography. *J Am Coll Cardiol.* 1995; 26(4):870-878.
9. Matsunari I, Kanayama S, Yoneyama T, Matsudaira M, Nakajima K, Taki J et al. Myocardial distribution of (18)F-FDG and (99m)Tc-sestamibi on dual-isotope simultaneous acquisition SPET compared with PET. Eur J Nucl Med Mol Imaging. 2002; 29(10):1357-1364.
10. Bax JJ, Visser FC, Poldermans D, Van Lingen A, Elhendy A, Boersma E et al. Safety and feasibility of cardiac FDG SPECT following oral administration of Acipimox, a nicotinic acid derivative: Comparison of image quality with hyperinsulinemic euglycemic clamping in nondiabetic patients. J Nucl Cardiol. 2002; 9(6):587-593.
11. Knuuti MJ, Yki-Jarvinen H, Voipio-Pulkki LM, Maki M, Ruotsalainen U, Harkonen R et al. Enhancement of myocardial [fluorine-18]fluorodeoxyglucose uptake by a nicotinic acid derivative. J Nucl Med. 1994; 35(6):989-998.
12. Schinkel AF, Bax JJ, Valkema R, Elhendy A, van Domburg RT, Vourvouri EC et al. Effect of diabetes mellitus on myocardial 18F-FDG SPECT using acipimox for the assessment of myocardial viability. J Nucl Med. 2003; 44(6):877-883.
13. Schelbert HR, Beanlands R, Bengel F, Knuuti J, Dicarli M, Machac J et al. PET myocardial perfusion and glucose metabolism imaging: Part 2-Guidelines for interpretation and reporting. J Nucl Cardiol. 2003; 10(5):557-571.
14. De Boer J, Slart RH, Blanksma PK, Willemsen AT, Jager PL, Paans AM et al. Comparison of 99mTc-sestamibi-18F-fluorodeoxyglucose dual isotope simultaneous acquisition and rest-

stress 99mTc-sestamibi single photon emission computed tomography for the assessment of myocardial viability. Nucl Med Commun. 2003; 24(3):251-257.
15. Kool W, Willemsen ATM, Paans AMJ, Piers DA. Convolution based triple energy window crosstalk correction for DISA SPECT. [abstract]. J Nucl Med. 1997; 38(89).
16. Hendel RC, Corbett JR, Cullom SJ, DePuey EG, Garcia EV, Bateman TM. The value and practice of attenuation correction for myocardial perfusion SPECT imaging: a joint position statement from the American Society of Nuclear Cardiology and the Society of Nuclear Medicine. J Nucl Cardiol. 2002; 9(1):135-143.
17. Ficaro EP, Kritzman JN, Corbett JR. Development and clinical validation of normal Tc-99m sestamibi database: comparison of 3D-MSPECT to Cequal [abstract]. [abstract]. J Nucl Med. 1999; 40(suppl)(125P).
18. van der Geest RJ, Buller VG, Jansen E, Lamb HJ, Baur LH, van der Wall EE et al. Comparison between manual and semiautomated analysis of left ventricular volume parameters from short-axis MR images. J Comput Assist Tomogr. 1997; 21(5):756-765.
19. Bland JM, Altman DG. Statistical methods for assessing agreement between two methods of clinical measurement. Lancet. 1986; 1(8476):307-310.
20. Fleiss JL. Statistical methods for rates and proportions. 2nd ed. New York: 1981:212-236.
21. Srinivasan G, Kitsiou AN, Bacharach SL, Bartlett ML, Miller-Davis C, Dilsizian V. [18F]fluorodeoxyglucose single photon emission computed tomography: can it replace PET and thallium SPECT for the assessment of myocardial viability? Circulation. 1998; 97(9):843-850.
22. Camici PG, Wijns W, Borgers M, De Silva R, Ferrari R, Knuuti J et al. Pathophysiological mechanisms of chronic reversible left ventricular dysfunction due to coronary artery disease (hibernating myocardium). Circulation. 1997; 96(9):3205-3214.
23. Rahimtoola SH. The hibernating myocardium. Am Heart J. 1989; 117(1):211-221.
24. Bax JJ, Wijns W, Cornel JH, Visser FC, Boersma E, Fioretti PM. Accuracy of currently available techniques for prediction of functional recovery after revascularization in patients with left ventricular dysfunction due to chronic coronary artery disease: comparison of pooled data. J Am Coll Cardiol. 1997; 30(6):1451-1460.
25. Di Carli MF, Davidson M, Little R, Khanna S, Mody FV, Brunken RC et al. Value of metabolic imaging with positron emission tomography for evaluating prognosis in patients with coronary artery disease and left ventricular dysfunction. Am J Cardiol. 1994; 73(8):527-533.
26. Haas F, Haehnel CJ, Picker W, Nekolla S, Martinoff S, Meisner H et al. Preoperative positron emission tomographic viability assessment and perioperative and postoperative risk in patients with advanced ischemic heart disease. J Am Coll Cardiol. 1997; 30(7):1693-1700.
27. Lee KS, Marwick TH, Cook SA, Go RT, Fix JS, James KB et al. Prognosis of patients with left ventricular dysfunction, with and without viable myocardium after myocardial infarction. Relative efficacy of medical therapy and revascularization. Circulation. 1994; 90(6):2687-2694.
28. Canty J-MJ, Fallavollita JA. Resting myocardial flow in hibernating myocardium: validating animal models of human pathophysiology. Am J Physiol. 1999; 277(1 Pt 2):H417-H422.
29. Vanoverschelde JL, Wijns W, Depre C, Essamri B, Heyndrickx GR, Borgers M et al. Mechanisms of chronic regional postischemic dysfunction in humans. New insights from the study of noninfarcted collateral-dependent myocardium. Circulation. 1993; 87(5):1513-1523.
30. Vanoverschelde JL, Melin JA. The pathophysiology of myocardial hibernation: current controversies and future directions. Prog Cardiovasc Dis. 2001; 43(5):387-398.
31. Rambaldi R, Poldermans D, Bax JJ, Boersma E, Valkema R, Elhendy A et al. Dobutamine stress echocardiography and technetium-99m-tetrofosmin/fluorine 18-fluorodeoxyglucose single-photon emission computed tomography and influence of resting ejection fraction to assess myocardial viability in patients with severe left ventricular dysfunction and healed myocardial infarction. Am J Cardiol. 1999; 84(2):130-134.

32. Haldeman GA, Croft JB, Giles WH, Rashidee A. Hospitalization of patients with heart failure: National Hospital Discharge Survey, 1985 to 1995. Am Heart J. 1999; 137(2):352-360.
33. Slart RH, Que TH, van Veldhuisen DJ, Poot L, Blanksma PK, Piers DA et al. Effect of attenuation correction on the interpretation of 99mTc-sestamibi myocardial perfusion scintigraphy: the impact of 1 year's experience. Eur J Nucl Med Mol Imaging. 2003; 30(11):1505-1509.
34. Burt RW, Perkins OW, Oppenheim BE, Schauwecker DS, Stein L, Wellman HN et al. Direct comparison of fluorine-18-FDG SPECT, fluorine-18-FDG PET and rest thallium-201 SPECT for detection of myocardial viability. J Nucl Med. 1995; 36(2):176-179.
35. Martin WH, Delbeke D, Patton JA, Hendrix B, Weinfeld Z, Ohana I et al. FDG-SPECT: correlation with FDG-PET. J Nucl Med. 1995; 36(6):988-995.
36. Bax JJ, Visser FC, Blanksma PK, Veening MA, Tan ES, Willemsen TM et al. Comparison of myocardial uptake of fluorine-18-fluorodeoxyglucose imaged with PET and SPECT in dyssynergic myocardium. J Nucl Med. 1996; 37(10):1631-1636.
37. Chen EQ, MacIntyre WJ, Go RT, Brunken RC, Saha GB, Wong CY et al. Myocardial viability studies using fluorine-18-FDG SPECT: a comparison with fluorine-18-FDG PET. J Nucl Med. 1997; 38(4):582-586.

Chapter 6

Prediction of functional recovery after revascularization in patients with chronic ischemic left ventricular dysfunction: head-to-head comparison between ^{99m}Tc-sestamibi/FDG DISA SPECT and ^{13}N-ammonia/FDG PET.

Riemer H.J.A. Slart[1], Jeroen J. Bax[2], Dirk J. van Veldhuisen[3], Ernst E. van der Wall[2], Matthijs Oudkerk[4], Wim J. Sluiter[5], Rudi A.J.O. Dierckx[1], Jaep de Boer[6], Pieter L. Jager[1]

Department of Nuclear Medicine and Molecular Imaging[1], University Medical Center Groningen; Department of Cardiology[2], Leiden University Medical Center; Department of Cardiology[3], University Medical Center Groningen; Department of Radiology[4], University Medical Center Groningen; Department of Endocrinology[5], University Medical Center Groningen; Department of Nuclear Medicine[6], Diaconessenhuis Meppel, The Netherlands.

Submitted.

Abstract

Background: FDG PET is an important modality for myocardial viability assessment in patients with left ventricular (LV) dysfunction. Dual isotope simultaneous acquisition (DISA) SPECT may be an alternative to PET. The aim of this study was to compare the diagnostic performance of PET and DISA SPECT for the prediction of regional function, global LV function and LV remodelling in patients with LV dysfunction undergoing revascularization.

Methods and Results: Patients (n=47) with chronic coronary artery disease and LV dysfunction underwent DISA SPECT (with ^{99m}Tc-sestamibi and FDG) and PET (with ^{13}N-ammonia and FDG) on the same day. ROC analysis was applied to determine the optimal cutoff values in viability assessment. Segmental and global functional recovery as determined by serial MRI serving as the reference method for viability.

Of 264 revascularized dysfunctional segments, 143 (54%) recovered in function. For prediction of improvement in regional LV function, PET and DISA SPECT had similar sensitivity (90% vs 89%, (*P* = NS)) and specificity (86% vs 86%, (*P* = NS)). For prediction of improvement in global LV function, sensitivity was 83% for DISA SPECT and 86% for PET (*P* = NS), at specificity of 100% for both. Reverse LV remodeling occurred in viable patients after revascularization, whereas nonviable patients showed further LV dilatation after revascularization. Sensitivity and specificity for the prediction of LV reverse remodeling were similar for DISA SPECT and PET.

Conclusion: In patients undergoing revascularisation, DISA SPECT and PET predict the improvement in regional LV function, global LV function and LV remodeling equally well.

Key Words: myocardial viability, prediction, functional LV recovery, DISA SPECT, PET

Introduction

The assessment of myocardial viability has become an important aspect of the diagnostic and prognostic work-up of patients with coronary artery disease (CAD) and left ventricular (LV) dysfunction. Patients with viable myocardium benefit from revascularization, in terms of an improved LV function and a favourable long-term prognosis after revascularization (1,2).

Positron emission tomography (PET) imaging using fluoride –18 fluorodeoxyglucose (FDG) combined with a flow tracer (e.g. ^{13}N-ammonia) is an accurate non-invasive diagnostic technique to distinguish viable myocardium from scar tissue in patients with chronic coronary artery disease (2,3). However, for routine clinical use this PET technique is less available, more expensive and time consuming compared to (single photon emission computed tomography) SPECT. For the production of the required perfusion tracers such as ^{13}N-ammonia or ^{15}O-water, a cyclotron is necessary. Generator-produced Rubidium-82 chloride (^{82}Rb) can be used as an alternative perfusion PET tracer, but is relatively expensive, especially when infrequently used.

To meet the increasing demand for viability studies (4), substantial effort has been invested in the development of (SPECT) methods. Using extra-high energy collimators, FDG imaging is possible, and this may permit clinical use of FDG imaging on a large scale (5-7). Another advantage of SPECT is the possibility of dual-isotope simultaneous acquisition (DISA) in which a ^{99m}Tc-labeled myocardial perfusion agent and FDG can be performed in a single session. DISA SPECT allows for shorter duration of procedures, and guaranties an identical geometric registration of the different isotope images. Despite these potential advantages, DISA SPECT imaging has not been validated in a direct head-to-head comparison with PET imaging in patients with LV dysfunction, using optimal reference methods. Therefore, the aim of this study was to prospectively study the diagnostic performance of DISA SPECT and PET in the prediction of LV improvement after revascularization in the same group of patients with chronic ischemic LV dysfunction, using magnetic resonance imaging (MRI) before and after revascularision as the reference method, and coronary angiography for quality control. As the optimal cut-off points in viability assessment in DISA SPECT and PET imaging are unclear, we first performed receiver operating characteristics (ROC) analysis on DISA SPECT and PET data, and used the results in the final viability assessments. Finally, we evaluated the relation between patient characteristics and the prediction of LV improvement after revascularization.

Materials and methods

Patients

Between April 2000 and July 2003, we included 47 consecutive patients with chronic CAD and LV dysfunction (41 men, mean age 65 ± 9 years, range 41 to 82) referred for

revascularization to the University Hospital Groningen, a tertiary referral center for the north of the Netherlands. Thirty-four patients (72%) had a history of myocardial infarction (>3 months ago) and 14 patients (29%) had undergone previous revascularization (>3 months before the study). The mean LV ejection fraction (LVEF) in the patient group was 33 ± 12% at rest, estimated from equilibrium radionuclide angiography (ERNA) or gated myocardial perfusion SPECT. The patients had on average 2.4 ± 0.8 stenosed coronary arteries on coronary angiography. Ten patients had diabetes mellitus, that was well-regulated by combinations of oral hypoglycemics and insulin in all cases, as this is required for optimal FDG uptake and image quality. Patients with unstable angina or heart failure requiring hospitalization were excluded. None of the patients had cardiac events during the study and the 6-months follow-up period.

The study procedures are outlined in Figure 1. PET and DISA SPECT acquisition were performed on the same day. Assessment of contractile function by MRI was performed within one week after DISA SPECT/PET and was repeated 6 months after revascularization. All surgeons and cardiologists were blinded to the PET and DISA SPECT results. Coronary angiography was repeated 6 months after revascularization to exclude re-occlusion of the revascularized coronary arteries or bypass grafts. The study protocol was approved by the Medical Ethics committee of our institution and all patients gave written informed consent. To improve the quality of reporting the diagnostic accuracy of this study, the Standards for Reporting of Diagnostic Accuracy (STARD) stategy was used (8).

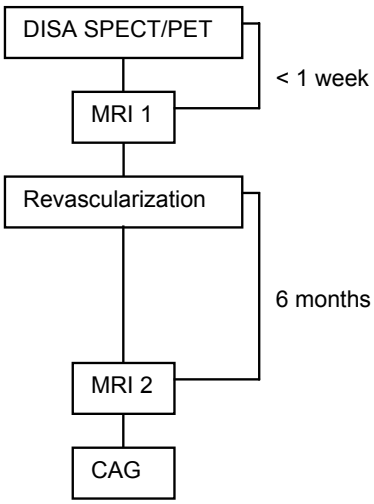

Figure 1. Schematic outline of the study procedures. CAG: coronary angiography.

Positron emission tomography

All anti-anginal medication and caffeine containing beverages were withdrawn at least 24 hours prior to the PET and SPECT studies. The PET and DISA SPECT protocol is outlined in Figure 2. Patients used a glucose-enriched breakfast. Ninety minutes prior to FDG injection, 500 mg acipimox (Nedios, Byk, The Netherlands), was administered orally to lower circulating free fatty acids (9). To prevent side-effects of acipimox (eg. skin rash), 250 mg of aspirin was administered orally 5 minutes before acipimox intake. Guided by the plasma glucose levels, 4 patients received additional insulin as previously described (10). In short, in patients with a plasma glucose level >9 mmol/L at baseline, 6 units of insulin were administered subcutaneously. When plasma glucose levels remained >9 mmol/L, additional insulin was administered.

We used an ECAT-951/31 PET scanner (Siemens/CTI, Knoxville, TN, USA), that acquires

31 planes over a total axial length of 10.8 cm. Following the transmission scan (using ^{68}Ge/^{68}Ga rod sources), 0.56 mg/kg/body dipyridamole was infused in 6 minutes. Two minutes after the end of the dipyridamole infusion, 400 MBq of ^{13}N-ammonia was injected. Dynamic data of ^{13}N-ammonia were then acquired over 15 minutes. After completion of the ^{13}N-ammonia data acquisition, 400 MBq of FDG was injected intravenously, followed by a PET dynamic acquisition procedure. The total FDG PET acquisition time was 40 minutes, with the last 20 minutes acquired in gated mode with 16 frames per cardiac cycle. The length of each gate was based on the current RR-interval. The RR-interval was allowed to vary by ± 10%. Data were corrected for attenuation using the transmission scan and were reconstructed using filtered back-projection (Hann filter: 0.5 pixels/cycle).
After manual reorientation, 12 short-axis images of FDG and ^{13}N-ammonia were obtained with a plane thickness of 7 mm at an in-plane resolution of approximately 7 mm. Myocardial tissue activity was corrected for spillover of activity from the LV cavity. For equal comparison of PET versus DISA SPECT, the frames of the last 8 minutes of the ^{13}N-ammonia acquisition were summed and used for further analysis. Similarly, all 16 frames of gated FDG PET were summed and used for further data analysis.

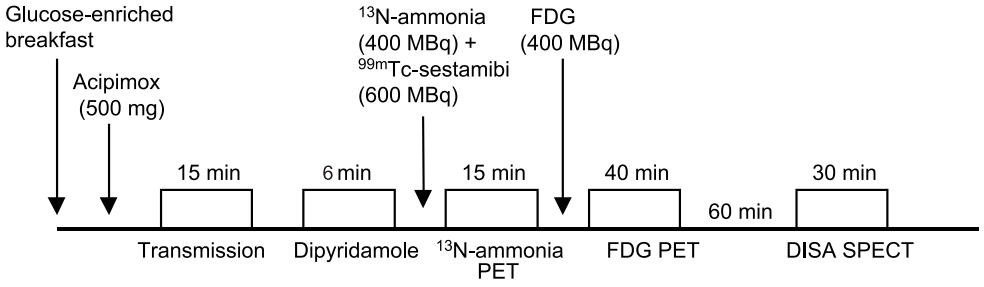

Figure 2. Schematic outline of the DISA SPECT and PET protocol

DISA SPECT

DISA SPECT acquisition was performed on the same day as the PET scan, 1 hour after the completion of the PET study (Figure 2). A Siemens MultiSPECT dual-headed gamma camera (Siemens Medical Systems, Hoffman Estates, IL, USA) with extra-high energy (EHE) collimators was used. EHE collimators are needed to permit imaging of the high energy (511 KeV) photons. The resolution of the EHE collimator is 10.4 mm full-width at half maximum (FWHM) for ^{18}F and 9.2 mm for ^{99m}Tc at 10 cm distance from the collimator face. Three energy windows were set at 140 (± 15%), 170 (± 20%) and 511 keV (±15%). Sixty-four projections were acquired over a circular orbit of 180° (from the 45° RAO to the 45° LPO position with 30 s per angle). The total acquisition time was 30 minutes.
Planar 140 keV images were corrected for scatter by subtraction of the 170 keV images using a convolution-based correction method (11,12). The planar FDG images were corrected for the decay of ^{18}F during acquisition, because the relative short half-life time of

^{18}F (110 min) may otherwise influence the image quality. Vertical and horizontal long-axis, and short-axis images of ^{99m}Tc-sestamibi and FDG were reconstructed using identical axes and filtered back projection with a Butterworth filter (Nyquist frequency 0.5, order 6 for both the FDG and ^{99m}Tc-sestamibi study). In this way identically oriented FDG and ^{99m}Tc-sestamibi images were obtained from the DISA SPECT acquisition.

Coronary angiography

Repeat coronary angiography was applied by a femoral approach using the standard Judkins technique and performed by a cardiologist blinded to all study data. After the procedure, a trained observer interpretated all angiographic findings independently. A significant re-stenosis or new stenosis was defined as >70% stenosis (percent luminal diameter narrowing).

MRI to assess contractile function

Images were acquired on a 1.5 Tesla MRI system (Vision, Siemens Medical Systems, Erlangen, Germany) equipped with high performance gradients (maximum gradient strength = 40 mT/m; maximum slew rate = 200 mT/m/ms). Patients were examined in the supine position using a flexible body array coil for signal reception. Scout images depicting the myocardium were acquired in the coronal and sagital imaging planes using a 2-D FLASH ECG-triggered sequence (one slice per heartbeat; TR = 40 – 100 ms, TE = 6 ms, flip angle = 58°, field of view (FOV) = 300 – 350 mm, slice thickness = 8 mm) after which the short-axis plane was determined. The short-axis plane was defined perpendicular to the LV long-axis from the center of the mitral annulus to the apex. Slices were acquired at 8 to10 LV base to apex short-axis locations during repeated breath-holds (± 15 seconds). Images were reconstructed using 2D-Fourier reconstruction with in-plane matrix of 128 x 256 (reconstructed voxel size = 17.6 mm^3). The TR was varied depending on the R-R interval of the patient and the number of cardiac phases to be imaged.

For analysis of data we used a Sun Sparc workstation (Sun Microsystems, Mountain View, CA, USA). Global LV function, i.e. LVEF, and LV volumes were derived from the MR images using previously validated automated software (MR Analytical Software System [MASS], Leiden, The Netherlands) (13). An improvement in LVEF ≥ 5% after revascularization was clinically considered significant (14). Reverse remodeling (reduction of LV end-diastolic and end-systolic volumes) of 10% in LVEDV and LVESV after revascularization was clinically considered significant (15).

Assessment of regional wall motion was performed visually by an experienced observer blinded to the clinical data and PET results. Baseline and follow-up MRI studies were interpreted in random order. A 17-segment model was used and each segment was assigned a wall motion score using a 4-point scoring system (1 = normal wall motion, 2 = hypokinesia, 3 = akinesia, 4 = dyskinesia). An improvement in regional wall motion post-revascularization by 1 grade or more was considered significant. Of note, a change from dyskinetic to akinetic was not considered to represent improvement in function, but a mechanical phenomenon (16).

ROC analysis and viability criteria for PET and DISA SPECT

Data from FDG PET and FDG SPECT, ^{13}N-ammonia PET and ^{99m}Tc-sestamibi SPECT were analysed quantitatively and displayed in a 17-segment polar map as recently proposed (17), using the 4D-MSPECT program, a commercially (Siemens Medical Systems, Hoffman Estates, Ill) available cardiac software package (18). Average counts per segment were obtained from the 17 segments and the measured counts were normalized to the segment with the highest average counts**.**

In general, segments are considered viable when FDG uptake is higher than perfusion tracer uptake (called a perfusion-metabolism mismatch). As the optimal decision level of this difference is not well described in the literature, ROC curve analysis was used both for PET and DISA SPECT to determine the optimal cutoff value for this difference in tracer uptake of FDG and perfusion, using recovery of function on MRI as the gold standard for viability (19,20). The output of ROC analysis is a area-under-the curve value between 0 and 1. The performance of a diagnostic test can be generally classified using this ROC AUC value, as follows: 0.90-1 = excellent, 0.80-0.90 = good. 0.70-0.80 = fair, 0.60-0.70 = poor, 0.50-0.60 = test without value.

Statistical analysis

Regional function

Descriptive results were expressed as mean ± SD. Patient data were compared using the Student *t* test for (un)paired data when appropriate. Fisher's exact test was used for categorical data. Sensitivity and specificity for the prediction of improvement of regional function were subsequently determined. McNemar's test was used to compare the sensitivity and specificity to predict improvement in regional function post-revascularization between DISA SPECT and PET.

Global function

Multivariate and univariate logistic regression analysis was performed to determine which variables best predicted improvement in LVEF after revascularization. The relation between the number of dysfunctional and viable (or non-viable) segments and the change in LVEF after revascularization was determined by linear regression analysis. Another ROC curve analysis was performed to determine the optimal number of dysfunctional but viable segments on PET and DISA SPECT, allowing discrimination between patients with and without improvement in LVEF (≥5%) (14). Sensitivity and specificity for the prediction of improvement in global LV function (LVEF) were subsequently determined. Sensitivity and specificity were also calculated to predict LV reverse remodelling (defined as a reduction by 10% or more in LV volumes). McNemar test was used to compare the sensitivity and specificity between DISA SPECT and PET to predict improvement in LVEF and LV reverse remodelling after revascularization. A *P*-value < 0.05 was considered significant.

Results

Forty-seven patients underwent revascularization, in particular 27 patients underwent CABG and 20 patients underwent PTCA (mean number of target vessels per patient: 2.1 ± 1). The procedures were uncomplicated. Repeat coronary angiography (to assess vessel- or graft-patency) was performed in 33 patients demonstrating that 4 bypass grafts were occluded and 5 lesions after PTCA showed re-stenosis. The remaining patients who did not undergo repeat coronary angiography did not have recurrent symptoms after revascularization.

Of all 799 myocardial segments in the 47 patients, 18 (2%) segments were excluded from further analysis because of technical reasons. Another 38 (4%) segments allocated to the vessels/grafts with a re-stenosis or occlusion were also excluded.

Data analysis was based on the remaining 743 segments. Of these, 421 (57%) segments had contractile dysfunction. Out of these 421 dysfunctional segments, 264 segments belonged to the distribution area of revascularized vessels. These 264 segments were used for the final analysis. Of these 264 revascularized segments, 174 (66%) were hypokinetic and 90 (34%) were a- or dyskinetic before revascularisation.

PET and DISA SPECT viability criterion assessment.

Using ROC analysis, a difference of 7% in relative segmental uptake was identified as the optimal difference between metabolism and perfusion (FDG uptake and ^{13}N-ammonia uptake) on PET, with an AUC value of 0.89 ± 0.02, considered very good – excellent. For DISA SPECT, this difference was 9% for FDG uptake and ^{99m}Tc-sestamibi uptake with an AUC value of 0.90 ± 0.02, considered excellent. The difference between PET and DISA SPECT was not significant (Figure 3).

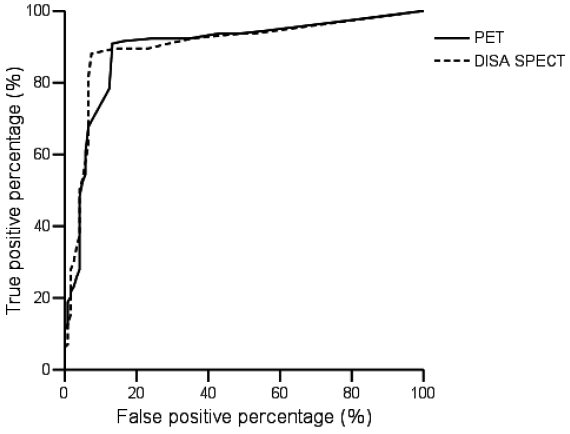

Figure 3. ROC curves for PET and DISA SPECT for the prediction of myocardial viability as defined by the difference between FDG and the perfusion tracer. The area under the curve (AUC) for PET of 0.89 ± 0.02 and for DISA SPECT is 0.90 ± 0.02 (*P* = NS).

Accuracy of PET vs DISA SPECT for the prediction of regional recovery

Of all 264 dysfunctional segments, 143 (54%) recovered in function on the follow-up MRI performed 6 months after revascularization (Figure 4). Of these 143 recovered segments, 130 (90%) segments were classified

as viable on PET imaging. Of the 121 segments without recovery, only 16 (13%) were incorrectly identified as viable by PET (*P* for difference <0.05). Therefore PET had a sensitivity for the prediction of viability and subsequent functional recovery of 90% at a specificity of 86%.

Viability on DISA SPECT was present in 128 (89%) segments with functional recovery, as compared to only 17 (14%) of the segments without functional recovery (*P* <0.05). Accordingly, the sensitivity for the prediction of functional recovery of DISA SPECT was 89% at a specificity of 86%. This performance of DISA SPECT and PET in the viability assessment and functional recovery prediction was not different (*P* =NS).

Sensitivity and specificity were also assessed for hypokinetic and a-/dyskinetic segments separately. Of the 174 hypokinetic segments, 108 (62%) showed recovery of function after revascularization. The sensitivity and specificity of PET imaging were 90% and 86%, whereas the sensitivity and specificity of DISA SPECT were 87% and 85%. Of the 90 a-/dyskinetic segments, 35 (38%) recovered in function after revascularization. The sensitivity and specificity of PET were 89% and 84% respectively and for DISA SPECT 87% and 83%. There was no significant difference between DISA SPECT and PET for the prediction of recovery.

Effect of revascularization on global LV function

The mean LVEF in the whole group of 47 patients improved from 33 ± 12% to 40 ± 14% (*P* < 0.001).

A strong direct linear relation was found between the number of viable segments on both PET and DISA SPECT and the magnitude of improvement in LVEF, suggesting that the extent of viability determined the magnitude of improvement in LVEF after revascularization (*P* <0.001) (Figure 5a and b). Similarly, a (weaker) inverse relation was observed between the number of non-viable segments on PET and DISA SPECT and the magnitude of improvement in LVEF (y = -1.6 + 11.4, *r* = 0.45, *P* < 0.005; y = -1.3 + 10.9, *r* = 0.39, *P* < 0.005, respectively).

In individual LVEF assessment, we found a clinically significant improvement in LVEF (≥ 5%) in 27 (57%) patients. The characteristics of the patients with and without improvement in LVEF are summarized in Table 1. Univariate analysis (including age, gender, previous myocardial infarction, NYHA class, LVEF, number of stenosed vessels, previous CABG/PTCA, diabetes, number of viable/nonviable segments on PET and DISA SPECT) indicated

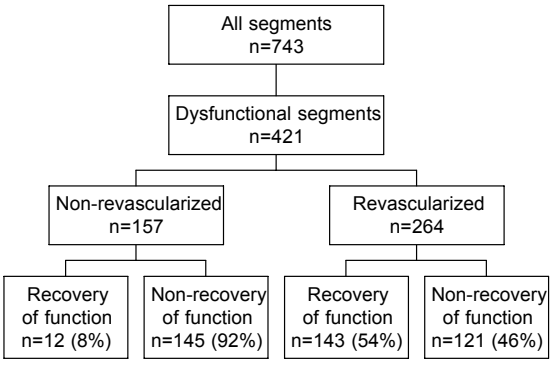

Figure 4. Recovery of dysfunctional segments after revascularization

that the number of viable segments on PET and DISA SPECT and the patient's age were the only predictors of improvement in LVEF after revascularization. Multivariate analysis showed that the number of viable segments was the strongest predictor for improvement in LVEF.

ROC analysis was used to assess the number of viable segments detected on PET and DISA SPECT and improvement of LVEF (⩾ 5%) after revascularization. The optimal cut-off level for a correct prediction of LVEF improvement was ⩾ 2 viable segments for PET

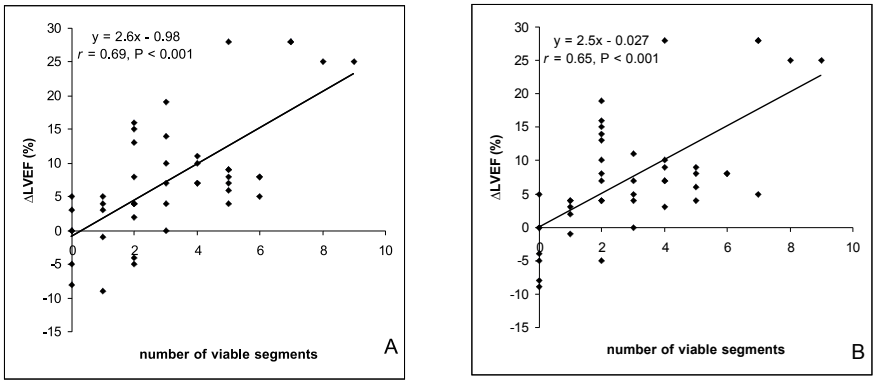

Figure 5. Scatterplots showing the relation between number of viable segments on PET (A) and DISA SPECT (B) and the change in LVEF after revascularization.

and DISA SPECT with an excellent accuracy (AUC 0.97 ± 0.02 and 0.96 ± 0.02 respectively, *P* = NS) (Figure 6). At this optimal cutoff level, sensitivity and specificity for the prediction of improvement in global LVEF for PET were 86% and 100% respectively, and for DISA SPECT 83% and 100%, respectively. This prediction performance of PET and DISA SPECT were similar (*P* = NS).

Effect of revascularization on LV remodeling.

After revascularization, the LVEDV and LVESV in patients with more than 2 viable revascularized segments estimated from PET (n = 31) and DISA SPECT (n = 30) decreased significantly (Table 2). Inversely, LVEDV and LVESV worsened significantly in patients considered non viable (who had < 2 viable revascularized segments) according to PET (n=16) and DISA SPECT (n=17) (Table 2).

The sensitivity and specificity of PET for the prediction of reverse remodeling of ≥ 10% (mL) in LVEDV was 95% and 65%, respectively, whereas the sensitivity and specificity of DISA SPECT was 95% and 69%, respectively (*P* = NS). The sensitivity and specificity of PET for the prediction of reverse modeling of ≥ 10 % (mL) in LVESV was 96% and 79%, respectively, whereas the sensitivity and specificity of DISA SPECT was 99% and 84%, respectively (*P*= NS).

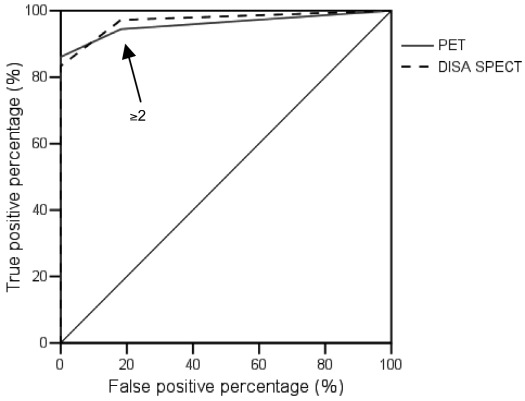

Figure 6. ROC curves for PET and DISA SPECT showing both the optimal cutoff level of 2 dysfunctional but viable segments (≥ 2) yielding highest sensitivity and specificity to predict LVEF improvement of ≥ 5% on patient basis. The area under the curve (AUC) for PET of 0.97 ± 0.02 and for DISA SPECT is 0.96 ± 0.02 (*P* = NS).

Table 1. Characteristics of patients with and without improvement in LVEF after revascularization.

	Pts with improved LVEF (n = 27)	Pts without improved LVEF (n = 20)	*P*-value
Age (yrs)	62 ± 9	68 ± 9	<0.05
Gender (M/F)	22/5	19/1	NS
Previous infarction	18 (66%)	16 (80%)	NS
NYHA class	2.8 ± 0.9	2.9 ± 0.9	NS
Diabetes	5	5	NS
Previous PTCA/CABG	10	4	NS
Nr stenosed vessels	2.6 ± 0.6	2.3 ± 1.1	NS
LVEF (%)	32 ± 12	33 ± 10	NS
LVEDV (mL)	145 ± 50	149 ± 74	NS
LVESV (mL)	98 ± 46	113 ± 82	NS
Nr.viable segs on SPECT	4.1 ± 2.2	1.8 ± 1.8	<0.001
Nr non-viable segs on SPECT	2.1 ± 2.3	3.0 ± 2.6	NS
Nr viable segs on PET	4.3 ± 2.1	1.8 ± 1.6	<0.001
Nr non-viable segs on PET	1.8 ± 2.2	3.0 ± 2.4	NS

CABG: coronary artery bypass grafting; LVEF: left ventricular ejection fraction;
NYHA: New York Heart Association; PTCA: percutaneous transluminal coronary angioplasty;
Segs: segments.

Discussion

FDG PET is considered the technique of choice for assessment of myocardial viability, and subsequent prediction of recovery of function post-revascularization. Head-to-head comparative studies between FDG imaging with PET and SPECT in patients undergoing revascularization have not been reported thusfar. The most important findings of this study can be summarized as follows. First, ROC curve analysis identified the optimal cut-off values for perfusion-FDG mismatches. For PET, a 7% difference between FDG activity and ^{13}N-ammonia activity was optimal and yielded a sensitivity and specificity of 90% and 86% to predict improvement of regional function. For SPECT, a 9% difference

Table 2. Ongoing remodeling or reverse remodeling of the left ventricle in viable patients (≥ 2 revascularized myocardial segments) or non viable patients (< 2 viable revascularized segments).

	Non viable patients							
	LVEDV Pre	LVEDV Post	mean difference	*P*	LVESV Pre	LVESV Post	mean difference	*P*
PET non viable	152±64	169±80	+17±36	<0.05	103±54	118±68	+15±31	<0.05
DISA non viable	154±62	169±77	+15±35	<0.05	105±53	119±66	+14±31	<0.05
	Viable patients							
	LVEDV Pre	LVEDV Post	mean difference	*P*	LVESV Pre	LVESV Post	mean difference	*P*
PET viable	145±58	122±63	-23±27	<0.002	102±59	76±59	-26±19	<0.001
DISA viable	146±57	123±62	-23±27	<0.002	101±59	75±59	-26±19	<0.001

LVEDV: left ventricular end-diastolic volume (mL); LVESV: left ventricular end-systolic volume (mL).

between FDG activity and ^{99m}Tc-sestamibi activity yielded a sensitivity and specificity of 89% and 86% (both NS versus PET). Second, for prediction of improvement in LVEF the sensitivities and specificities were good both for PET (86% and 100%) and for SPECT (83% and 100%, NS versus PET). Finally, for prediction of LV reverse remodeling the sensitivity and specificity were good for PET and SPECT, without significant differences. These results indicate that SPECT and PET have identical value in the evaluation of myocardial viability and prediction of functional recovery.

Comparison of modalities in previous studies: SPECT versus PET

The high spatial resolution, high-count-density images and the possibility for attenuation correction of PET, allows accurate assessment of regional uptake using FDG and ^{13}N-ammonia irrespective of weight or body habitus of patients. The poorer spatial resolution of SPECT, the lower sensitivity and the lack of attenuation correction in most cases may cause some discordance between SPECT and PET images (21,22). The clinical feasibility of imaging positron emitters such as FDG with EHE collimators SPECT techniques has been reported previously (23,24). Few studies have focused on the comparison of FDG SPECT and FDG PET, but showed a good agreement in the assessment of viability (25-29). The most detailed comparison was performed by the National Institutes of Health group (29). The investigators studied 28 patients with CAD and a mean LVEF of 33 ± 15%. These patients underwent both FDG SPECT and FDG PET after oral glucose loading with the addition of intravenous insulin if needed. Regional LV function was evaluated with gated SPECT or ERNA. When a 50% FDG uptake threshold was used to dis-

tinguish between viable and non-viable tissue, both techniques provided comparable information, yielding an agreement of 94%. Direct comparisons between DISA SPECT and PET are scarce (6). Fukuchi et al. (6) demonstrated an excellent relation between segmental FDG activities, measured with PET or DISA SPECT.
However, none of the previous studies compared PET and DISA SPECT in patients undergoing revascularization.
The imaging protocol used in the present study was not used previously, namely perfusion was assessed during pharmacological stress. Although omission of the resting perfusion images no longer allows discrimination between repetitively stunned myocardium (with normal resting perfusion) and hibernating myocardium (with reduced resting perfusion), this information is mainly of interest for research purposes. Other studies have demonstrated that resting perfusion was near normal in chronic dysfunctional myocardium (31). Vanoverschelde et al. (31) observed almost similar levels of perfusion with PET in regions with normal contraction and regions with chronic dysfunction. These authors showed that instead of resting flow, flow reserve was reduced in dysfunctional but viable myocardium (31). Based on their observations, Vanoverschelde and co-workers suggested that repeated ischemic attacks may result in chronic dysfunction, with flow remaining normal or mildly reduced—a condition referred to as repetitive stunning (32). The current DISA SPECT study however aims at providing a simple protocol for detection of viability of hibernating myocardium and dysfunctional myocardium based on reduced flow reserve.

DISA SPECT for the prediction of LV recovery: comparison with previous studies
In the current study, PET and DISA SPECT were compared directly in patients undergoing revascularization. First, the criteria for a mismatch were defined by ROC curve analysis. ROC analysis indicated that a 7% increase in FDG activity over ^{13}N-ammonia activity was optimal and yielded a sensitivity and specificity of 90% and 86% to predict improvement of regional function. These results are in line with the literature; pooling of 12 FDG PET studies yielded a sensitivity of 88% with a specificity of 73% (33) .
For DISA SPECT, a mismatch was defined by a 9% increase in FDG activity over ^{99m}Tc-sestamibi activity. This resulted in a sensitivity of 89% and a specificity of 86% with no significant difference from PET. Few SPECT studies have addressed the prediction of functional improvement after revascularization (34-37). All previous studies used sequential perfusion and FDG SPECT imaging, with thallium-201 as perfusion tracer. Bax et al. evaluated 55 patients with chronic CAD and depressed LV function (mean LVEF 39 ± 14%) with resting thallium-201 SPECT and FDG SPECT prior to revascularization and demonstrated a sensitivity of 84% and a specificity of 86% (35). The results of the current study are in line with these previous observations. The main advantage of DISA SPECT in comparison to PET or sequential thallium-201 and FDG SPECT acquisition is the perfect alignment between perfusion and FDG data.

Prediction of improvement in LVEF after revascularization

From a clinical point of view, improvement in LVEF is more important than improvement in regional LV function prediction (38-40). Accurate identification of patients who may improve in LVEF is important, since LVEF is an important prognostic parameter (41). In the present study, 27 patients (57%) showed improvement in LVEF (≥ 5%) after revascularization. In line with previous studies, the number of viable segments on PET and DISA SPECT were linearly related to the improvement in LVEF post-revascularization. Moreover, patients with 2 or more viable segments in either PET or SPECT had a high likelihood of functional recovery after revascularization. In particular, for PET the sensitivity and specificity were 86% and 100%, and for DISA SPECT these values were 83% and 100% (NS versus PET). Besides the presence of viability, the extent of scar tissue was also important for improvement of function post-revascularization; the number of nonviable segments was inversely related to the improvement in LVEF post-revascularization. Similar results were presented recently by Beanlands et al. using FDG PET (42). However, multivariate analysis in the current study demonstrated the superiority of viability (over scar tissue) for the prediction of improvement in LVEF.

Another clinically relevant issue is the relation between LV remodeling and viability. The data in the current study support the hypothesis that patients with viable myocardium do not only benefit from revascularization because of improvement in LVEF, but also by prevention of ongoing remodeling or even reverse LV remodeling after revascularization. Large trials have demonstrated the prognostic value of reverse remodeling for long-term outcome (43,44). In these trials, patients with viable myocardium showed a significant reduction in LVEDV and LVESV after revascularization. At least as important, patients with nonviable myocardium showed ongoing LV remodeling, with a significant increase in both LVEDV and LVESV after revascularization. These results indicate that revascularization per se, does not stop the remodeling process, and emphasize the value of viable myocardium for outcome after revascularization.

Limitations

Some limitations of this study need attention. First, repeated cardiac catheterization was not performed in all patients; however, none of the patients without repeated catheterization had recurrent symptoms. Second, functional follow-up was performed at 6 months after revascularization; this period may be too short to fully appreciate recovery of function; previous work demonstrated that recovery of function may occur up to one year after revascularization (45). Third, not all dysfunctional segments were revascularized mainly for technical reasons, but this affects the predictive accuracy of PET and DISA SPECT equally.

Conclusion

The current findings clearly establish the use of FDG imaging with SPECT. In this head-

to-head comparison between PET and DISA SPECT in patients undergoing revascularization, both techniques yielded a similar accuracy for the prediction of improvement in regional and global LV function. Also, both techniques were equally good in predicting reverse LV remodeling after revascularization in patients with viable myocardium. Therefore, this study provides convincing evidence that DISA SPECT is equivalent to PET, and serves as a good alternative to PET for the assessment of myocardial viability in patients considered for revascularization.

Acknowledgment

This study was supported by an educational unrestricted research grant (COG-AZG 2000-06) of the University Medical Center, Groningen, The Netherlands. Dr. D.J. van Veldhuisen is an Established Investigator of the Netherland Heart Foundation (Grant D976.017).

Reference List

1. Allman KC, Shaw LJ, Hachamovitch R, Udelson JE. Myocardial viability testing and impact of revascularization on prognosis in patients with coronary artery disease and left ventricular dysfunction: a meta-analysis. J Am Coll Cardiol. 2002; 39(7):1151-1158.
2. Tillisch J, Brunken R, Marshall R, Schwaiger M, Mandelkern M, Phelps M et al. Reversibility of cardiac wall-motion abnormalities predicted by positron tomography. N Engl J Med. 1986; 314(14):884-888.
3. Tamaki N, Kawamoto M, Tadamura E, Magata Y, Yonekura Y, Nohara R et al. Prediction of reversible ischemia after revascularization. Perfusion and metabolic studies with positron emission tomography. Circulation. 1995; 91(6):1697-1705.
4. Rizzello V, Poldermans D, Bax JJ. Assessment of myocardial viability in chronic ischemic heart disease: current status. Q J Nucl Med Mol Imaging. 2005; 49(1):81-96.
5. Delbeke D, Videlefsky S, Patton JA, Campbell MG, Martin WH, Ohana I et al. Rest myocardial perfusion/metabolism imaging using simultaneous dual-isotope acquisition SPECT with technetium-99m-MIBI/fluorine-18-FDG. J Nucl Med. 1995; 36(11):2110-2119.
6. Fukuchi K, Katafuchi T, Fukushima K, Shimotsu Y, Toba M, Hayashida K et al. Estimation of myocardial perfusion and viability using simultaneous 99mTc-tetrofosmin--FDG collimated SPECT. J Nucl Med. 2000; 41(8):1318-1323.
7. Sandler MP, Videlefsky S, Delbeke D, Patton JA, Meyerowitz C, Martin WH et al. Evaluation of myocardial ischemia using a rest metabolism/stress perfusion protocol with fluorine-18 deoxyglucose/technetium-99m MIBI and dual-isotope simultaneous-acquisition single-photon emission computed tomography. J Am Coll Cardiol. 1995; 26(4):870-878.
8. Bossuyt PM, Reitsma JB, Bruns DE, Gatsonis CA, Glasziou PP, Irwig LM et al. Towards complete and accurate reporting of studies of diagnostic accuracy: the STARD initiative. Fam Pract. 2004; 21(1):4-10.
9. Knuuti MJ, Yki-Jarvinen H, Voipio-Pulkki LM, Maki M, Ruotsalainen U, Harkonen R et al. Enhancement of myocardial [fluorine-18]fluorodeoxyglucose uptake by a nicotinic acid derivative. J Nucl Med. 1994; 35(6):989-998.

10. Schinkel AF, Bax JJ, Valkema R, Elhendy A, van Domburg RT, Vourvouri EC et al. Effect of diabetes mellitus on myocardial 18F-FDG SPECT using acipimox for the assessment of myocardial viability. J Nucl Med. 2003; 44(6):877-883.
11. Kool W, Willemsen ATM, Paans AMJ, Piers DA. Convolution based triple energy window crosstalk correction for DISA SPECT. [abstract]. J Nucl Med. 1997; 38(89).
12. De Boer J, Slart RH, Blanksma PK, Willemsen AT, Jager PL, Paans AM et al. Comparison of 99mTc-sestamibi-18F-fluorodeoxyglucose dual isotope simultaneous acquisition and rest-stress 99mTc-sestamibi single photon emission computed tomography for the assessment of myocardial viability. Nucl Med Commun. 2003; 24(3):251-257.
13. van der Geest RJ, Buller VG, Jansen E, Lamb HJ, Baur LH, van der Wall EE et al. Comparison between manual and semiautomated analysis of left ventricular volume parameters from short-axis MR images. J Comput Assist Tomogr. 1997; 21(5):756-765.
14. Bax JJ, Poldermans D, Elhendy A, Cornel JH, Boersma E, Rambaldi R et al. Improvement of left ventricular ejection fraction, heart failure symptoms and prognosis after revascularization in patients with chronic coronary artery disease and viable myocardium detected by dobutamine stress echocardiography. J Am Coll Cardiol. 1999; 34(1):163-169.
15. Senior R, Lahiri A, Kaul S. Effect of revascularization on left ventricular remodeling in patients with heart failure from severe chronic ischemic left ventricular dysfunction. Am J Cardiol. 2001; 88(6):624-629.
16. Arnese M, Fioretti PM, Cornel JH, Postma-Tjoa J, Reijs AE, Roelandt JR. Akinesis becoming dyskinesis during high-dose dobutamine stress echocardiography: a marker of myocardial ischemia or a mechanical phenomenon? Am J Cardiol. 1994; 73(12):896-899.
17. Hendel RC, Corbett JR, Cullom SJ, DePuey EG, Garcia EV, Bateman TM. The value and practice of attenuation correction for myocardial perfusion SPECT imaging: a joint position statement from the American Society of Nuclear Cardiology and the Society of Nuclear Medicine. J Nucl Cardiol. 2002; 9(1):135-143.
18. Ficaro EP, Kritzman JN, Corbett JR. Development and clinical validation of normal Tc-99m sestamibi database: comparison of 3D-MSPECT to Cequal [abstract]. [abstract]. J Nucl Med. 1999; 40(suppl)(125P).
19. Hanley JA, McNeil BJ. A method of comparing the areas under receiver operating characteristic curves derived from the same cases. Radiology. 1983; 148(3):839-843.
20. Metz CE. Basic principles of ROC analysis. Semin Nucl Med. 1978; 8(4):283-298.
21. Slart RH, Que TH, van Veldhuisen DJ, Poot L, Blanksma PK, Piers DA et al. Effect of attenuation correction on the interpretation of 99mTc-sestamibi myocardial perfusion scintigraphy: the impact of 1 year's experience. Eur J Nucl Med Mol Imaging. 2003; 30(11):1505-1509.
22. Slart RH, Bax JJ, Sluiter WJ, van Veldhuisen DJ, Jager PL. Added value of attenuation-corrected Tc-99m tetrofosmin SPECT for the detection of myocardial viability: comparison with FDG SPECT. J Nucl Cardiol. 2004; 11(6):689-696.
23. Sandler MP, Bax JJ, Patton JA, Visser FC, Martin WH, Wijns W. Fluorine-18-fluorodeoxyglucose cardiac imaging using a modified scintillation camera. J Nucl Med. 1998; 39(12):2035-2043.
24. Van Lingen A, Huijgens PC, Visser FC, Ossenkoppele GJ, Hoekstra OS, Martens HJ et al. Performance characteristics of a 511-keV collimator for imaging positron emitters with a standard gamma-camera. Eur J Nucl Med. 1992; 19(5):315-321.
25. Bax JJ, Visser FC, Blanksma PK, Veening MA, Tan ES, Willemsen TM et al. Comparison of myocardial uptake of fluorine-18-fluorodeoxyglucose imaged with PET and SPECT in dyssynergic myocardium. J Nucl Med. 1996; 37(10):1631-1636.
26. Burt RW, Perkins OW, Oppenheim BE, Schauwecker DS, Stein L, Wellman HN et al. Direct comparison of fluorine-18-FDG SPECT, fluorine-18-FDG PET and rest thallium-201 SPECT for detection of myocardial viability. J Nucl Med. 1995; 36(2):176-179.

27. Chen EQ, MacIntyre WJ, Go RT, Brunken RC, Saha GB, Wong CY et al. Myocardial viability studies using fluorine-18-FDG SPECT: a comparison with fluorine-18-FDG PET. J Nucl Med. 1997; 38(4):582-586.
28. Martin WH, Delbeke D, Patton JA, Hendrix B, Weinfeld Z, Ohana I et al. FDG-SPECT: correlation with FDG-PET. J Nucl Med. 1995; 36(6):988-995.
29. Srinivasan G, Kitsiou AN, Bacharach SL, Bartlett ML, Miller-Davis C, Dilsizian V. [18F]fluorodeoxyglucose single photon emission computed tomography: can it replace PET and thallium SPECT for the assessment of myocardial viability? Circulation. 1998; 97(9):843-850.
30. Canty J-MJ, Fallavollita JA. Resting myocardial flow in hibernating myocardium: validating animal models of human pathophysiology. Am J Physiol. 1999; 277(1 Pt 2):H417-H422.
31. Vanoverschelde JL, Wijns W, Depre C, Essamri B, Heyndrickx GR, Borgers M et al. Mechanisms of chronic regional postischemic dysfunction in humans. New insights from the study of noninfarcted collateral-dependent myocardium. Circulation. 1993; 87(5):1513-1523.
32. Vanoverschelde JL, Melin JA. The pathophysiology of myocardial hibernation: current controversies and future directions. Prog Cardiovasc Dis. 2001; 43(5):387-398.
33. Bax JJ, Patton JA, Poldermans D, Elhendy A, Sandler MP. 18-Fluorodeoxyglucose imaging with positron emission tomography and single photon emission computed tomography: cardiac applications. Semin Nucl Med. 2000; 30(4):281-298.
34. Bax JJ, Cornel JH, Visser FC, Fioretti PM, Van Lingen A, Reijs AE et al. Prediction of recovery of myocardial dysfunction after revascularization. Comparison of fluorine-18 fluorodeoxyglucose/thallium-201 SPECT, thallium-201 stress-reinjection SPECT and dobutamine echocardiography. J Am Coll Cardiol. 1996; 28(3):558-564.
35. Bax JJ, Cornel JH, Visser FC, Fioretti PM, Van Lingen A, Huitink JM et al. Prediction of improvement of contractile function in patients with ischemic ventricular dysfunction after revascularization by fluorine-18 fluorodeoxyglucose single-photon emission computed tomography. J Am Coll Cardiol. 1997; 30(2):377-383.
36. Bax JJ, Cornel JH, Visser FC, Fioretti PM, Huitink JM, Van Lingen A et al. F18-fluorodeoxyglucose single-photon emission computed tomography predicts functional outcome of dyssynergic myocardium after surgical revascularization. J Nucl Cardiol. 1997; 4(4):302-308.
37. Cornel JH, Bax JJ, Fioretti PM, Visser FC, Maat AP, Boersma E et al. Prediction of improvement of ventricular function after revascularization. 18F-fluorodeoxyglucose single-photon emission computed tomography vs low-dose dobutamine echocardiography. Eur Heart J. 1997; 18(6):941-948.
38. Meluzin J, Cerny J, Frelich M, Stetka F, Spinarova L, Popelova J et al. Prognostic value of the amount of dysfunctional but viable myocardium in revascularized patients with coronary artery disease and left ventricular dysfunction. Investigators of this Multicenter Study. J Am Coll Cardiol. 1998; 32(4):912-920.
39. Meluzin J, Cerny J, Nemec P, Frelich M, Stetka F, Spinarova L. Do the presence and amount of dysfunctional but viable myocardium affect the perioperative outcome of coronary artery bypass graft surgery? Int J Cardiol. 1999; 71(3):265-272.
40. Pagley PR, Beller GA, Watson DD, Gimple LW, Ragosta M. Improved outcome after coronary bypass surgery in patients with ischemic cardiomyopathy and residual myocardial viability. Circulation. 1997; 96(3):793-800.
41. White HD, Norris RM, Brown MA, Brandt PW, Whitlock RM, Wild CJ. Left ventricular end-systolic volume as the major determinant of survival after recovery from myocardial infarction. Circulation. 1987; 76(1):44-51.
42. Beanlands RS, Ruddy TD, deKemp RA, Iwanochko RM, Coates G, Freeman M et al. Positron emission tomography and recovery following revascularization (PARR-1): the importance of scar and the development of a prediction rule for the degree of recovery of left ventricular function. J Am Coll Cardiol. 2002; 40(10):1735-1743.

43. Bax JJ, Schinkel AF, Boersma E, Elhendy A, Rizzello V, Maat A et al. Extensive left ventricular remodeling does not allow viable myocardium to improve in left ventricular ejection fraction after revascularization and is associated with worse long-term prognosis. Circulation. 2004; 110(11 Suppl 1):II18-II22.
44. Mule JD, Bax JJ, Zingone B, Martinelli F, Burelli C, Stefania A et al. The beneficial effect of revascularization on jeopardized myocardium: reverse remodeling and improved long-term prognosis. Eur J Cardiothorac Surg. 2002; 22(3):426-430.
45. Bax JJ, Visser FC, Poldermans D, Elhendy A, Cornel JH, Boersma E et al. Time course of functional recovery of stunned and hibernating segments after surgical revascularization. Circulation. 2001; 104(12 Suppl 1):I314-I318.

SECTION IV

Gated FDG PET for the assessment of myocardial viability and left ventricular function

Hoofdstuk 7

Prediction of functional recovery after revascularization in patients with coronary artery disease and left ventricular dysfunction by gated FDG PET.

Riemer H.J.A. Slart[1], Jeroen J. Bax[2], Dirk J. van Veldhuisen[3], Ernst E. van der Wall[2], Rudi A.J.O. Dierckx[1], Jaep de Boer[4], Pieter L. Jager[1]

Department of Nuclear Medicine and Molecular Imaging[1], University Medical Center Groningen; Department of Cardiology[2], Leiden University Medical Center; Department of Cardiology[3], University Medical Center Groningen; Department of Nuclear Medicine[4], Diaconessenhuis Meppel, The Netherlands.

Submitted

Abstract

Background: Gated FDG PET is an attractive technique for detection of viability as its permits assessment of both myocardial glucose metabolism and wall contraction within one study. In this study the value of FDG uptake and wall thickening is analyzed by gated FDG PET for the prediction of recovery of regional and global left ventricle function in patients with coronary artery disease after revascularization.
Methods: Thirty-eight patients with chronic coronary artery disease and left ventricular dysfunction were included. Patients underwent a gated FDG PET protocol and an additional MRI within 1 week to assess regional wall motion and global ventricular function. MRI and coronary angiography were repeated 6 months after revascularization.
Results: Of all 213 revacularized dysfunctional segments, 133 (62%) exhibited recovery of function on the follow-up MRI. Receiver operating characteristic (ROC) curve analysis calculated a cutoff level of ≥50% FDG uptake yielded the highest sensitivity and specificity (93% and 85%, respectively) on gated FDG PET for prediction of LV recovery after revascularization. Using wall thickening (WT) as a predictor of functional LV recovery, ROC analysis showed ≥10% as the most optimal cut off level for the highest sensitivity and specificity (89% and 78%, respectively). The number of viable segments with FDG uptake and WT were the strongest predictors for the improvement in LVEF after revascularization. Reverse LV remodeling occurred in viable patients, whereas nonviable patients showed further LV dilatation after revascularization. Specificity for the prediction of LV reverse remodeling were similar for FDG uptake and WT, although sensitivity was higher using FDG ≥50% uptake criterion.
Conclusion: The observations in the present study provide further support for the use of FDG PET to predict outcome after revascularization. Segments with ≥50% FDG uptake or ≥10% WT have a high likelihood to improve in function post-revascularization. Patients with ≥3 viable segments according to these criteria have a high likelihood to improve in LVEF and will not suffer ongoing LV dilatation. Preserved (≥50%) FDG uptake is slightly superior to preserved (≥10%) WT to predict outcome.

Keywords: myocardial viability, gated FDG PET, wall thickening, functional LV recovery.

Introduction

The assessment of myocardial viability has become an important aspect of the diagnostic and prognostic work up of patients with coronary artery disease and left ventricular (LV) dysfunction. Patients with viable myocardium have been demonstrated to benefit from revascularization, with an improvement in LV function and a favourable prognosis after revascularization (1-4).

Positron emission tomography (PET) imaging using fluorine –18 fluorodeoxyglucose (FDG) combined with a flow tracer (eg, ^{13}N-ammonia) is an accurate non-invasive diagnostic technique to distinguish viable myocardium from scar tissue in patients with chronic coronary artery disease (4,5). However, recent studies have suggested that regional FDG uptake alone is also predictive of improvement of function, and may be more practical than combination with a flow tracer study in the clinical setting. Even from a single tracer study, more information can be derived than uptake alone. In particular, wall thickening (WT) on gated acquisitions could be used as markers of viability. Therefore, the aim of this study was to evaluate both FDG uptake and WT from a single gated FDG PET study, as predictors of functional recovery after revascularization. In addition, we analyzed the optimal cutoff values in FDG uptake and WT in the present study.

Materials and methods

Patients

Thirty-eight consecutive patients with chronic coronary artery disease and LV dysfunction (33 men, mean age 65 ± 8 years, range 41 to 80) referred for revascularization were included. Twenty-eight patients (73%) had a history of myocardial infarction (>3 months ago) and 8 patients (21%) had undergone previous revascularization (>3 months before the study). The mean LV ejection fraction (LVEF) in the patient group was 32 ± 10% at rest, estimated by previous radionuclide ventriculography or gated ^{99m}Tc-tetrofosmin SPECT. The patients had on average 2.5 ± 0.7 stenosed coronary arteries on angiography. Ten patients had diabetes mellitus, which was well-regulated by oral hypoglycemics and/or insulin, necessary for optimal FDG image quality. Patients with unstable angina and/or heart failure requiring hospitalization were excluded. None of the patients had cardiac events during the study. Assessment of contractile function, LV vol-

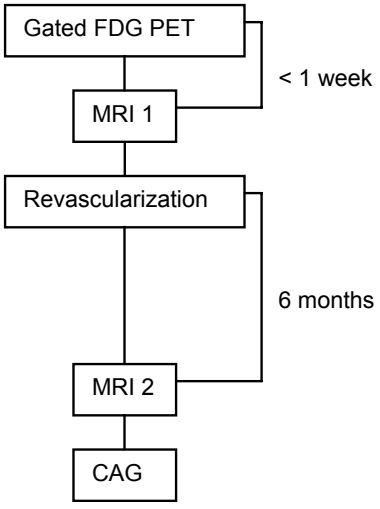

Figure 1. Schematic outline of the study procedures. CAG: coronary angiography.

umes and LVEF by MRI was performed within one week of gated FDG PET and was repeated 6 months after revascularization (see schematic outline; Figure 1). All surgeons and cardiologists were blinded to the gated FDG PET results. Coronary angiography was repeated 6 months after revascularization to exclude re-occlusion of the revascularized coronary arteries or bypass grafts. The study protocol was approved by the local Medical Ethics committee and all patients gave written informed consent.

Positron emission tomography

Patients had a glucose-enriched breakfast. Ninety minutes prior to FDG injection, acipimox (500 mg) was administered orally to lower the circulating free fatty acids (6). To prevent side-effects of acipimox (eg. skin rash), 250 mg of aspirin was administered orally 5 minutes before acipimox intake. Guided by the plasma glucose levels, patients received additional insulin as previously described (7). In short, in patients with a plasma glucose level >9 mmol/L at baseline, 6 units of insulin were administered subcutaneously. When plasma glucose levels remained >9 mmol/L, additional insulin was administered.

PET acquisition was performed on an ECAT-951/31 PET system (Siemens/CTI, Knoxville, TN, USA) imaging 31 planes over a total axial length of 10.8 cm (see schematic outline; Figure 2). Following the transmission scan (^{68}Ge/^{68}Ga rod sources), 400 MBq of FDG was injected intravenously, followed by the PET dynamic acquisition procedure. The total FDG PET acquisition time was 50 minutes, with the last 20 minutes acquired in gated mode with 16 frames per cardiac cycle. The myocardial count rate was higher than 10 kcps (true coincidents). The length of each gate was optimized for the current RR-interval. The RR-interval was allowed to vary by ± 10%. Data were corrected for attenuation using the transmission scan and were reconstructed using filtered back-projection (Hann filter: 0.5 pixels/cycle).

After manual reorientation, 12 short-axis images of FDG were obtained with a plane thickness from 7 to 9 mm at an in-plane resolution of approximately 7 mm. Myocardial tissue was corrected for spillover of activity from the blood pool in the LV myocardium. The dynamic PET studies were transformed into static studies and frames of gated FDG PET were summed and used for further data analysis.

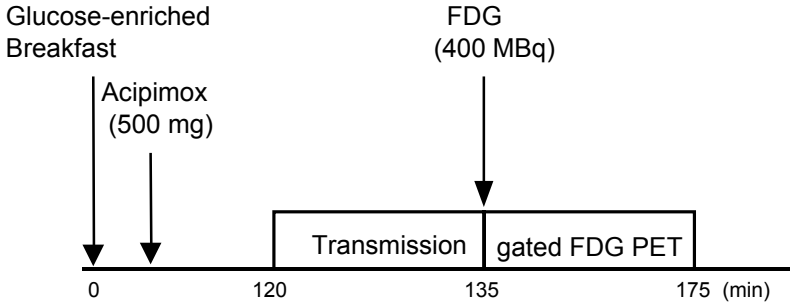

Figure 2. schematic outline of the gated FDG PET protocol.

MRI to assess contractile function

Images were acquired on a 1.5 Tesla MRI system (Vision, Siemens Medical Systems, Erlangen, Germany) equipped with high performance gradients (maximum gradient strength = 40 mT/m; maximum slew rate = 200 mT/m/ms). Patients were examined in the supine position using a flexible body array coil for signal reception.

Scout images depicting the myocardium were acquired in the coronal and sagital imaging planes using a 2-D FLASH ECG-triggered sequence (one slice per heartbeat; TR = 40 – 100 ms, TE = 6 ms, flip angle = 58°, field of view (FOV) = 300 – 350 mm, slice thickness = 8 mm) after which the short-axis plane was determined. The short-axis plane was defined perpendicular to the LV long-axis from the center of the mitral annulus to the apex. Slices were acquired at 8 to 10 LV base to apex short-axis locations during repeated breath-holds (± 15 seconds). Images were reconstructed using 2D-Fourier reconstruction with in-plane matrix of 128 x 256 (reconstructed voxel size = 17.6 mm3). The TR was varied depending on the R-R interval of the patient and the number of cardiac phases to be imaged.

A Sun Sparc workstation (Sun Microsystems, Mountain View, CA, USA) was used for further analysis of data. Global LV function, i.e. LVEF, and LV volumes were derived from the MR images using previously validated automated software (MR Analytical Software System [MASS], Leiden, The Netherlands) (8). An improvement in LVEF ≥5%, and reduction ≥10% in LVEDV and LVESV after revascularization were considered clinically meaningful (9).

Assessment of regional wall motion was performed visually by an experienced observer blinded to the clinical data and PET results. Moreover, baseline and follow-up MRI studies were interpreted in random order. A 17-segment model was used and each segment was assigned a wall motion score using a 4-point scoring system (1 = normal wall motion, 2 = hypokinesia, 3 = akinesia, 4 = dyskinesia). An improvement in regional wall motion post-revascularization by 1 grade or more was considered significant. Of note, a change from dyskinetic to akinetic was not considered improvement in function, but rather is considered as a mechanical phenomenon (10).

Coronary angiography

Repeat coronary angiography was applied by a femoral approach using the standard Judkins technique and performed by a cardiologist blinded to all study data. After the procedure, a trained observer interpreted all angiographic findings independently. A significant re-stenosis or new stenosis was defined as >70% stenosis (percent luminal diameter narrowing).

Gated FDG PET: data analysis and viability criteria

Data from the gated FDG PET studies were re-orientated to short-axis, horizontal and vertical long-axis sections. Data of FDG was analyzed quantitatively and displayed in a 17-segment polar map as recently proposed (11), using the quantitative gated SPECT (QGS) program (version 3; Cedars-Sinai Medical Center, Los Angeles, CA), a commer-

cially (Siemens Medical Systems, Hoffman Estates, Ill) available cardiac software package (12,13). Average segmental counts were calculated from the 17 segments and normalized to the segment with the highest average counts.
WT was automatically calculated and expressed in a 17-segment polar map as the percentage increase in wall thickness from the end-diastolic to the end-systolic phase. Receiver operating characteristic (ROC) curve analysis was used both for FDG uptake and WT to determine the optimal cutoff value for prediction of improvement in regional and global LV function (using MRI as the gold standard) (14,15). The performance of a variable can be classified using the area under the curve with 0.90-1 = excellent, 0.80-0.90 = good, 0.70-0.80 = fair, 0.60-0.70 = poor and 0.50-0.60 = test without value.

Statistical analysis
Descriptive results were expressed as mean ± SD. Patient data were compared using the Student's *t* test for (un)paired data when appropriate. Pairwise deletion Mann-Whitney statistics was used to compare the difference between areas under the curve (determined by ROC curve analysis) for FDG uptake and WT. Sensitivity and specificity for the prediction of improvement in regional function were subsequently determined. McNemar's test was used to compare the sensitivity and specificity of FDG uptake and WT for prediction of improvement post-revascularization.
Univariate logistic regression analysis was performed to determine which variables best predicted improvement in LVEF post-revascularization. The relation between the number of dysfunctional and viable segments and the change in LVEF after revascularization was determined by linear regression analysis. ROC curve analysis was performed to determine the optimal number of dysfunctional but viable segments (according to FDG uptake and WT), allowing discrimination between patients with and without improvement in LVEF ≥ 5% (16). Sensitivity and specificity to predict improvement in LVEF were subsequently determined. Sensitivity and specificity were also calculated for prediction of LV reverse remodeling (defined as a reduction ≥10% in LV volumes). McNemar test was used to compare the sensitivity and specificity between FDG uptake and WT to predict improvement in LVEF and LV reverse remodeling after revascularization. A *P*-value < 0.05 was considered significant.

Results

Thirty-eight patients underwent revascularization, in particular 23 patients underwent CABG and 15 patients underwent PTCA (mean number of target vessels per patient: 2.5 ± 0.7). The procedures were uncomplicated. Repeat coronary angiography (to assess vessel- or graft-patency) was performed in 27 patients demonstrating that 3 bypass grafts were occluded and 3 lesions after PTCA showed re-stenosis. The patients who did not undergo repeat coronary angiography did not have recurrent symptoms after revascularization, and grafts/vessels were considered patent.

Of all 646 myocardial segments in the 38 patients, 2 (0.3%) segments were excluded from further analysis because of technical reasons. Another 27 (4%) segments allocated to the vessels/grafts with re-stenosis or occlusion were also excluded.
Data analysis was based on the remaining 617 segments. Of these, 359 (58%) segments had contractile dysfunction, with 213 segments belonging to the distribution area of revascularized vessels. These 213 segments were used for the final analysis. Of these 213 revascularized segments, 145 (68%) were hypokinetic and 68 (32%) were a- or dyskinetic before revascularization.

Prediction of improvement of regional function

Using ROC analysis, a segmental FDG uptake value of ≥50% was identified as the optimal cutoff value, with an area under the curve of 0.91 ± 0.03. For WT on gated FDG PET, an optimal cutoff value of 10% WT was identified with an area under the curve of 0.89 ± 0.03. The difference between both areas under the curve was not significant (Figure 3).
Of all 213 dysfunctional segments, 133 (62%) improved in function on the follow-up MRI (Figure 4). Of these 133 recovered segments, 125 (93%) segments were classified as viable using the cutoff value of 50% FDG uptake. Of the 80 segments without recovery, only 12 (15%) were incorrectly identified as viable by FDG uptake. Accordingly, FDG uptake had a sensitivity of 93% with a specificity of 85% for the prediction of recovery of regional function post-revascularization. Using the cutoff value of 10% WT, 119 (89%) of 133 segments with functional recovery were considered viable, as compared to only 18 (22%) of the segments without recovery. Hence, the sensitivity and specificity were 89% (NS vs FDG uptake) and 78% (P <0.05 vs FDG uptake) respectively.
The results of 190 (89%) segments between FDG uptake and WT were concordant, whereas 23 (11%) segments showed discordance. Out of these 23 segments, 17 (74%) segments were correct with FDG uptake, and 6 (26%) segments with WT.
Sensitivity and specificity were also assessed for hypokinetic and a-/dyskinetic segments separately, by using the same cutoff values of FDG uptake and WT. Of the 145 hypoki-

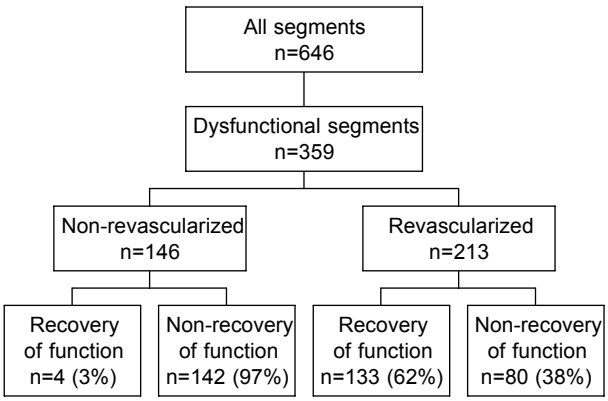

Figure 3. Recovery of dysfunctional segments after revascularization

netic segments, 93 (64%) showed recovery of function post-revascularization. The sensitivity and specificity for FDG uptake were 94% and 86%, whereas the sensitivity and specificity for WT were 91% (NS vs FDG uptake) and 78% (P <0.05 vs FDG uptake). Of the 68 a-/dyskinetic segments, 30 (44%) recovered in function after revascularization. The sensitivity and specificity for FDG uptake were 91% and 85% as compared to 86% (NS vs FDG uptake) and 79% (P <0.05 vs FDG uptake) for WT.

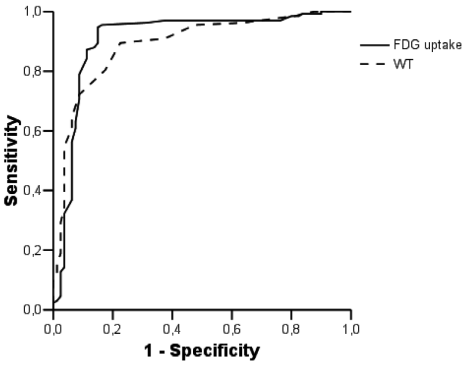

Figure 4. ROC curves for the prediction of improvement in regional function post-revascularization using percentage FDG uptake (area under curve 0.91 ± 0.03) and wall thickening (area under curve 0.89 ± 0.03, NS versus % FDG uptake). The optimal cutoff values were ≥50% for FDG uptake and ≥10% for wall thickening.

Prediction of improvement in LVEF

The mean LVEF in the 38 patients improved from 32 ± 10% to 39 ± 12% (P < 0.001).

An improvement in LVEF ≥5% was observed in 24 (63%) patients. The characteristics of the patients with and without improvement in LVEF are summarized in Table 1. Univariate analysis (including age, gender, previous myocardial infarction, NYHA class, LVEF, number of stenosed vessels, previous CABG/PTCA, diabetes and number

Table 1. Characteristics of patients with and without improvement in LVEF after revascularization

	Pts with improved LVEF (n = 24)	Pts without improved LVEF (n = 14)	*P*-value
Age (yrs)	64 ± 7	67 ± 8	NS
Gender (M/F)	24/6	14/0	NS
Previous infarction	18 (75%)	12 (85%)	NS
Diabetes	6 (25%)	3 (21%)	NS
Previous PTCA/CABG	7 (29%)	3 (21%)	NS
Nr stenosed vessels	2.5 ± 0.7	2.7 ± 0.6	NS
LVEF (%)	31 ± 11	32 ± 8	NS
LVEDV (mL)	141 ± 45	160 ± 65	NS
LVESV (mL)	99 ± 45	110 ± 54	NS
NYHA class pre-revascularization	3.0 ± 1.1	3.2 ± 1.1	NS
Nr FDG viable segs	4.5 ± 2.2	1.5 ± 1.3	<0.001
Nr FDG non-viable segs	1.2 ± 1.8	2.2 ± 2.1	NS
Nr WT viable segs	4.7 ± 2.0	1.5 ± 1.2	<0.001
Nr WT non-viable segs	1.3 ± 1.8	2.1 ± 2.3	NS

CABG: coronary artery bypass grafting; LVEDV: left ventricular end-diastolic volume; LVEF: left ventricular ejection fraction; LVESV: left ventricular end-systolic volume; NYHA: New York Heart Association; PTCA: percutaneous transluminal coronary angioplasty; Segs: segments; WT: wall thickening.

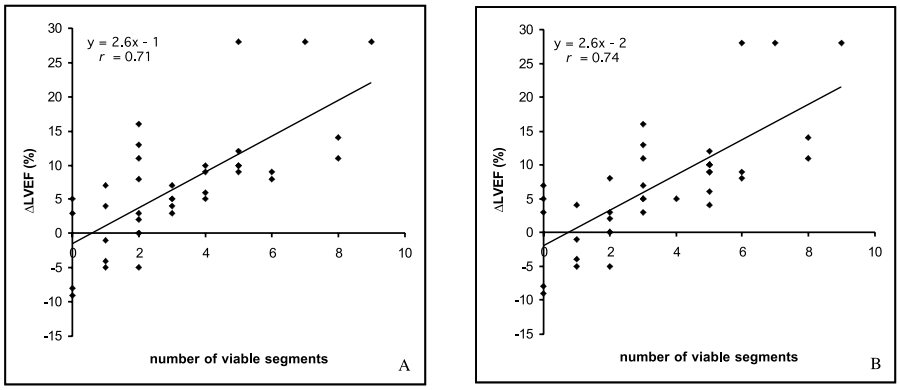

Figure 5. scatterplots showing the relation between the number of viable segments with ≥50% FDG uptake (panel A) and ≥10% wall thickening (panel B) and the change in LVEF after revascularization.

of viable/nonviable segments) indicated that the number of viable segments according to both FDG uptake or WT were the only predictors of improvement in LVEF after revascularization (Table 1). A correlation was observed between the number of revascularized, viable segments on both FDG uptake and WT and the magnitude of improvement in LVEF, indicating that the extent of viability directly determined the magnitude of improvement in LVEF post-revascularization (P <0.001) (Figures 5A and 5B).

ROC curve analysis showed that ≥3 viable segments on FDG uptake or WT had the highest accuracy to predict improvement in LVEF, with a comparable area under the curve (0.87 ± 0.03 versus 0.87 ± 0.02, NS, see Figure 6). This resulted in a sensitivity and specificity of 87% and 85% for FDG uptake and 75% (P <0.05 vs FDG uptake) and 85% (NS vs FDG uptake) for WT.

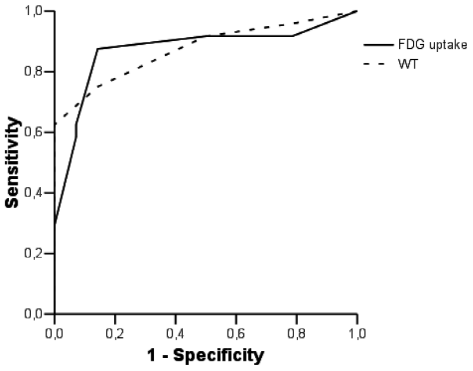

Figure 6. ROC curves for the prediction of improvement in LVEF post-revascularization improvement (LVEF ≥5%) using the number of viable segments with preserved (≥50%) FDG uptake (area under curve 0.87 ± 0.03) and the number of viable segments with preserved (≥10%) wall thickening (area under curve 0.87 ± 0.02, NS versus % FDG uptake). The optimal cutoff values were ≥3 viable segments, both for FDG uptake and wall thickening.

Prediction of LV reverse remodeling

Based on ROC curve analysis, the optimal cutoff level for prediction of LV reverse remodeling (reduction in LVEDV or LVESV ≥10%) was considered ≥3 viable segments on both

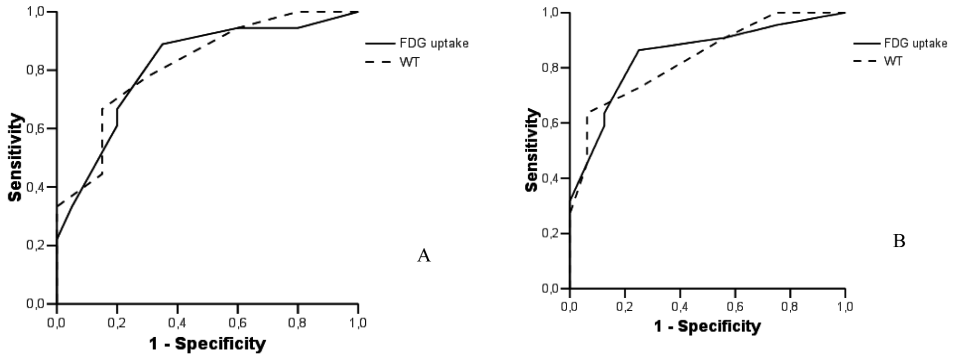

Figure 7. Panel A: ROC curves for the prediction of (≥10%) reduction in LVEDV post-revascularization using the number of viable segments with preserved (≥50%) FDG uptake (area under curve 0.82 ± 0.07) and the number of viable segments with preserved (≥10%) wall thickening (area under curve and 0.82 ± 0.07; *P* = NS versus % FDG uptake). The optimal cutoff values were ≥3 viable segments, both for FDG uptake and wall thickening.
Panel B: ROC curves for the prediction of (≥10%) reduction in LVESV post-revascularization using the number of viable segments with preserved (≥50%) FDG uptake (area under curve : 0.85 ± 0.06) and the number of viable segments with preserved (≥10%) wall thickening (area under curve and 0.83 ± 0.06; *P* = NS versus % FDG uptake). The optimal cutoff values were ≥3 viable segments, both for FDG uptake and wall thickening.

FDG uptake and WT (Figure 7). Patients with ≥3 viable segments on both FDG uptake and WT demonstrated a significant reduction in LVEDV and LVESV. Conversely, patients with less than 3 viable segments demonstrated ongoing LV remodeling with a significant increase in LV volumes (Table 2). FDG uptake had a sensitivity and specificity of 89% and 65% to predict reverse LV remodeling, as compared to 78% (*P* <0.05 vs FDG uptake) and 70% (NS vs FDG uptake) for WT.

Discussion

The most important findings of this study can be summarized as follows. ROC curve analysis identified the optimal cutoff values for FDG uptake and WT as 50% tracer uptake and 10% WT. These cutoff values yielded good sensitivity for the detection of viability of 93% and 89% (NS) respectively with a specificity of 85% and 78% (*P* <0.05) respectively. In 74% of the discordant segments, FDG uptake predicted regional recovery correctly in comparison to WT. For prediction of improvement in LVEF the sensitivities for FDG uptake and WT were 87% and 75% respectively (P <0.05) with a specificity of 85% both. For prediction of reverse LV remodeling, the sensitivities were 89% and 78% (*P* <0.05) for FDG uptake and WT respectively, with specificities of 65% and 70% (NS).

Table 2. Left ventricular remodeling (reverse and ongoing) in viable patients (≥3 viable segments with preserved FDG uptake or WT) or nonviable patients (<3 viable segments with preserved FDG uptake or WT).

Viable patients

	LVEDV Pre	LVEDV Post	mean difference	*P*	LVESV Pre	LVESV Post	mean difference	*P*
FDG≥50%	138±44	117±31	-21±27	<0.05	94±43	69±36	-25±21	<0.02
WT≥10%	138±45	116±38	-21±29	<0.05	95±44	69±36	-25±21	<0.02

Nonviable patients

	LVEDV Pre	LVEDV Post	mean difference	*P*	LVESV Pre	LVESV Post	mean difference	*P*
FDG≥50%	162±16	184±77	+21±35	<0.02	115±54	133±64	+18±31	<0.02
WT≥10%	167±62	188±72	+21±35	<0.02	117±51	135±61	+18±31	<0.02

LVEDV: left ventricular end-diastolic volume (mL); LVESV: left ventricular end-systolic volume (mL); WT: wall thickening.

FDG uptake as a marker for functional recovery

Many studies (n=22) have employed FDG PET to evaluate tissue viability and predict improvement of regional and global function after revascularization (2,17-20). The minority of these studies (n=4) used the relative FDG uptake value, normalized to the peak of activity, in order to predict functional recovery after revascularization (2,17,18,20). The cutoff values for FDG uptake varied from 50% to 65% in these previous FDG PET studies and were chosen arbitrarily. Two studies actually reported the accuracy to predict outcome after revascularization. Baer et al. performed FDG PET in 42 patients with LV dysfunction (LVEF 40 ± 13%) to predict functional recovery, using ≥50% FDG uptake as threshold value (2). Transesophageal echocardiography was used to assess wall motion before and 4-6 months after revascularization. Sensitivity was similar, but specificity was considerably lower compared to our study for the prediction of improvement of regional function. Schmidt et al. performed FDG PET in 40 patients with LV dysfunction (LVEF 42 ± 10%) to predict functional recovery, using ≥50% FDG uptake as threshold value (20). MRI was used to assess wall motion before and 4-6 months after revascularization. Sensitivity and specificity were 100% and 73% for the prediction of outcome. The current findings are in line with these results, although a higher specificity was noted in the present study. This may be due to the fact that ROC curve analysis was used to optimize results.

Wall thickening as a marker for functional recovery

A relatively new approach is the use of WT on gated FDG PET for the assessment of myocardial viability. The initial studies evaluating preserved WT as a marker of viability were performed with use of MRI. Perrone-Filardi et al. were the first to report on the use of MRI for assessment of WT to evaluate viability (21). In 25 patients with chronic LV dysfunction (LVEF 28 ± 10%), the authors demonstrated that dysfunctional but viable segments (according to FDG PET) had preserved WT on MRI. Since the patients did not

undergo revascularization, improvement of function could not be studied.
Few studies have performed a comparison between WT derived from gated FDG PET and MRI (22-24). With the newer software algorithms, WT can now be assessed from gated SPECT or PET imaging. Comparative studies in normal individuals reported good correlations between gated FDG PET and MRI for the assessment of regional WT (22). Waiter et al. compared gated FDG PET with MRI for the assessment of WT in a pilot study including 9 patients with ischemic heart disease and reduced LV function (24). Wall thickening on MRI and PET was assessed visually, using a three point grading scale; agreement between the 2 techniques was 81%. When MRI was considered the gold standard for WT, gated FDG PET had a sensitivity and specificity of 79% and 82% to assess preserved WT. Improvement of function post-revascularization has not been studied using WT on gated FDG PET. However, several SPECT studies with ^{99m}Tc-labeled agents have aimed at predicting functional recovery post-revascularization based on preserved WT (25-29). Stolfuss et al. evaluated 19 patients (mean LVEF 35 ± 7%) and reported a sensitivity of 82% with a specificity of 54% to predict functional recovery using gated ^{99m}Tc-tetrofosmin SPECT; the authors analyzed WT visually, using a semi-quantitative five-point scoring method and combined the WT results with the perfusion data (27). In the current study, a comparable sensitivity (89%) and specificity were noted with a higher specificity (78%) was noted. A potential explanation for the higher specificity observed in the current study may be related to the superior spatial resolution of PET as compared to SPECT. Also, attenuation correction as used with PET may allow a superior detection of WT as compared to SPECT.

Which parameter to predict recovery?
In the current study, 2 parameters obtained with FDG PET to assess viability were evaluated: percentage FDG uptake and percentage WT. This head-to-head comparison in patients undergoing revascularization, demonstrated that sensitivity for both approaches was comparable (93% versus 89%), whereas specificity was higher for percentage FDG uptake (85% versus 78%, P <0.05). This observation can be related to the fact that WT may not entirely reflect active contraction, but can also occur as a passive process (tethering) in partially infarcted areas. Indeed, studies using echocardiography have shown that subendocardial infarction frequently resulted in hypokinesia (not akinesia) which did not improve in function after revascularization (30). Also, studies using MRI have demonstrated that special tagging techniques are needed to differentiate active contraction in hypokinetic segments from passive motion (tethering) (31).
Other studies have frequently compared FDG uptake with regional perfusion in order to assess regions with perfusion-metabolism mismatch as marker of viability (5,32,33). These studies generally showed the highest accuracy to predict functional outcome post-revascularization (19). Regional perfusion was not assessed in the current study, and therefore this approach could not be directly compared with percentage FDG uptake or WT. However, the results of our study, using WT in combination with FDG uptake for the prediction of functional recovery, is comparable to these previous studies using perfusion-metabolism mismatch as marker of viability.

Clinical implications

From a clinical point of view, improvement in LVEF is more important than improvement in regional LV function prediction (34-36). Accurate identification of patients who may improve in LVEF is important, since LVEF is an important prognostic parameter (37). In the present study, 24 patients (63%) showed improvement in LVEF (≥5%) after revascularization. In line with previous studies, the number of viable segments on gated FDG PET was linearly related to the improvement in LVEF post-revascularization. Moreover, patients with 3 or more viable segments using either FDG uptake or WT had a high likelihood of functional recovery post-revascularization, although sensitivity was somewhat higher with FDG uptake as compared to WT (85% versus 75%, $P < 0.05$).

Another clinically relevant end-point is prediction of reverse LV remodeling after revascularization. The data in the current study support the hypothesis that patients with viable myocardium do not only benefit from revascularization in terms of improvement in LVEF, but also by prevention of ongoing LV remodeling or even reverse remodeling after revascularization. Large trials have demonstrated the prognostic value of LV volumes for long-term outcome, and therefore identification of patients with a high likelihood of prevention of ongoing LV remodeling or even reverse remodeling is important (38,39). At least as important is the observation that patients with nonviable myocardium showed ongoing LV remodeling after revascularization, with a significant increase in LV volumes. These results indicate that revascularization per se, does not necessarily stop the remodeling process, and stress the value of viability assessment to identify patients who may benefit from revascularization. The results in the current study indicate that both percentage FDG uptake and WT are useful markers to assess viability and predict benefit from revascularization.

Limitations

Some limitations of this study need attention. First, repeat cardiac catheterization was not performed in all patients; however, none of the patients without repeat catheterization had recurrent symptoms. Second, functional follow-up was performed at 6 months after revascularization; this period may be too short to fully appreciate recovery of function; previous work demonstrated that recovery of function may occur up to one year after revascularization (40).

Conclusion

The observations in the present study provide further support for the use of FDG PET to predict outcome after revascularization. Segments with ≥50% FDG uptake or ≥10% WT have a high likelihood to improve in function post-revascularization. Patients with ≥3 viable segments according to these criteria have a high likelihood to improve in LVEF and will not suffer ongoing LV dilatation. Preserved (≥50%) FDG uptake is slightly superior to preserved (≥10%) WT to predict outcome.

Acknowledgement

We thank Nic J.G.M. Veeger for statistical assistance.

Reference List

1. Allman KC, Shaw LJ, Hachamovitch R, Udelson JE. Myocardial viability testing and impact of revascularization on prognosis in patients with coronary artery disease and left ventricular dysfunction: a meta-analysis. J Am Coll Cardiol. 2002; 39(7):1151-1158.
2. Baer FM, Voth E, Deutsch HJ, Schneider CA, Horst M, de Vivie ER et al. Predictive value of low dose dobutamine transesophageal echocardiography and fluorine-18 fluorodeoxyglucose positron emission tomography for recovery of regional left ventricular function after successful revascularization. J Am Coll Cardiol. 1996; 28(1):60-69.
3. Bax JJ, Cornel JH, Visser FC, Fioretti PM, Van Lingen A, Reijs AE et al. Prediction of recovery of myocardial dysfunction after revascularization. Comparison of fluorine-18 fluorodeoxyglucose/thallium-201 SPECT, thallium-201 stress-reinjection SPECT and dobutamine echocardiography. J Am Coll Cardiol. 1996; 28(3):558-564.
4. Tillisch J, Brunken R, Marshall R, Schwaiger M, Mandelkern M, Phelps M et al. Reversibility of cardiac wall-motion abnormalities predicted by positron tomography. N Engl J Med. 1986; 314(14):884-888.
5. Tamaki N, Kawamoto M, Tadamura E, Magata Y, Yonekura Y, Nohara R et al. Prediction of reversible ischemia after revascularization. Perfusion and metabolic studies with positron emission tomography. Circulation. 1995; 91(6):1697-1705.
6. Knuuti MJ, Yki-Jarvinen H, Voipio-Pulkki LM, Maki M, Ruotsalainen U, Harkonen R et al. Enhancement of myocardial [fluorine-18]fluorodeoxyglucose uptake by a nicotinic acid derivative. J Nucl Med. 1994; 35(6):989-998.
7. Schinkel AF, Bax JJ, Valkema R, Elhendy A, van Domburg RT, Vourvouri EC et al. Effect of diabetes mellitus on myocardial 18F-FDG SPECT using acipimox for the assessment of myocardial viability. J Nucl Med. 2003; 44(6):877-883.
8. van der Geest RJ, Buller VG, Jansen E, Lamb HJ, Baur LH, van der Wall EE et al. Comparison between manual and semiautomated analysis of left ventricular volume parameters from short-axis MR images. J Comput Assist Tomogr. 1997; 21(5):756-765.
9. Senior R, Lahiri A, Kaul S. Effect of revascularization on left ventricular remodeling in patients with heart failure from severe chronic ischemic left ventricular dysfunction. Am J Cardiol. 2001; 88(6):624-629.
10. Arnese M, Fioretti PM, Cornel JH, Postma-Tjoa J, Reijs AE, Roelandt JR. Akinesis becoming dyskinesis during high-dose dobutamine stress echocardiography: a marker of myocardial ischemia or a mechanical phenomenon? Am J Cardiol. 1994; 73(12):896-899.
11. Hendel RC, Corbett JR, Cullom SJ, DePuey EG, Garcia EV, Bateman TM. The value and practice of attenuation correction for myocardial perfusion SPECT imaging: a joint position statement from the American Society of Nuclear Cardiology and the Society of Nuclear Medicine. J Nucl Cardiol. 2002; 9(1):135-143.
12. Germano G, Kavanagh PB, Berman DS. An automatic approach to the analysis, quantitation and review of perfusion and function from myocardial perfusion SPECT images. Int J Card Imaging. 1997; 13(4):337-346.
13. Germano G, Erel J, Lewin H, Kavanagh PB, Berman DS. Automatic quantitation of regional myocardial wall motion and thickening from gated technetium-99m sestamibi myocardial perfu-

sion single-photon emission computed tomography. J Am Coll Cardiol. 1997; 30(5):1360-1367.
14. Hanley JA, McNeil BJ. A method of comparing the areas under receiver operating characteristic curves derived from the same cases. Radiology. 1983; 148(3):839-843.
15. Metz CE. Basic principles of ROC analysis. Semin Nucl Med. 1978; 8(4):283-298.
16. Bax JJ, Poldermans D, Elhendy A, Cornel JH, Boersma E, Rambaldi R et al. Improvement of left ventricular ejection fraction, heart failure symptoms and prognosis after revascularization in patients with chronic coronary artery disease and viable myocardium detected by dobutamine stress echocardiography. J Am Coll Cardiol. 1999; 34(1):163-169.
17. Kitsiou AN, Bacharach SL, Bartlett ML, Srinivasan G, Summers RM, Quyyumi AA et al. 13N-ammonia myocardial blood flow and uptake: relation to functional outcome of asynergic regions after revascularization. J Am Coll Cardiol. 1999; 33(3):678-686.
18. Knuesel PR, Nanz D, Wyss C, Buechi M, Kaufmann PA, von Schulthess GK et al. Characterization of dysfunctional myocardium by positron emission tomography and magnetic resonance: relation to functional outcome after revascularization. Circulation. 2003; 108(9):1095-1100.
19. Knuuti J, Schelbert HR, Bax JJ. The need for standardisation of cardiac FDG PET imaging in the evaluation of myocardial viability in patients with chronic ischaemic left ventricular dysfunction. Eur J Nucl Med Mol Imaging. 2002; 29(9):1257-1266.
20. Schmidt M, Voth E, Schneider CA, Theissen P, Wagner R, Baer FM et al. F-18-FDG uptake is a reliable predictory of functional recovery of akinetic but viable infarct regions as defined by magnetic resonance imaging before and after revascularization. Magn Reson Imaging. 2004; 22(2):229-236.
21. Perrone-Filardi P, Bacharach SL, Dilsizian V, Maurea S, Frank JA, Bonow RO. Regional left ventricular wall thickening. Relation to regional uptake of 18fluorodeoxyglucose and 201Tl in patients with chronic coronary artery disease and left ventricular dysfunction. Circulation. 1992; 86(4):1125-1137.
22. Porenta G, Kuhle W, Sinha S, Krivokapich J, Czernin J, Gambhir SS et al. Parameter estimation of cardiac geometry by ECG-gated PET imaging: validation using magnetic resonance imaging and echocardiography. J Nucl Med. 1995; 36(6):1123-1129.
23. Sinha S, Sinha U, Czernin J, Porenta G, Schelbert HR. Noninvasive assessment of myocardial perfusion and metabolism: feasibility of registering gated MR and PET images. AJR Am J Roentgenol. 1995; 164(2):301-307.
24. Waiter GD, Al Mohammad A, Norton MY, Redpath TW, Welch A, Walton S. Regional myocardial wall thickening assessed at rest by ECG gated (18)F-FDG positron emission tomography and by magnetic resonance imaging. Heart. 2000; 84(3):332-333.
25. Kang WJ, Lee DS, Paeng JC, Kim KB, Chung JK, Lee MC. Prognostic value of rest (201)Tl-dipyridamole stress (99m)Tc-sestamibi gated SPECT for predicting patient-based clinical outcomes after bypass surgery in patients with ischemic left ventricular dysfunction. J Nucl Med. 2003; 44(11):1735-1740.
26. Mabuchi M, Kubo N, Morita K, Makino Y, Matsui Y, Murashita T et al. Prediction of functional recovery after coronary bypass surgery using quantitative gated myocardial perfusion SPECT. Nucl Med Commun. 2003; 24(6):625-631.
27. Murashita T, Makino Y, Kamikubo Y, Yasuda K, Mabuchi M, Tamaki N. Quantitative gated myocardial perfusion single photon emission computed tomography improves the prediction of regional functional recovery in akinetic areas after coronary bypass surgery: useful tool for evaluation of myocardial viability. J Thorac Cardiovasc Surg. 2003; 126(5):1328-1334.
28. Petretta M, Storto G, Acampa W, Sansone V, Evangelista L, Spinelli L et al. Relation between wall thickening on gated perfusion SPECT and functional recovery after coronary revascularization in patients with previous myocardial infarction. Eur J Nucl Med Mol Imaging. 2004; 31(12):1599-1605.
29. Stollfuss JC, Haas F, Matsunari I, Neverve J, Nekolla S, Ziegler S et al. 99mTc-tetrofosmin

SPECT for prediction of functional recovery defined by MRI in patients with severe left ventricular dysfunction: additional value of gated SPECT. J Nucl Med. 1999; 40(11):1824-1831.
30. Cornel JH, Bax JJ, Elhendy A, Poldermans D, Vanoverschelde JL, Fioretti PM. Predictive accuracy of echocardiographic response of mildly dyssynergic myocardial segments to low-dose dobutamine. Am J Cardiol. 1997; 80(11):1481-1484.
31. Garot J, Bluemke DA, Osman NF, Rochitte CE, McVeigh ER, Zerhouni EA et al. Fast determination of regional myocardial strain fields from tagged cardiac images using harmonic phase MRI. Circulation. 2000; 101(9):981-988.
32. Gerber BL, Vanoverschelde JL, Bol A, Michel C, Labar D, Wijns W et al. Myocardial blood flow, glucose uptake, and recruitment of inotropic reserve in chronic left ventricular ischemic dysfunction. Implications for the pathophysiology of chronic myocardial hibernation. Circulation. 1996; 94(4):651-659.
33. vom-Dahl J, Eitzman DT, al Aouar ZR, Kanter HL, Hicks RJ, Deeb GM et al. Relation of regional function, perfusion, and metabolism in patients with advanced coronary artery disease undergoing surgical revascularization. Circulation. 1994; 90(5):2356-2366.
34. Meluzin J, Cerny J, Frelich M, Stetka F, Spinarova L, Popelova J et al. Prognostic value of the amount of dysfunctional but viable myocardium in revascularized patients with coronary artery disease and left ventricular dysfunction. Investigators of this Multicenter Study. J Am Coll Cardiol. 1998; 32(4):912-920.
35. Meluzin J, Cerny J, Nemec P, Frelich M, Stetka F, Spinarova L. Do the presence and amount of dysfunctional but viable myocardium affect the perioperative outcome of coronary artery bypass graft surgery? Int J Cardiol. 1999; 71(3):265-272.
36. Pagley PR, Beller GA, Watson DD, Gimple LW, Ragosta M. Improved outcome after coronary bypass surgery in patients with ischemic cardiomyopathy and residual myocardial viability. Circulation. 1997; 96(3):793-800.
37. White HD, Norris RM, Brown MA, Brandt PW, Whitlock RM, Wild CJ. Left ventricular end-systolic volume as the major determinant of survival after recovery from myocardial infarction. Circulation. 1987; 76(1):44-51.
38. Bax JJ, Schinkel AF, Boersma E, Elhendy A, Rizzello V, Maat A et al. Extensive left ventricular remodeling does not allow viable myocardium to improve in left ventricular ejection fraction after revascularization and is associated with worse long-term prognosis. Circulation. 2004; 110(11 Suppl 1):II18-II22.
39. Mule JD, Bax JJ, Zingone B, Martinelli F, Burelli C, Stefania A et al. The beneficial effect of revascularization on jeopardized myocardium: reverse remodeling and improved long-term prognosis. Eur J Cardiothorac Surg. 2002; 22(3):426-430.
40. Bax JJ, Visser FC, Poldermans D, Elhendy A, Cornel JH, Boersma E et al. Time course of functional recovery of stunned and hibernating segments after surgical revascularization. Circulation. 2001; 104(12 Suppl 1):I314-I318.

Hoofdstuk 8

Comparison of gated positron emission tomography with magnetic resonance imaging for evaluation of left ventricular function in patients with coronary artery disease.

Riemer H.J.A. Slart[1], Jeroen J. Bax[2], Richard M. de Jong[3], Jaep de Boer[1]; Hildo J. Lamb[4], Piet H. Mook[5], Antoon T.M. Willemsen[1], Willem Vaalburg[1]; Dirk J. van Veldhuisen[3], Pieter L. Jager[1]

Department of Nuclear Medicine and Molecular Imaging[1], University Medical Center Groningen, Department of Cardiology[2], Leiden University Medical Center, Department of Cardiology[3], University Medical Center Groningen, Department of Radiology[4], Leiden University Medical Center, Department of Radiology[5], University Medical Center Groningen, The Netherlands.

J Nucl Med 2004 Feb;45(2):176-82.

Abstract

The aim of this study was to compare left ventricular (LV) volumes and regional wall motion (RWM) determined by PET with those determined by the reference technique, cardiovascular MRI.

Methods: LV end-diastolic volume (LVEDV), LV end-systolic volume (LVESV), and LV ejection fraction (LVEF) were measured and RWM was scored in 38 patients with chronic coronary artery disease using both gated FDG PET and MRI. A 9-segment model was used for PET and MRI to assess RWM.

Results: Good correlations were observed between MRI and gated PET for all parameters (*r* values ranging from 0.91 to 0.96). With PET, there was a significant but small underestimation of LVEDV and LVEF. Mean ± SD LVEDV, LVESV, and LVEF for MRI and gated PET was 131 ± 57 mL, 91 ± 12 mL, 33 ± 12% and 117 ± 56 mL, 85 ± 51 mL, 30 ± 11%, respectively. For regional wall motion, an agreement of 85% was found, with a kappa statistic of 0.79 (95% confidence intervals 0.70 to 0.89, SE 0.049).

Conclusion: LV volumes, LVEF and region wall motion can be assessed with gated FDG PET and correlate well with these parameters assessed by MRI.

Key words: gated FDG PET, left ventricular volumes, LVEF, regional wall motion, MRI.

Introduction

Left ventricular ejection fraction (LVEF), left ventricular end-diastolic volume (LVEDV) and left ventricular end-systolic volume (LVESV) are important prognostic parameters in patients with chronic coronary artery disease (CAD) and left ventricular (LV) dysfunction (1). Hence, accurate assessment of LVEF and LV volumes in these patients is important and several non-invasive techniques are available for this purpose, including 2D echocardiography (2), magnetic resonance imaging (MRI) (3), and radionuclide ventriculography (4). Positron emission tomography (PET) is a well-established technique for the imaging and quantification of myocardial metabolism and perfusion. Metabolic imaging with ^{18}F-fluorodeoxyglucose (FDG) is considered the gold standard for assessment of viability (5,6). Electrocardiographically (ECG) gated PET with FDG offers the unique potential combining LV function and myocardial metabolism assessments in a single PET examination. Limited data are available on the accuracy of gated PET compared with the accuracy of MRI for the assessment of LVEF, LV volumes and regional wall motion in patients with depressed LV function (7-11). Most of these studies were performed with other techniques, including gated SPECT, left ventriculography, and 2D echocardiography, to compare LV function, LV volumes and regional wall motion function with those determined by gated PET. MRI is considered the gold standard for determining parameters of LV function. The aim of this study was to compare the accuracy of gated PET with that of MRI (serving as the gold standard) for the assessment of LV function, LV volumes, and regional wall motion in patients with chronic CAD and depressed LVEF.

Materials and methods

Patients

The inclusion criteria were angiographically proven CAD and impaired LV function documented on 2D echocardiography or LV angiography by use of an ejection fraction cutoff value of approximately 45%. Exclusion criteria were unstable angina pectoris or heart failure requiring hospitalization, cardiac pacemakers or intracranial clips, arrhythmias making ECG gating impossible, and claustrophobia.

Thirty-eight patients (28 men and 10 women; mean age 66 ± 9 yrs) with clinically diagnosed CAD were evaluated in this study. All patients underwent an ECG gated FDG PET scan and ECG triggered MRI within one week.

Twenty-eight patients had a previous myocardial infarction (all > 6 months before the study) and 17 patients exhibited Q waves on the electrocardiogram (8 anterior, 5 inferior, 2 both and 2 lateral) (Table 1). These patients had 2.2 ± 0.7 vessels with a significant stenosis of more than 70% diameter reduction (7 patients had 1-vessel disease, 15 had 2-vessel disease and 16 had 3-vessel disease). Ten patients had type 1 or 2 diabetes, and 7 had systemic hypertension. Nine patients had undergone previous revascularization. Twenty-eight patients had angina pectoris (Canadian Cardiovascular Society class 1-4).

None of the patients had cardiac events or additional therapeutic interventions between the PET and MRI scans.

Table 1. Patient Characteristics

Parameter	Value*
Patients:	38
Male	28
Female	10
Mean ± SD age (y)	66 ± 9
Medical history:	
Myocardial infarction	28
Coronary angioplasty	7
Coronary artery bypass graft	2
Diabetes Mellitus	10
Systemic hypertension	7
CAD:	
One vessel	7
Two vessels	15
Three vessels	16
Angina pectoris	28

*Reported as number of patients unless indicated otherwise.
Canadian Cardiovascular Society classes 1-4.

PET scanning

All anti-anginal medication and caffeine containing beverages were withdrawn at least 24 h prior to the PET studies. Patients were prepared with a glucose-enriched breakfast, except diabetic patients. At 90 min before FDG injection, 500 mg of acipimox (a nicotinic acid derivative) was administered orally. To prevent side-effects of acipimox (eg. skin rash), 250 mg of aspirin was given just before acipimox intake. An euglycaemic hyperinsulinaemic glucose clamp was used in accordance with a standardized protocol as described by DeFronzo et al. (12) and Knuuti et al. (13) in patients with insulin-dependent diabetes mellitus

Gated FDG PET was performed on an ECAT-951/31 PET system (Siemens/CTI) imaging 31 planes over a total axial length of 10.8 cm. After the transmission scan (^{68}Ge/^{68}Ga rod sources) was performed, 400 MBq of FDG was injected intravenously, followed by the acquisition procedure. The total FDG acquisition time was 50 min, the last 20 min were in gated acquisition mode with 16 frames per cardiac cycle. The myocardial count rate was higher than 10 kcps coincident. All gated FDG PET scans were obtained in phased mode, that is, the length of each gate was optimized for the current RR-interval. The RR-interval was allowed to vary by ± 10%. Data were corrected for attenuation with the transmission scan and were reconstructed with filtered back-projection (Hann filter: 0.5 pixels/cycle). After manual reorientation, 12 short-axis images were obtained with a plane thickness from 7 to 9 mm at an in-plane resolution of approximately 7 mm.

PET data analysis

A quantitative gated single photon emission computed tomography (QGS) analysis program derived from Germano et al. (14-17) to assess LV volumes, LVEF and RWM was used to analyze the gated PET data. In brief, QGS segments the myocardium on the basis of LV short-axis images. Endocardial and epicardial surfaces are determined on the basis of count profiles that are fitted to asymmetric Gaussian curves. With myocardial size, shape, and location criteria, surface points can be determined even in regions without apparent radioactivity uptake. These calculations are performed for each gate, resulting in a determination of the myocardial surfaces as a function of the cardiac cycle. LVEF is calculated from the largest and smallest LV volumes, defined as end-diastole and end-systole (Figure 1). We applied this program to gated PET data without any changes or pre-processing except for a translation of the data to the required input format.

A 9-segment model, including 1 apical segment, 4 distal segments (anterior, lateral, inferior and septal) and 4 basal segments (anterior, lateral, inferior and septal), was used for PET. Each segment was assigned a wall motion score of 0 to 2: normal = 0, hypokinetic= 1, and akinetic/dyskinetic= 2.

A summed wall motion score was calculated for each patient as the sum of the individual scores of the 9 segments.

Also, the 9-segment polar map was used to display LV FDG uptake. Segments were scored according to a 4-point scoring system: 0 = normal (activity 75-100% of maximum), 1 = mild reduction (50-75%), 2 = severe reduction (25-50%), 3 = absent tracer uptake (activity 0-25%).

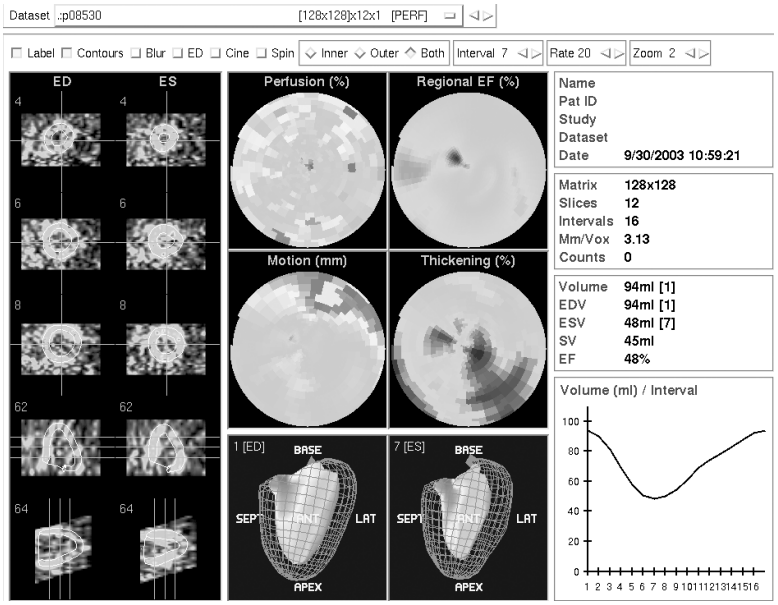

Figure 1. Image from QGS of the end-diastolic (A) and end-systolic (B) phases showing epicardial and endocardial borders of the left ventricle. SEPT = septal; LAT = lateral.

MRI acquisition

All images were acquired with patients in the supine by use of a 1.5 T MRI system (Siemens Vision, Siemens Medical Systems) with a flexible body array coil for signal reception. Spin-echo scout images were obtained in the coronal and sagital imaging planes, after which the short-axis plane was determined. The short-axis plane was defined perpendicular to the LV long-axis from the center of the mitral annulus to the apex. Slices of 8 mm were acquired at 8 to10 base-to-apex short-axis locations during repeated breath holds (± 15 s) with a 2D fast low-angle shot ECG triggered sequence with various repetition times (TRs). The field of view was 300 - 350 mm. Images were obtained in 128 x 256 matrices.

During 1 cardiac cycle of a breath hold, a limited number (5 – 10) of raw data lines were acquired for each TR for the succesive phases of the cardiac cycle. Therefore, the breath hold should span a number of cardiac cycles to fill the k-space. The TR ranged from 40 to 100 ms with an echo time of 6 ms depending on the R-R interval of the patient and the number of cardiac phases to be imaged.

MRI data analysis

A Sparc workstation (Sun Microsystems, Mountain View, CA) was used for further analysis. LV volumes were calculated from the MR images using previously validated automated software (MR Analytical Software System [MASS], Leiden, The Netherlands) (18). The details of this procedure have been described previously (18,19). In brief, the borders of the LV on short axes were outlined automatically, but when endocardial detection was unreliable, contours were corrected manually appropriate (Figure 2). The enclosed surface areas were measured automatically. Papillary muscles were regarded as being part of the LV cavity (19). Endocardial and epicardial borders were traced in all end-diastolic and end-systolic images; epicardial fat was excluded (19). The window width and window level settings were determined automatically by scaling to the maximum grey scale.

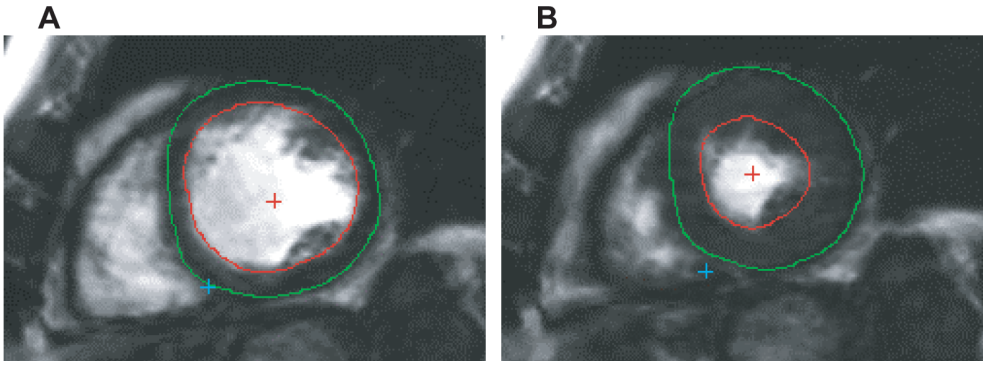

Figure 2. Transverse 2-chamber view of the end-diastolic (A) and end-systolic (B) phases of the left ventricle. Epicardial and endocardial contours are automatically drawn, but incorrect contours can be manually corrected.

LVESV and LVEDV were calculated and the related LVEF was subsequently derived. For the assessment of RWM, MRI images were visually interpreted by a single, experienced observer unaware of the PET results. A 9-segment model was used with the same scoring system as that described above; each segment was assigned a wall motion score by use of a 3-point scoring system (0 to 2 for normal to akinetic or dyskinetic).

Statistical analysis

Continuous data of EDV, ESV and LVEF values were expressed as mean ± SD and tested for statistical significance with the 2-tailed student's test for paired data. The agreement for segmental wall motion was assessed from 3 x 3 tables by use of weighted kappa statistics. Kappa values of <0.4, between 0.4 and 0.75, and >0.75 were considered to represent poor, fair to good, and excellent agreement, respectively, based on Fleiss classification (20). The kappa values are reported with their 95% confidence intervals (CI) and their SEs.

The agreements among LVESV, LVEDV, LVEF, and summed wall motion scores derived from the gated PET and MRI data were determined by linear regression (Pearson's correlation coefficient) and Bland-Altman analysis (21). The absence of a relation between the summed FDG defect score and the difference between LVEF measured by gated PET and MRI was evaluated by linear regression analysis (Pearson's correlation coefficient). For all tests, a *P* value of <0.05 was considered significant.

Ethics

All patients gave informed consent for the gated FDG PET and MRI study. The study was approved by the local research ethics committee.

Results

Non-gated FDG PET data

Twenty-six patients exhibited severe FDG defects (activity 0-25%), with a mean of 2.8 ± 1.6 segments per patient. In addition, 28 patients also exhibited moderate defects (score 1 or 2).

Regional wall motion by MRI and gated PET

Ten LV segments of two MRI studies were dropped from this investigation because of reduced quality resulting from patient movement.

On MRI, 159 segments exhibited normal wall motion, 118 demonstrated hypokinesia, and 55 akinesia or dyskinesia. On gated PET, 146 segments showed normal wall motion, 137 revealed hypokinesia, and 49 akinesia or dyskinesia. The agreement on a segmental basis is demonstrated in Table 2. An agreement of 85% was found with a kappa statistics of 0.79 (95% CI 0.70 to 0.89, SE 0.049), indicating excellent agreement. Importantly, 43 of 55 of the akinetic or dyskinetic segments (78%) on the MRI were identically classified

by gated PET and 102 of the 118 hypokinetic segments (86%) were also classified hypokinetic by gated PET. Hence, for the 173 dysfunctional segments on MRI, the exact agreement was 83% (with a kappa statistics of 0.79, 95% CI 0.68 to 0.90, SE 0.055). An agreement of 79% was found between FDG PET studies with segments showing ≤ 25% FDG uptake and akinetic or dyskinetic segments on MRI.

Virtually all disagreements between MRI and gated PET wall motion scores were a 1-grade difference (49/50; 98%). The relation between the summed wall motion scores was excellent (y =0.83x + 1.20, r =0.92, P <0.001) and is demonstrated in Figure 3. The agreement on a patient basis (expressed by the percentage of identically scored segments) varied from 67% to 100%, with a mean agreement of 85 ± 11% per patient; importantly, the agreement was > 85% in 21 patients. Three basal segments (anterior, lateral, inferior) and 2 distal segments (lateral and septal) exhibited the highest agreement (> 85%) (Figure 4). The basal anterior segment and the apex revealed the lowest agreement between the 2 techniques (70%).

Table 2. Agreement between MRI and gated FDG PET for assessment of Regional Wall Motion Score (RWMS)

	No. of segments with the following RWMS on gated PET			
RWMS on MRI	0	1	2	Total
0	136	22	1	159
1	10	103	5	118
2	0	12	43	55
Total	146	37	49	332

Agreement was excellent (85%; kappa statistic, 0.79)

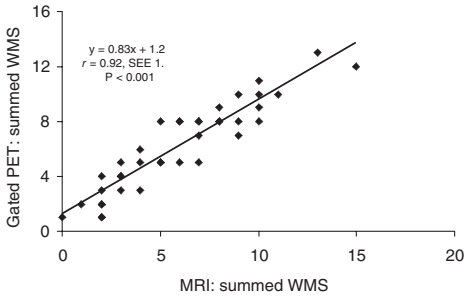

Figure 3. Relationship between the summed wall motion score (WMS) per patient on MRI and on gated FDG PET.

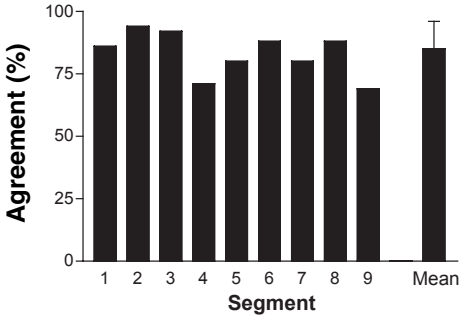

Figure 4. Agreement of regional wall motion score (RWMS) per segment on MRI and on gated FDG PET. Basal segments: 1 =anterior; 2 =lateral; 3 =inferior; 4=septal. Distal segments: 5 =anterior; 6 =lateral; 7 =inferior; 8 =septal; 9 =apical segment. Mean = mean agreement for all 9 segments ± SD.

LV volumes and LVEF evaluated by MRI and gated PET

The quantitative measurements of LV volumes and LVEF are shown in Table 3. LVESV measured by MRI ranged from 31 to 202 mL (mean 91 ± 12 mL). The corresponding values for gated PET (range 24 to 198 mL, mean 85 ± 51 mL, P =0.57) were slightly lower but not significantly different from MRI. Linear regression revealed a good correlation (y =0.91x + 2.0, r =0.94, P <0.0001) between LVESV measured by MRI and gated PET (Figure 5A). The Bland-Altman plot showed a mean difference of 12.5 ± 13.5 mL which was not significantly different from zero (P =0.57) (Figure 5B).

LVEDV measured by MRI ranged from 61 to 267 mL (mean 131 ± 57 mL). The corresponding values for gated PET were lower: LVEDV ranged from 41 to 242 mL (mean 117 ± 56 mL, P <0.01). Linear regression demonstrated a good correlation (y = 0.93x + 22.1, r = 0.91, P <0.001) between LVEDV measured by MRI and gated PET (figure 6A). The Bland-Altman plot showed a mean difference of 19.6 ± 18.7 mL, which was significantly different from 0 (Figure 6B).

LVEF measured by MRI ranged from 14% to 59% (mean 33 ± 12%). The corresponding values for gated PET were close to MRI but significantly different: LVEF ranged from 13%

Table 3. Measurements of LV volumes and LVEF by MRI and gated FDG PET

	Value determined by:		
Measurement	MRI	Gated PET	*P*
LVESV	91 ± 12	85 ± 51	0.57
Mean (mL)	31-202	24-198	
Range (mL)			
LVEDV			
Mean (mL)	131 ± 57	117 ± 56	<0.001
Range (mL)	61-267	41-242	
LVEF			
Mean (%)	33 ± 12	30 ± 11	<0.001
Range	14-59	13-55	

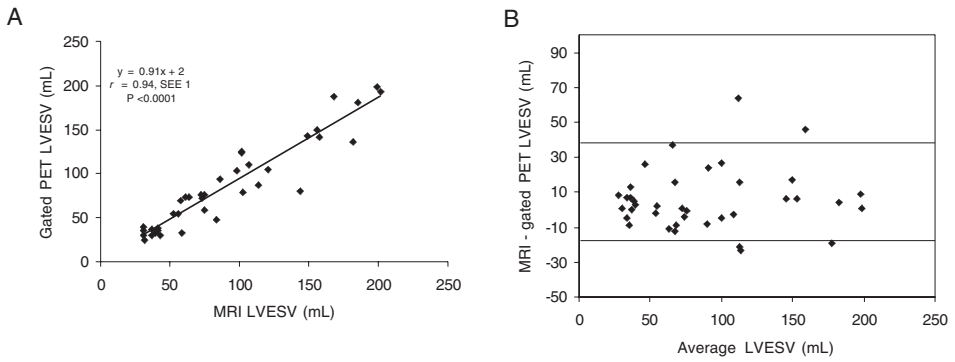

Figure 5. Relationship between LVESV assessed by MRI and gated FDG PET (A). Bland-Altman plot for LVESV without a systematic trend (B).

to 55% (mean 30 ± 11%, P <0.01). The results from the linear regression analysis showed a good correlation (y = 1.0x + 2.5, r = 0.96, P <0.001) between LVEF assessed by MRI and gated PET (Figure 7A). The Bland-Altman plot for LVEF showed a mean difference of 3.4 ± 2.2 %, which was significantly different from 0 (Figure 7B).

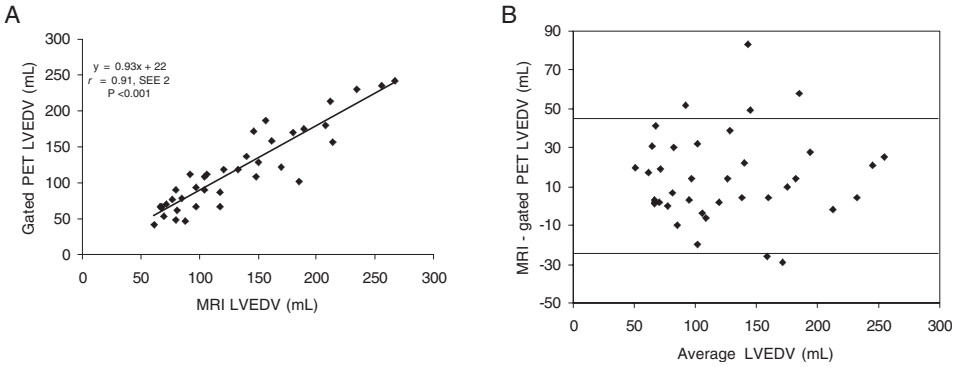

Figure 6. Relationship between LVEDV assessed by MRI and gated FDG PET (A). Bland-Altman plot for LVEDV without a systematic trend (B).

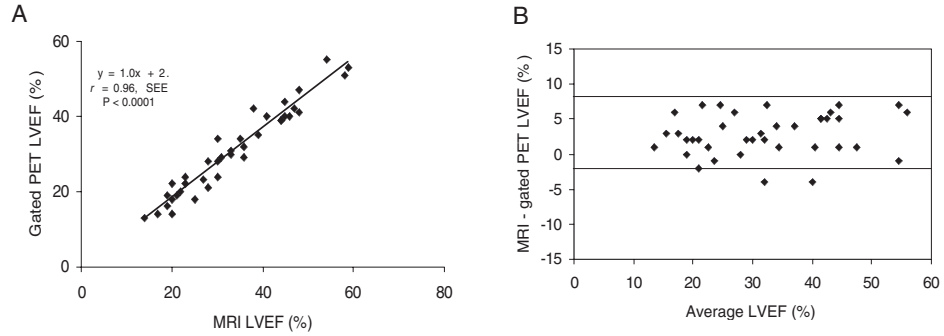

Figure 7. Relationship between LVEF assessed by MRI and gated FDG PET (A). Bland-Altman plot for LVEF without a systematic trend (B).

Variation in LV volumes and other parameters

The relation between various gated PET parameters and the difference between LV volumes assessed by MRI and gated PET was investigated. The underestimation of the LVEDV or LVESV by gated PET compared with MRI was not related to the number of akinetic and/or dyskinetic segments on gated PET, nor to the total number of segments with absent FDG uptake (activity, 0-25%).

Discussion

In this study, good correlations between gated PET and MRI were observed for the parameters regional wall motion, LVESV, LVEDV and LVEF.

For regional wall motion, the exact agreement between the 2 techniques was 85%. Virtually all differences were within 1 grade of regional wall motion. The largest share of discrepancies between the 2 modalities was attributable to 12 segments with hypokinesia on MRI that were classified as akinetic on gated PET.

The relatively small number of segmental discrepancies may be due to spatial misalignment of segments between the MRI and gated PET images volumes. Although segmental analysis is important, a more global analysis may also be relevant as an indication for intervention. From this point of view, it is important to note that the correlation between the summed wall motion score obtained with the 2 techniques was very good. When individual patients were considered, the mean exact agreement was 85% of all segments per patient (Figure 4). These data suggest that gated PET provides adequate clinical information on regional wall motion in nearly all patients with depressed LVEF. These results are comparable to those obtained by Vaduganathan et al. (22) who used a similar study protocol to compare gated SPECT versus MRI.

Few other studies have compared gated PET and MRI for assessment of LV function. Waiter et al. (8) compared regional myocardial wall thickening of gated PET at rest versus that on MRI and showed a segmental correlation of 81%. A disadvantage of their visual method of wall thickening scoring may be over- or underestimation of the regional LV function when a segment shows a high or low FDG uptake, respectively.

The correlations in our study between LV volumes measurements by gated PET and MRI were also very good, although both LVESV and LVEDV were lower with gated PET than with MRI.

Two possible explanations for this finding can be ruled out: No relationship was found between the underestimation of LV volumes by gated PET and the extent or severity of FDG defects, and no relationship was found between the extent or severity of regional wall motion abnormalities and underestimation of LV volumes.

Underestimation of LV volume measurements with gated PET may be attributable to automatic algorithms, differences in nature of the images, and variances in how algorithms operate. For example, MRI algorithms consider papillary muscles as being part of the LV cavity, whereas the gated PET algorithms merges papillary muscles into the myocardial wall, thereby reducing the cavity volume. The finding of underestimation of LVESV and LVEF is most likely due to the fact that the temporal resolution of gated FDG PET is lower than that of MRI. Also the used 2D (with septa) imaging on our PET scanner may result in lower sensitivity than modern instruments in the 3D mode. This 2D system may produce noisy data, which could contribute to the slight underestimation of cardiac volumes. PET data are reconstructed, and the use of different filter sets will influence LV volume measurements, as ia also the case with gated SPECT data (23). Patient motion or respiration motion may also influence the determination of LVEF, but appropriate

instruction to the patient will at least reduce patient motion.
Despite these differences in LV measurement techniques, the correlations between gated PET and MRI for assessment of LV volumes, LVEF and RWM were high.
Schaefer et al. also evaluated LV function and regional wall motion of gated FDG PET in comparison with MRI in 30 patients, using also QGS for gated FDG PET quantification (24). They also found a high correlation between gated FDG PET and MRI for EDV, ESV and LVEF (r =0.96, r =0.97, and r =0.95, respectively). They found a total agreement of both techniques in all region wall motion scoring classifications of 76%, a fraction lower than our finding of 85%. This small difference is may be due to used gates of 8 per cardiac cycle instead of 16.
Willemsen et al. (17) compared the same QGS program (originally developed for gated SPECT), suitable for PET systems, with equilibrium radionuclide angiography (ERNA) in 20 patients with CAD. They observed a high correlation between the QGS program and ERNA in LVEF measurement and a slight underestimation of LVEF (y= -5.9 + 0.90 (ERNA) – EF; r =0.86) by gated PET.
Gated PET probably better estimates LVEF, LVEDV and LVESV as obtained by the standard, MRI, than does gated SPECT (25). This situation probably results from the higher spatial resolution of PET than of SPECT, a fact that minimizes the uncertainty in the exact position of the myocardial wall. In addition, the small LV volume problem, common with gated SPECT, is less present with gated PET, because of the higher spatial resolution of PET. The algorithm of Germano et al. is based on detection of the myocardial wall from short-axis slices, but the exact wall position is subsequently corrected, based on validation studies by means of segmentation algorithm that has been empirically determined from SPECT studies (16). As gating of SPECT data has added greatly to the clinical value of myocardial SPECT, gating of PET data may contribute even more to the value of PET. LV function estimated by gated PET may be of additional value to the observer-dependent ultrasound results. Combining regional wall motion with according perfusion-metabolism match and mismatch patterns can be beneficial for interpretation. Gated PET results therefore argue in favor of cardiac PET studies in general.
Other PET techniques, including gated blood-pool PET after red blood-cell labeling with $C^{15}O$, also provides information about LV volumes and function but do not provide information about metabolism (26,27). A major advantage of the gated FDG PET technique is the integration of the assessment of myocardial metabolism and contractile function. In combination with PET myocardial perfusion imaging, gated FDG PET permits a complete LV evaluation, using a single technique for the evaluation of major clinical parameters, including metabolism, flow reserve and LV function. Obtaining functional information of the LV requires no additional scanning time or tracer injection. Therefore, successful assessment of cardiac function by gated FDG PET without the need for other clinical modalities will reduce significantly the time needed and the costs of prerevascularization examinations. Also, the single-technique approach inherently has the advantage of a very good image alignment, which allows the 3D comparison of regional function versus myocardial perfusion and metabolism.

Conclusion

Gated FDG PET permits the assessment of LV volumes, LVEF and RWM and all these parameters correlated well with those determined by MRI. Gated FDG PET can be performed easily following a dynamic FDG acquisition protocol, and the data will facilitate the integration of the assessment of myocardial metabolism and contractile function by PET without additional scanning time or patient burden.

Acknowledgement

We greatly acknowledge Dirk Schuiling for analyzing the MRI studies and Hans Hillege for statistical assistance.

Reference List

1. White HD, Norris RM, Brown MA, Brandt PW, Whitlock RM, Wild CJ. Left ventricular end-systolic volume as the major determinant of survival after recovery from myocardial infarction. Circulation. 1987;76:44-51.
2. Starling MR, Crawford MH, Sorensen SG, Levi B, Richards KL, O'Rourke RA. Comparative accuracy of apical biplane cross-sectional echocardiography and gated equilibrium radionuclide angiography for estimating left ventricular size and performance. Circulation. 1981;63:1075-1084.
3. Van der Wall EE, Vliegen HW, De Roos A, Bruschke AV. Magnetic resonance imaging in coronary artery disease. Circulation. 1995;92:2723-2739.
4. Wackers FJ, Berger HJ, Johnstone DE, et al. Multiple gated cardiac blood pool imaging for left ventricular ejection fraction: validation of the technique and assessment of variability. Am J Cardiol. 1979;43:1159-1166.
5. Di Carli MF. Predicting improved function after myocardial revascularization. Curr Opin Cardiol. 1998;13:415-424.
6. Tamaki N, Kawamoto M, Tadamura E et al. Prediction of reversible ischemia after revascularization. Perfusion and metabolic studies with positron emission tomography. Circulation. 1995;91:1697-1705.
7. Hattori N, Bengel FM, Mehilli J, et al. Global and regional functional measurements with gated FDG PET in comparison with left ventriculography. Eur J Nucl Med. 2001;28:221-229.
8. Waiter GD, Al-Mohammad A, Norton MY, Redpath TW, Welch A, Walton S. Regional myocardial wall thickening assessed at rest by ECG gated (18)F-FDG positron emission tomography and by magnetic resonance imaging. Heart. 2000;84:332-333.
9. Hoffmeister HM, Helber U, Franow A, et al. ECG-gated 18F-FDG positron emission tomography. Int J Cardiovasc Imaging. 2002;18:363-372.
10. Maruyama A, Hasegawa S, Paul AK, et al. Myocardial viability assessment with gated SPECT Tc-99m tetrofosmin % wall thickening: comparison with F-18 FDG-PET. Ann Nucl Med. 2002;16:25-32.
11. Hör G, Kranert WT, Maul FD, et al. Gated metabolic positron emission tomography (GAPET) of the myocardium: 18F-FDG-PET to optimize recognition of myocardial hibernation. Nucl Med

Commun. 1998;19:535-545.
12. DeFronzo RA, Tobin JD, Andres R. Glucose clamp technique: a method for quantifying insulin secretion and resistance. Am J Physiol. 1979;237:E214-223.
13. Knuuti MJ, Nuutila P, Ruotsalainen U et al. Euglycemic hyperinsulinemic clamp and oral glucose load in stimulating myocardial glucose utilization during positron emission tomography. J Nucl Med. 1992;33:1255-1262.
14. Germano G, Kavanagh PB, Berman DS. An automatic approach to the analysis, quantification and review of perfusion and function from myocardial perfusion SPECT images. Int J Card Imaging. 1997;13:337-346.
15. Germano G, Erel J, Lewin H, Kavanagh PB, Berman DS. Automatic quantification of regional myocardial wall motion and thickening from gated technetium-99m sestamibi myocardial perfusion single-photon emission computed tomography. J Am Coll Cardiol. 1997;30:1360-1367.
16. Germano G, Kiat H, Kavanagh PB, et al. Automatic quantification of ejection fraction from gated myocardial perfusion SPECT. J Nucl Med. 1995;36:2138-2147.
17. Willemsen ATM, Siebelink HJ, Blanksma PK, Paans AMJ. Automatic ejection fraction determination from gated myocardial FDG-PET data. J Nucl Card. 1999;6:577-582.
18. Van der Geest RJ, Jansen E, Buller VGM, Reiber JHC. Automated detection of left ventricular epi- and endocardial contours in short-axis MR images. Comput Cardiol. 1997;21:33-36.
19. Pattynama PMT, Lamb HJ, Van der Velde EA, Van der Wall EE, De Roos A. Left ventricular measurements with cine and spin-echo MR imaging: a study of reproducibility with variance component analysis. Radiology. 1993;187:261-268.
20. Fleiss JL. Statistical methods for rates and proportions. 2nd ed. New York, NY: Wiley, 1981;Chapter 13:212-236.
21. Bland JM, Altman DG. Statistical methods for assessing agreement between two methods of clinical assessment. Lancet. 1986;1:307-310.
22. Vaduganathan P, He Z, Vick GW, Mahmarian JJ, Verani MS. Evaluation of left ventricular wall motion, volumes, and ejection fraction by gated myocardial tomography with Tc-99m tetrofosmin: a comparison with cine magnetic resonance imaging. J Nucl Cardiol. 1998;6:3-10.
23. Wright GA, McDade M, Martin W, Hutton I. Quantitative gated SPECT: the effect of reconstruction filter on calculated left ventricular ejection fractions and volumes. Phys Med Biol. 2002;21:N99-105.
24. Schaefer WM, Lipke CSA, Nowak B et al. Validation of an evaluation routine for left ventricular volumes, ejection fraction and wall motion from gated cardiac FDG PET: a comparison with cardiac resonance imaging. Eur J Nucl Med. 2003;30:545-553.
25. Ioannidis JPA, Trikalinos TA, Danias PG. Electrocardiogram-gated single- photon emission computed tomography versus cardiac magnetic resonance imaging for the assessment of left ventricular volumes and ejection fraction. A meta-analysis. J Am Coll Cardiol. 2002;39:2059-2068.
26. Rajappan K, Livieratos L, Camici PG, Pennell DJ. Measurement of ventricular volumes and function: a comparison of gated PET and cardiovascular magnetic resonance. J Nucl Med. 2002;43:806-810.
27. Boyd HL, Gunn RN, Marinho NVS, et al. Non-invasive measurement of left ventricular volumes and function by gated positron emission tomography. Eur J Nucl Med. 1996;23:1594-1602.

Chapter 9

9.1 Summary

Differentiation between viable and non-viable myocardium in patients with coronary artery disease and left ventricular (LV) dysfunction plays a major role in decision making for revascularization. New noninvasive techniques may improve the accuracy for the detection of viable myocardium, but careful evaluation of these new techniques is needed before clinical use.

SECTION I: General introduction and outline of the thesis. **Chapter 1** presents an overview about the different conventional and new nuclear imaging techniques and backgrounds for the detection of myocardial viability.

SECTION II: evaluates the value of attenuation correction in myocardial perfusion scintigraphy and viability detection. **Chapter 2** describes the value of attenuation correction (AC) in myocardial perfusion imaging, before and after a 1-year experience period. Non-uniform attenuation of the emitted radiation may produce severe artefacts, which may result in fixed defects on SPECT images that can easily be mistaken for myocardial infarction. The addition of transmission scans, by using line array of gadolinium-153 rods may help in distinguishing attenuation artefacts from myocardial infarction. In this study of patients referred for MPI, both non-corrected (NC) and AC images were analysed by three independent readers shortly after implementation of AC. The same images were re-analysed 1 year later. Results were compared with gold standards for ischemia and infarction based on coronary angiography, follow-up, ultrasound and gated blood pool imaging. We conclude that AC improves interpretation of myocardial perfusion studies. With AC, specificity is increased and sensitivity is similar as compared with NC images. However, AC requires experience and is associated with a learning curve.

Chapter 3 evaluates the value of AC of gated ^{99m}Tc-tetrofosmin SPECT for the detection of myocardial viability in comparison with the reference method FDG SPECT. Both the NC and AC ^{99m}Tc-tetrofosmin SPECT images were compared with the FDG images. By use of AC, the agreement between ^{99m}Tc-tetrofosmin and FDG imaging improved from 84% to 90%. Similar observations were made when the analysis was restricted to the dysfunctional segments. We conclude that addition of AC to gated ^{99m}Tc-tetrofosmin SPECT significantly improved the detection of myocardial viability in patients with chronic coronary artery disease, although as compared with FDG SPECT imaging minimal underestimation of viability remained.

SECTION III: evaluates the value of DISA SPECT for the detection of myocardial viability. In **Chapter 4,** we investigated whether DISA SPECT yields additional information for the assessment of myocardial viability in comparison with rest-stress ^{99m}Tc-sestamibi. Nineteen patients with known coronary artery disease and irreversible perfusion defects on previous rest-stress ^{99m}Tc-sestamibi test studies were analyzed. DISA SPECT was performed using energy windows of 140 (±15%), 170 (±20%) and 511 keV (±15%). Ima-

ges of 140 keV were corrected for scatter by subtraction using the 170 keV window. FDG and ^{99m}Tc-sestamibi images were visually scored for a perfusion-metabolism mismatch pattern. There was an excellent correlation between the ^{99m}Tc-sestamibi uptake detected in the single and dual isotope acquisition. The average difference between the dual and single isotope ^{99m}Tc-sestamibi uptake was 1.2%, which is very low. Of the 79 regions with irreversible perfusion defects on previous rest-stress ^{99m}Tc-sestamibi, six regions in five patients showed a perfusion-metabolism mismatch pattern. We conclude that DISA SPECT does not affect the quality of the ^{99m}Tc-sestamibi images. Furthermore, ^{99m}Tc-sestamibi/FDG DISA SPECT may show viability in a small but significant number of regions with irreversible perfusion defects on rest-stress ^{99m}Tc-sestamibi.

The quality of DISA SPECT is excellent, however the agreement for the assessment of myocardial viability with the reference method positron emission tomography (PET) is unclear. Therefore, in **Chapter 5,** 58 patients with chronic coronary artery disease and LV dysfunction were studied with DISA SPECT and PET. Patients underwent a one-day dipyridamole stress ^{99m}Tc-sestamibi/FDG DISA SPECT and ^{13}N-ammonia/FDG PET protocol. Within 1 week, resting MRI was performed to assess contractile function. Comparison of PET and DISA SPECT data was performed using both visual and quantitative analysis. The correlation of normalized activities of the flow tracers ^{99m}Tc-sestamibi and ^{13}N-ammonia was good, ($r = 0.82$; $P < 0.001$). The correlation between both FDG studies was also good ($r = 0.83$; $P < 0.001$). The agreement for the detection of viability for all segments between DISA SPECT and PET was 82%; in dysfunctional segments only, the agreement was also 82%.

When the DISA SPECT data were analyzed visually, the agreement between DISA SPECT and PET was 83%. Moreover, there was no difference between visual and quantitative DISA SPECT analysis for the detection of viability ($P < 0.001$). We conclude that this study showed an overall good agreement between ^{99m}Tc-sestamibi/^{18}FDG DISA SPECT and PET for the assessment of myocardial viability in patients with severe left ventricular dysfunction. Quantitative or visual analysis of the SPECT data did not influence the agreement with PET, suggesting that visual assessment may be sufficient for clinical purposes.

Patients with LV dysfunction who have viable myocardium are the patients at highest risk because of the potential for ischemia but at the same time benefit most from revascularization, due to functional LV improvement. It is important to identify viable myocardium in these patients. Unclear is the value of DISA SPECT in comparison with PET for the prediction of LV recovery in patients with LV dysfunction.

Therefore, in **Chapter 6**, 47 patients with chronic coronary artery disease and LV dysfunction underwent DISA SPECT (with ^{99m}Tc-sestamibi and FDG) and PET (with ^{13}N-ammonia and FDG) to evaluate the value for the prediction of LV recovery. PET and DISA SPECT data were analyzed quantitatively. MRI was used to assess LV function (regional function, LVEF and LV volumes) before and 6 months after revascularization. For prediction of improvement of regional LV function, PET and DISA SPECT had comparable sensitivity (90% and 89% respectively) and specificity (86% both). For prediction of improvement in LVEF,

sensitivities were 83% for DISA SPECT and 86% for PET (specificities both 100%). Reverse LV remodeling occurred in viable patients after revascularization, whereas nonviable patients showed further LV dilatation after revascularization. Accuracy to predict LV reverse remodeling was similar for DISA SPECT and PET. We conclude that DISA SPECT and PET have comparable accuracy to predict improvement in (regional and global) LV function and reverse LV remodeling.

Although DISA SPECT is an accurate method, PET remains a valuable technique for the assessment of myocardial viability in nuclear medicine institutes equipped with PET cameras. However PET is a comprehensive, time-consuming technique. Gated FDG PET might be a novel technique to reduce the acquisition time. Therefore, ***SECTION IV*** evaluates the value of gated FDG PET for the assessment of myocardial viability. In **Chapter 7**, the value of FDG uptake and wall thickening was analyzed by gated FDG PET for the prediction of recovery of regional and global left ventricular function in 38 patients with coronary artery disease after revascularization. Patients underwent a gated FDG PET protocol and an additional MRI within 1 week to assess regional wall motion and global ventricular function. MRI and coronary angiography were repeated 6 months after revascularization.

Receiver operating characteristic (ROC) curve analysis yielded a cutoff level of ≧50% where FDG uptake gave the highest sensitivity and specificity (93% and 85%, respectively) for prediction of LV recovery after revascularization. Using wall thickening (WT) as a predictor of functional LV recovery, ROC analysis showed ≧10% as the optimal cut off level for the highest sensitivity and specificity (89% and 78%, respectively). The number of viable segments with FDG uptake and WT were the strongest predictors for the improvement in LVEF after revascularization. Reverse LV remodeling occurred in viable patients, whereas nonviable patients showed further LV dilatation after revascularization. Specificity for the prediction of LV reverse remodeling were similar for FDG uptake and WT, although sensitivity was higher using FDG ≥50% uptake criterion.

We conclude that segments with ≥50% FDG uptake or ≥10% WT on gated FDG PET have a high likelihood to improve in function post-revascularization. Patients with ≥3 viable segments according to these criteria have a high likelihood to improve in LVEF and will not suffer ongoing LV dilatation. Preserved (≥50%) FDG uptake is slightly superior to preserved (≥10%) WT to predict outcome.

Gated FDG PET can be used for the assessment of LV volumes, LV ejection fraction (LVEF) and wall motion. Importantly is the accuracy of gated FDG PET for the assessment of these parameters. However, comparative studies with the reference method MRI are scarce. Therefore, the aim of the study in **Chapter 8** was to compare left ventricular (LV) volumes and regional wall motion determined by gated FDG PET with those determined by the reference technique MRI. LV end-diastolic volume (LVEDV), LV end-systolic volume (LVESV), and LVEF were measured and regional wall motion was scored in 38 patients with chronic coronary artery disease by both gated FDG PET and MRI. Good correlations were observed between MRI and gated PET for all parameters (*r* values ranging from 0.91 to 0.96). With PET, there was a significant but small underestimation of

LVEDV and LVEF. LVEDV, LVESV, and LVEF for MRI were 131 ± 57 mL, 91 ± 12 mL, and 33% ± 12%, respectively, and those for gated PET were 117 ± 56 mL, 85 ± 51 mL, and 30% ± 11%, respectively. For regional wall motion, an agreement of 85% was found, with a kappa-statistic of 0.79. We conclude that LV volumes, LVEF, and regional wall motion can beassessed with gated FDG PET and correlated well with these parameters assessed by MRI.

9.2 Future perspectives

9.2.1 General

The number of patients with chronic ischemic heart disease will increase, (partially) due to increasing life expectancy in the Western world. This will further increase the demand on health care. Identification of viable yet jeopardized myocardium helps in selecting patients for whom LV dysfunction, secondary to chronic ischemic heart disease, may improve after revascularization. Therefore, reasonably priced, accurate and patient friendly imaging techniques are needed to fulfil these tasks.
Many nuclear medicine-, radiological techniques and different radiopharmaceuticals are used for the assessment of myocardial viability and LV function, as described in the introduction chapter.

9.2.2 SPECT

Conventional rest-stress gated myocardial perfusion SPECT is a widely used technique for the assessment of myocardial ischemia and LV function, with a good accuracy to assess coronary artery disease. Furthermore, myocardial perfusion scintigraphy is a thoroughly validated technique in comparison with other imaging techniques and has the highest classification for clinical indication according to the international classification system. The addition of gating to SPECT substantially increases the accuracy of the test and has now become the standard. Attenuation correction also increases the accuracy of myocardial perfusion scintigraphy for the detection of ischemia and viability, as confirmed in this thesis, but is less used. Gated myocardial perfusion SPECT also allows the assessment of myocardial viability. Preserved wall thickening and wall motion on gated SPECT indicates viable myocardium. As tracers, ^{201}Thallium and ^{99m}Tc-labeled perfusion tracers (^{99m}Tc-sestamibi and ^{99m}Tc-tetrofosmin) can be used to assess viability. Preserved uptake of these tracers may indicate viability in regions with contractile dysfunction. In rare equivocal cases other techniques complement SPECT.
Although perfusion imaging gives a reasonable impression of viability, imaging using the metabolic tracer FDG is the best method to detect preserved viability. FDG is a tracer for PET imaging, but is also possible with conventional gamma cameras nowadays by using extra-high energy collimators. The current findings in our study clearly establish the use of FDG imaging with SPECT. In the head-to-head comparison between PET and DISA SPECT in patients undergoing revascularization, both techniques yielded a similar accu-

racy for the prediction of improvement in regional and global LV function. Also, both techniques were equally good in predicting reverse LV remodeling after revascularization in patients with viable myocardium. Therefore, this study provides evidence that DISA SPECT is equivalent to PET, and serves as a good alternative to PET for the assessment of myocardial viability in patients considered for revascularization. However, DISA SPECT is not widely implemented on nuclear departments presently, attributable to:

1. The lack of clinical evidence of cardiac DISA SPECT for the detection of myocardial viability in comparison with the conventional rest-stress myocardial perfusion scintigraphy. Our study, however indicates that DISA SPECT is a good alternative for the assessment of myocardial viability and this technique should be implemented clinically and considered for reimbursement. Patients with a LV-dysfunction based on a myocardial infarction or ischemia, should be referred to DISA SPECT for the detection of ischemia and preserved viability.
2. The availability of FDG. Due to better distribution of PET cameras, the use of FDG becomes more practical. Furthermore, the wide availability of SPECT systems will easily lead to the implementation of DISA SPECT imaging in nuclear medicine departments.
3. The opinion that myocardial perfusion SPECT is sufficient for the detection of myocardial viability. In specific cases FDG is of additional value for the detection of preserved viability.

9.2.3 PET

FDG and additional myocardial perfusion imaging with PET is believed to be one of the most accurate methods for the detection of myocardial viability by demonstrating high sensitivity and specificity values. Unlike SPECT, PET can be performed in a static as well as in a dynamic imaging mode. Dynamic acquisition allows absolute quantification of myocardial metabolism and perfusion, by using tracer kinetic models. Static PET acquisition is based on the regional activity distribution, divided by the peak of activity. The accuracy of static and dynamic PET for the detection of myocardial viability is comparable.

PET may be an attractive technique for the detection of myocardial ischemia and viability in patients suspected of endothelial dysfunction or multiple coronary vessel disease, because of the benefits of absolute quantification of myocardial perfusion, flow reserve and metabolism.

Finally, gated FDG PET is an attractive PET technique, because this technique is less time-consuming and reveals an accurate assessment of myocardial viability and LV function, as demonstrated in this thesis.

9.2.4 MRI and echocardiography

Magnetic resonance imaging and echocardiography are other potent diagnostic tools for myocardial viability assessment. MRI and echocardiography can detect myocardial viabi-

lity, using dobutamine stress to assess contractility reserve. Also delayed enhancement (with the contrast media gadolinium) seems to be a reliable marker of scar tissue as compared with ^{201}Thallium or FDG. Another area of interest with MRI is the assessment of myocardial ischemia using gadolinium and vasodilators like adenosine or dipyridamole.
However, MRI and echocardiography are also accompanied by several disadvantages: the reproducibility of echocardiography is moderate, because this depends on the experience of the echocardiographist; dobutamine stress MRI is a relative unattractive protocol for patients, attributable to the length of the procedure and the unpleasant side-effects of dobutamine while laying in the narrow gantry of the MRI; contrast agents are non-specific and cellular processes are not visualized in the way nuclear medicine techniques do; the clinical experience with MRI is limited compared with nuclear imaging techniques; the limitation of MRI and the presence of pacemakers and defibrillators. This last issue may be of particular importance in patients with heart failure, who will frequently have undergone implantation of these devices.

9.2.5 Computed tomography (CT)

CT is not generally used for the assessment of myocardial viability. However, CT may be additional as an AC device in myocardial perfusion scintigraphy. The high photon flux produced by CT generates better correction than the lower flux methods incorporating radioactive sources, such as the array of gadolinium-153 rods, as used in our studies. With the introduction of PET-CT or SPECT-CT systems, CT may be applied as a new attenuation correction tool.
Another potential application of these systems is the possibility of obtaining coronary calcium scores at the same imaging session as the SPECT scan for the assessment of coronary risk. The clinical value of coronary calcium scoring is at this time still an open question in clinical practice and its applicability and significance needs to be explored.
An intriguing possibility is the potential value of CT coronary angiography performed together with SPECT rest-stress perfusion imaging. Multislice CT (MSCT) scanners have been found to have sufficient resolution to image coronary arteries with invasive coronary angiography. There are limitations in visualizing lesions in the smallest distal vessels, and in the presence of heavy calcifications. The latter limitation can be overcome with the aid of the SPECT perfusion results.
It is conceivable that patients with known or suspected disease could be studied with sequential stress-rest perfusion imaging, CT angiography, calcium scoring, ventriculography, and FDG metabolism, allowing acquisitions of superimposed images of both coronary anatomy, perfusion, wall motion, and viability. This complete set of spatially mapped information could add precision and ease to decision-making for interventions planning. This proposition still needs to be evaluated in clinical studies, because the experience of PET- or SPECT-CT is lacking at present.

9.3 Conclusions

Cardiac imaging techniques in nuclear medicine play an important role for the noninvasive evaluation of myocardial viability in patients with coronary artery disease. FDG is a very accurate tracer for the assessment of myocardial metabolism. DISA SPECT is an important technique to detect myocardial viability. With the new developments in AC, gated FDG PET and combined cameras (PET- or SPECT-CT), the accuracy for the detection of myocardial ischemia and viability will be further improved with fewer different techniques. The improved infrastructure of PET (and PET-CT) scanners in combination with the availability of FDG have set the stage for more widespread use of PET(-CT) and probably for DISA SPECT for indications shown to be of benefit. Patients with LV-dysfunction based on a myocardial infarction or ischemia should be referred to DISA SPECT for detection of ischemia and preserved viability. The potential clinical success of nuclear cardiology for the assessment of myocardial viability will contribute to optimal patient selection for coronary revascularization, which is advantageous for patient and society.

Chapter 10

10.1 Samenvatting

Patiënten met kransslagaderlijden en een verminderde linker hartkamer functie (= linker ventrikel (LV) functie) van het hart kunnen zeer gebaat zijn bij een dotterbehandeling of een hartomleiding. De LV functie en de prognose van de patiënt kunnen aanzienlijk verbeteren na deze behandelingen. Wel is het erg belangrijk dat voorafgaande aan de ingreep nauwkeurig vastgesteld wordt hoeveel levensvatbaar, (herstelbaar (vitaal) en niet-levensvatbaar (niet-vitaal = hartinfarcering)) hartspierweefsel aanwezig is. Het is alleen zinvol gebleken patiënten met voldoende vitaal hartspierweefsel te dotteren of te opereren. Bij onvoldoende vitaal hartspierweefsel is het meestal beter de patiënt met medicijnen te behandelen.
Nieuwe nucleair geneeskundige technieken kunnen mogelijk de nauwkeurigheid voor het aantonen van vitaal hartspierweefsel verhogen, echter goede evaluatie van deze nieuwe technieken is noodzakelijk voordat deze klinisch toegepast kunnen worden.

DEEL I: Algemene introductie en doelomschrijving van dit proefschrift. **Hoofdstuk 1** geeft een overzicht van de verschillende conventionele en nieuwe nucleaire afbeeldingstechnieken en hun achtergronden voor het detecteren van vitaal hartspierweefsel.
DEEL II: evalueert de toegevoegde waarde van verzwakkingscorrectie bij de myocardperfusiescintigrafie en de detectie van vitaliteit in het hart. **Hoofdstuk 2** beschrijft de toegevoegde waarde van de verzwakkingscorrectie als nieuwe techniek bij de myocardperfusiescintigrafie, zonder en met 1 jaar klinische ervaring met verzwakkingscorrectie.
Het achterwege laten van verzwakkingscorrectie kan leiden tot artefacten in het myocardperfusiescintigram (uitgevoerd met single positron emission computed tomography (SPECT)). Deze artefacten zijn zogenaamde irreversibele defecten op de SPECT scan die verward kunnen worden met een hartinfarct. Een verzwakkingsartefact wordt veroorzaakt door zich over het hart projecterend weefsel (bijvoorbeeld een borst) dat de gamma-straling absorbeert. Met behulp van verzwakkingscorrectie kunnen er zogenaamde transmissiescans vervaardigd worden. Met deze transmissiescans, waarbij gebruik gemaakt wordt van radioactieve lijnbronnen (gadolinium-153), kan er onderscheid worden gemaakt tussen verzwakkingsartefacten en hartinfarcering. In onze studie werden de zowel niet-verzwakkingsgecorrigeerde als verzwakkingsgecorrigeerde hartstudies door 3 verschillende nucleair geneeskundigen beoordeeld op het moment dat het verzwakkingscorrectie systeem net geïntroduceerd was op de afdeling nucleaire geneeskunde. Dezelfde hartstudies werden 1 jaar later opnieuw door dezelfde nucleair geneeskundigen beoordeeld. De resultaten van de beoordelingen werden vergeleken met het coronair angiogram, de klinische bevindingen, echocardiografie en de MUGA van de patiënten. Wij concluderen dat verzwakkingscorrectie de interpretatie van myocardperfu-

siescintigrafie verbetert. Na verzwakkingscorrectie neemt de specificiteit van het hartonderzoek toe, maar de sensitiviteit blijft onveranderd hoog in vergelijking met het niet-verzwakkingsgecorrigeerde hartonderzoek. Uit het onderzoek blijkt verder dat er sprake is van een leercurve in de interpretatie van verzwakkingsgecorrigeerde hartonderzoeken.

Hoofdstuk 3 evalueert de waarde van verzwakkingsgecorrigeerde gated ^{99m}Tc-tetrofosmin SPECT voor het detecteren van vitaliteit in het hart in vergelijking met de referentie methode FDG SPECT. ^{99m}Tc-tetrofosmin SPECT afbeeldingen, met en zonder verzwakkingscorrectie, werden vergeleken met de FDG SPECT afbeeldingen. Na verzwakkingscorrectie nam de overeenkomst tussen gated ^{99m}Tc-tetrofosmin SPECT en FDG SPECT toe van 84% naar 90%. Overeenkomstige bevindingen werden gezien wanneer alleen die delen van de LV met verminderde wandbewegingen werden geanalyseerd. Wij concluderen dat toevoeging van verzwakkingscorrectie aan gated ^{99m}Tc-tetrofosmin SPECT de detectie van vitaliteit in het hart bij patiënten met kransslagaderlijden duidelijk verbetert. Echter een kleine onderschatting ten op zichte van de FDG SPECT blijft bestaan.

DEEL III: evalueert de waarde van dual isotope simulataneous acquisition (DISA) SPECT voor het detecteren van vitaal hartspierweefsel. Het voordeel van DISA SPECT is dat 2 verschillende isotopen gelijktijdig afgebeeld kunnen worden, waarbij een ^{99m}Tc-gelabelde tracer de perfusie en FDG het metabolisme in het hart afbeeldt. Dit is mogelijk doordat de fotonenergie van ^{99m}Tc en ^{18}F van elkaar verschillen. Door vervolgens verschillende energievensters op de gammacamera te gebruiken kunnen de 2 isotopen van elkaar onderscheiden worden. DISA SPECT draagt bij tot een kortere duur van het onderzoek en geeft tevens een identieke geometrische registratie van de 2 verschillende isotopen.

In **Hoofdstuk 4** hebben we onderzocht of de scankwaliteit van ^{99m}Tc-sestamibi door de FDG van DISA SPECT wordt beïnvloed. Tevens werd gekeken of DISA SPECT een toegevoegde waarde heeft voor het detecteren van vitaliteit in het hart in vergelijking met de conventionele rust-stress ^{99m}Tc-sestamibi scan. In dit onderzoek werden 19 patiënten met kransslagaderlijden en irreversibele perfusiedefecten eerst met een voorafgaande rust-stress ^{99m}Tc-sestamibi scan in kaart gebracht. DISA SPECT werd uitgevoerd met energie vensters van 140 (±15%), 170 (±20%) en 511 keV (±15%). Planaire 140 keV afbeeldingen werden gecorrigeerd voor strooistraling door middel van een subtractie venster van 170 keV. FDG en ^{99m}Tc-sestamibi afbeeldingen van de DISA SPECT werden visueel beoordeeld met betrekking tot perfusie-metabolisme mismatch. Er bleek een uitstekende correlatie te zijn tussen ^{99m}Tc-sestamibi opname op de conventionele rust scan en die op de DISA SPECT scan. Van de 79 segmenten in de linker ventrikel met een irreversibel perfusiedefect op de conventionele rust-stress ^{99m}Tc-sestamibi, waren er 6 segmenten in 5 patiënten met een perfusie-metabolisme mismatch, passend bij restvitaliteit. Wij concluderen dat de DISA SPECT techniek de kwaliteit van de ^{99m}Tc-sestamibi afbeeldingen niet beïnvloedt. Bovendien toont ^{99m}Tc-sestamibi/FDG DISA SPECT rest-vitaliteit aan in een klein, maar significant aantal segmenten van de linker ventrikel.

De kwaliteit van DISA SPECT is uitstekend, maar onduidelijk is wat de klinische waarde van DISA SPECT is in het detecteren van vitaliteit in het hart in vergelijking met de posi-

tron emissie tomografie (PET) scan. De PET scan wordt beschouwd als de gouden standaard om vitaliteit in het hart op te sporen.
Daarom werden in de volgende studie, in **Hoofdstuk 5,** achtenvijftig patiënten met kransslagaderlijden en slechte LV functie (LV ejectie fractie 33 ± 12%) bestudeerd. De patiënten ondergingen op dezelfde dag een dipyridamol (persantin) stress ^{99m}Tc-sestamibi/FDG DISA SPECT scan en ^{13}N-ammonia/FDG PET scan. Binnen 1 week werd er bij deze patiënten een rust MRI verricht om de contractiele functie van de linker ventrikel vast te leggen. De PET en DISA SPECT gegevens werden zowel visueel als kwantitatief geanalyseerd. De kwantitatieve correlatie tussen de perfusietracers ^{99m}Tc-sestamibi and ^{13}N-ammonia was goed, ($r = 0.82$; $P < 0.001$), evenals de correlatie tussen beide FDG studies ($r = 0.83$; $P < 0.001$). De overeenkomst tussen DISA SPECT en PET op segment niveau voor het detecteren van vitaliteit in de linker ventrikel was 82%; wanneer alleen naar dysfunctionele segmenten gekeken werd, was de overeenkomst eveneens 82%.
Wanneer de DISA SPECT gegevens visueel geanalyseerd werden, was de overeenkomst tussen DISA SPECT en PET 83%. Opvallend was, dat er geen verschil was tussen de visuele and kwantitatieve DISA SPECT analyse ($P < 0.001$). Deze studie toont een goede overeenkomst aan tussen ^{99m}Tc-sestamibi/FDG DISA SPECT en PET voor het detecteren van vitaliteit in het hart bij patiënten met een ernstige LV dysfunctie. Kwantitatieve of visuele analyse van de DISA SPECT scan tonen een goede overeenkomst met PET, hetgeen aangeeft dat visuele beoordeling volstaat in de klinische praktijk.
Patiënten met een ernstige LV dysfunctie als gevolg van ischemisch, doch vitaal hartspierweefsel, hebben een verhoogde kans op een fatale hartaandoening. Deze patiënten zijn gebaat bij een revascularisatie van de kransslagaderen, omdat er een grote kans bestaat dat de LV functie hierna zal verbeteren.
Daarom ondergingen zevenenveertig patiënten met kransslagaderlijden en LV dysfunctie zowel een DISA SPECT (met ^{99m}Tc-sestamibi en FDG) als een PET (met ^{13}N-ammonia en FDG) onderzoek, zoals beschreven in **Hoofstuk 6**. De gegevens van de PET en de DISA SPECT studie werden kwantitatief geanalyseerd. De MRI werd gebruikt om de LV functie (regionale functie, LVEF en LV volumes) zowel voor als 6 maanden na de revascularisatie te bepalen. PET en DISA SPECT hadden een vergelijkbare sensitiviteit, respectievelijk 90% en 89%, en specificiteit (beide 86%) voor het voorspellen van het verbeteren van de regionale LV functie. De sensitiviteit voor het voorspellen van LVEF verbetering was voor DISA SPECT 83% en voor PET 86% (specificiteit 100% voor beide technieken). Afname van het LV volume na de revascularisatie, zogenaamde “reverse remodeling”, kwam voor bij patiënten met aangetoonde vitaliteit in het hart. Echter bij patiënten zonder aangetoonde vitaliteit nam het volume van de linker ventrikel verder toe (“ongoing remodeling”). DISA SPECT en PET hadden een vergelijkbare voorspellende waarde voor een afname of toename van de LV volume na revascularisatie. Wij concluderen dat DISA SPECT en PET even goed voorspellen of de (regionale and globale) LV functie en het LV volume zullen verbeteren na revascularisatie.
Alhoewel DISA SPECT een goede methode is, blijft PET alsnog een waardevolle techniek voor het aantonen van vitaliteit in het hart. Echter PET is een vrij langdurig onder-

zoek. Een nieuwe techniek, gated FDG PET, biedt hierin uitkomst. Daarom evalueren we in ***DEEL IV*** de waarde van gated FDG PET voor het detecteren van vitaliteit in het hart. In **Hoofdstuk 7** wordt de mate van FDG opname in de LV en de mate van wandverdikking van de LV gebruikt om te kunnen voorspellen of de regionale en globale LV functie bij 38 patiënten met kransslagaderlijden na revascularisatie zullen herstellen. De patiënten ondergingen binnen 1 week zowel een gated FDG PET scan als een MRI om de regionale en globale LV functie vast te leggen. De MRI en het coronair angiogram werden 6 maanden na revascularisatie herhaald.
Een FDG opname van 50% of meer gaf de hoogste sensitiviteit en specificiteit (respectievelijk 93% en 85%) in het voorspellen van LV functie verbetering na revascularisatie. Een wandverdikking van 10% of meer gaf de hoogste sensitiviteit en specificiteit (89% en 78%, respectievelijk) ter voorspelling van de LV verbetering na revascularisatie. Van alle verschillende parameters hadden het aantal vitale hartsegmenten voor zowel de FDG opname als de wandverdikking de beste voorspellende waarde voor een verbetering in LVEF na revascularisatie. Afname in LV volume trad op bij patiënten met voldoende vitaliteit in het hart. Daarentegen trad bij patiënten met onvoldoende vitaliteit in het hart een toename (=verslechtering) op van het LV volume. De specificiteit van de FDG opname en wandverdikking was gelijk voor het voorspellen van LV volume verbetering. De sensitiviteit van de FDG opname was echter beter dan de wandverdikking.
We concluderen dat LV segmenten met 50% of meer FDG opname of een wandverdikking van 10% of meer een goede kans op herstel hebben na revascularisatie. Patiënten met 3 of meer vitale hartsegmenten, gebaseerd op de bekende FDG- en wandverdikkingscriteria, hebben na revascularisatie een goede kans op herstel van de LVEF zonder verdere LV dilatatie. De FDG opname bleek in het algemeen wel een iets betere voorspeller voor het herstel van LV functie en volume dan de wandverdikking.
Gated FDG PET kan ook gebruikt worden voor het kwantificeren van het volume, de ejectie fractie en de wandbewegingen van de linker ventrikel. Hierbij is van belang om de nauwkeurigheid van gated FDG PET voor deze verschillende parameters vast te leggen. Echter, vergelijkende studies met de MRI (gouden standaard) zijn schaars. Het doel van **Hoofdstuk 8** was om de nauwkeurigheid van gated FDG PET in vergelijking met de MRI vast te stellen. Bij 38 patiënten met kransslagaderlijden werd het LV eind-diastolisch volume (LVEDV), LV eind-systolisch volume (LVESV) en de LVEF bepaald met gated FDG PET en de MRI. Tevens werd bij deze patiëntengroep de wandbewegingen beoordeeld. Voor alle parameters waren de correlaties tussen MRI en gated FGD PET hoog (r –waarden varieerden van 0.91 tot 0.96). Met PET was er wel een kleine onderschatting van de LVEDV en LVEF. De gemiddelde LVEDV, LVESV en LVEF bepaald met MRI waren respectievelijk 131 ± 57 ml, 91 ± 12 ml en 33% ± 12%, en voor gated FDG PET was dit respectievelijk 117 ± 56 ml, 85 ± 51 ml en 30% ± 11%. De overeenkomst in beoordeling van de regionale wandbewegingen tussen gated FDG PET en MRI was 85%, met een kappa van 0.79. Wij concluderen dat met gated FDG PET de LV volumes, de LVEF en de regionale wandbewegingen goed te bepalen zijn en dat deze parameters goed correleren met de MRI bevindingen.

10.2 Toekomstblik

10.2.1 Algemeen

Door de verbeterde levensverwachting zal het aantal patiënten met een chronische, ischemische (op basis van zuurstoftekort) hartaandoening stijgen. Hierdoor zal de druk op de gezondheidszorg, om beeldvorming van deze hartaandoeningen te verrichten, toenemen. Het vaststellen van vitaal hartspierweefel is van belang om te kunnen voorspellen of de LV functie van hartpatiënten zal herstellen na revascularisatie. Daarom is het noodzakelijk dat er betaalbare, nauwkeurige en patiëntvriendelijke afbeeldingsapparatuur beschikbaar is om hieraan te kunnen voldoen. Nucleair geneeskundige technieken spelen hierbij een belangrijke rol.
Op dit moment zijn er verschillende nucleair geneeskundige technieken en radiofarmaca in gebruik ter bepaling van vitaliteit in een dysfunctioneel hart, zoals beschreven in de introductie.

10.2.2 SPECT

De reguliere rust-stress gated myocard perfusie SPECT is een veelgebruikte en goede techniek voor het bepalen van ischemie en de LV functie. De myocardperfusiescintigrafie SPECT is een goed gevalideerde techniek in vergelijking met andere afbeeldingstechnieken. De myocardperfusiescintigrafie SPECT staat hoog geclassificeerd als klinische indicatie. Door de recente toevoeging van gating aan de SPECT techniek is de nauwkeurigheid van myocardperfusiescintigrafie verder substantieel toegenomen. Verzwakkingscorrectie heeft er eveneens toe geleid dat de nauwkeurigheid van de myocardperfusiescintigrafie voor het detecteren van ischemie en vitaliteit in het hart is verbeterd, zoals in dit proefschrift is bevestigd. Gated SPECT verbetert ook de detectie van vitaliteit in de linker ventrikel. Wandverdikking en wandbeweging op de gated SPECT duidt op vitaal hartspierweefsel. De tracers ^{201}Thallium and ^{99m}Tc-gelabelde perfusietracers (^{99m}Tc-sestambi en ^{99m}Tc-tetrofosmin) kunnen gebruikt worden om vitaliteit in de linker ventrikel aan te tonen. Voldoende opname van deze tracers in gebieden van de linker ventrikel met verminderde wandbeweging duidt op vitaal hartspierweefsel. In specifieke gevallen zijn andere technieken aanvullend om rest-vitaliteit in het hart aan te tonen.
Ofschoon de myocardperfusiescintigrafie een goede indruk geeft van vitaliteit in de linker ventrikel, blijft beeldvorming met FDG een van de beste methoden om vitaliteit aan te tonen. FDG wordt gewoonlijk als tracer bij de PET beeldvorming gebruikt. Echter FDG beeldvorming is tegenwoordig ook mogelijk op de conventionele gamma-camera (FDG SPECT), waarbij gebruikt gemaakt wordt van extra hoge energie (EHE) collimatoren. Dit maakt het mogelijk om FDG op grotere schaal voor de cardiologische beeldvorming te gebruiken. De bevindingen van ons onderzoek bevestigen dat goede FDG beeldvorming mogelijk is op een conventionele gammacamera. Uit ons onderzoek komt naar voren dat PET en DISA SPECT een vergelijkbare voorspellende waarde hebben m.b.t. verbetering van de regionale en globale LV functie bij patiënten na revacularisatie. De DISA SPECT techniek lijkt hiermee een goed alternatief te zijn voor PET. Op dit moment is de DISA

SPECT techniek nog beperkt aanwezig op verschillende nucleair geneeskundige afdelingen en daar is een aantal verklaringen voor te geven:

1. Het tot nu toe ontbreken van een goede klinische evaluatie van DISA SPECT voor het detecteren van vitaliteit in het hart. Onze studie geeft nu duidelijk aan dat DISA SPECT een betrouwbare techniek is voor het detecteren van vitaliteit in het hart. De weg is nu vrij om DISA SPECT te implementeren als klinisch diagnosticum. Een belangrijke doelgroep zijn met name patiënten met een LV dysfunctie veroorzaakt door een infarct of ischemie.
2. De beperkte beschikbaarheid van FDG. Inmiddels is het aantal PET camera's sterk uitgebreid en is bovendien FDG eenvoudiger verkrijgbaar. Gecombineerd met de zeer uitgebreide aanwezigheid van conventionele gamma-camera's op de diverse nucleair geneeskundige afdelingen moet het mogelijk zijn DISA SPECT systemen in te voeren.
3. De misvatting dat myocardperfusiescintigrafie alleen, voldoende is voor het bepalen van vitaliteit in het hart. FDG heeft een toegevoegde waarde om rest-vitaliteit in het hart vast te stellen, zoals ook in ons onderzoek naar voren komt.

10.2.3 PET

FDG in combinatie met een perfusietracer wordt gezien als een van de nauwkeurigste methoden voor het detecteren van vitaliteit in het hart. De PET scan kan zowel statisch als dynamisch verricht worden. Het voordeel van de dynamische PET scan is, dat de perfusie en het metabolisme van het hartspierweefsel gekwantificeerd kunnen worden met behulp van kinetische tracer modellen. De statische PET scan is gebaseerd op een semikwantitatieve analyse, waarbij de activiteit in de verschillende regio's van de linker ventrikel vergeleken wordt met de regio met de hoogste activiteit (ratio bepaling). De nauwkeurigheid van de statische en de dynamische PET scan voor het detecteren van hartvitaliteit liggen overigens dicht bij elkaar.

Wanneer conventionele SPECT technieken geen uitsluitsel bieden, kan PET een aanvullende techniek zijn voor het detecteren van ischemie en vitaliteit in het hart. Met name bij patienten met verdenking op endotheeldysfunctie of meertaks/hoofdstamlijden van de kransslagaderen is de kwantificatie van de perfusie, de perfusiereserve en het metabolisme zinvol.

De PET scan uitgevoerd met een rust-, stress-perfusie- en FDG onderdeel is voor de patient een vrij langdurige procedure. Dit probleem kan omzeild worden door gebruik te maken van gated FDG PET. Gated FDG PET wordt zonder een perfusietracer uitgevoerd, maar kan wel op een betrouwbare manier vitaliteit aantonen in een dysfunctionele linker ventrikel, zoals bevestigd in dit proefschrift.

10.2.4 MRI en echocardiografie

Magnetische resonantie beeldvorming en echocardiografie zijn andere potentiële technieken om vitaliteit in het hart vast te stellen. MRI en echocardiografie kunnen met dobutamine stress de reserve-contractiliteit van de linker ventrikel vaststellen. Verder kan met

contrastvloeistof hartinfarcering (zogenaamde late enhancement) opgespoord worden. De betrouwbaarheid van deze methode komt goed overeen met die van ^{201}Tl of FDG. Een andere toepassing van de MRI is het vaststellen van ischemie in het hart met behulp van de contrastvloeistof gadolinium in combinatie met de vasodilatoren adenosine of dipyridamole.
Er zijn echter ook beperkingen aan de MRI en de echocardiografie: de reproduceerbaarheid van de echocardiografie is vrij matig, omdat de kwaliteit van het echo-onderzoek sterk afhankelijk is van de ervaring van de onderzoeker; het dobutamine stress MRI onderzoek is een relatief patiënt onvriendelijk onderzoek, vanwege de duur van het onderzoek, de mogelijke bijwerkingen van dobutamine en het liggen in een kleine ruimte; gadolinium is relatief aspecifiek en geeft niet de cellulaire processen weer zoals de nucleair geneeskundige tracers; de beperkte klinische ervaring met MRI in vergelijking met de nucleair geneeskundige technieken; de contra-indicatie bij patiënten met een pacemaker of defibrillator. Dit laatste punt is met name van belang bij patiënten met hartfalen, die steeds vaker met pacemakers of defibrillatoren uitgerust worden.

10.2.5 Computed tomography (CT)

De CT is vrij recent in de cardiologische beeldvorming geïntroduceerd en staat hiermee nog aan het begin van de ontwikkeling. De CT wordt in het algemeen niet gebruikt voor het aantonen van vitaliteit van het hart. De CT kan wel aanvullend zijn als een verzwakkingscorrectiesysteem met betrekking tot de myocardperfusiescintigrafie. De hoge fotonenstroom die door de CT geproduceerd wordt, geeft een betere verzwakkingscorrectie dan de lage fotonenstroom bij de geïncorporeerde radioactieve lijnbronnen, zoals de gadolinium-152 lijnbronnen in onze studie. Met de introductie van de geïntegreerde PET-CT of SPECT-CT kan de CT eenvoudig worden toegepast als een verzwakkingscorrectiesysteem.
Met deze geïntegreerde camerasystemen is het eveneens mogelijk om een calciumscore van de kransslagaderen te berekenen. De calciumscore is mogelijk een interessante diagnosticum voor risicostratificatie van kransslagaderlijden.
Een andere mogelijkheid van SPECT-CT is het gelijktijdig afbeelden van de kransslagaders middels angiografie en myocardperfusiescintigrafie. Multislice CT (MSCT) scans beschikken over voldoende resolutie om met behulp van contrastvloeistof kransslagaderen af te beelden. Er zijn wel beperkingen in het in beeld brengen van de kleinste vaatstructuren, met name bij ernstige verkalkingen. In dit geval kunnen de SPECT bevindingen een uitkomst bieden.
Het is denkbaar dat patiënten met kransslagaderlijden of de verdenking hierop, geanalyseerd kunnen worden op één camera, met de mogelijkheid om gelijktijdig stress-rust perfusie, angiografie, calciumscore, ventriculografie en FDG metabolisme te bepalen. Alle belangrijke gegevens worden dan tijdens 1 cameraprocedure vastgelegd. Dit complete overzicht van gegevens kan gebruikt worden voor snelle en accurate besluitvorming met betrekking tot eventuele revascularisatie.

10.3 Conclusies

Nucleaire geneeskunde speelt een belangrijke rol binnen de niet-invasieve cardiologische beeldvorming voor het visualiseren van vitaliteit in het hart bij patiënten met kransslagaderlijden. FDG heeft zich hierin bewezen als een nauwkeurige tracer voor het bepalen van vitaliteit in het hart. DISA SPECT is een belangrijke aanvullende techniek voor het detecteren van vitaliteit in het hart. Met de nieuwe ontwikkelingen, zoals verzwakkingscorrectie, DISA SPECT, gated FDG PET en gecombineerde camerasystemen (PET-CT en SPECT-CT), neemt de nauwkeurigheid voor het bepalen van ischemie en vitaliteit in het hart toe. Door de verbeterde beschikbaarheid van PET (en PET-CT) camera's en FDG nemen de mogelijkheden voor cardiologische beeldvorming met FDG toe, dit geldt met name voor DISA SPECT. Het klinisch succes van de nucleaire cardiologie ligt in het nauwkeurig bepalen van ischemie en vitaliteit in het hart, hetgeen zal leiden tot een optimale patiënten selectie voor revascularisatie.

Dankwoord

Klaar, …maar nog niet voordat ik een aantal mensen erg wil bedanken voor hun steun en inzet bij het tot stand komen van dit proefschrift.
Het proefschrift is zeker niet zonder slag of stoot tot stand gekomen. Promoveren gaat gelukkig gepaard met een leercurve, waarbij het opzetten, uitvoeren en uitwerken van het onderzoek steeds beter gaan verlopen. Zonder de hulp van velen was dit echter niet mogelijk geweest.

Om te beginnen wil ik alle patiënten erg bedanken die aan mijn onderzoek hebben meegedaan. Met name het DISA SPECT onderzoek vereiste een lang uithoudingsvermogen van de patiënten. Ik hoop dat het hen verder goed gaat.

Mijn hoofdpromotor Prof. dr. D.J. van Veldhuisen. Beste Dirk Jan, je enthousiaste inzet, toegankelijkheid en adviezen heb ik als plezierig ervaren tijdens mijn onderzoeksperiode en dit heeft tot een goede samenwerking geleid. Het is gelukt om het proefschrift voor de zomervakantie af te ronden en hierin heb jij een belangrijke bijdrage gehad. Ik heb er veel vertrouwen in dat we in de toekomst de samenwerking voort kunnen zetten met betrekking tot nieuwe nucleair cardiologische projecten.

Mijn promotor Prof. dr. E.E. van der Wall. Beste Ernst, ik wil je bedanken voor de prettige contacten en je adviezen op nucleair cardiologisch gebied, waarbij je een goed oog had voor de kernpunten van het onderzoek. Ik vind het eervol dat je mijn promotor wilt zijn en mij de mogelijkheid gaf om de nucleaire cardiologische contacten met Leiden te versterken.

Mijn co-promotor Dr. P.L. Jager. Beste Piet, ik ben je veel verschuldigd voor alle tijd die je in mij hebt geïnvesteerd. Je bent op veel terreinen thuis en daar heb ik steeds dankbaar gebruik van gemaakt. Soms was ik wel eens teleurgesteld over je kritische correcties in mijn artikelen, maar ik kon me er uiteindelijk vaak goed in vinden. Je bent een zeer plezierige collega om mee samen te werken op de afdeling.

Mijn co-promotor Dr. J.J. Bax. Beste Jeroen, ook jou ben ik zeer veel dank verschuldigd voor de professionele ondersteuning tijdens mijn onderzoeksperiode. Vele E-mails en gekoppelde bijlagen hebben er toe geleid dat de artikelen uiteindelijk de juiste vorm kregen. Ik vind je betrokkenheid bij de vele wetenschappelijke lijnen bijzonder. Je weet daar vaak veel uit te halen.

Dr. J. de Boer. Beste Jaep, jij bent de grondlegger van het DISA SPECT onderzoek. Het idee kwam van jou en het is je gelukt stimuleringsgeld van het UMCG te krijgen om daarmee het onderzoek op te starten. Nadat je het UMCG verliet om je als nucleaire geneeskundige in Meppel te vestigen, heb ik het stokje van het onderzoek overgenomen.

Ondanks je drukke bezigheden in de periferie hebben we een aantal avonden bij elkaar gezeten om de gang van zaken door te nemen. Ik heb dit altijd heel waardevol gevonden, waarbij je een scherpe en nuchtere blik had over hoe het onderzoen verder zou moeten gaan. Ik heb je altijd als een erg grote steun op afstand ervaren.

De leden van de beoordelingscommissie, Prof. dr. R.A.J.O. Dierckx, Prof.dr. F. Zijlstra en Prof.dr. B.L.F. van Eck-Smit, wil ik bedanken voor de bereidwilligheid om het proefschrift te bekritiseren en te opponeren tijdens de verdediging.

Dr. D.A. Piers. Beste Bert, bedankt dat je mij destijds voor de opleiding hebt aangenomen, ondanks dat ik min of meer toevallig met de nucleaire geneeskunde in aanraking kwam. Ook kreeg ik de mogelijkheid van je om na het afronden van de opleiding aan te blijven als staflid van de afdeling Nucleaire Geneeskunde. Daarbij kreeg ik veel ruimte van je om mijn promotieonderzoek verder af te werken, hetgeen ik zeer gewaardeerd heb. Je nuchtere blik en brede kennis van zaken hebben mij in de eerste fase van het onderzoek verder geholpen. De stoel voor de dinsdagochtendbesprekingen blijft voor je gereserveerd.

Dr. P.K. Blanksma. Beste Paul, ook jij bent betrokken geweest bij de beginselen van het DISA SPECT onderzoek. Van je PET expertise op cardiologisch gebied heb ik destijds ook veel gebruik gemaakt. Ik ben dan nu ook blij dat ik je het eindresultaat van mijn onderzoek kan overdragen.

Mijn achtereenvolgende kamergenoten Dr. Ir. L. Poot en Drs. K.P. Koopmans.
Beste Lieke, leuke conversaties hebben we gehad op onze kamer en bedankt voor je ondersteuning tijdens mijn onderzoek. Je koe is niet meer.
Beste Klaas-Pieter, bedankt voor je computerondersteuning. Binnenkort gaan we een motortochtje maken.

Dr. Ir. A.T.M. Willemsen. Beste Antoon, je maakt je niet snel druk, maar als het echt moest gebeuren dan ging je er toch voor. Tja, cardiologische beeldvorming, geloof me, is meer dan de moeite waard.

Tonnie Wiegman wil ik bedanken voor het uitwerken van de vele DISA SPECT studies. Uiteindelijk heb ik de uitwerkingen niet kunnen gebruiken, maar ze gaven me wel inzicht in hoe het anders moest.

Dan de paranimfen, Freerk van der Sluis en Koos Mantel.
Beste Freerk, we kennen elkaar al vanaf het begin van de geneeskunde studie. Misschien ben ik af en toe te wetenschappelijk bezig in jouw ogen als huisarts in Friesland, maar na een stevig zeiltochtje met de boot (niet altijd schadevrij) van je ouders op de Friese meren hebben we het er al snel niet meer over. De zomer staat weer voor de

deur.... . Ik ben blij dat je me op 27 juni bij wilt staan.
Beste Koos (Sieuwko), geweldig dat ook jij de rol van paranimf aan wilde nemen. Ook wij kennen elkaar al sinds het begin van de geneeskunde studie, maar jij hebt besloten ondertussen iets anders te gaan doen. Vele uurtjes hebben we aan de stamtafel in der Witz gepraat over het wel en wee in de wereld en natuurlijk over onszelf. Je hebt altijd een luisterend oor voor mijn verhalen.

Alle medewerkers van de afdeling Nucleaire Geneeskunde en het voormalige PET-centrum (ondertussen gefuseerd tot de afdeling Nucleaire Geneeskunde en Moleculaire Beeldvorming) hebben hun steentje bijgedragen aan dit onderzoek. Rika v.d. Werff, Bea Vennema-Hermse, Alice Staal-Kloosstra, Ilse Sewnandan, Erna van der Wijk en Arja Hoekman van het secretariaat van de afdeling Nucleaire Geneeskunde en het PET-centrum zorgden voor goede planning en het snel afwerken van de DISA SPECT studies. De medewerkers van het laboratorium van de afdeling Nucleaire Geneeskunde en het PET-centrum wil ik bedanken voor het bereiden van de radiofarmaca. Soms was er een tweede “run” ammonia nodig wanneer de eerste onvoldoende was, maar dat mocht de pret niet drukken. De medisch nucleair werkers zijn altijd ontzettend behulpzaam geweest voor het verrichten van de hartstudies, zelfs soms in hun middagpauze. In het bijzonder wil ik Hans ter Veen, Geertje Akkerman, Remco Koning, Marijke Broersma, Hedy Vrakking, Clara Lemstra, Judith Streurman, Johan Wiegers, Yvonne Reitsma, Yvonne van der Knaap, Sabiene Boerdijk, Sharon Jonkman en Annemiek Stiekema hiervoor bedanken.

Mr. Annie van Zanten, manager bedrijfsvoering, wil ik bedanken voor de vele “zaakjes” die geregeld moesten worden. Deze werden altijd direct opgepakt en uitgevoerd.

Prof. dr. P.A. Kaufmann, from the Nuclear Cardiology Section, Cardiovascular Center, University Hospital Zurich, Switzerland. Dear Philipp, I want to thank you for your willingness to be part of the committee on 27 June.

Ook wil ik Dr. J. de Sutter, afdeling cardiologie, Universitair Ziekenhuis Gent, België, bedanken voor zijn bereidwilligheid om te opponeren tijdens de verdediging van mijn proefschrift.

Dr. Wim J. Sluiter, drs. Nic J.G.M. Veeger en dr. Hans L. Hillega wil ik bedanken voor de statistische ondersteuning.

Het gouden duo van het secretariaat van de afdeling Cardiologie, Olga Klompstra en Alma Guikema, wil ik bedanken voor de goede ondersteuning tijdens mijn onderzoeksperiode. Jullie stonden altijd klaar om te helpen en bovendien was de sfeer altijd erg prettig. Ik kom gauw weer eens langs.

Het secretariaat van de hartcatheterisatie, met name Alice Kanning, Gerda Boven-Faber, Manon Bus, Jannet Elderman-Bartels, Liesje Sebo en het secretariaat van de afdeling Thoraxchirurgie, met name Jessica Volders en Anneke Hamming wil ik erg bedanken voor beschikbaar stellen van “het schriftje” op de HC en het telkens doorsturen van de patiëntenwachtlijst.

Bob Hoogenboom van Siemens Medical Systems Nederland wil ik bedanken voor de softwarematige ondersteuning van de DISA SPECT studies. Regelmatig kwam je naar Groningen om mij te helpen. Dit is van essentieel belang geweest voor het onderzoek. Ik hoop dat je nog een keer een top-10 hit scoort met je muziekband.

De MRI afdeling en in het bijzonder de laboranten Peter Kappert, Titia van Echten en Anita Kuiper wil ik bedanken voor de MRI verrichtingen, ook al was het soms passen en meten in het schema.

Dr. P.H. Mook. Beste Piet, veel dank voor de MRI ondersteuning. Zonder jou was het niet veel geworden, simpelweg omdat er destijds geen cardiologische MRI expertise aanwezig was in het ziekenhuis. Zelfs thuis kon ik je benaderen om de MASS perikelen aan je voor te leggen.

En natuurlijk wil ik mijn ouders bedanken voor de mogelijkheden die zij mij altijd hebben geboden. Mijn moeder voor haar onvoorwaardelijke steun. Mijn vader voor zijn gedachtegoed, helaas ben je er niet meer.

Tot slot, lieve Henriëtte, bedankt voor het bijwerken van enkele hoofdstukken van dit proefschrift. Straks de koffers pakken en op naar Havanna.

List of Publicaties

Papers about viability detection and attenuation correction

Slart RHJA, Bax JJ, van Veldhuisen DJ, van der Wall EE, Oudkerk M, Sluiter WJ, de Boer J, Jager PL. Prediction of functional recovery after revascularization in patients with chronic ischemic left ventricular dysfunction: head-to-head comparison between ^{99m}Tc-sestamibi/^{18}FDG DISA SPECT and ^{13}N-ammonia/FDG PET. Submitted, 2005.

Slart RHJA, Bax JJ, van Veldhuisen DJ, MD, van der Wall EE, Dierckx RA, de Boer J, Jager PL. Prediction of functional recovery after revascularization in patients with coronary artery disease and left ventricular dysfunction by gated FDG PET. Submitted 2005.

Slart RHJA, Bax JJ, van Veldhuisen DJ, van der Wall EE, Dierckx RA, Jager PL. Imaging techniques in nuclear cardiology for the assessment for myocardial viability. Submitted, 2005

Slart RHJA, Bax JJ, de Boer J, Willemsen ATM, Mook PH, Oudkerk M, van der Wall EE, van Veldhuisen DJ, Jager PL. Comparison of ^{99m}Tc-sestamibi/^{18}FDG DISA SPET with PET for the detection of viability in patients with coronary artery disease and left ventricular dysfunction. In press: Eur J Nucl Med Mol Imaging, 2005

Slart RHJA, Bax JJ, Sluiter WJ, van Veldhuisen DJ, Jager, PL. Added value of attenuation corrected ^{99m}Tc-tetrofosmin SPECT for the detection of viability: Comparison with FDG SPECT. J Nucl Cardiol 2004 Nov-Dec;11(6):689-96.

Slart RHJA, Jager PL, de Boer J. FDG SPECT and ^{99m}Tc-MIBI/FDG DISA SPECT: comparable with FDG PET for the detection of myocardial viability. Ned.Tijdschr. v. Nucl. Geneesk 2004 Jul;26(2):39-45.

Slart RHJA, Bax JJ, de Jong RM, de Boer J, Lamb HJ, Mook P, Willemsen ATM, Vaalburg W, van Veldhuisen DJ, Jager PL. Comparison of gated positron emission tomography with magnetic resonance imaging for evaluation of left ventricular function in patients with coronary artery disease. J Nucl Med 2004 Feb;45(2):176-82.

Slart RHJA, Que TH, van Veldhuisen DJ, Poot L, Blanksma PK, Piers DA, Jager PL. Performance of ^{99m}Tc-sestamibi myocardial perfusion scintigraphy before and after 1 year of attenuation correction experience. Eur J Nucl Med Mol Imaging 2003 Nov;30(11):1505-9.

De Boer J, **Slart RHJA,** Blanksma PK, Willemsen AT, Jager PL, Paans AM, Vaalburg W, Piers DA. Comparison of ^{99m}Tc-sestamibi-^{18}F-fluorodeoxyglucose dual isotope simultaneous acquisition and rest-stress ^{99m}Tc-sestamibi single photon emission computed tomo-

graphy for the assessment of myocardial viability. Nucl Med Commun 2003 Mar;24(3):251-7.

Slart RHJA, de Boer J, Jager PL, Piers DA. Added value of attenuation-corrected myocardial perfusion scintigraphy in a patient with dextrocardia. Clin Nucl Med 2002 Dec;27(12):901-2.

Slart RHJA, de Boer J, Jager PL, Piers DA. Resolution of myocardial perfusion defects after attenuation correction in a patient with dextrocardia. New Adv Nucl Cardiol 2002;2(3)15-6.

Other papers

Van der Vleuten PA, **Slart RHJA**, Tio RA, Van der Horst ICC, MD, Van Veldhuisen DJ, Dierckx RA, Zijlstra F. Feasibility of repeated left ventricular ejection fraction analysis with sequential single-dose radionuclide ventriculography. In press: Nucl Med Commun 2005.

(Gated SPECT) Myocardperfusiescintigrafie, een belangrijk diagnositicum in de klinische cardiologie. Bavelaar-Croon CDL, **Slart RHJA**, Bax JJ, Van der Wall EE. Submitted, 2005.

Van Waarde A, Maas B, Doze P, **Slart RHJA**, Frijlink HW, Vaalburg W, Elsinga PH.
PET studies of human airways using an inhaled beta-adrenoceptor antagonist, *S*-^{11}C-CGP 12388. Submitted, 2005.

De Jong RM, Willemsen ATM, **Slart RHJA**, Blanksma PK, Van Waarde A, Cornel JH, Vaalburg W, Van Veldhuisen DJ, Elsinga, PH.Myocardial b-adrenoceptor downregulation in idiopathic dilated cardiomyopathy measured in vivo with PET using the new radioligand (S)-[^{11}C]CGP12388. In press: Eur J Nucl Med Mol Imaging 2005.

Slart RHJA, Phan TTH, Talsma MD, Jager PL. Different Splenic Uptake of ^{99m}Tc-sulfur colloid and ^{99m}Tc-heat-denatured red blood cells in an infant with complete situs inversus. Clin Nucl Med 2004 Sep;29(9):590-591.

Tio RA, Tan ES, Jessurun AJ, Veeger N, Jager PL, **Slart RHJA**, de Jong RM, Pruim J, Hospers GAP, Willemsen ATM, de Jongste MJL, van Boven AJ, Zijlstra F. PET for evaluation of differential myocardial perfusion dynamics after VEGF gene therapy and laser therapy in end-stage coronary artery disease. J. Nucl Med 2004 Sep;45(9):1437-43.

Slart RHJA, Poot L, Piers DA, van Veldhuisen DJ, Nichols K, Jager PL. Gated blood-pool SPECT automated versus manual left ventricular function calculations. Nucl Med Com-

mun 2004 Jan;25(1):75-80

Slart RHJA, Poot L, Piers DA, van Veldhuisen DJ, Jager PL. Evaluation of right ventricular function by NuSMUGA software: gated blood-pool SPECT versus first-pass radionuclide angiography. Int J Cardiovasc Imaging 2003 Oct;19(5):401-7.

Slart RHJA, Jager PL, Poot L, Piers DA, Cohen Tervaert J-W, Stegeman CA. Clinical value of gallium-67 scintigraphy in assessment of disease activity in Wegener's granulomatosis. Ann Rheum Dis 2003 Jul;62(7):659-62.

Jager PL, **Slart RHJA,** Corstens FH, Hoekstra OS, Teule JJ, Oyen WJ. PET-CT: a matter of opinion? **:** Eur J Nucl Med Mol Imaging 2003 Mar;30(3):470-1.

Jager PL, **Slart RHJA**, Pruim J, Oostenbrug LE, van der Werf TS. Three patients with massive pulmonary embolism. Ned Tijdschr Geneeskd 2002 Apr 20;146(16):779.

Jager PL, **Slart RHJA**, Piers DA. Clinical thinking and decision making in practice. A nurse with acute pain between shoulder blades. Ned Tijdschr Geneeskd 2000 Feb 19;144(8):396.

Slart RHJA, de Jong JW, Haeck PW, Hoogenberg K. Lytic skull lesions and symptomatic hypercalcaemia in bone marrow sarcoidosis. J Intern Med 1999 Jul;246(1):117-20.

Slart RHJA, Yu AL, Yaksh TL, Sorkin LS. An animal model of pain produced by systemic administration of an immunotherapeutic anti-ganglioside antibody. Pain 1997 Jan;69(1-2):119-25.

Landesz M, Kamps A, **Slart RHJA,** Siertsema JV, van Rij G. Morphometric analysis of the corneal endothelium with three different specular microscopes. Doc Ophthalmol 1995;90(1):15-28.

Abstracts/posters/presentations

about viability detection and attenuation correction

Slart RHJA, Jager PL, Que TH, Piers DA. Clinical evaluation of profile attenuation correction: preliminary analysis. Centers of excellence meeting Siemens, Sept 2000, Chicago, USA. [oral presentation].

Jager PL, **Slart RHJA**, Que TH, Piers DA. Advanced and future Nuclear Cardiology. Centers of Excellence meeting Siemens, Sept 2002, Chicago, USA.

Jager PL, **Slart RHJA**, Poot L, Que TH, Piers DA. Initial impact of Profile™ attenuation correction (AC) on the interpretation of myocardial perfusion imaging (MPI). J Nucl Med, May 2001 42 (5):175P. Society of Nuclear Medicine [poster].

De Boer J, **Slart RHJA**, Blanksma PK, Willemsen ATM, Jager PL, Paans AM, Vaalburg W, Piers DA. Comparison of ^{99m}Tc-sestamibi-^{18}F-fluorodeoxyglucose dual isotope simultaneous acquisition and rest-stress ^{99m}Tc-sestamibi single photon emission computed tomography for the assessment of myocardial viability. International Conference of Nuclear Cardiology, Apr 2003 Florence, Italy [poster].

Slart RHJA, Que TH, van Veldhuisen DJ, Poot L, Blanksma PK, Piers DA, Jager PL. Performance of ^{99m}Tc-sestamibi myocardial perfusion scintigraphy before and after 1 year of attenuation correction experience. International Conference of Nuclear Cardiology, Apr 2003 Florence, Italy [poster discussion].

Slart RHJA, Bax JJ, van Veldhuisen DJ, van der Wall EE, Oudkerk M, Jager PL, de Boer J. Prediction of improvement of functional recovery after revascularization in patients with coronary artery disease and left ventricular dysfunction by ^{99m}Tc-sestamibi/^{18}F-FDG DISA SPECT and ^{13}N-ammonia/^{18}F-FDG PET. Ned Tijdschr Nucl Geneesk, 2005.Nederlandse Vereniging voor Nucleaire Geneeskunde, November 2004, Nieuwegein [oral presentation].

Slart RHJA, Jager PL, Poot L, Que TH, Piers DA. Initial impressions of Profile™ attenuation correction on the interpretation of myocardial perfusion imaging. Ned Tijdschr Nucl Geneesk 2002;24:p19. Nederlandse Vereniging voor Nucleaire Geneeskunde, November 2001, Den Haag [oral presentation].

Jager PL, **Slart RHJA**, Poot L, Que TH, Piers DA. Added value of Profile™ attenuation correction in myocardial perfusion imaging (MPI). Ned Tijdschr Nucl Geneesk 2002;24:p18. Nederlandse Vereniging voor Nucleaire Geneeskunde, November 2001, Den Haag.

Slart RHJA, Bax JJ, de Jong RM, de Boer J, Lamb HJ, Mook PH, Willemsen ATM, Vaalburg W, van Veldhuisen DJ, Jager PL. Comparison of gated positron emission tomography with magnetic resonance imaging for evaluation of left ventricular function in patients with coronary artery disease. Ned Tijdschr Nucl Geneesk 2003;25:p25. Nederlandse Vereniging voor Nucleaire Geneeskunde, April 2003, Groningen [oral presentation].

Slart RHJA, Bax JJ, Sluiter WJ, van Veldhuisen DJ, Jager PL. Added value of attenuation corrected ^{99m}Tc-tetrofosmin SPECT for the detection of viability: Comparison with ^{18}F-FDG SPECT. Eur J Nucl Med Mol Imaging 31: S274, Aug 2004. European Association of Nuclear Medicine, Sept 2004, Helsinki, Finland [oral presentation].

Slart RHJA, Bax JJ, Sluiter WJ, van Veldhuisen DJ, Jager PL. Added value of attenuation corrected ^{99m}Tc-tetrofosmin SPECT for the detection of viability: Comparison with ^{18}F-FDG SPECT. European Society of Cardiology, workgroup Nuclear Cardiology, Mar 2004, Kitzbuhel, Austria [oral presentation].

Other abstracts/posters/presentations

Slart RHJA, Poot L, van Veldhuisen DJ, Jager PL. Evaluation of left and right ventricular function: gated blood-pool SPECT versus planar gated blood-pool and first-pass imaging. International Conference of Nuclear Cardiology, Apr 2003 Florence, Italy [poster].

Slart RHJA, Jager PL, Poot L, Piers DA, Cohen Tervaert JW, Stegeman CA. The clinical value of gallium-67 scintigraphy in Wegener's granulomatosis. Eur J Nucl Med Mol Imaging 2001;28 (8):S553. European Association of Nuclear Medicine, Aug 2001, Napoli, Italy [poster discussion].

Van Waarde A, Elsinga PH, Doze P, Jager PL, **Slart RHJA**, Frijlink HW, Vaalburg W. PET studies of human airways using inhaled ^{11}C-CGP 12388. J Nucl Med 2002; 43 (5): 350P. Society of Nuclear Medicine, June 2002, Los Angeles, USA [poster].

Curriculum vitae

Riemer Harmand Johan Anne Slart werd geboren in Emmercompascuum op 10 april 1969. Hij volgde zijn middelbare schoolopleiding te Emmen. In 1987 begon hij met de studie chemische technologie aan de Hogere Technische School te Groningen. In 1988 werd de overstap gemaakt naar de studie geneeskunde aan de Rijksuniversiteit te Groningen. Tijdens de studie geneeskunde werkte hij mee aan het onderzoek “Morphometric analysis of the corneal endothelium with three different specular microscopes” op de afdeling Oogheelkunde onder leiding van Prof. Dr. G. van Rij en Dr. M. Landesz. De officiële wetenschappelijke stage getiteld “An animal model of pain produced by systemic administration of an immunotherapeutic anti-ganglioside antibody” werd verricht in San Diego, Californië (VS) onder leiding van Prof. Dr. T.L. Yaksh en Dr. L.S. Sorkin. Na het afronden van de co-schappen in het Medisch Spectrum Twente te Enschede behaalde hij in 1997 het artsexamen. Na 2 maanden gewerkt te hebben bij de GG & GD startte hij met de opleiding nucleaire geneeskunde (opleider: dr. D.A. Piers). Tijdens het laatste jaar van de opleiding begon hij met het promotieonderzoek onder leiding van promotores Prof. Dr. D.J. van Veldhuisen, Prof. Dr. E.E. van der Wall en co-promotores Dr. P.L. Jager en Dr. J.J. Bax. In september 2001 rondde hij de opleiding tot nucleair geneeskundige af en werd vervolgens staflid, werkzaam op de afdeling Nucleaire Geneeskunde en Moleculaire Beeldvorming in het Universitair Medisch Centrum Groningen met cardiologie als aandachtsgebied.